CYTOTOXICITY OF HEXAVALENT CHROMATE COMPOUNDS IN CH310T1/2 CELLS AND CYTOMODULATION BY SODIUM ARSENITE AND METHANOL EXTRACT OF *Rauvolfia vomitora* (Afzel) IN MICE.

By

KAZEEM AKINYINKA AKINWUMI

BSc., MSc. Biochemistry, Ibadan.

A thesis in the Department of BIOCHEMISTRY

Submitted to the Faculty of Basic Medical Sciences in partial fulfillment of the requirements of the award of the Degree of

DOCTOR OF PHILOSOPHY

of the

UNIVERSITY OF IBADAN

FBRUARY, 2015

CERTIFICATION

I certify that this work was carried out by KAZEEM AKINYINKA AKINWUMI in the Cancer Research and Molecular Biology Laboratories, Department of Biochemistry, University of Ibadan.

---------- ----------

Supervisor Date

Oyeronke Odunola, PhD

Director, Cancer Research and Molecular Biology

Laboratories,

Department of Biochemistry

University of Ibadan.

DEDICATION

The thesis is dedicated to Almighty God for His mercy and favours throughout my educational pursuit

ACKNOWLEDGEMENTS

All praises and adoration are due to God almighty; that is able to do all things. I thank God for His favours, mercies and protection throughout the duration. This thesis would not have been possible without the help and encouragement of so many people. I express my gratitude to the Head of Department, Prof. O.O. Olorunsogo for his fatherly advice and providing enabling environment in the Department, which aided the completion of this work. I would like to thank my supervisor and mentor, Dr. Oyeronke Adunni Odunola who nurtured me academically from B.Sc. to Ph.D. I appreciate the cordial relationship I enjoyed throughout my stay in the laboratory. I am grateful for her love, kindness, encouragement and support over the period of my stay. I also thank her for the guidance and taking time out to correct this thesis. May God reward you abundantly.

My appreciation goes to the former Director of the Cancer Research and Molecular Biology, Prof. A.O. Uwaifo for stimulating my interest in Cancer Research and more importantly, introducing me to Dr. Joe Landolph in whose laboratory a substantial part of this work was carried out. I am equally gratefully to Prof. E.O. Faronmbi for his care, advice and support. My sincere thanks go to Drs. Gbadegesin, Owunmi and Adaramoye for their invaluable comments and suggestions that greatly improved the quality of this work. Also, my special thanks go all my Lecturers in the Department for the knowledge imparted that provided a formidable foundation for this degree. All the non-teaching staff including Mr Isiaka and Eric is appreciated.

My sincere gratitude goes to the Vice Chancellor of Bells University, Prof. I. A. Adeyemi and the management staff for allowing me to go on study leave with pay to University of Southern California, Los Angeles in order to carry out my research. The Executive Secretary, National University Commission, Prof Julius Okojie, who through the NUC provided the air ticket to and from Los Angeles, is appreciated. I also thank Mr. Mayaki, the Director of Protocol and Special Duties in NUC for his moral support and encouragement.

I am very grateful to my host and mentor at the Department of Molecular Microbiology and Immunology, University of Southern California, Los Angeles, USA, Dr. Joseph R. Landolph.

His daily guidance, support, mentorship, encouragement and extremely kindness are worthy of emulation. His family members, Alice, Joe III and Louis Landolph are also appreciated for their hospitality and friendship throughout my stay in Los Angeles. I appreciate the assistance given to me by members of the Laboratory like Prethi, Sara, Sid, Shira, Megan, Sophia, Shelly, Will, Oliver, Ibukun, Laureen, Ahmed, Khalid and Justin. Douglas Hauser, Anthony Rodriguez, Ernesto and Eric Baron are appreciated for teaching me electron microscopy. Many thanks goes to Dr. John Mata & his laboratory members at the Department of Basic Medical Sciences, College of Osteopathic Medicine of the Pacific , University of Health Sciences, Lebanon, Oregon USA. The genes expression studies reported in this thesis were done in his laboratory. I also appreciate the hospitality and warm embrace received from the Harley as well as Maggie and Jessse Mata.

I acknowledge without reservation the encouragement and support of Ayo and Labake Akerele, High Chief (Dr.) Olufemi Olaifa, Prof. F.A.A. Adeniyi, Prof. L. A. Bamidele, Ayo Adedoja, Lekan Ilesanmi, Eco, Bode, Ismail Adeyemo, Kola Bada, Ali Gafar, Taofeeq Yaqeen and my colleagues at Bells University of Technology. Dami, Debbie, Aminat, Jumoke, and Ola Olajumoke are all appreciated for their support and secretariat assistance.

My family members, Washi, Hammed, Zainab, Hafeez and Mutiat are appreciated for their forbearance, support and prayers. Finally, I thank my parents, for encouraging me to tread this path. I appreciate your prayers, love and care that contributed immensely to my academic success. My prayer is that you both live long to enjoy the fruit of your labour.

ABSTRACT

Exposure to certain hexavalent chromate compounds (HCC) causes lung and colon cancers. Their mechanisms of cytotoxicity are unclear, but believed to be affected by ascorbate and particle size. However, their role is not clearly defined. Co-exposure with sodium arsenite (SA) is common, but its effect on HCC toxicity is unknown. Current therapy has side effects, necessitating the search for antidote from unexplored natural products such as *Rauvolfia vomitora* (RV). This study therefore investigates the effect of particle size and ascorbate on cytotoxity of selected HCC [lead chromate ($PbCrO_4$), barium chromate ($BaCrO_4$), strontium chromate ($SrCrO_4$) and potassium dichromate ($K_2Cr_2O_7$)] in C3H10T1/2 cells and cytomodulatory effects of SA and RV in mice.

The effect of ascorbate, dehydroascorbate and particle size on HCC cytotoxicity in C3H10T1/2 cells was determined by measuring survival fraction and yield of foci by microscopy. Actin and cellular ultrastructure disruption and induction of cell death were assessed by electron and fluorescent microscopy. The molecular mechanisms of cytotoxicity and transformation were evaluated in eighty-four cell death genes using real time (RT^2) gene array, while cell cycle analysis was done by flow cytometry. Leaves of RV were air dried, powdered and extracted with methanol. Forty male mice (20-25g) were divided into 8 groups of 5 Swiss albino mice each and treated with water (control), RV (275 mg/Kg), SA (2.5 mg/kg), $K_2Cr_2O_7$ (12 mg/Kg), SA + $K_2Cr_2O_7$, RV + SA, RV + $K_2Cr_2O_7$, RV + SA + $K_2Cr_2O_7$. *Rauvolfia vomitora* was given orally for seven days, while $K_2Cr_2O_7$ and SA were administered on day seven. Serum aspartate and alanine aminotransferases (AST and ALT), catalase, glutathione-S-transferase (GST), glutathione and malondialdehyde (MDA) levels were determined by spectrophotometry. Micronucleated polychromatic erythrocytes (mPCEs) were evaluated by microscopy. Data were analysed using ANOVA and Student's t- test at $p= 0.05$.

Survival fraction of control cells was 1.0, treatment with $PbCrO_4$ and ≤ 12.5 µM ascorbate or ≤ 2 µM dehydroascorbate decreased it to 0.4. The 15-20 µM ascorbate and 3-4 µM dehydroascorbate reversed it to 0.7. Exposure of cells to small (≤ 3 µm) and large particles (≤ 8 µm) of $PbCrO_4$, $BaCrO_4$ and $SrCrO_4$ resulted in a dose-dependent decrease in survival. The total foci were higher for $PbCrO_4$ (3.8) with large particles and $BaCrO_4$ (6.6) with small particles. Phagocytosis of particles was time-dependent. The HCC treatment led to G2/M and S phase arrest, anucleation, actin disruption and mixed cell death. Thirty-four cell death genes including Bax and Casp3 were up-regulated by 4 folds and six including Bcl-2 and Traf2 were down-regulated in treated cells. Twenty-one anti-apoptotic and autophagy genes including Atg5 and Bcl-2 were up-regulated in $PbCrO_4$ transformed cells. The $K_2Cr_2O_7$ and/ or SA significantly increased mPCEs, AST, ALT, catalase and MDA levels while glutathione and GST were reduced. The RV restored the markers towards normal values.

Cytotoxicty of chromate compounds is particle size and ascorbate dependent. The cytotoxicity might be due to actin disruption, micronuclei induction and cell cycle arrest. Methanol extract of *Rauvolfia vomitora* modulated the toxicity in mice.

Keywords: Hexavalent chromate compounds, Sodium arsenite, *Rauvolfia vomitora*, Cytotoxicity

Word counts: 494

TABLE OF CONTENTS

CHAPTER SIX

LIST OF FIGURES

LIST OF TABLES

ABBREVIATIONS

ALT - Alanine aminotransferase

AO	-	Acridine orange
AST	-	Aspartate aminotransferase
ATM	-	Ataxia telangiectasia-mutated gene
ATP	-	Adenosine triphosphate
BacMam	-	Baculovirus with a mammalian promoter
BAL	-	British anti lewisite
Bis-AAF-R110		Bis-alanylalanyl-phenylalanyl-rhodamine 110
BME	-	Basal eagle medium
CAT	-	Catalase
CHK	-	Checkpoint kinase
CHO	-	Chinese hamster ovary
CIN	-	Chromosomal Instability
CYD	-	Cytochalasin D
DD	-	Death domain
DED	-	Death effector domain
DFFA	-	DNA fragmentation factor A
DISC	-	Death-inducing signaling complex
DMPS	-	2,3-dimercaptopropane 1-sulphonate
DNA	-	Deoxyribonucleic Acid
DPBS	-	Dulbecco's Phosphate Buffered Saline 1X
DTNB	-	5, 5-dithiobis 2-nitrobenzoic acid
EDTA	-	Ethylenediaminetetraacetic Acid
EDX	-	Energy-dispersive X-ray analysis
EPA	-	Environmental Protection Agency
ESR	-	Eectron spin resonance
FBS	-	Fetal bovine Serum
FCS	-	Fetal calf serum

FP	-	Fluorescent protein
FRIN	-	Forestry Research Institute of Nigeria
GF-AFC	-	Glycylphenylalanyl-aminofluorocoumarin
GFP	-	Green fluorescent protein
GST	-	Glutathione S-Transferases
GPx	-	Glutathione Peroxidase
GSSG	-	Glutathione Disulphide
GSH	-	Reduced Glutathione
GRd	-	Glutathione-Reductase Enzyme
HPV	-	Human papillomavirus
IARC	-	International Agency for Research on Cancer
LSCM	-	Laser scanning confocal microscopy
LUTH	-	Lagos University Teaching Hospital
MCA	-	3-methyl cholanthrene
MDA	-	Malondialdehyde
MMC	-	Mouse mesangial cells
MN	-	Micronucleus
MOM	-	Mitochondrial outer membrane
MOMP	-	mitochondrial outer membrane permeabilization
MPCEs	-	micronucleated polychromatic erythrocytes
MPT	-	Mitochondrial permeability transition
MTOR	-	Mammalian target of rapamycin
NADH	-	Reduced form of nicotinamide adenosine dinucleotide
NBS	-	Nile blue sulfate
NR	-	Neutral red
NSCs	-	Neural stem cells
PCE	-	Polychromatic erythrocytes

PCR	-	Polymerase chain reaction
PI	-	Propidium iodide
PI3K	-	Phosphatidylinositol-3-kinase
RNA	-	Ribonucleic acid
ROS	-	Reactive oxidative Species
RV	-	*Rauvolfia vomitora*
SA	-	Sodium arsenite
SHE	-	Syrian hamster embryo
SOD	-	Superoxide Dismutase
TBA	-	2-thiobarbituric acid
TBARS	-	Thiobarbituric acid reactive substances
TEM	-	Transmission electron microscopy
TNF	-	Tumor necrosis factor
TOR	-	Target of rapamycin
TRITC	-	Tetramethylrhodamine
TUNEL	-	Terminal dUTP Nick End-Labeling
USC	-	University of Southern California
PCD	-	Programmed Cell Death
NER	-	Nucleotide Excicion Repair
GFP	-	Green Flourescent Protein

CHAPTER ONE

1.0 INTRODUCTION

Cancer, a category of diseases that are characterized by the uncontrolled growth and spread of abnormal cells in the body is a major threat to human existence. In the year 2000 only, cancer accounted for 6.2 million deaths, 22.4 million persons living with cancer and 10.1 million new cases where discovered globally (Vincent *et al.*, 2004). Africa is not left out of the monster ravaging lives. International Agency for Research on Cancer (IARC), reported that about 681,000 new cancer cases and 512,400 cancer deaths occurred in 2008 in Africa and these data are expected to be doubled by the year, 2030 (Ferlay *et al.*,2008). Cancer incidence has been on the increase in the continent probably due to the adoption of western ways of life and diets as well as industrialisation. Interestingly, exposure to pollutants, toxicants and contaminants from these industries increases the age specific incidence of cancer and is estimated to increase the global burden of cancer annually to 15 million by 2020 with a lot of new cases from Africa (Klehues *et al.*, 2003). Hexavalent chromate is one of these pollutant and contaminants. Regulatory bodies across the globe have not only declared it a human carcinogen, but one of the 33 compounds that possess the greatest potential health threat in urban areas (OSHA, 2006; NTP, 2005; IARC, 1990).

Chromium is a wide spread element in the environment. It is found naturally in rocks, soil, plants,animals, volcanic dust and gases (Saygi *et al*., 2008; Li *et al*., 2009; Pouzar *et al*., 2009; Wise *et al*., 2009). It exists mainly in two forms, Cr (III) and Cr (VI). Cr (III) occurs naturally, but Cr (VI) is rarely found in nature. It is produced mainly from commercial and industrial processes. The Chromium (III) is essential for carbohydrate and lipid metabolism, while the Cr (VI) can be toxic and carcinogenic. Human beings get exposed to hexavalent chromate via water, food and by direct contact to the skin (Son *et al.*, 2010). In addition, millions of workers worldwide are estimated to be occupationally exposed to chromate (VI) compounds in an array of industries such as pigment production, chrome plating, stainless steel welding, cement, textile, printing, photography, paint, wood preservatives, lithography plastics, ceramics, glass and leather tanning (Cheng *et al.*, 2014; Urbano *et al*, 2008). Also, effluents from various industries such as plating, tanning, painting, pigment production and metallurgy contain hexavalent chromate that may contaminate natural waters (Cheng *et al.*, 2014; Tziritis *et al.*, 2012; Cossich

et al., 2002; Liu *et al.*, 2001; Fishbein, 1981). Furthermore, defective organ prostheses manufactured from chrome alloys also accounts for human exposure to the toxic hexavalent chromium (Michel *et al.*, 1991). Non-occupational exposure to Cr occurs from automobile emissions, fossil fuel combustion, waste incineration and cigarette smoke (Tian *et al.*, 2012; Cong *et al.*, 2010). It has been estimated that cigarettes produced in the United States contain 0.24–6.3 mg Cr/kg (ASTDR, 2000; IARC, 1990). In the environment, elevated levels of chromate (VI) have been reported ipppn areas near landfills, hazardous waste disposal sites, chromate industries and highway. Moreover, the Environmental Protection Agency EPA (1999) noted that approximately, 1.7 X 10^5 tons of Cr is released into the atmosphere every year. Consequently therefore, there is widespread inadvertent inhalation of chromate by the general populace especially in the developing countries. A summary of the different sources of human exposure to chromate (VI) is shown in Figure 1.1.

Chronic and acute exposure to hexavalent chromium results in many undesirable effects including, hepatic failure, anaemia, thrombocytopenia, spontaneous abortions, ulcers, dermal damage, gastrointestinal bleeding, renal failure, intravascular haemolysis, liver damage, respiratory disturbances, coma and even death (Lin *et al.*, 2009; Das and Mishra, 2008; IARC, 1990). Moreover, the International Agency for Research on Cancer (IARC, 1990) has classified chromium (VI) as human carcinogen based on the weight of evidences from experimental studies. For instance, consistent associations have been found between employment in the chromium industries and significant risk for respiratory cancer (Landolph, 1994; Biedermann and Landolph, 1990; IARC, 1994; Gibbs *et al.*, 2000). More recent studies also disclosed excess risk of lung cancer death resulting from occupational exposure to Cr (VI) compounds (Kuo *et al.*, 2006; Park *et al.*, 2004; Gibb *et al.*, 2000). Cr (VI) carcinogenesis in humans follows a linear, no-threshold dose-response curve (De Flora, 2000). Furthermore, statistical studies have found a 25% risk of dying from lung cancer with the permissible exposure of 52µg/m^3 in 1971 (Gibbs *et al*., 2000), so this standard was lowered to 5µg/m^3 by U.S. Occupational Safety Health Administration in 2006 (OSHA, 2006). Unfortunately, this new standard still expects 10-45 deaths for every 1,000 exposed workers (Gibb *et al*., 2000).

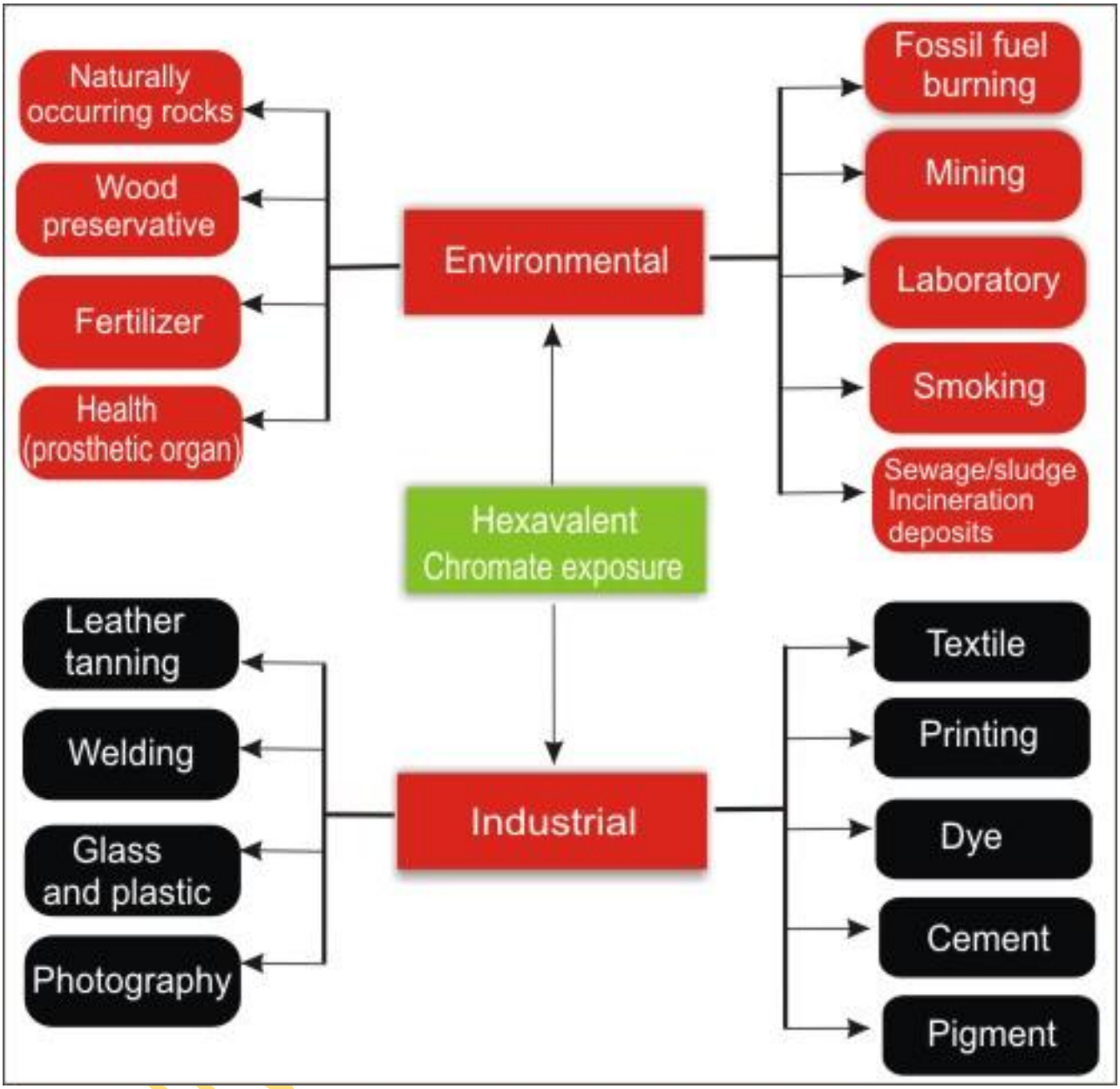

Figure 1.1: Common Sources of Exposure to Hexavalent Chromate in the Environment

Similarly, the genotoxicity and mutagenicity of chromium compounds have all been demonstrated in man and animals (Stohs and Bagchi, 1995; Mount and Hockett, 2000). Many animal experiments and *in vitro* experiments have further supported these epidemiology reports by showing that Cr (VI) compounds induce DNA damage, cytotoxicity, and neoplastic growth (NIOSH, 2005).

Once inside cell, hexavalent chromate can be reduced to the Cr (III) under physiological conditions, producing reactive intermediates, including Cr (V), Cr (IV), and Cr (III). These active intermediates may bind directly to DNA forming stable DNA-chromium complexes, DNA strand breaks, DNA-DNA cross links (Hodges *et al*., 2001). Similarly, chromium metabolism has been shown to be accompanied by the generation of reactive oxygen species (ROS) that presumably trigger oxidative damage to DNA (Zhang *et al*., 2001) and consequent cell deatb (D'Agostini *et al*., 2002). It has also been reported that Cr (VI) induced oxidative damage in tissue either through production of free radicals/ lipid peroxidation or by alteration of cellular antioxidant capacity (Quinteros *et al.,* 2008). For instance Cr (VI) treatment was reported to increase the level of lipid peroxidation in rat and mice (Arreola- Mendoza *et al*., 2006; Perez *et al*., 2004). Moreover, recent studies showed that Cr (VI) alter the activities of antioxidant enzymes, including glutathione peroxidase, catalase and superoxide dismutase (Fatima and Mohamood, 2007; Luca *et al*., 2007). Furthermore, generation of reactive oxygen species (ROS), stimulation of lipid peroxidation and alteration of antioxidant reserves have been suggested to be major contributors to Cr (VI)-exposure related diseases (Luca *et al.*, 2007; Valko *et al.*, 2006).

Despite progress in understanding of Cr (VI) toxic potential, the specific mechanisms of Cr (VI)-induced toxicity and carcinogenesis is still complex and not clearly elucidated. For instance, epidiemiology studies have repeated showed that exposure to insoluble chromate (VI) compounds causes cancers of the respiratory system including lung cancers, whereas this has not been convincingly demonstrated *in vitro*. Disparities in results have also been obtained in different cells exposed to hexavalent chromate. Although, hexavalent chromate toxicity are thought to be affected by particle sizes and the type as well as the amount of intracellular reductant present at the time of exposure, different results have been reported by different researchers. Furthermore, the toxicity of hexavalent chromate may also be compounded by co-

exposure with other environmental toxicant such as arsenic and cigarette smoke. Moreover, phytochemicals such as antioxidant in diet and medicinal plants may also affect toxicological outcome of hexavalent chromate exposure.

This work therefore investigates the effect of particle size and ascorbate on cytotoxity of selected hexavalent chromate compounds [lead chromate ($PbCrO_4$), barium chromate ($BaCrO_4$), strontium chromate ($SrCrO_4$)] in C3H10T½ cells. In addition, the cytomodulation of potassium dichromate ($K_2Cr_2O_7$) and sodium arsenite toxicity by methanol extract of *Rauvolfia vomitora*, a medicinal plant that is traditionally used for treating tumours was also investigated in mice.

1.1 JUSTIFICATION

Despite the overwhelming evidences from epidemiological and animal studies concerning the strong potency of insoluble hexavalent chromates as human carcinogen, effort to establish the carcinogenesis of hexavalent chromate compounds in vitro has only yielded limited success.

For instance, Patierno *et al.* (1988) reported that $PbCrO_4$ induced a weak morphological transformation in CH310T½ cells. The weak transformation was ascribed to a number of factors including particle size that limits its uptake (Patierno *et al.*, 1988). The particle size distribution of inhaled aerosols has important consequences for deposition in the lung. Penetration of an inhaled particle through the airways generally increases with decreasing particle size for particles. Chromate particles $\leq$ 3 µM are deposited in the bronchial tree where chromium-induced cancers occur (IARC, 1990). Moreover, workers in chromate related industries are exposed to different sizes of the compounds, but the role of particle size in chromate (VI) toxicity has not been reported.

Inadequate or lack of ascorbate in culture has also been suggested to result in low mutation and morphological transformation in chromate treated cells (Holmes *et al.*, 2008). Ascorbate is the fastest and main reductant of hexavalent chromate, generating reactive intermediates and free radicals (Fig 1.2) that can interact with cellular macromolecules (Costa and Klein, 2008; Zhitkovich *et al.*, 2005). *In vivo*, ascorbate levels are quite high (about 1 mM). However, the levels of ascorbate in tissue culture media are quite low and therefore inadequate to reduce

chromate. The only source of ascorbate in tissue culture media is supplied by fetal bovine serum (FBS). The level of ascorbate supplied by 10 % FBS usually use in tissue culture is only about 50 μM , which is 20 times lower than that found *in vivo* (Zhitkovich, 2005). Therefore, experiments on mutagenesis and other toxic effects of hexavalent chromium in tissue culture may underestimate its mutagenic, genotoxic, and cell-transforming activities (Zhitkovich, 2005; Costa and Klein, 2008). Addition of ascorbate or dehydroascorbate to culture media of hexavalent chromate treated cells would therefore mimic *in vivo* condition and may produce toxicity data there are more relevant to human exposure.

The mode of action for the carcinogenicity observed with chromate needs to be more clearly understood in order to reduce the risks associated with human interaction with chromate compounds. The lack of clear mechanistic information regarding chromate cytotoxicity is believed to be partly due to the number of different oxidation states of this metal that may play a role in its carcinogenicity. In addition multiple oxidation and binding pathways have been proposed to account for the wide assortment of DNA lesions observed in cellular systems.

Chromate (VI) toxicities are complicated by co-exposure with other environmental toxicant like cigarette smoke, UV and other heavy metals (Salnikow and Zhitkovich, 2008). For instance, arsenic is another carcinogenic heavy metal that is concomitantly inhaled or ingested with hexavalent chromate. Co-exposure to chromate and arsenic is common in drinking water, cigarette smoke, beverages and some fungicides (Maduabuchi *et al*, 2007). However, there is dearth of information concerning the toxic effect of co-exposure to both metals.

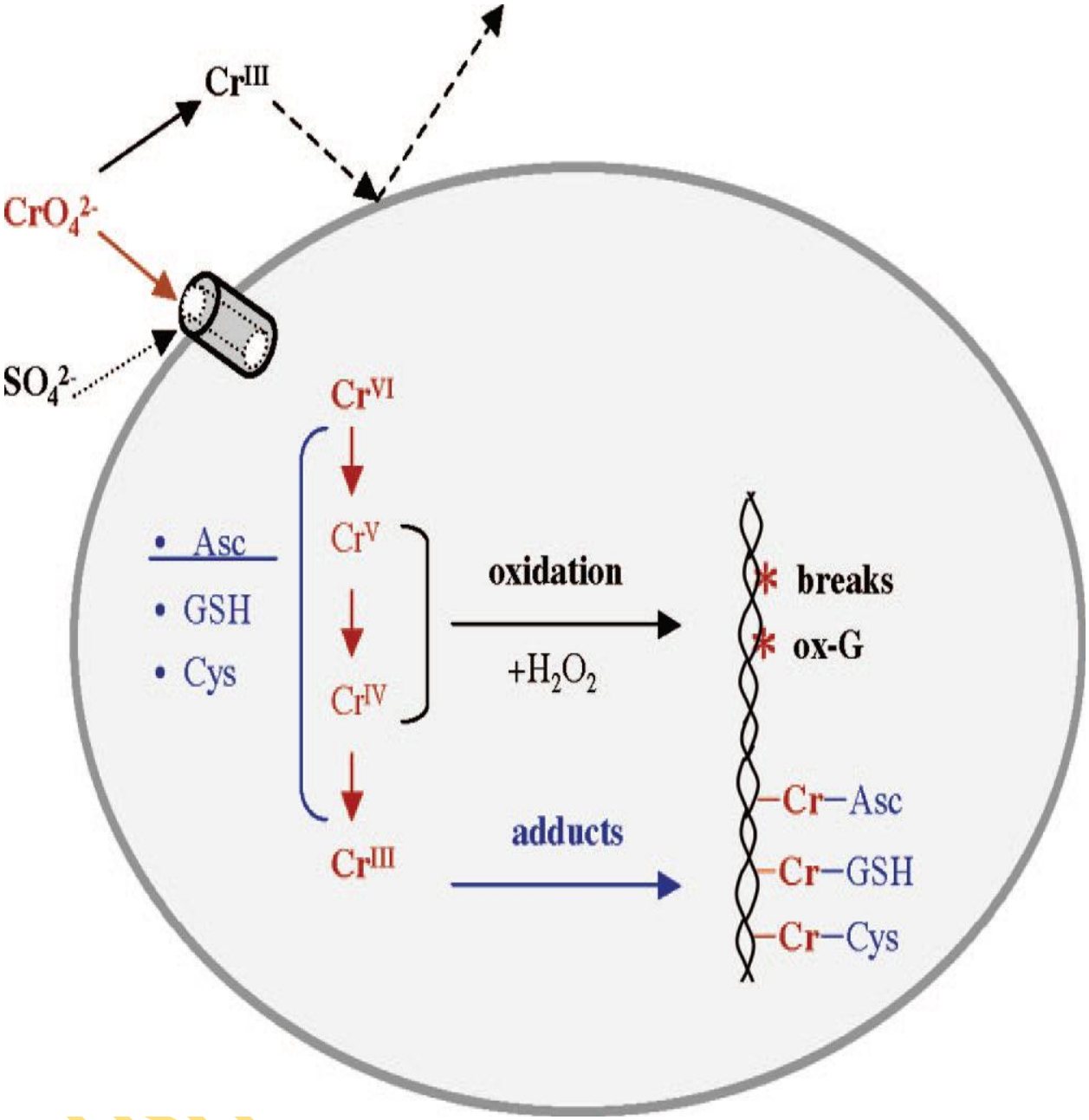

Figure 1.2: Major steps in uptake, metabolism, and formation of DNA damage by Cr (VI) (Zhitkovich *et al.*, 2005)

Despite the numerous sources of exposure to chromium and its attendant health effects, there is still no known safe and effective antidote for preventing or treating chromate toxicity. The use of metal chelators such as ethylenediaminetetraacetic acid (EDTA), British Anti Lewisite (BAL), sodium 2,3-dimercaptopropane 1-sulfonate (DMPS) and meso 2,3-dimercaptosuccinic acid have been proposed. However, metal chelators have been reported to possess side effects that limit their use. For instance, vomiting, headache, lachrymation, and salivation, profuse sweating, chest and abdominal pain, anxiety and decreased plasma concentration of essential metal like Zn, Mo and Cu are associated with chelation treatment (Shi *et al.*, 2004). The search for a safe and effective antidote against chromate (VI) and arsenic toxicity had led scientist to exploit the use of dietary antioxidants and medicinal plants with antioxidant properties in attenuating the toxic effects caused by exposure to heavy metals (Guha *et al.*, 2009; Arreola *et al*., 2006; Perez *et al*.,2004, Fatima and Mohamood, 2007). The usefulness of *Rauvolfia vomitora* (RV), a herb that is traditionally used to manage cancer related problems in the management of hexavalent chromate and arsenite toxicities is not known.

Rauvolfia vomitoria is a medicinal plant that is widely distributed in the humid tropical secondary and low land forests of Africa (Sofowora, 1993). It belongs to the family Apocynaceae and grows to a height of about 15m. Among the Yoruba speaking people of Nigeria, it is popularly known as "Asofeyeje" meaning bearing fruits for the birds, while the Igbo people in Nigeria and Ashantes of Ghana call it Akanta and Pempe respectively. The plant has found wide applications in traditional medicine across the world. Traditionally, different part of the plant found wide applications in the treatment of many diseases such as mental illness, tumours, liver problems, hypertension and fever (Amole *et al*., 2009; Akpanabiatu *et al* , 2009; Bemis, 2006). In addition, its tissue lipid lowering-effect, blood pressure lowering, antipyretic, analgesic, haematinic, aphrodisiac, purgative, dysenteric, abortive, insecticidal, anti psychotic, anticonvulsant properties have all been documented (Amole et al, 2009; Obembe,1994; Principe , 1989). Extract from the plant have also been reported to inhibit the growth of bacterial, viral, fungal and parasitic pathogens (Amole *et al*, 1993). Preliminary investigations show that the plant is rich in antioxidant, flavonoids, and polyphenols and could protect against CCl_4 induced hepatotoxicity (Akinwumi *et al.*, 2011).

However to date, no information exists in literature about the effect of consumption of *Rauvolfia vomitora* against hexavalent chromate and arsenic intoxification. Therefore, a study was undertaken in this thesis to investigate the effect of pretreatment of mice with methanol extract of RV on the clastogenic and hepatotoxic potential of potassium dichromate and sodium arsenite.

1.3 Aim of the Study

The overall aim of this work is to investigate the cytotoxity of three hexavalent chromate compounds [lead chromate ($PbCrO_4$), barium chromate ($BaCrO_4$), and strontium chromate ($SrCrO_4$),] in C3H10T½ cells and cytomodulatory effects of sodium arsenite and *Rauvolfia vomitora* (Afzel) on potassium dichromate ($K_2Cr_2O_7$) indued toxicity in mice.

1.3.1. Specific Objectives

Specifically this work was designed to investigate:

(i) The effect of ascorbate or dehydroascorbate on the cytotoxicity of $PbCrO_4$ in CH310T½ cells.

(ii) The effect of particles size on the cytotoxicity and transformation of CH310T½ cells treated with $PbCrO_4$, $BaCrO_4$ and $SrCrO_4$.

(iii) The effect of $PbCrO_4$, $BaCrO_4$ and $SrCrO_4$ treatment on cell death, actin disruption and cell cycle kinetics.

(iv) The mRNA expression profile of cell death related genes in chromate treated and transformed cells.

(v) The effect of *Rauvolfia vomitora* (RV) on potassium chromate (VI) toxicity alone and in combination with sodium arsenite by monitoring liver function, oxidative stress and clastogenic markers in mice.

CHAPTER TWO

LITERATURE REVIEW

2.1 Cancer

Cancer remains a major health problem and is responsible for one in eight deaths worldwide. (Berghe, 2012). There were 12.7 million new cancer cases and about 21,000 cancer deaths per day worldwide in 2008 (Ferlay *et al.*, 2010). Also, an estimated 68.5% increase in cancer incidence and 73.7% cancer deaths is expected by the year 2030 if urgent intervention strategies are not taken(ACS, 2010; Ferlay *et al.*, 2010). A recent survey of the global incidence of cancer shows that the age-adjusted cancer incidence in the Western world is above 300 cases per 100,000 population, whereas that in Asian countries is less than 100 cases per 100,000 (Messinaand and Hilakivi-Clarke, 2009). Observational studies have suggested that lifestyle risk factors such as tobacco, obesity, alcohol, sedentary lifestyle, high-fat diet, radiation, infections and exposure to environmental toxicant are major contributors to the high incidence of cancer. In addition, an increase in cancer cases was observed among immigrants from Asian to Western countries (Anand *et al.*, 2008; Shu *et al.*, 2009).Thus, a good percentage of cancer deaths may be prevented by modifying the diet composition (i.e. content of fiber, polyphenols, fat/oil, protein, spices, cereals, etc.) and regular physical exercise (Tennant *et al.*, 2010; Anand *et al.*, 2008; Boffetta *et al.*, 2010). Diet modifies the genome and determines stress adaptative responses, metabolism, immune homeostasis and the physiology of an organism (Huang *et al.*, 2011*;* vel Szic *et al.*, 2010)

All cancers involve the malfunction of genes that control cell growth, division, repairs and death (Vogelstein and Kinzler, 2004; Hanahan and Weinberg, 2000). Only a minority of cancers are caused by germline mutations, while the vast majority (90%) is linked to somatic mutations and environmental factors (Anand *et al.*, 2008). Damage to genes may be due to internal factors, such as hormones or the metabolism of nutrients within cells, or external factors, such as tobacco, chemicals, and sunlight. Most cancers evolve through multiple changes resulting from a combination of hereditary and environmental factors. Certain types of cancer can be prevented by eliminating exposure to tobacco and other carcinogen that initiate or accelerate cancer development. Cancer is treated with surgery, radiation, chemotherapy, hormones, and immunotherapy. However, it well known that many treatment regimens cause mild to

devastating and even fatal side effects. For instance, bevacizumab the best known drug for colorectal cancer can have terrible side effects, including gastrointestinal perforations, serious bleeding, severe hypertension, clot formation, and delayed wound healing. Therefore, there is renewed effort to discover new anticancer agents with less toxic effects from natural products such as plants.

2.2 Carcinogenesis

Carcinogenesis is a multistep process by which a normal cell is transformed into cancer (Vogelstein and Kinzler, 2004; Hanahan and Weinberg, 2000). Three main stages are involved: initiation, promotion and progression (Figure 2.1). During initiation, normal cells are exposed to stress (ROS) and/or a carcinogen (Figure 2.1). Initiation results in an increased capacity of the cells to survive or decrease capacity to die. This initial event results in a selective growth advantage that allows cells to accumulate more mutations or epigenetic changes that facilitate "selection" of cells through clonal selection and expansion. As carcinogenesis progresses, the neoplastic cells consistently acquire essential alterations in cell physiology which are known as the "hallmarks of cancer" (Hanahan and Weinberg, 2000). These include sustaining proliferative signaling, evading growth suppressors, resisting cell death, enabling replicative immortality, inducing angiogenesis, and activating invasion and metastasis (Fig 2.2). Underlying these hallmarks are genomic instability and inflammation. Genomic instability generates the genetic diversity that expedites their acquisition, while inflammation fosters multiple hallmark functions. In addition, reprogramming of energy metabolism and evasion of immune destruction were recently added to the list (Hanahan and Weinberg, 2011). Furthermore, tumors exhibit another dimension of complexity. They contain a repertoire of recruited, presumably normal cells that contribute to the acquisition of hallmark traits by creating the ''tumor microenvironment'' (Hanahan and Weinberg, 2011).

Environmental carcinogen represents a key contributor to human cancers. Exposure to many carcinogen such as heavy metals and other carcinogenic chemicals have detrimental effects on health and are considered to contribute substantially to the increasing global incidence of cancer and other public health diseases (Figure 2.3). They are well known to mediate a wide variety of toxic effects such as cell cycle arrest and DNA damage or genotoxicity. However, oxidative stress induced by a surge in cellular Reactive Oxygen Species (ROS) production and

dysregulation of cell death are two leading mechanisms in the etiology, progression and promotion of several human cancers (Rodgrio *et al.*, 2009).

2.3 Reactive Oxygen Species

Reactive oxygen species (ROS) are implicated as possible underlying pathogenic mechanisms in the initiation and progression of cancer. A free radical can be defined as any molecular species capable of independent existence that contains an unpaired electron in an atomic orbital (Lobo *et al.*, 2010). Most radicals are unstable and highly reactive. They can either donate an electron to or accept an electron from other molecules, therefore behaving as oxidants or reductants (Cheeseman and Slater, 1993). The most important oxygen-containing free radicals in many disease states are hydroxyl radical, superoxide anion radical, hydrogen peroxide, oxygen singlet, hypochlorite, nitric oxide radical, and peroxynitrite radical (Figure 2.4). These highly reactive species are capable of damaging biologically relevant molecules such as DNA, proteins, and carbohydrates (Young and Woodside, 2001). In addition, ROS could initiates fatty acid peroxidation in the nucleus and membranes of cells (Figure 2.5). Injury to the macromolecules by ROS in generally termed oxidative stress. Oxidative stress results when production of ROS exceeds the capacity of cellular antioxidant defenses to remove these toxic species (Shen *et al.*, 2011; Limon-Pacheco and Gonsebatt, 2009). Oxidative stress usually leads to cell damage and homeostatic disruption.

Free radicals including reactive oxygen species and reactive nitrogen species are generated by the human body by various endogenous systems, exposure to different physiochemical conditions, or pathological states; and thus, they participate in the pathogenesis of many of diseases including cancer. The different mechanisms by which reactive oxygen and nitrogen species, oxide and their biological metabolites initiates carcinogenesis is summarised in Figure 2.6. The initiation, promotion, and progression of cancer have been linked to the imbalance between ROS and the antioxidant defense system. ROS has been shown to cause at least 100 different types of DNA lesions, including base modifications, singe-strand breaks and double-

strand breaks and interstrand crosslinks (Xu *et. al.*, 2014; Cadet *et. al.*, 1997). In addition, numerous investigators have proposed participation of free radicals in carcinogenesis, mutation, and transformation. It is clear that their presence in biosystem could lead to mutation,

transformation, and ultimately cancer (Lobo *et al*., 2010). A summary of the different mechanism employed by ROS / RNS in inducing cancer is presented in Figure 2.7. The oxidative stress and cancer promoting activities of radicals can be decreased by antioxidant.

2.4 Antioxidant

An antioxidant is a molecule that is stable enough to donate an electron to a rampaging free radical in order to neutralize it and reducing its capacity to damage cells. These antioxidants delay or inhibit cellular damage mainly through their free radical scavenging property (Halliwell, 1995). Antioxidants are mainly responsible for converting or transforming free radicals into molecules that are less harmful in the cell. They therefore decrease oxidative stress induced carcinogenesis by a direct scavenging of ROS and/or by inhibiting cell proliferation secondary to the protein phosphorylation. Antioxidants may also act as hydrogen donor, electron donor, peroxide decomposer, singlet oxygen quencher, enzyme inhibitor, synergist and metal-chelating agents (Krinsky *et al.*, 1992). Both enzymatic and nonenzymatic antioxidants exist in the intracellular and extracellular environment to detoxify ROS (Lobo *et al.*, 2010).

Non-enzymatic antioxidants include low-molecular-weight antioxidants (Figure 2.7), which can interact with free radicals and terminate the chain reaction before vital molecules are damaged. These include glutathione, ubiquinol, and uric acid produced during normal metabolism in the body. Others such as carotenoids, flavonoids, vitamin E (α-tocopherol), vitamin C (ascorbic acid), β-carotene, selenium and copper, are supplied in diet. Water-soluble molecules, such as vitamin C, are potent radical scavenging agents in the aqueous phase of the cytoplasm, whereas lipid soluble forms, such as vitamin E and carotenoids, act as antioxidants within lipid environments. Selenium, copper, zinc, and manganese are also important elements, since they act as cofactors for antioxidant enzymes. Selenium is considered particularly important in protecting the lipid environment against oxidative injury, as it serves as a cofactor for glutathione peroxidase (GSH-Px) (Halliwell and Gutteridge, 1999).

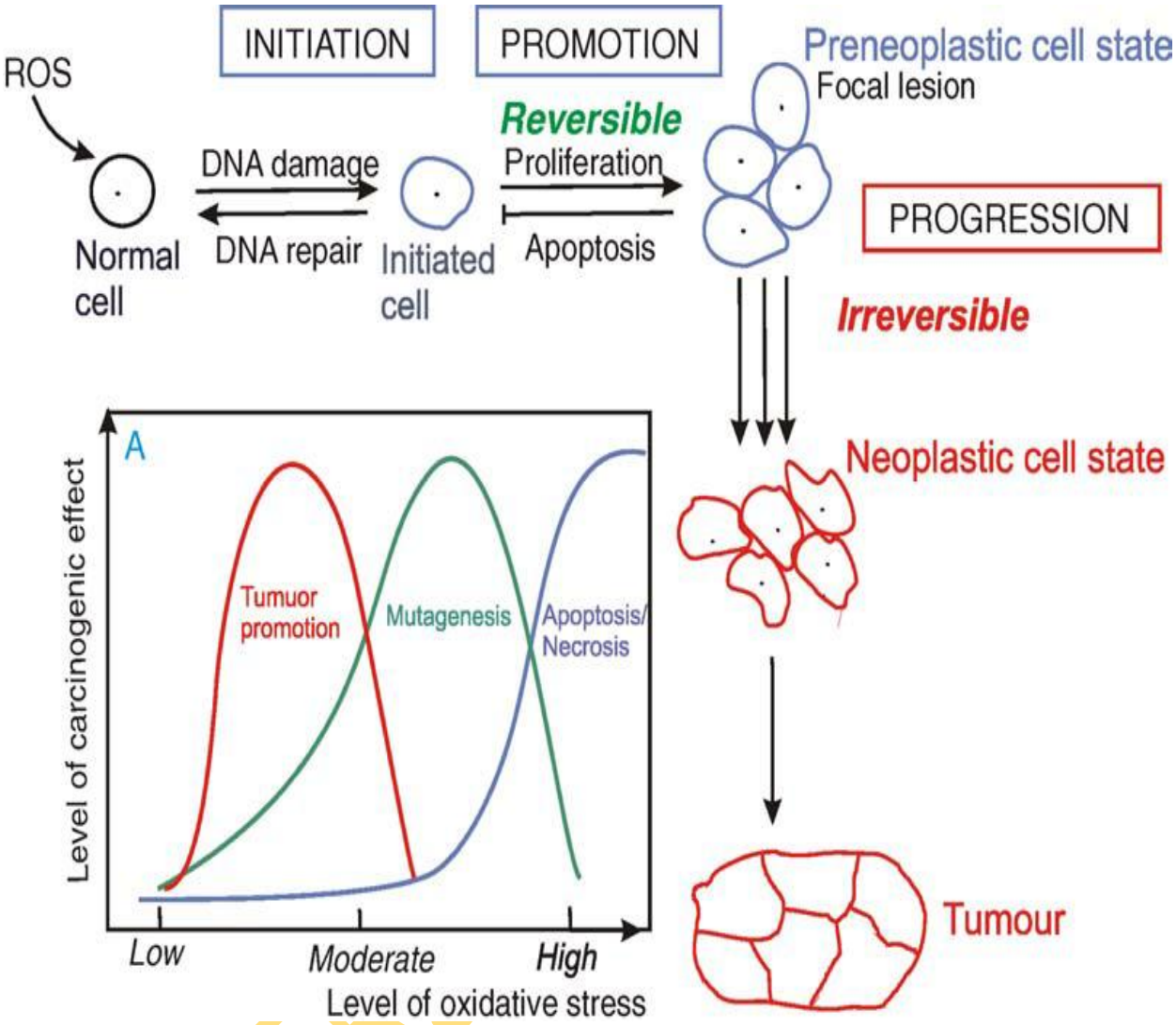

Figure. 2.1: Three stages model of carcinogenesis and the level of carcinogenic effect vs. level of free radicals at various stages of carcinogenic process (inset A) (Valko *et al.*, 2006).

.

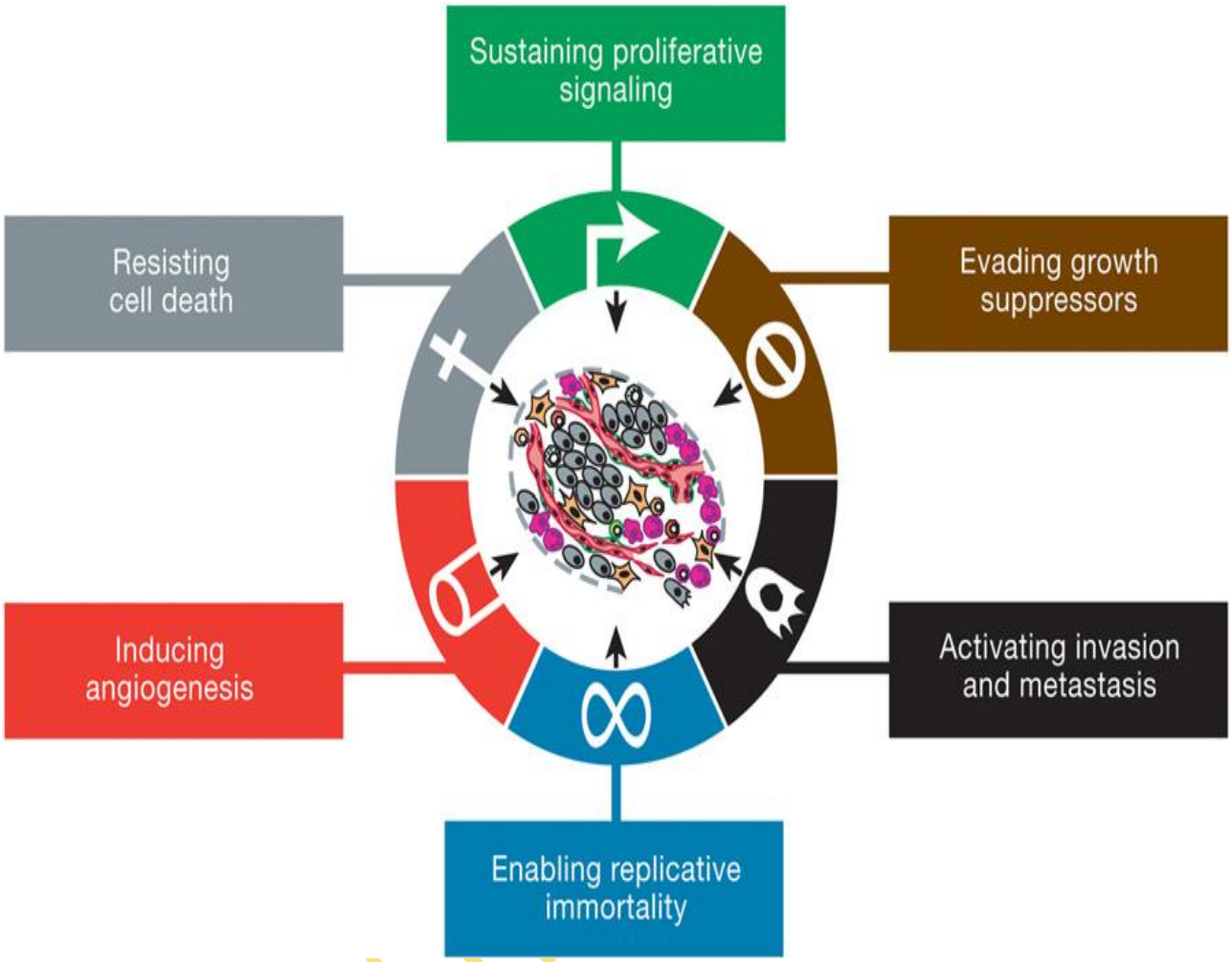

Figure 2.2: The Hallmarks of Cancer (Hanahan and Weinberg, 2011)

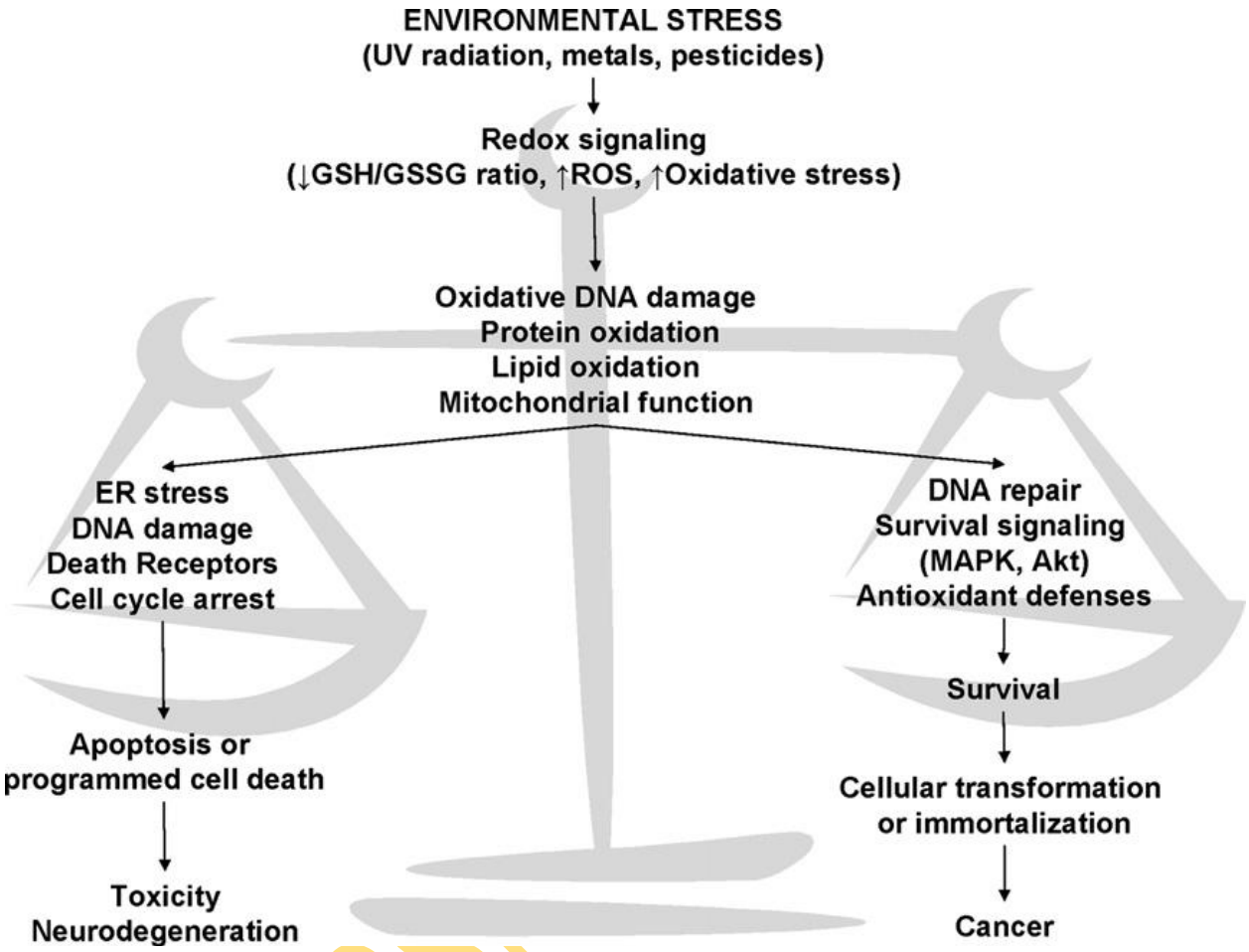

Figure 2.3: Environmentally induced cell death and transformation (Rodgrio *et al.*, 2009)

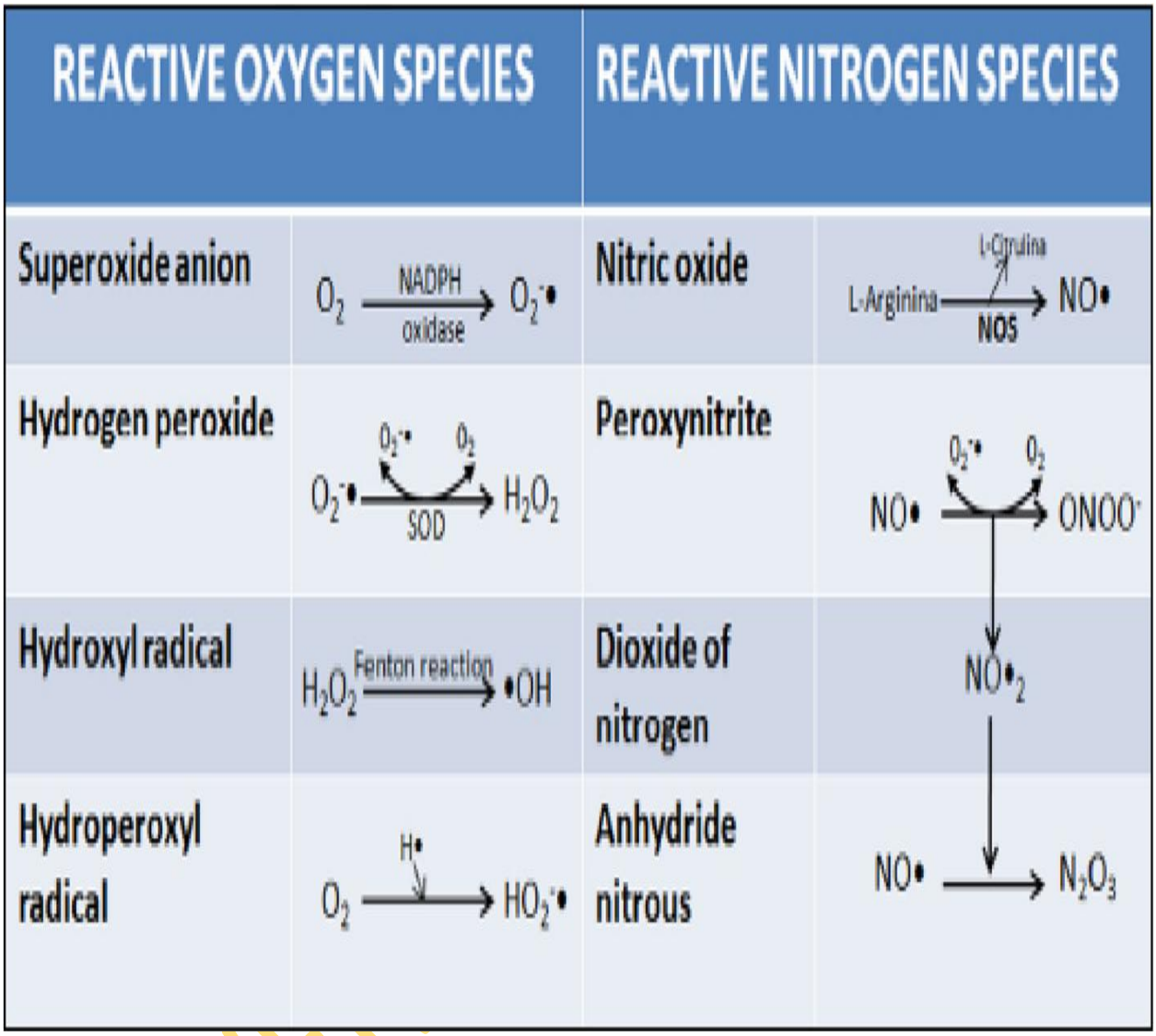

Figure 2.4: Some commonly encountered reactive oxygen and nitrogen reactive species (Ríos-Arrabal *et al.*, 2013)

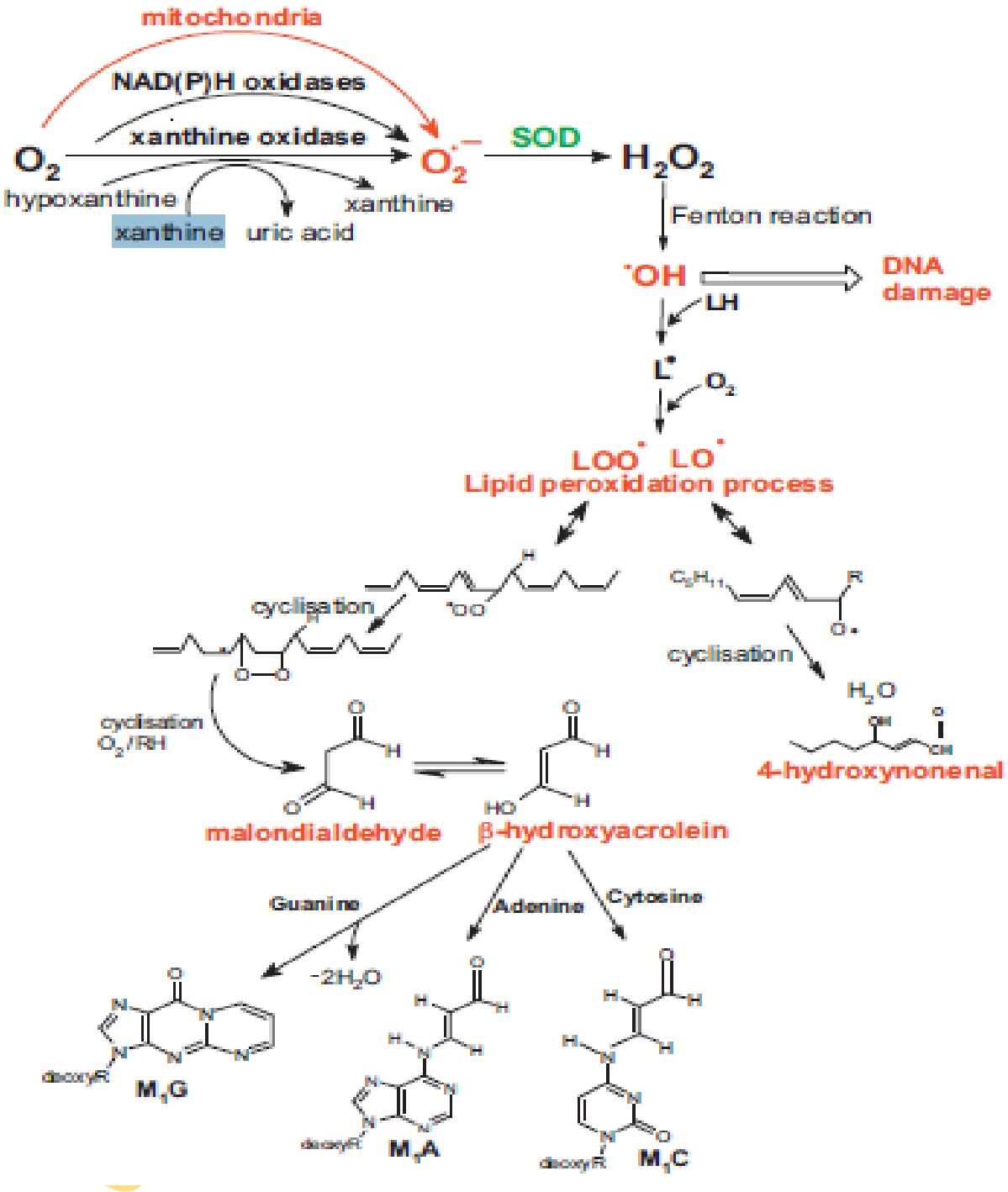

Figure 2.5: ROS formation and the lipid peroxidation process (Jomovaa and Valko, 2011).

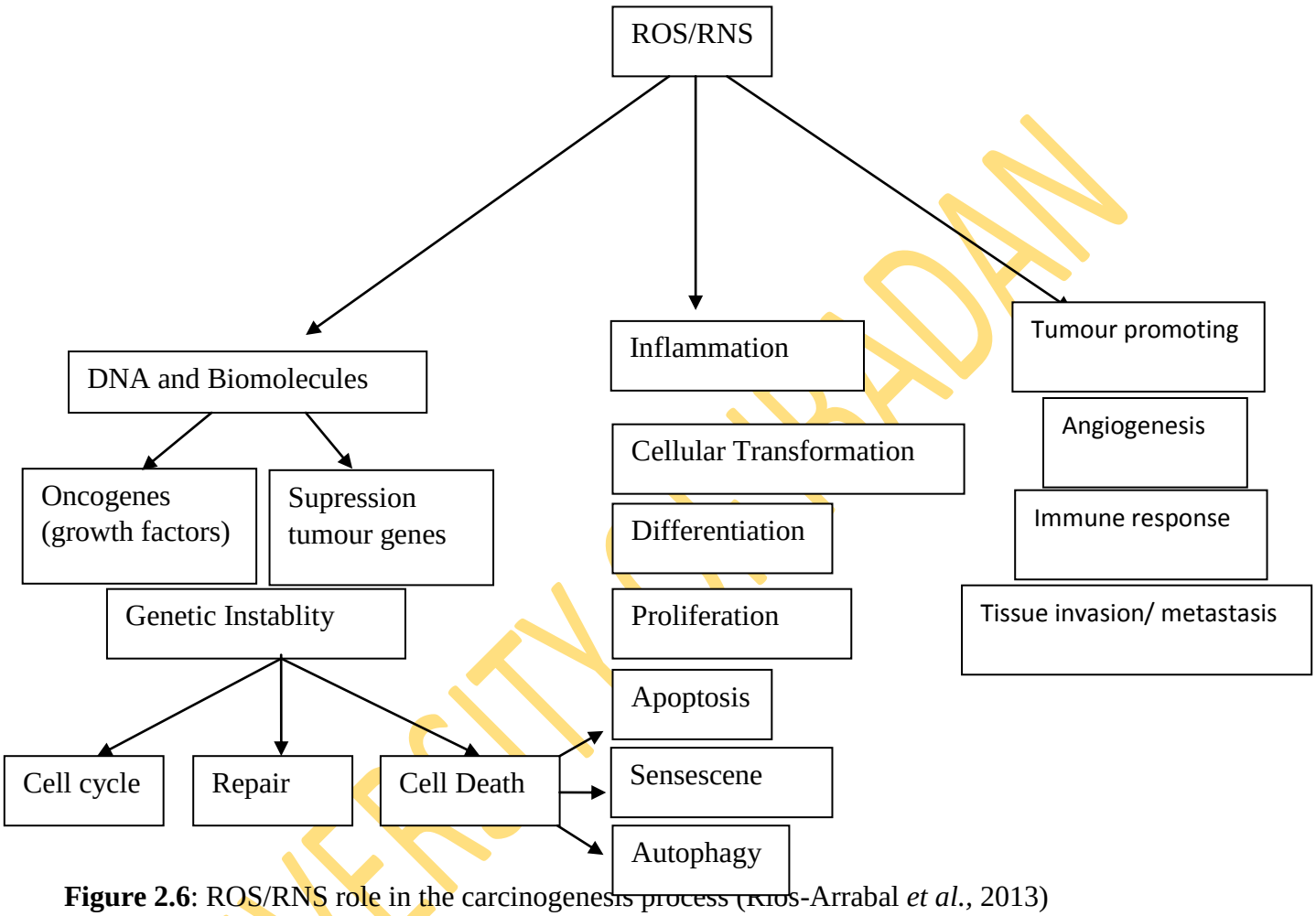

Figure 2.6: ROS/RNS role in the carcinogenesis process (Ríos-Arrabal *et al.*, 2013)

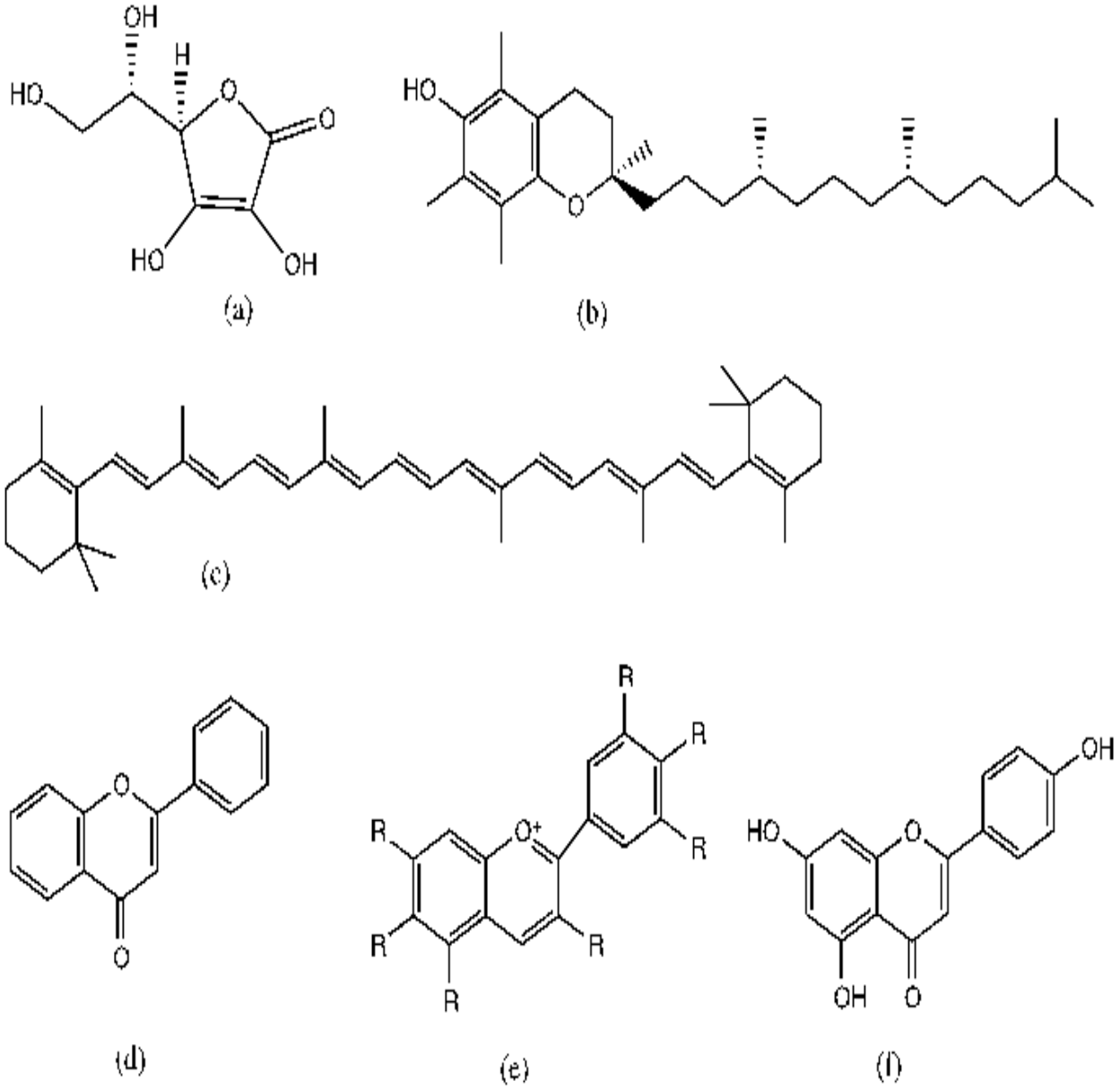

Figure 2.7: Chemical Structures of some antioxidants. (a) Ascorbic Acid, (b) VitaminE, (c) β- Carotene, (d) Flavonoid, (e) Anthocyanin, (f) Polyphenol.

Examples of enzymic antioxidant include peroxisomal catalase (CAT), superoxide dismutase (SOD), glutathione S-transferases (GST) and glutathione peroxidase (GPx). Many of the enzymatic and non enzymatic antioxidants are exploited as bio-markers of oxidative stress in the body.

2.41 BIOMARKERS OF OXIDATIVE STRESS

(A) Glutathione

Glutathione is also an important antioxidant compound responsible for maintaining intracellular redox homeostasis. This redox balance is altered under hypoxia conditions, as in the case of tumors, with the production of ROS and NO•. Glutathione exists in reduced (GSH) and oxidized (glutathione disulphide, GSSG) states. In its reduced state, it sequesters ROS, which is transformed and recycled by the action of the glutathione-reductase enzyme (GRd). The electron source used by this enzyme is coenzyme NADPH, which is mainly derived from the phosphate pentose pathway.

The main protective roles of glutathione against oxidative stress as summarized by Masella *et al.* (2005) are presented below:

(a) Glutathione is a cofactor of several detoxifying enzymes against oxidative stress, e.g. glutathione peroxidase (GPx), glutathionetransferase etc;

(b) GSH participates in amino acid transport through the plasma membrane;

(c) GSH scavenges hydroxyl radical and singlet oxygen directly, detoxifying hydrogen peroxide and lipid peroxides by the catalytic action of glutathione peroxidase;

(d) Glutathione is able to regenerate the most important antioxidants, Vitamins C and E, back to their active forms; glutathione can reduce the tocopherol radical of Vitamin E directly, or indirectly, *via* reduction of semidehydroascorbate

(B) SUPEROXIDE DISMUTASE (SOD)

Superoxide dismutases **(**SODs) are metal-containing proteins that catalyze the removal of superoxide, generating water peroxide as a final product of the dismutation. Three isoforms have been found in all eukaryotic cells, but their location differs inside the cell. The copper-zinc SOD isoform is present in the cytoplasm, nucleus, and plasma, while the manganese SOD isoform is primarily located in mitochondria (Limon-Pacheco and Gonsebatt, 2009). Iron SOD is found in

the stroma of chloroplast in addition to prokayotic organisms. SOD is nuclear encoded and SOD genes have been shown to be sensitive to environmental stresses presumably due to increased ROS formation. SOD destroys $O_2^{\bullet -}$ with remarkably high reaction rates, by successive oxidation and reduction of the transition metal ion at the active site in a "Ping-Pong" type mechanism (Mates *et. al.*,1999).

(C) CATALASE

The intracellular level of H_2O_2 is regulated by a wide range of enzymes, the most important being catalase and peroxidases. Catalase is a tetramer of four polypeptide chains, each over 500 amino acids long. It contains four porphyrin heme (iron) groups that allow the enzyme to react with the hydrogen peroxide. It is a common enzyme found in nearly all living organisms exposed to oxygen and it is usually located in the peroxisome (Alberts *et al*., 2002). It efficiently catalyzes the decomposition of hydrogen peroxide to water and oxygen (Valko *et al.,* 2006; Chelikani, 2004). Catalase has one of the highest turnover rates for all enzymes: one molecule of catalase can convert approximately 6 million molecules of hydrogen peroxide to water each minute and is a very important enzyme in protecting the cell from oxidative damage by reactive oxygen species (Valko *et al.*, 2006). Infact, decreased capacity of a variety of tumours for detoxifying hydrogen peroxide is linked to a decreased level of catalase (Valko *et al.*, 2006)

(D) **Glutathione Transferases**

The glutathione transferases (GSTs; also known as glutathione S-transferases) are major phase II detoxification enzymes found mainly in the cytosol. In addition to their role in catalyzing the conjugation of electrophilic substrates to glutathione (GSH), these enzymes also carry out a range of other functions. They have peroxidase and isomerase activities, they can inhibit the Jun N-terminal kinase and thus protecting cells against H_2O_2-induced cell death (Sheehan *et al*., 2001). They can bind non-catalytically to a wide range of endogenous and exogenous ligands. Cytosolic GSTs of mammals have been particularly well characterized, and were originally classified into Alpha, Mu, Pi and Theta classes on the basis of a combination of criteria such as

substrate/inhibitorspecificity, primary and tertiary structure similarities and immunological identity (Sheehan *et al*., 2001).

2.5 CELL DEATH

Cell death is a sequence event that culminates in cessation of biological activity of the cell. It is one of the most crucial events in the evolution of disease in any tissue or organ. It results from diverse causes, including ischemia infections, toxins, and immune reactions. Cell death is also a normal and essential process in embryogenesis, the development of organs, and the maintenance of homeostasis. Cell death plays a crucial role in many physiological processes and diseases. It is a process that is both complementary and antagonistic to cell division for the maintenance of tissue homeostasis (Dunai *et al*., 2011). Three major types of cell death have been described based on cell morphology: apoptosis, autophagic cell death, and necrosis / necroptosis (Chunlan, 2013).

2.6 APOPTOSIS

Apoptosis, also referred to as type I cell death. Apoptosis is characterized by distinct morphological characteristics and energy-dependent biochemical mechanisms. One of the early events during apoptosis is cell dehydration. Loss of intracellular water results in condensation of the cytoplasm followed by a change in cell shape and size. Cells that are originally round may become elongated and smaller. Another change, perhaps the most characteristic feature of apoptosis, is condensation of nuclear chromatin. The condensation starts at the nuclear periphery, and the condensed chromatin often takes on a concave shape resembling a half-moon, or sickle. The condensed chromatin has a uniform, smooth appearance, with no evidence of any texture normally seen in the nucleus. DNA in condensed (pycnotic) chromatin exhibits hyperchromasia, staining strongly with fluorescent or light absorbing dyes. The nuclear envelope disintegrates; lamin proteins undergo proteolytic degradation, followed by nuclear fragmentation (karyorrhexis). Many of the nuclear fragments stain uniformly with DNA dyes and are scattered throughout the cytoplasm. The nuclear fragments, together with constituents of the cytoplasm (including intact organelles), are then packaged and enveloped into apoptotic bodies. The

apoptotic bodies are then shed from the dying cell. Appearance of membrane blebs on the plasma membrane is another important characteristics feature of apoptosis.

Biochemical changes such as the activation of caspases and/or endonucleases are important characteristics in the process of typical apoptosis induction (Arends *et al.*, 1990; Patel *et al.*, 1996). Caspase-3 is a key apoptotic executioner caspases, being activated by proteolytic cleavage due to caspase-8 and caspase-9 (Annunziato *et al.*, 2003; Qu and Qing, 2004; Son *et al.*, 2006). Although internucleosomal fragmentation is a hallmark of apoptosis, recent studies have revealed that cellular DNA is not always fragmented into nucleosomal ladders in apoptotic cells, thus apparently depending on cell type (Oberhammer *et. al.*, 1993). Other features of apoptosis include mobilization of intracellular ionized calcium (McConkey *et al.*, 1989), activation of trans glutaminase which cross-links cytoplasmic proteins (Piacentini *et al.*,1995), loss of microtubules (Endersen *et al.*, 1995), loss of asymmetry of the phospholipids on the plasma membrane leading to exposure of phosphatidyl serine on the outer surface (Hale *et al.*, 1996 ; Evenson, *et al.*,1993), and other plasma membrane changes which precondition remnants of the apoptotic cell to become a target for phagocytic cells. The duration of apoptosis may vary, but generally is short, even shorter than the duration of mitosis (Darzynkiewicz *et al.*, 1997). Many of these changes appeared to be unique to apoptosis, and have become markers used to identify this mode of cell death biochemically, by microscopy or cytometry (Darzynkiewicz *et al.*, 1997).

Apoptosis plays a critical role in a number of physiological functions such as fetal development or tissue homeostasis regulation (Siegel, 2006). In addition to these physiological roles, considerable evidence suggests that changes in apoptosis play a major role in the development of various diseases. Indeed, in cancer, inhibition of apoptosis leads to anarchic division of cells and favors tumor development (Debunne *et al.*, 2011). In contrast, over activation of apoptosis contributes to the aggravation of various cardiovascular diseases such as atherosclerosis, myocardial, infarction, and heart failure (Fadeel and Orrenius, 2005).

Mitochondria play an important task in apoptosis induced both by caspase-dependent and -independent pathways. Bcl-2 and Bcl-xL are the major anti-apoptotic proteins integrated in mitochondrial membrane. These proteins prevent apoptosis through either hetero dimerization

with pro-apoptotic proteins, or their direct pore forming effects on the outer membrane of mitochondria (Gross *et al.*, 1999; Harris and Thompson, 2000; Nechushtan *et al.*, 2001). Many apoptogen induce apoptosis by reducing the cellular levels or activity of the antiapoptotic Bcl-2 family such as Bcl-2 and Bcl-xL

2.6.1. Mechanisms of Apoptosis

The mechanisms of apoptosis are highly complex and sophisticated, involving an energy-dependent cascade of molecular events (Fig 2.7). There are two main apoptotic pathways: the extrinsic or death receptor pathway and the intrinsic or mitochondrial pathway. Recent evidences show that the two pathways are linked and that molecules in one pathway can influence the other (Igney and Krammer, 2002). Additionally, T-cell mediated cytotoxicity and perforin-granzyme pathway can also activate the killing of cells (El More, 2007).

In the intrinsic pathway, which is more ancient, stimuli such as cellular damage or lack of essential factors cause mitochondrial outer membrane permeabilization (MOMP), a step that is controlled by the proapoptotic and antiapoptotic proteins of the Bcl-2 family. The critical molecules are Bax and Bak, which, following activation, assemble in the lipid pore, forming MOMP (Chipuk *et al.*, 2006; Youle and Strasser, 2009). Once the MOMP is functional, the released cytochrome c binds to the cytosolic protease-activating factor-1 (Apaf-1), forming the apoptosome, the caspase-9 activating complex, that recruits and activates the initiator caspase-9, whereas Smac/Diablo antagonizes the X-chromosome-linked inhibitor of apoptosis (XIAP) thereby ensuring propagation of apoptosis (Pop and Salvesen, 2009).

In the extrinsic apoptotic pathway, activation of the initiator caspases-8 and -10 is mediated by the extracellular ligands that bind to death receptors on the cell surface. The death receptors are transmembrane proteins belonging to the tumor necrosis factor (TNF) receptor superfamily. Ligand binding triggers a conformational change in the cytoplasmic domain of the receptor exposing the death domain (DD) that recruits the adaptor proteins via their own DD. In addition to the DD, some adaptor proteins contain a death effector domain (DED). The complex between the death receptor and the adaptor protein's DED is called the death-inducing signaling complex (DISC), which recruits the initiator caspase-8 to DISC, thereby enabling its activation (Oberst e*t*

al., 2010). The execution phase downstream of caspase-8 activation is cell-type specific. In type I cells, the amount of DISC-processed caspase-8 allows for the direct activation of sufficient amounts of the executioner caspases-3 and -7 to finalize apoptosis. However, in type II cells the DISC-mediated caspase- 8 activation is insufficient for efficient apoptosis triggering and caspase-8, rather than directly activating the executioner caspases activates Bid, thereby creating an amplification loop through recruitment of the mitochondrial pathway to help finishing up dysfunctional or superfluous cells.

The perforin/granzyme pathway can induce apoptosis via either granzyme B or granzyme A. The extrinsic, intrinsic, and granzyme B pathways converge on the same terminal, or execution pathway (Figure 2.8). This pathway is initiated by the cleavage of caspase-3 and results in DNA fragmentation, degradation of cytoskeletal and nuclear proteins, cross-linking of proteins, formation of apoptotic bodies, expression of ligands for phagocytic cell receptors and finally uptake by phagocytic cells. The granzyme A pathway activates a parallel, caspase-independent cell death pathway.

2.6.2. Apoptosis and Cancer.

The normal mechanisms of cell cycle regulation are dysfunctional in cancer cells. This is usually caused by over proliferation of cells and/or decreased removal of cells (King and Cidlowski, 1998). In fact, suppression of apoptosis during carcinogenesis is thought to play a central role in the development and progression of some cancers (Kerr *et al*., 1994). There are a variety of molecular mechanisms that tumor cells use to suppress apoptosis. Tumor cells can acquire resistance to apoptosis by the expression of anti-apoptotic proteins such as Bcl-2 or by the down-regulation or mutation of pro-apoptotic proteins such as Bax. The expression of both Bcl-2 and Bax is regulated by the *p53* tumor suppressor gene (Miyashita, 1994). Certain forms of human B cell lymphoma have over expression of Bcl-2, and this is one of the first and strongest lines of evidence that failure of cell death contributes to cancer (Vaux *et al*., 1988). Another method of apoptosis suppression in cancer involves evasion of immune surveillance (Smyth *et al*., 2001).

Certain immune cells (T cells and natural killer cells) normally destroy tumor cells via the perforin/granzyme B pathway or the death-receptor pathway. In order to evade immune

destruction, some tumor cells will diminish the response of the death receptor pathway to FasL produced by T cells. This has been shown to occur in a variety of ways including down regulation of the Fas receptor on tumor cells. Other mechanisms include expression of nonfunctioning Fas receptor, secretion of high levels of a soluble form of the Fas receptor that will sequester the Fas ligand or expression of Fas ligand on the surface of tumor cells (Cheng *et al*., 1994; Elnemr *et al.*, 2001). In fact, some tumor cells are capable of a Fas ligand-mediated "counterattack" that results in apoptotic depletion of activated tumor infiltrating lymphocytes (Koyama *et al.*, 2001).

The ataxia telangiectasia-mutated gene (ATM) has also been shown to be involved in tumorigenesis via the ATM/*p53* signaling pathway . The ATM gene encodes a protein kinase that acts as a tumor suppressor. ATM activation, via ionizing radiation damage DNA, stimulates DNA repair and blocks cell cycle progression. One mechanism through which this occurs is ATM dependent phosphorylation of *p53* (Kurz and Lees-Miller, 2004). p53 then signals growth arrest of the cell at a checkpoint to allow for DNA damage repair or can cause the cell to undergo apoptosis if the damage cannot be repaired. This system can also be inactivated by a number of mechanisms including somatic genetic/epigenetic alterations and expression of oncogenic viral proteins such as the HPV, leading to tumourigenesis. Other cell signaling pathways can also be involved in tumor development. For example, upregulation of the phosphatidylinositol 3-kinase/AKT pathway in tumor cells renders them independent of survival signals. In addition to regulation of apoptosis, this pathway regulates other cellular processes, such as proliferation, growth, and cytoskeletal rearrangement.

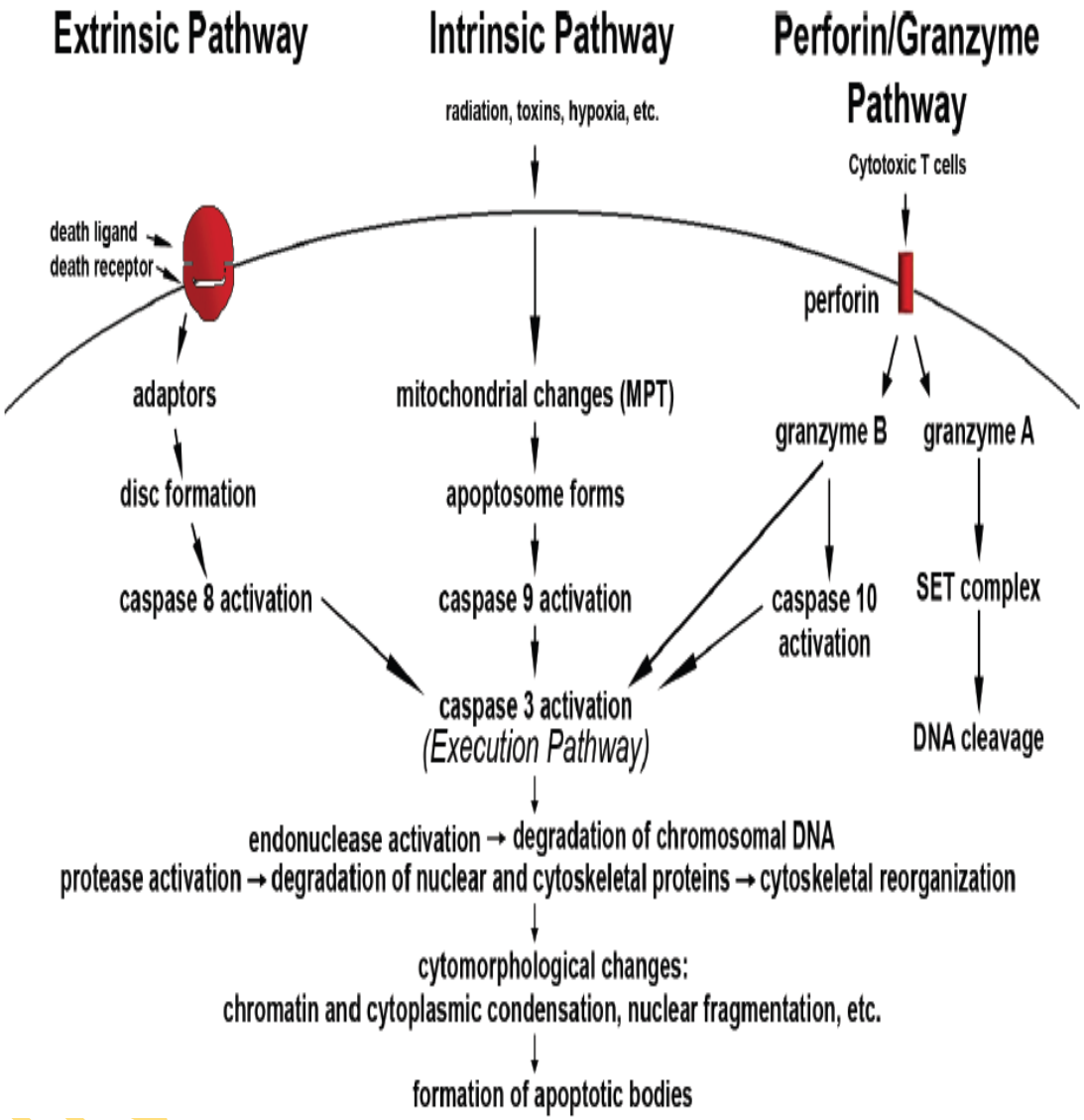

Figure 2.8: Schematic representation of apoptotic events. (El more, 2007)

Alterations of various cell signaling pathways can result in dysregulation of apoptosis and lead to cancer. The p53 tumor suppressor gene is a transcription factor that regulates the cell cycle and is the most widely mutated gene in human tumorigenesis (Wang and Harris, 1997). The critical role of *p53* is evident by the fact that it is mutated in over 50% of all human cancers. The *p53* gene can activate DNA repair proteins when DNA has sustained damage and hold the cell cycle at the G1/S regulation point on DNA damage recognition. It can also initiate apoptosis if the DNA damage proves to be irreparable. Tumourigenesis can occur if this system goes awry. If the *p53* gene is damaged, then tumor suppression is severely reduced. The p53 gene can be damaged by radiation, chemicals and viruses such as the Human papillomavirus (HPV). People who inherit only one functional copy of this gene will most likely develop Li–Fraumeni syndrome, which is characterized by the development of tumors in early adulthood.

2.6.3. Assays for Apoptosis

Complex signaling cascade and its multiple regulation points are exploited in the assessment of apoptosis. There are a large variety of assays available, but each assay has advantages and disadvantages which may make it acceptable to use for one application but inappropriate for another application (Watanabe *et al*., 2002; Otsuki *et al*., 2003). Therefore, when choosing methods of apoptosis detection in cells, tissues or organs, understanding the advantages and disadvantages of each assay is crucial.

Based on methodology, apoptosis assays, can be classified into six major groups:

(i) Cytomorphological alterations
(ii) DNA fragmentation
(iii) Detection of caspases, cleaved substrates, regulators and inhibitors
(iv) Membrane alterations
(v) Detection of apoptosis in whole mounts
(vi) Mitochondrial assays.

2.6.3.1 Cytomorphological Alterations

The evaluation of hematoxylin and eosin-stained tissue sections with light microscopy allows the visualization of apoptotic cells. Although a single apoptotic cell can be detected with this method, confirmation with other methods may be necessary. The morphological events of apoptosis are rapid and the fragments are quickly phagocytized. Considerable apoptosis may occur in some tissues before it is histologically apparent. Also, this method detects the later events of apoptosis, so cells in the early phase of apoptosis will not be detected. Semi-ultrathin sections from an epoxy-resin-embedded block can be stained with toluidine blue or methylene blue to reveal intensely stained apoptotic cells when evaluated by standard light microscopy. This methodology depends on the nuclear and cytoplasmic condensation that occurs during apoptosis. The tissue and cellular details are preserved with this technique and surveys of large tissue regions are distinct advantages. However, smaller apoptotic bodies will not be detected and healthy cells with large dense intracellular granules can be mistaken for apoptotic cells or debris. Additionally, there is loss of antigenicity during processing so that immunohistological or enzyme assays cannot be performed on the same tissue. However, this tissue may be used for transmission electron microscopy (TEM).

Transmission electron microscopy is considered the gold standard for confirmation of apoptosis. This is because categorization of an apoptotic cell is irrefutable if the cell contains certain ultrastructural morphological characteristics (White and Cinti, 2004). These characteristics are: (1) electron-dense nucleus (marginalization in the early phase); (2) nuclear fragmentation; (3) intact cell membrane even late in the cell disintegration phase; (4) disorganized cytoplasmic organelles; (5) large clear vacuoles; and (6) blebs at the cell surface. As apoptosis progresses, these cells will lose the cell-to-cell adhesions and will separate from neighboring cells. During the later phase of apoptosis, the cell will fragment into apoptotic bodies with intact cell membranes and will contain cytoplasmic organelles with or without nuclear fragments. Phagocytosis of apoptotic bodies can also be appreciated with TEM. The main disadvantages of TEM are the cost, time expenditure, and the ability to only assay a small region at a time. Other disadvantages include the difficulty in detecting apoptotic cells due to their transient nature and the inability to detect apoptotic cells at the early stage.

2.6.3.2 DNA Fragmentation

The DNA laddering technique is used to visualize the endonuclease cleavage products of apoptosis (Wyllie, 1980). It involves extraction of DNA from a lysed cell homogenate followed by agarose gel electrophoresis. These results in a characteristic "DNA ladder" with each band in the ladder separated in size by approximately 180 base pairs. This methodology is easy to perform, has a sensitivity of 1×10^6 cells (i.e., level of detection is as few as 1,000,000 cells), and is useful for tissues and cell cultures with high numbers of apoptotic cells per tissue mass or volume, respectively. However, it is not recommended in cases with low numbers of apoptotic cells. There are other disadvantages to this assay. DNA fragmentation occurs in the later phase of apoptosis. Therefore, the absence of a DNA ladder does not eliminate the potential that cells are undergoing early apoptosis. Additionally, DNA fragmentation can occur during preparation making it difficult to produce a nucleosome ladder. Furthermore, necrotic cells can also generate DNA fragments.

The TUNEL (Terminal dUTP Nick End-Labeling) method is used to assay the endonuclease cleavage products by enzymatically end-labeling the DNA strand breaks. Terminal transferase is used to add labeled UTP to the 3'-end of the DNA fragments. The dUTP can then be labeled with a variety of probes to allow detection by light microscopy, fluorescence microscopy or flow cytometry. The assays are available as kits and can be acquired from a variety of companies. This assay is also very sensitive, allowing detection of a single cell via fluorescence microscopy or as few as 100 cells via flow cytometry. It is also a fast technique and can be completed within 3 hours. The disadvantages are cost and the unknown parameter of how many DNA strand breaks are necessary for detection by this method. This method is also subject to false positives from necrotic cells and cells in the process of DNA repair and gene transcription. For these reasons, it should be paired with another assay.

2.6.3.3 Detection of Caspases, Cleaved Substrates, Regulators and Inhibitors

There are more than 13 known caspases (procaspases or active cysteine caspases) that can be detected using various types of caspase activity assays (Gurtu *et al*., 1997). There are also immunohistochemistry assays that can detect cleaved substrates such as PARP and known cell

modifications such as phosphorylated histones (Love *et al*., 1999; Talasz *et al*., 2002). Fluorescently conjugated caspase inhibitors can also be used to label active caspases within cells (Grabarek *et al*., 2002). Caspase activation can be detected in a variety of ways including western blot, immunoprecipitation and immunohistochemistry. Both polyclonal and monoclonal antibodies are available to both pro-caspases and active caspases.

One method of caspase detection requires cell lysis in order to release the enzymes into the solution, coating of microwells with anti-caspases; followed by detection with a fluorescent labelled substrate. Detection of caspase activity by this method usually requires 1×10^5 cells. This technique allows selection for individual initiator or execution caspases. It also allows for rapid and consistent quantification of apoptotic cells. The major disadvantage is that the integrity of the sample is destroyed thereby eliminating the possibility of localizing the apoptotic event within the tissue or determining the type of cell that is undergoing apoptosis. Another disadvantage is that caspase activation does not necessarily indicate that apoptosis will occur. Moreover, there is tremendous overlap in the substrate preferences of the members of the caspase family, affecting the specificity of the assay.

2.6.3.4 Apoptosis PCR microarray

Apoptosis PCR microarray is a relatively new methodology that uses real-time PCR to profile the expression of at least 112 genes involved in apoptosis (Hofmann *et al*., 2001; Vallat *et al*., 2003). These PCR microarrays are designed to determine the expression profile of genes that encode key ligands, receptors, intracellular modulators, and transcription factors involved in the regulation of programmed cell death. Genes involved in anti-apoptosis can also be assessed with this methodology. Comparison of gene expression in cells or tissues can be performed between test samples and controls. This type of assay allows for the evaluation of the expression of a focused panel of genes related to apoptosis and several companies offer apoptosis pathway-specific gene panels. Hierarchical cluster analysis of genes can reveal distinct temporal expression patterns of transcriptional activation and/or repression. However, interpretation of the results can be confounded by the large number of analyzed genes and by the methodological complexity. This methodology uses a 96-well plate and as little as 5 nanograms of total RNA.

Every mRNA, or transcript, is labeled with a marker, such as a fluorescent dye. A real-time PCR instrument is used for expression profiling. The location and intensity of the resulting signals give an estimate of the quantity of each transcript in the sample. The microarray test should be combined with a different methodology to confirm

2.6.3.5 Membrane Alterations

Externalization of phosphatidyl serine residues on the outer plasma membrane of apoptotic cells allows detection via Annexin V in tissues, embryos or cultured cells. Once the apoptotic cells are bound with FITC-labeled Annexin V, they can be visualized with fluorescent microscopy. The advantages are sensitivity (can detect a single apoptotic cell) and the ability to confirm the activity of initiator caspases. The disadvantage is that the membranes of necrotic cells are labeled as well. Therefore a critical control is to demonstrate the membrane integrity of the phosphatidylserine-positive cells. Since loss of membrane integrity is a pathological feature of necrotic cell death. Necrotic cells will stain with specific membrane-impermeant nucleic acid dyes such as propidium iodide and trypan blue. Likewise, the membrane integrity of apoptotic cells can be demonstrated by the exclusion of these dyes. The transfer of phosphatidylserine to the outside of the cell membrane will also permit the transport of certain dyes into the cell in a unidirectional manner. As the cell accumulates dye and shrinks in volume, the cell dye content becomes more concentrated and can be visualized with light microscopy. This dye-uptake bioassay works on cell cultures, does not label necrotic cells, and has a high level of sensitivity (can detect a single apoptotic cell).

2.6.3.6 Detection of Apoptosis in Whole Mounts

Apoptosis can also be visualized in whole mounts of embryos or tissues using dyes such as acridine orange (AO), Nile blue sulfate (NBS), and neutral red (NR) (Zucker *et al*., 2000). Since these dyes are acidophilic, they are concentrated in areas of high lysosomal and phagocytotic activity. The results would need to be validated with other apoptosis assays because these dyes cannot distinguish between lysosomes degrading apoptotic debris from degradation of other debris such as microorganisms. Although all of these dyes are fast and inexpensive, they have certain disadvantages. AO is toxic and mutagenic and quenches rapidly under standard conditions whereas NBS and NR do not penetrate thick tissues and can be lost during preparation

for sectioning. Lyso- Tracker Red is another dye that acts in a similar way; however this dye can be used with laser confocal microscopy to provide 3-dimensional imaging of apoptotic cells. This dye is stable during processing, penetrates thick tissues and is resistant to quenching. This dye can be used for cell culture as well as whole mounts of embryos, tissues, or organs.

2.6.3.7. Mitochondrial Assays

Mitochondrial assays and cytochrome *c* release allow the detection of changes in the early phase of the intrinsic pathway. Laser Scanning Confocal Microscopy (LSCM) creates submicron thin optical slices through living cells that can be used to monitor several mitochondrial events in intact single cells over time (Darzynkiewicz *et al*., 1999). Mitochondrial permeability transition (MPT), depolarization of the inner mitochondrial membrane, Ca^{2+} fluxes, mitochondrial redox status, and reactive oxygen species can all be monitored with this methodology. The main disadvantage is that the mitochondrial parameters that this methodology monitors can also occur during necrosis. The electrochemical gradient across the mitochondrial outer membrane (MOM) collapses during apoptosis, allowing detection with a fluorescent cationic dye. In healthy cells this lipophilic dye accumulates in the mitochondria, forming aggregates that emit a specific fluorescence. In apoptotic cells the MOM does not maintain the electrochemical gradient and the cationic dye diffuses into the cytoplasm where it emits a fluorescence that is different from the aggregated form. Other mitochondrial dyes can be used that measure the redox potential or metabolic activity of the mitochondria in cells. However, these dyes do not address the mechanism of cell death and should be used in conjunction with other apoptosis detection methods such as a caspase assay. Cytochrome *c* release from the mitochondria can also be assayed using fluorescence and electron microscopy in living or fixed cells (Scorrano *et al*., 2002). However, cytochrome *c* becomes unstable once it is released into the cytoplasm (Goldstein *et al*., 2000). Therefore a non-apoptotic control should be used to ensure that the staining conditions used are able to detect any available cytochrome *c*. Apoptotic or anti-apoptotic regulator proteins such as Bax, Bid, and Bcl-2 can also be detected using fluorescence and confocal microscopy (Tsien, 1998; Zhang *et al*., 2002). However, the fluorescent protein tag may alter the interaction of the native protein with other proteins. Therefore, other apoptosis assays should be used to confirm the results.

2.7 NECROSIS

Necrosis, also referred to as type III cell death is characterized by an increase in cell volume, the swelling of organelles and the rupture of the plasma membrane and is largely considered an accidental type of cell death (Kroemer and Levine, 2008). During necrosis, the mitochondria swell with apparently intact nuclei, and no DNA fragmentation. Necrosis is an uncontrolled and passive process that usually affects large fields of cells whereas apoptosis is controlled and energy-dependent and can affect individual or clusters of cells. However, Necroptosis, a regulated necrotic cell death triggered by broad caspase inhibition in the presence of death receptor ligands and is characterized by necrotic cell death morphology and the activation of autophagy (Degterev *et al*., 2005).

Necrotic cell injury is mediated by two main mechanisms; interference with the energy supply of the cell and direct damage to cell membranes. Some of the major morphological changes that occur with necrosis include cell swelling; formation of cytoplasmic vacuoles; distended endoplasmic reticulum; formation of cytoplasmic blebs; condensed, swollen or ruptured mitochondria; disaggregation and detachment of ribosomes; disrupted organelle membranes; swollen and ruptured lysosomes; and eventually disruption of the cell membrane (Kerr *et al*., 1972; Majno and Joris, 1995). This loss of cell membrane integrity results in the release of the cytoplasmic contents into the surrounding tissue, sending chemotatic signals with eventual recruitment of inflammatory cells. Apoptotic cells do not release their cellular constituents into the surrounding interstitial tissue and are quickly phagocytosed by macrophages or adjacent normal cells, there is essentially no inflammatory reaction (Savill and Fadok, 2000; Kurosaka *et al*., 2003). It is also important to note that pyknosis and karyorrhexis are not exclusive to apoptosis and can be a part of the spectrum of cytomorphological changes that occurs with necrosis (Cotran *et al*., 1999). Some of the major morphological features of apoptosis and necrosis are presented in table 2.1 and shown in Figure 2.9.

2.8 Autophagy

Autophagic cell death also referred to as type II cell death. Autophagy (also called autophagocytosis) is evolutionary conserved intracellular system that enables cells to degrade and recycle cellular components (Mihalache, 2012). The word autophagy derives from Greek and means to eat oneself. It is also referred to as type II cell death, is a degradative lysosomal

pathway that is characterized by the accumulation of cytoplasmic material in the vacuoles for bulk degradation by lysosomal enzymes. Distinctive feature of type II PCD (or autophagic cell death) is the presence of autophagosomes and autophagolysosomes (Barth *et. al.*, 2011; Ogier-Denis and Codogno, 2003; Edinger and Thompson, 2004), which are the executors of self-degradation. Autophagosomes are spherical structures consisting of double bilayered membranes with diameters of about 500 nm (Noda, 2009). Other morphology features associated with autophagy are marked modifications of the mitochondrial structure such as condensation of the mitochondrial matrix, dilatation of the intercristal spaces and budding of the outer mitochondrial membranes (a morphologic sign of mitochondrial fission), which may be critical for the segregation of dysfunctional mitochondria and their subsequent autophagic removal. Other authophagy related ultra structural modifications includes: dilatation of the rough endoplasmic reticulum and golgi complex, presence of cytoplasmic lipid droplets and peripheral chromatin condensation.

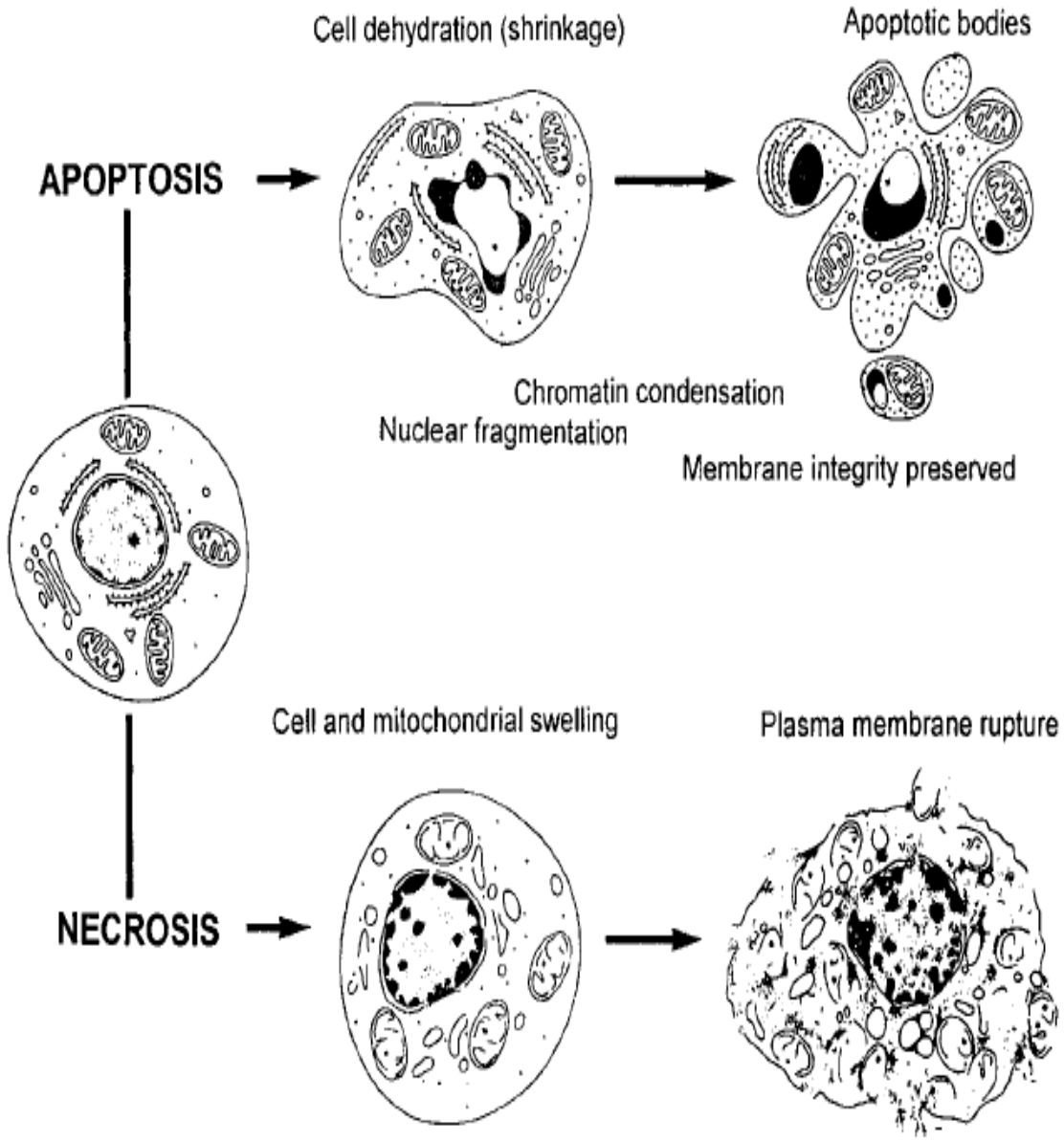

Figure 2.9: Some common morphologic features of apoptosis and necrosis (Darzynkiewicz *et al*, 1997)

Table 2.1: Comparison of morphological features of apoptosis and necrosis

Apoptosis	Necrosis
Single cells or small cluster of cells	Often contiguous cells
Cell shrinkage and convolution	Cell swelling
Pyknosis and Karyorrhexis	Karyolysis, pyknosis and karyorrhexis
Intact cell membrane	Disrupted cell membrane
Cytoplasm retained in apoptotic bodies	Cytoplasm released
No inflammation	Inflammation usually present

The phenomenon of autophagy occurs in a wide range of eukaryotic organisms from yeast to mammals during starvation, cell and tissue development, and cell death (Levine and Klionsky, 2004). Autophagy is critical to the process of embryo development because some animal models have shown that the lack of autophagy leads to arrest, delays or defects in development (Adastra *et al.*, 2011). The physiological role of autophagy enables cellular homeostasis by removing damaged or surplus organelles in order to ensure survival (Yang *et al*., 2008). In addition, amino acids and fatty acids that are produced from the degradation of component of the cells in autolysosomes can be used for protein synthesis or be oxidized by the mitochondrial electron transport chain to produce ATP for cell survival under starvation conditions (Levine and Yuan, 2005). Paradoxically, autophagy can also lead to cell death by depleting the cell's organelles and critical proteins (Zhang *et al.*, 2011). It also plays a role in cells of the immune system. In addition, autophagy represents an adaptive response to cellular and environmental stress, such as nutrient deprivation or growth factor withdrawal (Park *et al.*, 2013; Moreau *et al.*, 2010). Other stress factors such as pathogens, chemicals, radiation, hypoxia, and ROS might induce autophagy.

Dysregulation of autophagy has been implicated in a wide range of disease processes, including aging-related disorders, infection and immunity, inflammation, cancer and cardiomyopathy (Levine and Kroemer, 2008; Chiarelli *et al.*, 2012). Recent studies have linked autophagy with neurodegenerative disease such as Alzheimer's and Huntington's disease (Chiarelli *et al.*, 2012). The molecular mechanisms of autophagosome formation are conserved in evolution and involve several autophagy related genes. One of these genes is atg5, whose product, autophagy related gene 5 (ATG5) conjugates with ATG12, to generate an E3 ubiquitin ligase-like enzyme required for autophagy (Geng *et a*l., 2008). Mice deficient in the atg5 gene die on the first day after birth (Kuma *et al.*, 2004). In addition to the ATG5–ATG12 conjugate, the ATG8 (LC3) conjugation system is also essential for autophagosome formation (Geng *et a*l., 2008; Tacham and Simon, 2010). Once formed, autophagosomes then merge with lysosomes to form autolysosomes whose contents are degraded by lysosomal hydrolases (Geng *et a*l., 2008).

2.8.1 Types of Autophagy

In mammalian cells, three types of autophagy are recognised depending on the way of delivery of material subjected to degradation to lysosomes, and include macroautophagy, microautophagy and chaperone-mediated autophagy (Klionsky and Emr, 2000; Cuervo, 2004). Macroautophagy plays a major role in intracellular degradation and is often used as a synonym for autophagy (Yoshimori, 2004). During macroautophagy, portions of cytoplasm, and even entire organelles, are sequestered in a double-membrane organelle called autophagosome. Such organelles are subjected to a number of subsequent changes including membrane transformation, acidification, and, finally, fusion with lysosomes or late endosomes, resulting in the formation of autophagolysosomes or amphisomes, respectively. Although macroautophagy is generally considered a non-selective process, there have been reports of selective autophagy of peroxisomes and mitochondria (Yokota, 1993). The origin and nature of the autophagic sequestering membrane (phagophore) is not well understood. However, it has been proposed that phagophore formation occur either by de novo synthesis, or by utilisation of pre-existing cytoplasmic membranes.

The process when lysosomes sequester cytoplasmic components in invaginations of lysosomal membranes is termed microautophagy (Dice, 2000). Digestion of the internalised material occurs after disappearance of the vesicle membrane. Microautophagy accounts for the degradation of peroxisomes and some cytosolic proteins.

Chaperone-mediated autophagy is a selective pathway responsible for degradation of certain cytosolic proteins after their direct transport through the lysosomal membrane by means of molecular chaperones (Dice, 2000; Cuervo, 2004). Proteins selected for this type of autophagy, contain a specific amino acid sequence (KFERQ: lysinephenylalanine- glutamate-arginine-glutamine), which is recognised by a heatshock type chaperone protein, and is transported to the lysosomal-associated membrane protein type 2a (LAMP-2a) for translocation into the lysosomal lumen (Cuervo, 2004).

2.8.2 Regulation of Autophagy

The exact mechanism of regulating autophagy-induced is unclear. However, a number of agents and conditions have been reported to regulate autophagy. Nutrient deprivation is a potent inducer

of autophagy, while amino acids, being the final product of autophagic degradation of proteins, act as negative feedback regulators (Blommaart *et al*., 1997). An important part of nutrient dependent regulation pathway is the serine/threonine kinase mammalian TOR (target of rapamycin). Inhibition of MTOR by rapamycin induces autophagy even in presence of amino acids (Blommaart *et al*., 1997). Although the exact mechanism of amino acid regulation of MTOR activity is not yet understood, it has been shown that activation of MTOR by nutrients induces phosphorylation of proteins involved in the initial step of autophagy, resulting in their disassembling and inhibition of autophagy (Levine and Klionsky, 2004; Meijer and Codogno, 2004). MTOR has also been found to be sensitive to depletion of ATP (Dennis *et al*., 2001).

In addition to nutrients, autophagy is also regulated by some hormones especially insulin and glucagon. Activation of the insulin receptor induces activity of class I phosphatidylinositol-3-kinase (PI3K), with consequent activation of a cascade of intermediate enzymes, finally resulting in upregulation of MTOR and inhibition of autophagy (Levine and Klionsky, 2004). A MTOR independent insulin receptor associated pathway has also be been described (Saeki *et al.*, 2003). Activation of the pathway also results in inhibition of autophagy. Glucagon, on the other hand, activates autophagy by inhibiting MTOR via a protein kinase A-related mechanism (Kimball *et al.*, 2004).

Autophagosome formation is controlled mainly by class III phosphatidylinositol 3-kinase (PI3K) and Atg6, and elongation of the autophagosomal membrane is mediated by two ubiquitin-like conjugation systems: the conjugation of Atg12 to Atg5, which is localized together with Atg16 to the phagophore and, downstream of it, the Atg8 conjugation to phosphor ethanolamine (PE), which decorates both the phagophore and the autophagosomal membrane (Fujita *et al.*, 2008; Hanada *et al*., 2007). Atg8–PE undergoes deconjugation by the Atg4 protease, a step regulated by ROS that allows recycling of this protein (Scherz-Shouval *et al.*, 2008). Atg4 also is responsible for the priming of Atg8 by cleaving its C terminus, which exposes a glycine residue (Kirisako *et al.*, 2000).

Although a number of additional proteins, such as heterotrimeric G proteins, Ras, protein kinases A and B were reported to regulate autophagy, their role and mechanisms of action are not yet well understood (Levine and Klionsky, 2004; Meijer and Codogno, 2004).

2.8.2 Autopagy and Oxidative Stress

It is generally accepted that ROS induce autophagy (Xu, *et al.*, 2006*;* Matsui *et al.*, 2007), and that autophagy, in turn, serves to reduce oxidative damage (Marino, 2004; Scherz-Shouval *et al.*, 2007; Pelicano *et al.*, 2004). Many cellular stresses can cause induction of autophagy such as endoplasmic reticulum stress or mitochondrial dysfunction (Marin˜o, 2004; Matsui *et al.*, 2007) Oxidative stress has been shown to induce autophagy under starvation and ischemia/reperfusion conditions (Matsui *et al.*, 2007; Scherz-Shouval *et al.*, 2007) Under oxidative stress, reactive oxygen species (ROS) including free radicals such as superoxide ($O_2^{\cdot}$), hydroxyl radical ($HO^{\cdot}$) and hydrogen peroxide (H_2O_2) are generated at high levels inducing cellular damage and cell death (Pelicano *et al.*, 2004). This cell death often involves induction of apoptosis through caspase activation. Blockage of caspase activation causes degradation of catalase and increased ROS generation leading to cell death. The degradation of catalase is mediated by autophagy indicating a role for autophagy in caspase-independent cell death (Yu *et al.*, 2006). Furthermore, ROS contribute to caspase-independent cell death in macrophages (Shouval *et al.*, 2007). Under starvation conditions, ROS production is increased and is required for induction of autophagy (Scherz-Shouval *et al.*, 2007). The mechanism involved in oxidative stress induced autophagy-related cell death is unknown.

2.8.4 Detection of Autophagy

2.8.4.1. Transmission Electron Microscopy

Autophagy was first described by transmission electron microscopy (TEM) about half century ago (Glick *et al.*, 2010; Ashford, 1962). Till date, TEM remains one of the most widely used and sensitive techniques to detect the presence of autophagic vesicles (Eskelinen, 2008; Klionsky *et al.*, 2008). TEM has recently been used to great effect in combination with tomographical approaches to identify regions of the endoplasmic reticulum as the likely origin of autophagosomes in mammalian cells (Hayashi-Nishino, 2009; Yla-Anttila *et al.*, 2009). TEM characterizes autophagy qualitatively, as early autophagic compartments (autophagosomes) containing morphologically intact cytosol or organelles, or as late, degradative autophagic structures (autolysosomes) containing partially degraded cytoplasmic as well as organelle material. The major limitation of TEM in analyzing autophagy is that it is not objectively quantitative. Thus, while TEM remains an important qualitative approach to monitor steady state

levels of autophagy and to gain structural insight to the unique inter-relationship between phagophore membranes and other organelles, additional techniques are needed in conjunction with TEM to quantify steady-state levels of autophagy and autophagic flux.

2.8.4.2. Monitoring Autophagy by Fluorescence microscopy

In addition to electron microscopy, earlier studies of autophagy relied heavily on cell staining and fluorescent microscopy. In particular, the over-expression of GFP–LC3, in which GFP (green fluorescent protein) is expressed as a fusion protein at the amino terminus of LC3, was widely used to measure autophagy (Kadowaki and Karim, 2009). These studies were limited, however, by several issues: (a) counting GFP-positive punctate structures in order to quantify relative levels of autophagy is a laborious and arguably subjective task, despite the use of computer software; (b) overexpressed GFP–LC3 can be incorporated into protein aggregates independent of autophagy; (c) transfection procedures used to introduce exogenous GFP–LC3 has been shown to induce autophagy; (d) GFP–LC3 is sensitive to acid pH and ceases to fluoresce once autophagosomes fuse with the lysosome, resulting in the inability to look at end-stages of autophagy (Kuma *et al.*, 2007; Kimura *et al.*, 2007).

2.8.5 Autophagy and Tumor Cell Survival

The predominant role of autophagy in cancer cells is to confer stress tolerance, which serves to maintain tumor cell survival (Degenhardt *et al.*, 2006). Knockdown of essential autophagy genes in tumor cells has been shown to confer or potentiate the induction of cell death (White and DiPaola, 2009). Cancer cells have high metabolic demands due to increased cellular proliferation, and *in vivo* models, exposure to metabolic stress was shown to impair survival in autophagy-deficient cells compared with autophagy- proficient cells (Mathew *et al.*, 2009). Basal levels of autophagy were increased in human pancreatic cancer cell lines and tumor specimens, and they were shown to enable tumor cell growth by maintaining cellular energy production (Yang *et al*., 2011).

Cancer cells that survive chemotherapy and/or radiation activate autophagy to enable a state of dormancy in residual cancer cells that may contribute to tumor recurrence and progression (Lu *et al.*, 2008). Inhibition of autophagy in tumor cells has been shown to enhance the efficacy of

anticancer drugs supporting its role in cytoprotection. Recent report indicate that human cancer cell lines bearing activating mutations in H-ras or K-ras have high basal levels of autophagy even in the presence of abundant nutrients (Guo *et al.*,2011). Suppression of essential autophagy proteins was shown to inhibit cell growth in those cells. Indicating that autophagy maintains tumor cell survival and suggesting that blocking autophagy in tumors that are addicted to autophagy, such as Ras-driven cancers, may be an effective treatment approach.

2.9 HEXAVALENT CHROMATE

Chromium was discovered in 1797 as part of the mineral crocoite, used as pigment due to its intense coloration. It derived its name from the Greek word "χρώμα" (chroma- color) (Santos and Rodriguez, 2012). Chromium is the 21st most abundant element in Earth's crust with an average concentration of 100 ppm, ranging in soil between 1 mg/kg and 3000 mg/kg; in sea water from 5 µg/L to 800 µg/L and in rivers and lakes between 26 µg/L and 5.2 mg/L (Santos and Rodriguez, 2012). Normally, Cr is mined from chromate but native deposits are not unheard off. One of the most interesting characteristics of this metal is its hardness and high resistance to corrosion and discoloration. The importance of these proprieties resulted among others in the usage of this metal in the development of stainless steel, which together with chrome plating and leather tanning, are the most important applications of this element (Santos and Rodriguez , 2012).. These industries are also the main sources of Cr pollution in the environment. Chromium is highly soluble under oxidizing conditions and forms, exhibiting a wide range of possible oxidation states (from -2 to +6), The trivalent [Cr (III)] and hexavalent [Cr(VI)] are the most stable forms. Naturally occurring chromium is usually present as Cr(III), while hexavalent chromium in the environment is almost entirely derived from human activities. Hexavalent chromium is especially of great interest not only because of its toxic effects on industrial workers, but the high risk of exposure to hexavalent chromium that still exists for the general public.

2.9.1 Physicochemical properties of chromium and its principal ions

Chromium (atomic number 24, relative atomic mass 51.996) occurs in each of the oxidation states from -2 to +6, but only the 0 (elemental metal form), +2, +3 and +6 states are common. Divalent chromium (+2) is unstable in most compounds as it is easily oxidized to the trivalent form by air. Only the trivalent Cr(III) and hexavalent Cr(VI) forms are more common and important for human health (Skovbjerg *et al*., 2006).

The relationship between the hexavalent and trivalent states of chromium is described by the equation:

$Cr_2O_7^{2-} + 14H^+ + 6e^- \Longrightarrow 2Cr^{3+} + 7H2O + 1{:}33\ eV$

Considering the high electric potential of conversion of Cr^{6+} to Cr^{3+}, Cr^{3+} rarely occur in biological systems. However, reduction of Cr (VI) occurs spontaneously in the organism unless present in an insoluble form. For instance, in blood, Cr(VI) is rapidly reduced to Cr (III). Thus, once Cr (VI) has penetrated the membrane of the red blood cell it is reduced to Cr (III). Cr (III) becomes bound to cellular constituents making it unable to leave the erythrocyte. Chromium (VI) exists in solution as ionic species which are dependent on pH. At basic and neutral pH, Cr (VI) is largely in chromate form. The dichromates species becomes dominat at lower pH. Some physicochemical properties of some selected hexavalent chromate compounds are summarized in Table 2.2. Both chromate and dichromate have tetrahedral arrangements of coordinated oxygen groups (Figure 2.10). Hexavalent chromate is a potent oxidant at highly acidic pH and any organic molecule with oxidizable groups can promote its reduction to Cr (III). Increasing pH enhances the stability of Cr (VI), particularly at near neutral and alkaline pH. The strong pH effect on Cr(VI) reduction is demonstrated by the findings that human gastric juice was capable of reducing approximately 70% of Cr(VI) after a 30-min incubation at pH 1.4 but was completely ineffective at pH 7.0 (Donaldson *et al*., 1996). The presence of Fe^{2+} is important for abiotic reduction of Cr (VI) under anaerobic conditions in soil and underground water. Uptake and reduction by microorganisms is another detoxification process for Cr (VI), although it is limited by the ability of resistant bacteria striving in contaminated water to rapidly extrude Cr(VI) (Branco *et al*., 2008).

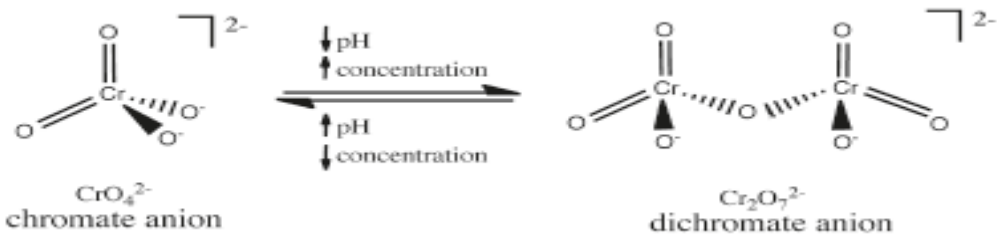

Figure 2.10: Structure of chromate and dichromate.

2.9.2 Uses of Chromium Compounds

The resistance of chromium to ordinary corrosive agents at room temperature makes it useful in electroplating and protective coating. It is also used in non-ferrous and ferrous alloys. Ferrous alloys, mainly stainless steels, account for most of the consumption (Shadreck and Mugadza, 2013). These steels have a wide range of mechanical properties as well as being corrosion and oxidation resistant (Bielicka *et al.*, 2005). In addition, chromium and its compounds are very useful in everyday life, as presented in Table 2.2. It is used on a large scale in many different industries, including metallurgical, electroplating, production of paints and pigments, tanning, wood preservation, chromium chemicals production, and pulp and paper production (Zayed and Terry, 2003).

2.9.3 Contamination of the Environment by Hexavalent Chromate

Industrial activities associated with the direct release of Cr (VI) into the soil and water is the most important source of Cr (VI) contamination in the atmosphere. Pollution with various forms of Cr results from its numerous uses in the chemical industry, production of dyes, wood preservation, leather tanning, chrome plating, manufacturing of various alloys, and many other applications and products (IARC,1990; ASTDR,2000). Incineration and emissions from cars create ambient pollution with Cr (VI)- and Cr(III)-containing particles, which leads to low-level inhalation exposures by large segments of the general population and increases Cr levels in surface waters (Zhitkovich, 2011). Chromate can travel over significant distances if introduced into a water source. The permissible level of chromium was lowered to 0.1 ppm due to the emergence of new information about amounts of chromium being released into the environment (Clifford and Chau, 1998). Between the years 1987 and 1993, there were 2,876,055 pounds of chromium released into bodies of water in the United States and 196,880,624 pounds released on land.

The contamination stems from the mining, smelting, and wood treatment industries. Again, in 2006, the standard was further lowered from 52 to 5 µg/m3 of air as an 8 hour time-weighted average for hexavalent chromium. Some of the chromate may be reduced to Cr (III), but the portion that remains in the hexavalent form will be carried downstream (Fandeur, 2007).

Large scale environmental pollution with Cr (VI) results from anthropogenic contamination of drinking water discharges of toxic Cr(VI) by cooling towers (Pellerin, 2000). Improper disposal of millions of tons of incompletely processed chromite ore also contribute to the pollution of the environment by hexavalent chromate (Stern *et al.*, 1998). In addition, hundreds of the large toxic waste sites in the U.S. known as Superfund sites contain Cr as a major contaminant (ASTDR, 2000). Furthermore, the presence of Cr(VI) in drinking water can also result from the oxidation of naturally occurring Cr(III) by Mn(III/IV) oxides in birnessite (Oze *et al.*, 2007), a common mineral that coats weathered grains and fractures in Cr-rich ultramafic rocks and serpentinites that are enriched with chromite [$FeCr(III)_2O_4$]. In addition to birnessite, the presence of two other Mn (IV) oxide containing minerals, asbolane and lithiophorite, has also been associated with the formation of Cr(VI) from natural Cr(III) (Fandeur *et al.*,2009). Examination of four minerals made of Mn oxides (birnessite, cryptomelane, todorokite, and hausmannite) showed that birnessite had the highest ability to oxidize Cr (III) under laboratory conditions. Furthermore, environmental contamination with Cr (III) can also generate Cr (VI) through oxidation reactions with water chlorination products, Ca and Mn oxides as well as photoxidation (Apte *et al.*, 2006; Dai *et al.*, 20003; Pilay *et al*., 2003; Clifford and Chau, 1988).

Table 2–1. Chemical and physical properties of select hexavalent chromium compounds

Compound	Molecular weight	Boiling point (°C)	Melting point (°C)	Solubility		
				Cold water		Other
				g/100 cc	°C	
Ammonium chromate	152.07	—	Decomposes at 180	40.5	30	Insoluble in alcohol; slightly soluble in NH_3, acetone
Ammonium dichromate	252.06	—	Decomposes at 170	30.8	15	Soluble in alcohol; insoluble in acetone
Barium chromate	253.32	—	—	0.00034	160	Soluble in mineral acid
Calcium chromate (dehydrate)	156.07	—	$-2H_2O$, 200	16.3	20	Soluble in acid, alcohol
Chromium (VI) oxide (chromic acid)	99.99	Decomposes	196	67.45	100	Soluble in alcohol, ether, sulfuric acid, nitric acid
Lead chromate	323.19	Decomposes	844	0.0000058	25	Soluble in acid, alkali; insoluble in acetic acid
Lead chromate oxide	546.39	—	—	Insoluble	—	Soluble in acid, alkali
Potassium chromate	194.19	—	968.3 975	62.9 36	20 20	Insoluble in alcohol
Potassium dichromate	294.18	Decomposes at 500	Triclinic becomes monoclinic at 241.6; Melting point is 398	4.9 102	0 100	Insoluble in alcohol
Silver chromate	331.73	—	Decomposes	0.0014	—	Soluble in NH_4OH, KCN
Sodium chromate	161.97	—	19.92	87.3	30	Slightly soluble in alcohol; soluble in MeOH
Sodium dichromate	261.97	Decomposes at 400 (anhydrous)	—	238 (anhydrous) 180	0 20	Insoluble in alcohol
Strontium chromate	203.61	—	—	0.12	15	Soluble in HCl, HNO_3, acetic acid, NH_4 salts
Zinc chromate	181.36	—	—	Insoluble	Insoluble	Soluble in acid, liquid NH_3; insoluble in acetone

Source: The Merck Index [2006].

Table 2.2: Uses of Chromate Compounds

Form	Uses
Cr(O)	Stainless steel production Alloy production Metal and alloy manufacturing
Cr(III)	Metal and alloy manufacturing Brick lining Chrome plating Leather tanning Textiles
Cr(VI)	Copying machine toner Chrome plating Leather tanning Textiles Copying machine toner

2.9.4 Routes of Exposure.

Occupational and non occupational exposure to chromate occurs through air, drinking water and direct skin contact (Son *et al*, 2010). The degree of exposure via the three routes is summarised in table 2.3.

Air

The bronchial tree is the primary target organ for carcinogenic effects of chromium (VI). Inhalation of chromium-containing aerosols is therefore a major concern with respect to exposure to chromium compounds. The retention of chromium compounds from inhalation, based on a 24-hour respiratory volume of 20 m^3 in urban areas with an average chromium concentration of 50 ng/ m^3, is about 3–400 ng. Individual uptake may vary depending on concomitant exposure to other relevant factors, e.g. tobacco smoking, and on the distribution of the particle sizes in the inhaled aerosol. Chromium has been determined as a component of cigarette tobacco produced in the United States, its concentration varying from 0.24 to 6.3 mg/kg (IARC,1990), but no clear information is available on the fraction that appears in mainstream tobacco smoke

Table 2.3: Levels of daily chromium intake by humans from different routes of exposure

Route of exposure	Daily intake	Absorption
Foodstuff	<200 µg	<10 µg
Drinking water	0.8–16 µg	<1 µg
Ambient air	<1000 ng	<5 ng

Drinking-water

The concentration of chromium in water varies according to the type of the surrounding industrial sources and the nature of the underlying soils For instance, an analysis of 3834 tap-water samples in representative cities of the United States showed a chromium concentration ranging from 0.4 to 8 µg/litre (EPA, 1984)

Food

The daily chromium intake from food is difficult to assess because studies have used methods that are not easily comparable. The chromium intake from typical North American diets was found to be 60–90 µg/day *(*Pellerin *et al.*, 2000*)* and may be generally in the range 50–200 µg/day. The chromium content of British commercial alcoholic beverages was reported to be slightlyhigher than that of wines produced in the United States, namely 0.45 mg/litre for wine, 0.30 mg/litre for beer, and 0.135 mg/litre for spirits *(*EPA,1984*)*.

2.9.5. Toxicokinetics

Although studies on the biokinetics of chromium are limited, it is believed that the rate of uptake in the airways is greatly governed by the size distribution of the inhaled particles and by the water solubility of the compounds *(*ATSDR, 2012*)*. Large particles (> 10 µm) of inhaled Cr (VI) compounds are deposited in the upper respiratory tract, while smaller particles can reach the lower respiratory tract. Some of the inhaled Cr (VI) is reduced to trivalent chromium (Cr [III]) in the epithelial or interstitial lining fluids within the bronchial tree. The extracellular reduction of Cr (VI) to Cr (III) limits the cellular uptake of chromium because Cr(III) compounds cannot enter cells as readily as Cr(VI) compounds. Cr (VI) compounds are tetrahedral oxyanions (Figure 2.9) that can cross cell membranes. Cr (III) compounds are predominantly octahedral structures to which the cell membrane is practically impermeable.

Absorption of water-soluble chromium (VI) compounds occurs rapidly by inhalation exposure although the extent of uptake is difficult to quantify. An estimate of pulmonary absorption, after chromium (III) chloride deposition in the lungs indicates that approximately 5% is absorbed within a few hours (EPA, 1984). A number of studies on the fate of chromium (VI) and chromium (III) following intratracheal administration have provided some information on

pulmonary retention and absorption of chromium compounds (Edel and Sabbioni, 1985; Weigand *et al.*, 1984). Chromium(III) is retained to a greater extent in the lungs than is chromium(VI) (Edel and Sabbioni, 1985) Chromates with low water solubility are mainly cleared to the gastrointestinal tract, whereas more soluble chromates are absorbed into the blood *(*Weigand *et al.*, 1984*).*

Absorption of chromium in the gastrointestinal tract is not greater than5% after oral exposure (EPA). Studies on the uptake of chromium (VI) compounds in the gastrointestinal tract show that that the rate of uptake is to is heavily dependent on the solubility of the compounds (IARC, 1990). Data from *in vitro* studies indicate that gastrointestinal juices are capable of reducing chromium (VI) to chromium (III). However, data from *in vivo* studies are insufficient to demonstrate whether this reduction process has the capacity to eliminate any differences in absorption between ingested chromium(VI) and chromium(III) compounds (EPA, 1984). Pulmonary cells have been shown *in vitro* to have some capacity to reduce hexavalent chromium. However, this capacity is low compared to that of liver cells (WHO, 2009). Tests on female experimental animals showed that absorbed chromium (III) and chromium (VI) can be transported to a limited extent to the fetus *in utero*. However, available data do not allow quantitative estimates of fetal exposure. In humans, the chromium concentration in the tissues of newborn babies has been found to be higher than that found later in life. There is a significant decline in concentration in children until about 10 years of age. Subsequently, there is a slight increase in the lung tissue concentration, but a slight decrease in other tissues.

Chromium is transported by the blood and distributed to other organs. The most significant retention occurs in the spleen, liver, kidney and bone marrow (WHO, 2000; Weber, 1983). Studies conducted by the National Toxicology Programme (NTP) in male rats and female mice orally exposed to chromium (VI) for 2 years also showed dose-related and time-dependent increases in total chromium concentrations in red blood cells, plasma, and in several organs. The total chromium content of the red cells was higher than that of plasma (IARC, 1990).

In both animals and humans, elimination of absorbed chromate from the body is biphasic, with a rapid phase, representing clearance from the blood, and a slower phase, representing clearance from tissues. The principal route of elimination is urinary excretion and it accounts for a little

over 50%. Fecal excretion accounts for only 5%. The remaining chromium is deposited into deep body compartments, such as bone and soft tissue. Elimination from these tissues proceeds very slowly; the estimated half-time for whole-body chromium elimination is 22 days for chromium(VI) and 92 days for chromium(III) following intravenous administration (EPA, 1984).

2.9.6. Metabolism of Chromate VI compounds.

Structural similarity of chromate ion to phosphate and sulfate (Figure 2.1) allows its easy entry through the general sulfate channels (Zhitkovich *et al.*, 2005). As with abiotic reactions, cellular reduction of Cr (VI) yields thermodynamically stable Cr(III) (Levina *et al.*, 2007; Ortega *et al.*, 2005). Efficient uptake of Cr(VI) followed by Cr(III) trapping via its binding to macromolecules leads to a massive accumulation of Cr relative to its extracellular concentrations, ranging from 10- to 20-fold after 3-h exposures to about 100-fold after 24-h exposures (Reynolds *et al.,* 2007*;* Messer *et al.,* 2006*).* With the apparent exception of bacteria producing hyperoxidized Mn (III/IV), biological systems lack the ability to reoxidize Cr(III) to Cr(VI) (Murray *et al*., 2007). Extracellular reduction of Cr (VI) is a detoxification process that produces poorly permeable nontoxic Cr (III) (Fig. 2.3). Studies of reduction activities in tissue homogenates and biological fluids showed that ascorbate (Asc) was the principal biological reducer of Cr (VI), accounting for 80-95% of its metabolism (Standeven and Wetterhahn, 1992; Suzuki *et al.*, 1991)

A combined activity of Asc and small thiols glutathione (GSH) and cysteine is responsible for >95% of Cr (VI) reduction in vivo. Tissue concentrations of GSH and Asc are not usually dramatically different, and the predominant role of Asc stems from its very high rate of Cr(VI) reduction. At physiological 1mM concentration, $t_{1/2}$ for Cr (VI) reduction by Asc was 1 min vs 60.7 min for GSH and 13.3min for Cys (Quievryn, 2003). Despite its slower rate of reduction, GSH is more important for Cr (VI) metabolism than Cys due to its higher cellular concentrations.

Depending on the nature of the reducing agent, its concentration, and stoichiometry, Cr (VI) reduction reactions generate variable amounts of transient products such as Cr (V), Cr (IV), and sulfur- and carbon-based radicals (Lay *et al.*, 1998; Stearn, 1994). The biological antioxidants, GSH-, cysteine-, and Asc derived radicals formed in Cr (VI) reactions are unreactive toward DNA (Guttmann *et al.,* 2008). However, in the presence of H_2O_2, the Cr intermediate formed can

catalyze Fenton-type reactions, generating highly reactive OH• radicals (Luo *et al.*, 1996) Formation ROS and direct oxidizing abilities of Cr (V) are the two main processes contributing to the induction of oxidative stress in Cr (VI)-treated cells (Slade *et al*., 2007; Sugden *et al.*, 2001)

All the biological reducers convert Cr(VI) to Cr(III) with varying mechanisms of reduction. Kinetic analyses suggest that Cys acts almost exclusively as a one-electron reducer that is consistent with the presence of strong Cr (V) signal in Cys-driven reactions (Quievryn, *et al.*, 2001). Reduction by GSH can proceed via either one- or two-electron reactions (Lay *et al.*, 1998). Asc is a highly efficient two-electron donor, yielding Cr (IV) as the first reduction intermediate and dehydroascorbic acid as the oxidized product. The presence of Cr (V) is only detectable under non physiological conditions of equimolar or higher ratio of Cr (VI) to Asc (Lay *et al.*, 1998). Insufficient amounts of Asc for the completion of Cr (VI) reduction in these reactions were responsible for a transient appearance of Cr (V), likely resulting from comproportionation of Cr (IV) and Cr (VI). Severe Asc deficiency of human and nonhepatic rodent cells in standard cultures raises concerns that studies with cultured cells may not accurately recapitulate genotoxic properties of Cr (VI) in vivo (Messer *et al*, 2007*;* Salnikow and Zhitkovich, 2008; Salnikow *et al*., 2004). The Asc depleted state of cultured cells results from the absence of the essential vitamin in the most common types of synthetic growth media. The additions of 10% serum to the media theoretically supplies only 10% of normal vitamin C levels. The actual levels of Asc in the growth media are lower due to its loss during the preparation and storage of serum. The half-life of Asc at 37 ^{0}C in cell culture media is 6-7 h (Bergsten, 1990). Recently fed cells can contain up to 50-60 µM vitamins C, but in many cases, its levels are dramatically lower or undetectable. Even when cells start with 50- 60 µM Asc, they become completely depleted of Asc after 24-48 h in culture (Karaczyn, 2006). Physiological concentrations of vitamin C in white blood cells and epithelial tissues are usually in the 1-2 mM range (Bergsten, 1990).

2.9.7 Health Effects of Hexavalent Chromate Exposure

Exposure to hexavalent chromate is associated with cancer and non cancer effects.In addition exposure to hexavalent also lead to geneotoxicty, induction of micronuclei, oxidative stress and actin disruption.

2.9.7.1 Nonmalignant Effects

Inhalation of Cr(VI) has been shown to cause ulceration of the nasal mucosa, perforation of the nasal septum, asthma, bronchitis, pneumonitis, inflammation of the larynx and liver, while exposure due to dermal contact of Cr(VI) compounds can induce skin ulcers, allergies, dermatitis, dermal necrosis and dermal corrosion (Bielicka *et al*., 2005). Chronic and acute exposure to chromate (VI) has been reported to cause kidney and liver damage, pulmonary congestion and edema, epigastric pain, erosion and discoloration of teeth, and perforated ear drums. Other effects of exposure to chromates include eye injury, leukocytosis, leukopenia, eosinophilia, (NIOSH, 2003; Johansen *et al*., 1994). Anemia, thrombocytopenia, infertility, birth defects, spontaneous abortions, ulcers, gastrointestinal bleeding, renal failure, intravascular haemolysis, liver damage, respiratory disturbances, coma and even death have all been reported. to be associated with chromate (VI) exposure (Lin *et al.,* 2009; Loubieres *et al.,* 1999; Bonde and Ernst, 1992).

2.9.7.2 Malignant Effects

Particulate hexavalent chromium compounds are well established human respiratory toxins and carcinogens that are used commercially in welding, chrome plating, chrome pigmenting, leather tanning, and in the ferrochrome industry (Beaver, 2009). Occupational exposure to Cr (VI) in these industries and are associated with fibrosis, fibrosarcomas, adenocarcinomas and squamous cell carcinomas of the lung (Beaver, 2009). Epidemiological studies in the USA indicated a 10 to 30 fold- increased risk of lung cancer among workers in the chromate industry compared to the general population (Das and Mishra, 2008). A positive correlation was also found between the duration of exposure and lung cancer death (Das and Mishra, 2008). Upon inhalation, chromium

particles accumulate at the bifurcations of the bronchi and the concentration of Cr in these regions of the lung can reach up to 15.8 mg/g tissue (dry weight) (Ishikawa *et al*., 1994a; Ishikawa *et al*., 1994b). Autopsy of the lungs of chromate workers show higher lung-Cr burdens correlate with increased lung tumor incidence (Ishikawa, *et al*., 1994b; Ishikawa, *et al.*, 1994a). Epidemiological studies in Europe, Japan and the United States have consistently shown that workers in the chromate production industry have an elevated risk of respiratory disease including: fibrosis, perforation of the nasal septum, development of nasal polyps, hyperplasia of the bronchial epithelium, lung fibrosarcomas, adenocarcinomas and squamous cell carcinomas (IARC, 1990; Ishikawa, *et al*., 1994b; Ishikawa, *et al*., 1994a; Dalager *et al*., 1980).

Animal studies of chromate exposure by inhalation or intratracheal/intrabronchial instillations illustrate that the slightly soluble and highly insoluble particulate Cr (VI) such as zinc, lead, strontium and sintered calcium chromate consistently induced lung tumors (Landolph *et al.*, 1994*;* Levy *et al*., 1986; Hueper *et al*., 1959; Steffee and Baettjer, 1965).

2.9.7.3 Genotoxicity

Inaddition, Cr (VI) is a potent genotoxin and initiates a variety of cellular and molecular damage that includes Cr-DNA adducts, DNA single and double strand breaks,**,** alkali labile sites, chromosomal aberrations, DNA-protein cross-links and apoptosis (Salnikow *and* Zhitkovich, 2008; Zhitkovich, 2005; O'Brien *et al*., 2003). The present understanding of Cr (VI)-induced genotoxicity is based on Wetterhahn's uptake-reduction model (Standeven and Wetterhahn, 1989):

(i) the active transport of Cr(VI) into cells through anion channels for soluble chromates through phagocytosis for insoluble compounds such as $PbCrO_4$);

(ii) the intracellular reduction of Cr(VI) with the formation of potentially DNA-damaging Cr (V/IV) intermediates (which can be stabilized by intracellular ligands) and organic radicals;

(iii) the formation of kinetically inert Cr(III) complexes, such as highly genotoxic DNA–Cr(III)–protein and DNA–Cr(III)–DNA cross-links, as a result of such reduction

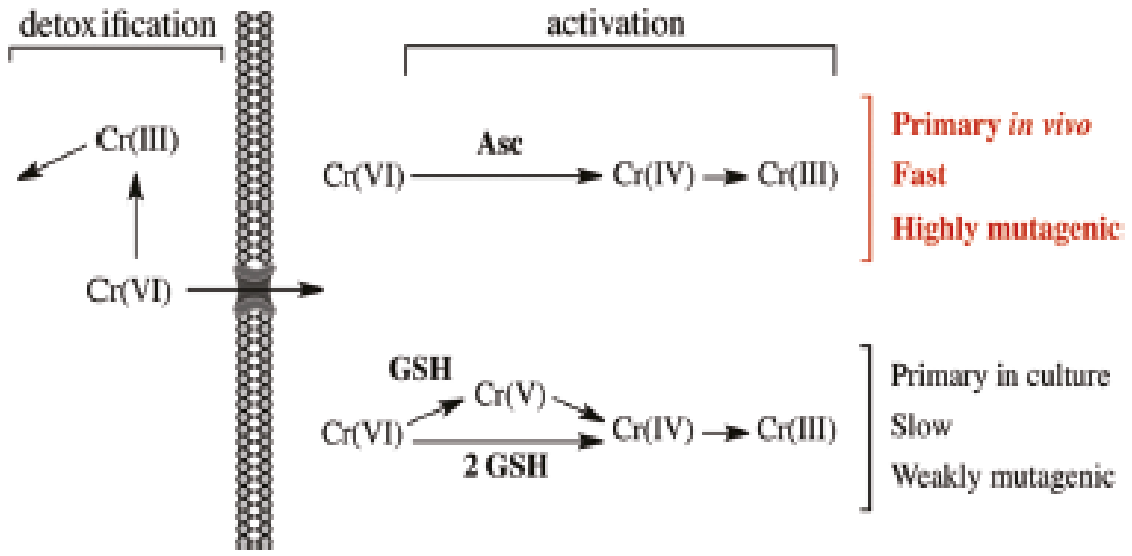

Figure 2.11: Metabolism of Hexavalent Chromate (Zhitkovich, 2011)

The most common type of DNA damage associated with chromate (VI) exposure is Cr-DNA binding (adducts). It has been detected in reduction reactions in different cultured cells and in vivo (Zhitkovich *et al.*, 2005). Cr-DNA adducts are a heterogeneous groupthat includes binary [Cr(III)-DNA] and several ternary [ligand- Cr(III)-DNA] adducts where the ligand can be Asc, GSH, cysteine, or histidine. All four ternary adducts have been detected in Cr (VI)-treated cells and are readily formed during in vitro Cr (VI) metabolism (Zhitkovich *et al.*, 1995). Cr (VI) also causes the formation of protein-Cr(III)- DNA cross-links, which are rare lesions and whose main toxicological significance could lie not necessarily in the contribution to genotoxic responses but rather in the inhibition of gene-specific expression (Schnekenburger *et al.*, 2007).

Binary Cr-DNA adducts are the most frequent DNA modifications in the in vitro reductions of Cr(VI). In Cr(VI) reactions with Asc and GSH, binary adducts accounted for 75-95% of the total DNA-bound Cr (Guttmann *et al*., 2008; Quievryn *et al.*, 2002).When normalized for recovery, Asc-Cr-DNA cross-links have been calculated to comprise 6% of Cr-DNA adducts in human A549 cells with restored Asc levels(Quievryn *et al.*, 2002). Cys-Cr- DNA and GSH-Cr-DNA accounted for 24 and 17% respectively of all DNA adducts in hamster CHO cells (Zhitkovich *et al.*, 1995) although these values were not been adjusted for recovery. Protein-Cr-DNA cross-links constitute only about 0.1% of total adducts immediately after Cr(VI) exposures (Zecevic , *et al.*, 2010) but their relative amounts are likely higher at later post exposure times due to delayed formation and slower repair relative to those of small Cr-DNA adducts (Zecevic *et al* , 2010; Macfie *et al.*, 2010).

Replication of adduct-carrying shuttle-vectors in human cells showed that the most abundant adduct, the binary Cr-DNA conjugate, was weakly mutagenic, whereas four ternary adducts containing DNA-cross-linked Asc, GSH, cysteine, and histidine were strongly mutagenic (Quievryn *et al.*, 2003; Voitkun *et al.*, 1998). In vitro reduction of Cr (VI) by purified Asc, GSH, or cysteine also led to the production of mutagenic and replication-blocking DNA lesions, as revealed by analyses of replicated progeny of shuttle-vector plasmids propagated in human fibroblasts (Guttmann *et al*., 2008; Quievryn *et al*, 2003; Zhitkovich, *et al*, 2001). Asc-driven metabolism of Cr (VI) in vitro resulted in the strongest mutagenic responses, while reactions with GSH showed low yields of mutagenic damage and GSH-Cr-DNA adducts (Guttmann *et al*., 2008; Quievryn *et al.*, 2003). These findings were corroborated by a strong potentiation of Cr (VI) mutagenicity in cells with restored Asc levels (Reynolds *et al.*, 2007). Blocking of Cr-DNA

binding during the reduction or dissociation of Cr-DNA adducts eliminated all mutagenic and replication-blocking responses in shuttle-vector plasmids incubated in Cr (VI) reactions containing Asc, GSH, or Cys (Guttmann *et al.*, 2008; Reynolds *et al.*, 2007; Quievryn *et al*, 2003). Thus, indicating a key role of Cr-DNA adducts in the mutagenicity and genotoxicity of Cr(VI) when metabolized by these three reductants. In agreement with these results, in vitro reduction reactions employing iron free reagents failed to generate detectable amounts of singlestrand breaks and abasic sites in DNA (Guttmann *et al.*, 2008; Quievryn *et al.*, 2003; Zhitkovich et *al.*, 2001). Inhibition of *in vitro* replication on DNA templates damaged in Cr (VI)-Asc reactions was also dependent on Cr-DNA binding (O'Brien *et al.*, 2002).

Involvement of Cr-DNA adducts in bacterial mutagenesis by Cr (VI) is indicated by higher yields of revertants in the Ames test using a NER-deficient Salmonella uvrA strain (Watanabe *et al.*, 1998). Cr(VI) mutagenicity in transgenic lacI mice was inhibited by GSH depletion, which points to the importance of non-oxidative mechanisms and GSH-Cr-DNA adducts in mutagenic responses in vivo (Cheng *et al.*, 2000). Cr (VI)-induced fold changes in the number of HPRT mutants were reported to be lower in NER-deficient clones of CHO cells grown under the standard Asc-deficient conditions which contrasts the positive role of NER in the removal of adducts and survival of CHO and human cells (O'Brien, *et al.*, 2005). The biological consequences of Cr-induced DNA damage include DNA and RNA polymerase arrest and mutagenesis/chromosomal abnormalities including induction of micronuclei (Reynolds *et al.*, 2007; De Flora *et al.*, 2006; Zhitkovich, 2005; Quievryn *et al.*, 2003; Stearns *et al.*, 1994, Suzuki, 1990; Borges *et al.*, 1991).

2.9.7.4 Micronuclei Formation

The micronucleus (MN) assay is an effective biomarker for the early detection of the changes related to cancer (Bonassi *et al.*, 2011). Micronuclei originate from chromosome fragments or whole chromosomes that are not included in the main daughter nuclei during nuclear division (Maffei *et al.*, 2014). Thus, MN are found in interphase cells as small, extranuclear bodies resulting from chromosome breaks and whole lagging chromosomes, which are not incorporated into the main nucleus during cell division. The formation of micronuclei during cell division process can be caused by chromosomal rearrangements, altered genome expression or

aneuploidy, all of which are associated with the chromosome instability phenotype, often observed in cancer patients (Fenech, 2002). The hypothesis of an association between MN frequency and cancer development is supported by a number of observations, the most substantial of which include the high MN frequency in untreated cancer patients and in subjects affected by cancer-prone congenital diseases (Bolognesi *et al.*, 2005; El-Zein *et al.*, 2006; Iarmarcovai, *et al.*, 2008). A number of international cohort studies have demonstrated that the MN frequency in the Peripheral Blood Lymphocytes of healthy subjects is a predictor of cancer risk (Bonassi *et al.* 2007; Fenech *et al.*, 2011). MN therefore, is exploited in assessing structural and numerical chromosomal alterations in genotoxicity testing. The frequency MN can be used to screen drug candidates and other test chemicals for both clastogenic and aneugenic potential (Seager *et al.*, 2014). Induction of micronuclei in *vivo* by hexavalent chromate appears to be dependent on the route of exposure. Several studies that have directly compared the micronucleus formation of Cr (VI) by administration in drinking water (or oral gavage) and ip injection suggest that only ip administration results in genotoxicity. Shindo *et al*. (1989) exposed two strains of mice (CD-1 and MS/Ae) to several concentrations of Cr (VI) via oral gavage and by ip injection. In both strains of mice, there was a dose-dependent decrease in polychromatic erythrocytes (PCEs) and an increase in micronucleated PCEs following ip injection of >10 mg/kg potassium chromate administration but not following gavage (Shindo *et al*., 1989). Similarly, De Flora *et al*. (2006) showed that ip administration of 17.7 mg/kg Cr (VI) to 8-month-old male BDF1 mice resulted in a significant increase in micronucleated PCEs, whereas gavage of the same dose did not. In another study, Bagchi et al. (2002), reported DNA damage in liver and brain tissue within 24–96 h after oral gavage of 6 mg/kg Cr (VI).

Recently, it has been demonstrated that chromosome fragments that are not incorporated into the nucleus at cell division (micronuclei formation) is the one of the major manifestations of heavy metal toxicity in tissue culture and animals (Yih *et al*., 2007). There are several possible hypotheses on the pathways of MN formation. Cytogenetic alterations in chromium (VI)-exposed cells in culture and *in vivo*, such as increased frequencies of chromosomal breaks and micronuclei, are suggested to be due to DNA double-strand breaks, produced by a cell-replication-dependent mechanism in the G2 phase of the cell cycle. The induction ROS found in chromate (VI)-exposed mammalian and plant cells may attack purine and pyrimidine bases and deoxyribose in DNA. This can cause DNA strand breakage, which can increase the probability of

chromosome/chromatid fragmentation. Thus, leading to MN formation. Chromate (VI) can binding to sulfhydryl groups and inactivate some important enzymes involved in DNA repair and expression, alter DNA repair mechanism, and cause an increase in MN frequency. Furthermore, some evidences suggest that chromate (VI) may interfere with microtubule assembly and spindle formation causes chromosomal lagging, chromosomal instability and possibly leads to a higher frequency of micronuclated cells (Reynolds *et al.*, 2007; Salnikow and Zhitkovich, 2008).

2.9.7.5 Hexavalent chromate and Oxidative Stress

In addition to intracellular reduction of Cr (VI) to Cr (III) by low molecular weight thiols such as glutathione (GSH) and cysteine, as well as antioxidants like ascorbate (Figure 2.13A) (O'Brien *et al*., 2003; Zhitkovich, 2005). It has been hypothesized that the process of Cr (VI) cytotoxicity and carcinogenesis can be triggered by the dysregulation of gene expression, cellular redox state, and DNA damage as a result of oxidative stress. Oxidative stress is the favoring of cellular oxidant production over that of antioxidants, which leads to the formation of reactive oxygen species (ROS), and damage to cellular RNA, DNA, proteins, and lipids (Klaunig and Kamendulis, 2004). It involves reduction of Cr (VI) to Cr (V) by molecular oxygen, which results in the generation of reactive oxygen species (ROS) (Liu and Shi, 2001). This in turn leads to the formation of hydrogen peroxide that can be removed by catalase, conjugation with GSH (perhaps competing with GSH-mediated Cr (VI) reduction), as well as by Fenton reactions with iron. Peroxide can also undergo Fenton reactions with Cr (V), thereby reforming Cr (VI) and hydroxide radicals (Liu and Shi, 2001). Thus, sustained exposure to Cr (VI) might lead to oxidative stress (Figure 2.13B). While the direct relationship between DNA-reactive oxygen species and chromium-induced DNA damage is heavily debated and unclear, there have been several studies supporting the role of ROS in Cr (VI)-induced genotoxicity, cytotoxicity, and oxidative stress (Patlolla *et al*., 2009; Azad *et al*., 2010). Pretreatment with free radical scavenger such as flavin adenine dinucleotide or vitamin E were also shown to markedly decrease Cr (VI)-induced single-strand breaks and cytotoxicity (Sugiyama *et al*., 1989). Furthermore, Shi *et al*. (1999) suggests that ROS contributes to the early effects of Cr (VI)-induced apoptosis via a p53-independent mechanism, whereas the apoptotic effects could be blocked in the presence of ROS scavengers, such as catalase, aspirin and N-acetyl-L-cysteine. Moreover, gene expression analysis of Cr(VI)-treated A549 cells showed increases in glutathione peroxidase, CuZnSOD, and MT-II (protects cells from toxicity and oxidative stress) gene expression, while NADH

ubiquinone oxidoreductase B18 subunit (a subunit of the mitochondrial respiratory chain complex I), glutathione peroxidase, and the sodium/potassium-transporting ATPase alpha 1 subunit (an ROS regulator) were up regulated in Cr(VI)-treated BEAS-2B cells (Andrew *et al.*, 2003). Similarly, Cr (VI)-induced expression of the HO1 gene was also shown in human dermal fibroblasts and A549 (Joseph *et al.*, 2008), however a report from O'Hara and colleagues contradicts these data (O'Hara *et al*., 2006).

Generally, the relationship between oxidative stress and Cr (VI)-induced cytotoxicity, genotoxicity, and potential carcinogenesis remains unclear. This has been ascribed to the non-uniform treatment protocols, conflicting data and controversial methods used for detection of Cr (VI)- induced oxidative stress. For instance, Martin *et al*. (1998) demonstrated that the high valence chromium species, bis(2-ethyl-2-hydroxybutyrato)oxochromate(V) [Cr(V)- EHBA], was able to independently induce the fluorescence of two dyes commonly used to detect ROS (2′,7′-dichlorofluorescin and dihydrorhodamine) in A549 cells that was not affected by treatment with radical scavengers (Martin *et al.*, 1998). Thus indicating that 2, 7′-dichlorofluorescin and dihydrorhodamine are more appropriate for the qualitative detection of Cr (V), rather than ROS production in the presence of Cr (VI). In addition, total dose over time and dose rate, as well as the relative ratios and availability of intracellular reductants and anti-oxidants may also determine the response to cells to oxidative stress or otherwise.

2.9.7.6. Actin Disruption

Actin is an important functional and structural protein common to all eukaryotic cells. The actin filaments are the major component responsible for the maintenance of global cell shape in fibroblast (Ujihara *et al*., 2008). The actin cytoskeleton has diverse function in the cell. It is essential for cell growth, maintenance of cell polarity and morphology, locomotion, phagocytosis, trafficking of organelles, signal transduction and cell division in fibroblasts and other cells. Disruption of the actin cytoskeleton elicits profound changes in cell survival and function. It may lead to disruption in signal transduction that may lead to cell death or enhanced survival.

It has been reported that apoptotic signals trigger actin cytoskeletal changes that result in release from the extracellular matrix, membrane blebbing, and condensation into apoptotic bodies in a

sequential fashion (Mills *et al.*, 1999). These events are linked with stress fiber loss and cortical actin reorganization, actinomyosin contraction of the actin ring, and dissolution of polymerized actin, respectively (Mills *et al.*, 1999). Actin reorganization and degradation has been viewed as a later consequence occurring only after a cell has committed to an apoptotic death. However, there is increasing evidence that perturbations of the actin cytoskeleton itself can initiate events that commit a cell to apoptosis. Loss of actin-based, integrin mediated cell matrix adhesion results in apoptosis in epithelial cells and other cell types (Frisch *et al*., 2001).

Direct disruption of the actin cytoskeleton with cytochalasin D (CYD) or jasplakinolide induces apoptosis of airway epithelial cells (White *et al*., 2001), HL-60 cells (Rao *et al.*, 1990), endothelial cells (Li *et al.*, 2003). EL4 T lymphoma cells (Korichneva, 1999) and NIH3T3 cells (Korichneva and Hammerlig,1999). However, Ailenberg and Silverman, 2003 reported that cytochalsin D disruption of mouse mesangial cells (MMC) caused it to undergo apoptosis, but it promoted cell survival in NIH 3T3 cells. Although, it was reported that soluble hexavalent chromium interfere with cytoskeletal actin in murine fibroblasts and hepatocytes (Li *et al*., 1992; Gunaratnam and Grant, 2004), the role of actin disruption in the cytotoxicity of hexavalent chromate is CH310T ½ mouse embryonic fibroblast is yet to be studied.

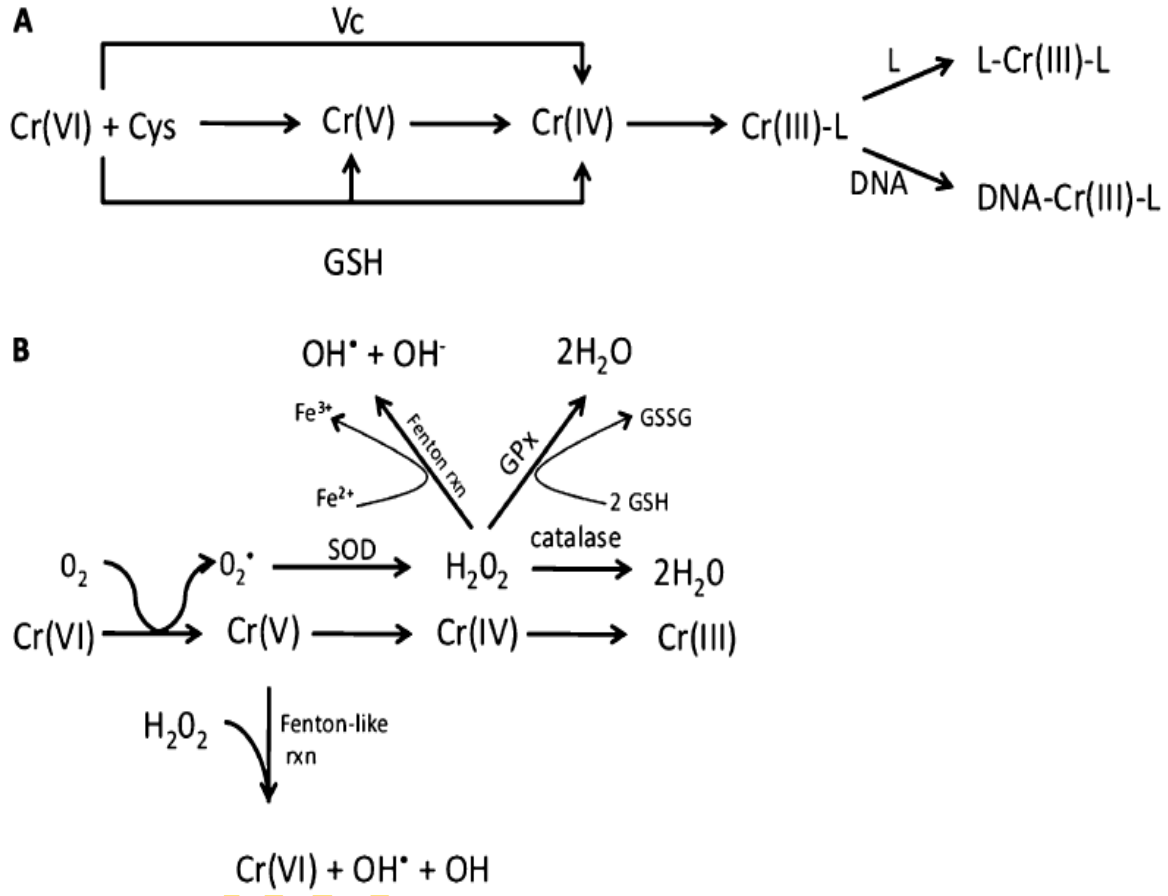

Figure 2.11: Reduction schemes for Cr (VI). (A) Reduction of Cr (VI) by low molecular weight ligands (L) (Zhitkovich, 2005). (B) Reduction of Cr (VI) by molecular oxygen (Liu and Shi, 2001). SOD, superoxide dismutase; Cys, cysteine; GSSG, oxidized GSH; GPx, glutathione peroxidase; Vc, ascorbate

2.10 Arsenic

It is widely distributed in nature in many forms and its compounds are used extensively as components of herbicides, insecticides, rodenticides, food preservatives, and drugs (Mustafa *et al.,* 2010; Baxley *et. al.,* 1981). Inhalation exposure to arsenic also occurs in other industrial settings such as lead, copper, and zinc smelting as well as fossil fuel combustion in power plants and semiconductor industry. The trivalent (arsenite) or pentavalent (arsenate) has a wide distribution. The most common inorganic trivalent arsenic compounds are arsenic trioxide, sodium arsenite, and arsenic trichloride. The pentavalent inorganic compounds are arsenic pentoxide, arsenic acid, and arsenates, such as lead arsenate and calcium arsenate. Arsenite is less excreted from the body relative to arsenate. Thus, arsenites are considered more toxic and carcinogenic than arsenate (Huang 2004; Kreppel *et al.*, 1993). Arsenite is extremely thiol-reactive. It can affect enzyme activities by binding to critical vicinal cysteinyl residues, such as those in the lipoamide of pyruvate dehydrogenase, tyrosine phosphatases, and enzymes involved in protein ubiquination. In general, arsenite is thought to be a sulfhydryl reagent having a high affinity mainly for vicinyl dithiols and thiols located near hydroxyls.

Ingestion of arsenite in drinking water presents the greatest hazard and this has been associated with many cancer and non cancer effects in affected populations (Hua *et al.,* 2004). Such effects include tumors at multiple sites including the skin, liver, lungs, urinary bladder and prostate (NRC, 1999; Lewis *et al.,* 1999). The increase in cancer risk observed in epidemiological studies is attributed mainly to the presence of inorganic trivalent arsenic (arsenite). Similarly, arsenite exposure has been linked to endemic arsenic dermatosis along with hyperkeratosis, maningioma, diabetes, hypertension, embryotoxicities, spontaneous abortion, adverse pregnancy outcomes, gangrene, and blackfoot disease (Yang *et al.* 2003; Tseng *et al.,* 2002.*;* Saha *et al.,* 1995). An early event in arsenic carcinogenesis is molecular alterations both in humans and animals which manifests in a dose dependent chromosomal breaks and alterations (Barns *et al.* 2002; Vega *et al.,* 1995). Recently, it was demonstrated that induction of micronuclei is one of the principal manifestations of arsenic toxicity in plants and animals (Odunola *et al.,* 2007*;* Yi e*t al.*, 2007). Several reports have also implicated oxidative stress in arsenic-induced cytotoxicity and genotoxicity (Valko *et al.*, 2006). Many other studies confirmed the generation of free radicals during arsenic metabolism in cells (Yamanaka *et al.,* 2007). Interestingly, experimental

evidences have shown that arsenic-induced generation of free radicals can cause cell damage and death through activation of oxidative sensitive signaling pathways (Kamat *et al.,* 2005). Arsenic-mediated generation of reactive oxygen species is a complex process which involves the generation of a variety of ROS including superoxide ($O_2^{\bullet -}$), singlet oxygen ($^1O_2$), the peroxyl radical ($ROO^{\bullet}$), nitric oxide ($NO^{\bullet}$), hydrogen peroxide (H_2O_2), dimethylarsinic peroxyl radicals ($[(CH3)_2AsOO^{\bullet}]$) and also the dimethylarsinic radical $[(CH3)_2As^{\bullet}]$. The exact mechanism responsible for the generation of all these reactive species is not yet clear.

In addition, it has been found that perturbation of signal transduction such as the JNK pathway occurred during arsenite induced malignant transformation. This confers resistant to apoptosis and thus, suggesting that apoptotic control mechanisms are disrupted as cells becomes transformed through arsenic exposure. This apoptotic disruption may allow damaged cells to inappropriately escape apoptosis and potentially proliferate, thereby providing initiating events in carcinogenic development. In addition, it has been found that perturbation of signal transduction such as the JNK pathway occurred during arsenite induced malignant transformation. This confers resistant to apoptosis and thus, suggesting that apoptotic control mechanisms are disrupted as cells becomes transformed through arsenic exposure. This apoptotic disruption may allow damaged cells to inappropriately escape apoptosis and potentially proliferate, thereby providing initiating events in carcinogenic development.

2.11. CANCER CHEMOPREVENTION

The prevention of cancer is one of the most important public health and medical practices of the 21st century. Cancer chemoprevention encompasses the concepts of inhibition, reversal, and retardation of the cancer process. It aims to halt or reverse the development and progression of pre-cancerous cells through use of non-cytotoxic nutrients and/or pharmacological agents during the period between tumor initiation and malignancy. Cancer chemoprevention is regarded as a promising avenue for cancer control (De Flora *et al.,* 2001). This strategy is based on the reduction of cancer incidence by increasing the public consumption of antimutagens and anticarcinogens common used. Chemopreventive agents can be divided into blocking and suppressing agents (Wattenberg, 1997). Blocking agents prevent carcinogens from reaching the target sites, undergoing metabolic activation or interacting with crucial cellular macromolecules such as DNA, RNA and proteins (Figure 2.13). For example, calcium can block bile acid uptake

into colonic epithelial cells. On the other hand, suppressing agents, inhibit the malignant transformation of initiated cells at either the promotion or the progression stage (Figure 2.13). The cellular and molecular events modulated by these chemopreventive phytochemicals include carcinogen activation/detoxification by xenobiotic metabolizing enzymes; DNA repair; cell-cycle progression; cell proliferation, differentiation and apoptosis; expression and functional activation of oncogenes or tumour-suppressor genes; angiogenesis and metastasis; and hormonal and growth-factor activity (Surh, 2003). They lower the risk of human cancer development via their radical scavenging, antioxidant, anti-inflammatory and antiproliferative activities (Kwak and Kensler, 2010; Parys *et al,* 2010; Surh, 2003). Some other agents such as retinoids induce terminal differentiation in aberrant epithelial cells and thus removing them from the replicating pool. Furthermore, many of the bioactive agents' acts by altering signal transduction pathways (Surh, 2003).

Cancer has no effective cure and conventional radiotherapy and chemotherapy with synthetic drugs used for treating cancer are limited by severe side effects such as immunosuppression, organ failure and infectious diseases which cause the death of patient after recovery from cancer (Barh, 2008). This has necessitated the search for chemopreventive agents from natural products including dietary and medicinal plant. These plants contain phytochemicals that are biologically active nonnutritive chemical compounds, which are responsible for the health promoting properties of varieties of medicinal plants. Several of these phytochemicals have been reported to inhibit the multistep process of carcinogenesis (Singh *et al.*, 2006) (Figure 2.14)

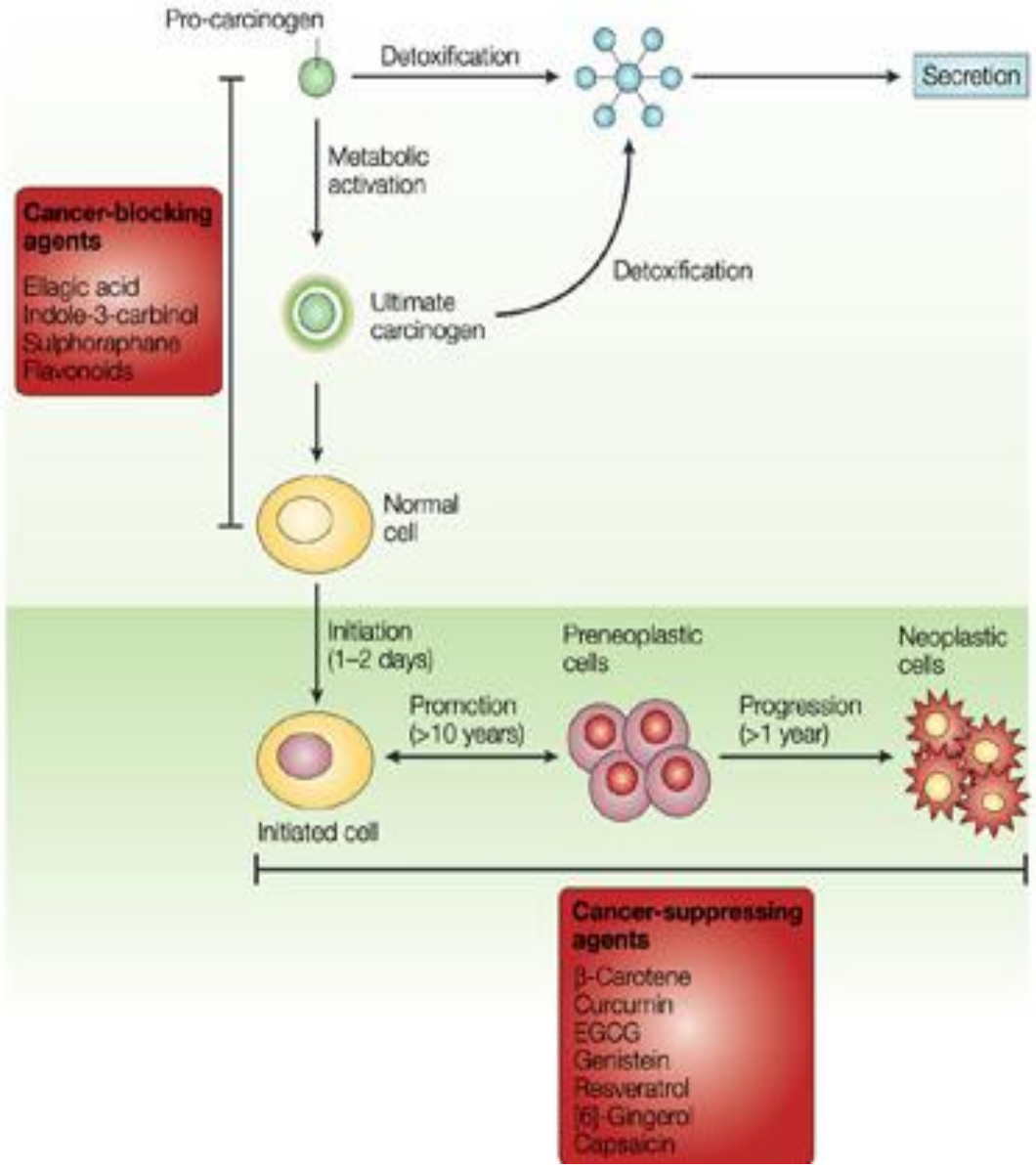

Figure 2.12: Interference of different stages of carcinogenesis by phytochemicals (Surh, 2003)

Garlic alone contains 30 cancer preventing compounds including selenium. Broccoli contains indole-3-carbinol as well as phenethylisothio-cyanate, a sulfur-containing compound that is being studied in the prevention of cancer. Soy products contain phytoestrogens such as genistein that contribute to the putative breast- and prostate-cancer-preventive activity of soya bean (Surh, 2003). Topical application of capsaicin, a pungent component of hot chilli pepper (*Capsicum annuum* L.) inhibited PMA-induced mouse-skin tumour formation and activation of Nf-kb (Han *et al.,* 2001). Both black and green tea contains an abundance of polyphenols such as catechins that have antioxidant and anti-cancer activity. Epigallocatechin gallate (EGCG), an antioxidant and chemopreventive polyphenol found in green tea has been shown to suppress malignant transformation in a PMA-stimulated mouse epidermal JB6 cell line by blocking activation of Ap1 or Nf-κb44 (Surh, 2003). Cur-cumin the most studied phytochemical and it is obtained from the spice, turmeric (Surh, 2003). It is both an anti-inflammatory agent and an antioxidant. In laboratory animals curcumin has been shown to inhibit colon, breast, and stomach cancer (Rukkumani *et al.,* 2004).

Although many herbs and species are been tested round the world for their cancer chemopreventive potentials, many are stilled unexplored or the scientific evidence of their traditional useage have not been properly investigated. One of such herbs *is Rauvolfia vomitoria*

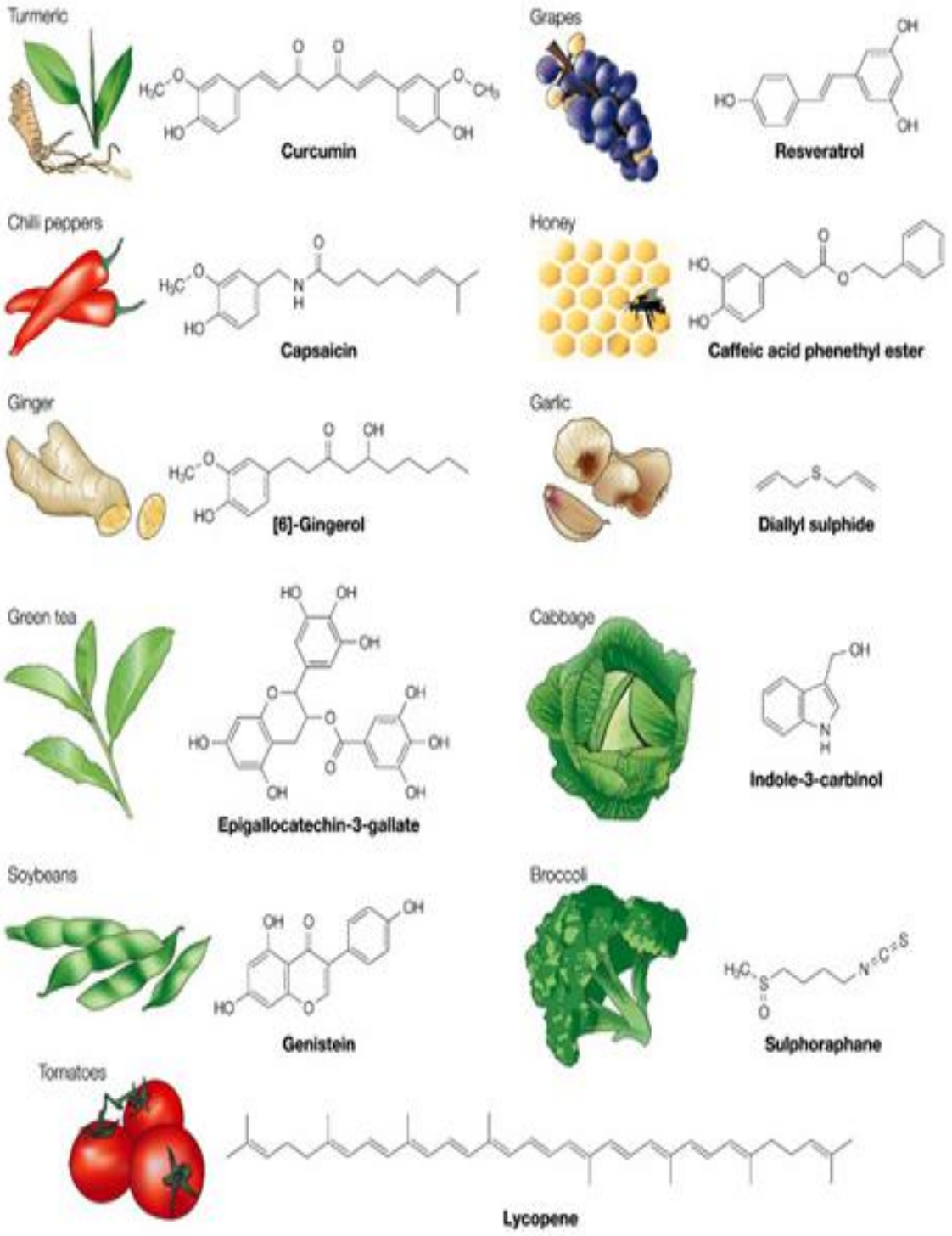

Figure 2.13: Chemopreventive phytochemicals and their dietary sources (Surh, 2003)

2.12. *Rauvolfia vomitora (Afzel)*

2.12.1 Classification

Family: - Apocynaceae.

Synonym(s):- Hylacium owariense Afzel, Rauvolfia Senegambia

Common names: - (English): swizzle stick, poison devil's-pepper

(Yoruba): Asofeyeje

(Hausa): Wadda

` (Igbo): Ntu oku

Organism type: tree, shrub

Kingdom: Plantae-Plants
Subkingdom: Tracheobionta-Vascular plants
Superdivision: Spermatophyta-Seed plants
Division: Magnoliophyta-Flowering plants
Class: Dicotyledonae
Subclass: Asteridae
Order: Gentiales
Family: Apocynaceae
Genus: *Rauvolfia*
Species: *vomitoria*

Figure 2.14: *Rauvolfia vomitora (Afzel) Plant* (Taken at Omi Adio, Ibadan)

2.12.2 Habitat and Distribution.

Rauvolfia vomitoria (RV) is a medicinal plant which native to in the humid tropical secondary forests of Africa (Sofowora,1993), but it has been introduce to Asia , Puerto Rico and Hawai'i . It naturally occurs in gallery forests, but is mostly found in forest re-growth where fallow periods are prolonged. RV is associated with palms, Trema guineensis and Combretum spp. RV is considered endangered species.

2.12.3 Description

The generic name Rauvolfia commemorates a 16th century German physician, Leonhart Rauvolf, who travelled widely to collect medicinal plants. The specific epithet vomitoria refers to the purgative and emetic properties of the bark. *Rauvolfia vomitoria. Rauvolfia vomitoria* is a shrub or small tree up to 8 m tall. The leaves grow in whorls of three and are elliptic and pointed at the end, 5-12 cm long and 3-6 cm wide. Flowers are tiny, sweet-scented, pale greenish-white and somewhat hairy inside. The orange fruits are shaped like small balls, each containing a single seed. Flowering occurs between August and October, while fruiting occurs between October and December.

2.12.4 Functional uses

The plant is rich nutrient such as crude protein (9.3-17%), crude fibre and ash (Ojo *et al.,* 2012*;* Mecha *et al,* 1980). The sweet-scented flowers are frequented by bees and therefore, exploited in apiculture. It is used as firewood for in Sierra Leone. The bark has good yields of bast fiber. The latex extruded from the young stems is used in rubber production. A yellow pigment obtained from the bark is useful in making dye. The seeds are used in making decorative necklaces. In Gabon, the bark and root powder, are mixed with water or palm oil to kill fleas and vermin.

2.12.5 Medicinal Uses

The plant has found wide applications in traditional medicine across the world. Traditional medicine practioner in Nigeria and other parts of Africa use different part of the plant in treating fever, general weakness, intestinal diseases, liver problems, mental illness, haemorrhoids, hypertension, snakebite and cholera (Amole, 2009; Bemis *et al.*, 2006; Obembe *et al.*, 1994; Akpanabiatu *et al.,* 2009; Waterman, 1986). Decoctions of the leaves of RV have a powerful

emetic and anti-swelling effect (Burkill, 1994). In addition, its tissue lipid lowering-effect, blood pressure lowering, antipyretic, analgesic, haematinic, aphrodisiac, purgative, dysenteric, abortive, insecticidal, anti psychotic, anticonvulsant properties have all been documented (Amole *et al.*, 2009; Obembe *et al.*, 1994; Principe, 1989). Extract from the plant have also been reported to inhibit the growth of bacterial, viral, fungal and parasitic pathogens (Amole *et al.*, 2006).

Furthermore, the plant has been reported to have anti-prostate cancer activity in both in vitro and in vivo model system. This mechanism of action has suggested to be via modulation of DNA damage and cell cycle control signaling pathways (Beljanski and Beljanski, 1999). Recently, Yu *et al.* (2013) reported that *Rauvolfia vomitora* inhibited the growth of 3 ovarian cancer cell lines and inhibited their colony formation in soft agar. In addition, it was shown that extract of RV suppressed tumour growth in mice (Yu *et al.*, 2013).

2.12.6 Phytochemical Constituents

The leaf of the plant is rich in alkaloids, flavonoids, tannin, saponins and tepernoid. (Ojo *et al.*, 2012). Extensive studies carried out on its chemical properties showed that the plant contains more than 50 active indole alkaloids (Table 2.5), each possessing remarkable pharmacological activities (Yu *et al.*, 2013; Iwu and Court, 1982*;* Pousset and Poisson, 1965). The main alkaloid present in *Rauvolfia* is the anti hypertensive and psychiatric agent, *reserpine.* The indole akaloids with yohimbane skeleton namely yohimbine, reserpine, rescinnamine, raucaffricine, ajmaline and ajmalicine have been isolated from the extract of RV (Yu *et al.*, 2013). A bioactive carboline alkaloid, alstonine, present in the root and leaf were previously shown to have anti cancer activity (Pettit *et al.*, 1994*;* Bemis *et al.*, 2006).

Table 2.5: Major alkaloids and their bioactivities isolated from the root of *Rauvolfia vomitoria* (Yu *et al.*, 2013).

Type	Alkaloids Detected	Activities Reported
Yohimbine	α-Yohimbine	Pre- and postsynaptic α_2-adrenoceptor inhibitor, stimulant and aphrodisiac effect, antidiabetic
18-Hydroxy-yohimbine	Reserpine	Antipsychotic, antihypertension, antidepression, anticancer, carcinogenesis
	Rescinnamine	Antihypertension
Heteroyohimbine	Aricine	Unknown
	Reserpiline	Antipsychotic, antigastric secretion, antihypertension
	Isoreserpiline	Antipsychotic
Dihydroindole	Sarpagine	Unknown
	Ajmaline	Antiarrhythmia, antifibrillation, cardiac and liver toxicity
	Sandwicine	Unknown
	Iso-sandwicine	Unknown
	Mitoridine	Unknown
	Rauvomitine	Unknown
	N-demethyl-rauvomitine	Unknown
	Purpeline	Unknown
	Seredamine	Unknown
	Suaveoline	Unknown
	Tetraphyllicine	Myocardial excitation
	Vomalidine	Unknown
	Serpentine	Antioxidant, possible anticancer
	Alstonine	Antipsychotic, possible anticancer
Ψ-Indoxyl	Isoreserpiline- Ψ-indoxyl	Unknown
Oxindole	Carapanaubine	Unknown
	Rauvoxine	Unknown

CHAPTER THREE

MATERIALS AND METHODS

3.1 EXPERIMENTAL ANIMALS

Forty male Wistar strain albino mice approximately 8-10 weeks old with average weight of 20g obtained from the Animal House of the University of Lagos Teaching Hospital (LUTH), Idi-Araba, Lagos State, Nigeria were used for the experiment. They were housed five per cage with wood shaven bedding in polypropylene cages under standard environmental conditions of 50± 10% relative humidity, 29 ± 2 ^{0}C temperature and 12 hours light and 12 hours dark cycle at the Experimental Animal House, Department of Chemical Sciences, Bells University of Technology, Ota, Ogun State, Nigeria. They were fed with mice pellet containing at least 20% protein, 3.5% fat, 9.0% fibre, 1.2% calcium, 0.7% phosphorus, vitamin, mineral per mix, antioxidant, antibiotics, carbohydrates etc from God First Feed Mill, Bodija, Ibadan, Nigeria and water *ad libitum*. A period of two weeks was allowed for the animals to acclimatize before the commencement of the experiment. Test and control substance were administered methanol extract of *Rauvolfia vomotora* (RV), potassium dichromate ($K_2Cr_2O_7$) and sodium arsenite (SA) as summarized in Figure 3.8. The RV was given orally for seven days, while potassium dichromate $K_2Cr_2O_7$ and SA were administered on day seven of the experiment.

3.2 PLANT COLLECTION AND EXTRACTION

Fresh leaves of *Rauvolfia vomotora* (RV) were collected from the Botanical Garden, University of Ibadan, Ibadan. The leaves identified by Mr. O.S. Shasanya and Osiyemi O.A. at the herbarium in the Forestry Research Institute of Nigeria (FRIN), Ibadan and voucher specimen deposited at the same herbarium (Voucher No: FHI108901). The fresh leaves were air dried for 8 weeks at room temperature, after which they were completely dried in a solar drier at 40 ^{0}C. It was then milled in a hammer- miller with mesh size 0.27µm. 100g of the powder obtained was soaked in 1000ml for 48 hours in 70% methanol and cold extraction carried out. The suspension obtained was filtered and concentrated with a rotary evaporator under reduced pressure at 40 ^{0}C. The percentage yield was 9.7 %. A dosage 275 mg/kg body weight corresponding to 1/25th of the LD 50 of RV (Amole *et al.*, 1993) was dissolved in distilled water and injected intraperitoneally into test animals.

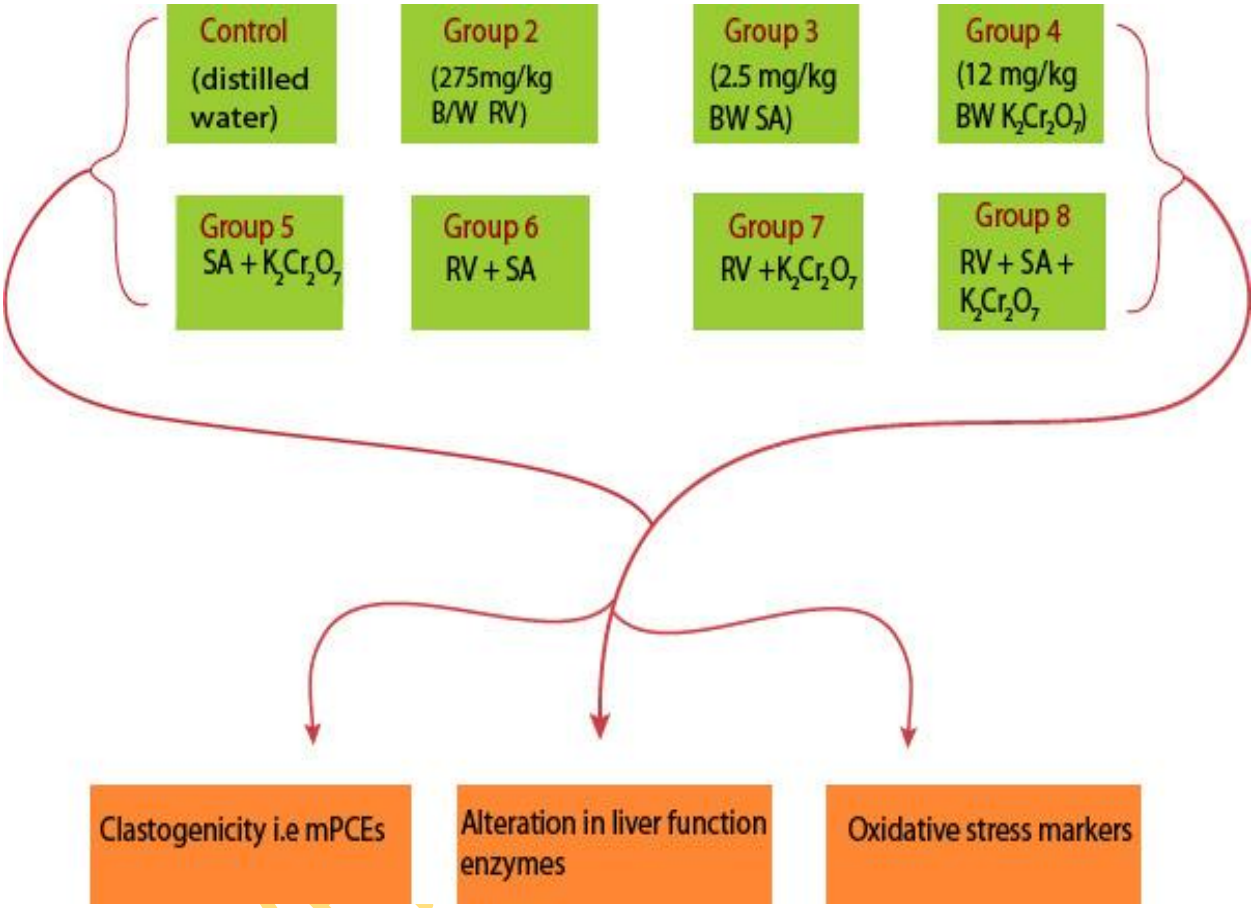

Figure 3.1: Protocol for the administration of test substances.

3.3 DETERMINATION OF PLATING EFFICIENCIES OF CH310T½ CELLS

Principle

The plating efficiency of cells also known as clonogenic cell survival assay determines the ability of a cell to proliferate indefinitely, thereby retaining its reproductive ability to form a large colony or a clone (Munshi *et al*, 2005). Loss of reproductive integrity and the inability to proliferate indefinitely are the most common mechanism of cell death. Therefore, a cell that retains its ability to synthesize proteins and DNA and go through one or two mitoses, but is unable to divide and produce a large number of progeny is considered dead. This is referred to as loss of reproductive integrity or reproductive death and it is the end point measured with cells in culture. In contrast, a clonogenic cell is reproductively active, retains its ability to divide and proliferate into a large colony of cells. The ability of a single cell to grow into a large colony that can be visualized with the naked eye or microscope is a proof that it has retained its capacity to reproduce. The loss of this ability as a function of dose of radiation or chemotherapy agent is described by the dose-survival curve

Reagents

10% Fetal Bovine Serum

50 ml fetal bovine serum was made up 500 ml with basal medium eagle (BME)

1% Crystal violet Stain

1 g of crystal violet is weighed and dissolved in 20 ml of methanol and made up to 100 ml with distilled water

Procedure

Once 10T½ cells from passage 7-8 had grown to 80% confluence, the standard steps of the plating efficiency protocol were conducted as follows: Medium was aspirated and 1ml of DPBS (Dulbecco's Phosphate Buffered Saline 1X) was added to the cells to remove serum-containing trypsin inhibitors. DPBS was aspirated and 1ml of trypsin was added back to each flask. Once a majority of the cells were detached from the vented flask, 1ml of medium containing 10% FBS was added to neutralize the trypsin. The cell suspension was then transferred to a centrifuge tube and centrifuged for 12 minutes at 3,000 rpm on an IEC-HN-S table top centrifuge. Next, the supernatant was aspirated, and the cell pellet was resuspended in 10 ml of BME containing 10% FBS. 1ml of the resuspended cell suspension was diluted 1:20 with PBS, aliquoted, and counted

using a Coulter Counter Model Zf (Coulter Electronics, Hialeah, Florida). The cells were then diluted to a concentration of 200,000 cells/5 ml, serially diluted 1:10 three more times, and seeded onto the 60-mm tissue culture dishes at 200 cells/dish in 5 ml of BME containing 5% fetal bovineserum (FBS). Five dishes per treatment group were seeded for plating efficiency determination. This method has been published in previous studies (Reznikoff *et al*, l973a, b; Landolph and Heidelberger, l979; Miura *et al*, l987; Patierno *et al*, l988). Two days after seeding, the media were changed and cells were cultured for additional 8 days. Cells were then fixed with methanol for 30 minutes, the methanol was removed by aspiration, and finally, the cells were stained with 1% crystal violet in water for one hour as previously described by Reznikoff *et al*., l973a. Colonies containing 20 or more cells were counted and averaged in the five dishes. Relative survival was determined as a percentage of survival of cells.

3.4 PHAGOCYTIC UPTAKE DETERMINATION

Principle

The entry of a toxin into the cell is a vital step that determines whether or not the toxin will exert a carcinogenic effect on the cell through mutagenic or epigenetic mechanisms (Muñoz and Costa, 2012). Therefore, the varying toxicities associated with toxic compounds may be dependent on how they are internalized and the degree of internalization of their particles

Reagents

70% Ethanol

70 ml of ethanol was mixed with 30 ml of distilled water.

1% Crystal violet Stain

1 g of crystal violet was dissolved in 20 ml of methanol and made up to 100 ml with distilled water

Procedure

The 10T½ cells were seeded at 2,000 cells in 60 mm dishes and treated after 24 hours. Two days later, cells were fixed with 70% ethanol, stained with 1 % crystal violet, and examined with a light microscope at 200x magnification. The amount of vacuolated and anucleated cells were scored in 100 cells in treated and control groups.

Alternatively, 500,000 logarithmic growing cells were seeded in 75ml flask and allowed to adhere overnight. Cells were treated and harvested by trypsinisation , fixed with ½ strength karnovsky's fixative for 2 h at 4 °C and post fixed in 2% osmium tetra oxide for 1hr, and rinsed

again three times in cacodylate buffer. The pellets were block stained in 1% uranyl acetate overnight. Cell pellets were washed in three changes of distilled water, gelatinized with 15% bovine serum albumin for 3 hours and dehydrated in graded ethanol. Subsequently, pellets were treated with a graded series of ethanol- propylene oxide as well as EPON-propylene oxide. Pellets were covered with EPON overnight and suspended in fresh pure EPON three times for at least three hours and embedded in beam capsules using pure EPON. Polymerization was thermally induced by incubating the samples overnight at 60°C. Semi thin plastic sections (1-2 µm) were cut with glass knives, stained uranyl acetate and evaluated for the percentage of cells containing chromate particle using a Scanscope Microscope.

3.5 SCANNING ELECTRON MICROSCOPY

Principle

The scanning electron microscope (SEM) uses a focused beam of high-energy electrons to generate a variety of signals at the surface of solid specimens. The signals derived from electron-sample interactions reveal information about the sample including external morphology (texture), chemical composition, and crystalline structure and orientation of materials making up the sample. The basic principle is that a beam of electrons is generated by a suitable source (e.g. tungsten filament or a field emission gun). The electron beam is accelerated through a high voltage (e.g. 20 kV) and pass through a system of apertures and electromagnetic lenses to produce a thin beam of electrons, then the beam scans the surface of the specimen and electrons emitted from the specimen are then collected by a suitably-positioned detector.

Reagents

0.2% Sodium Cacodylate Buffer

42.8g of sodium cacodylate was dissolved in 1 liter of double distilled water. The mixture was stirred until the sodium cacodylate was completely dissolved. The pH was adjusted to 7.2.

½ strength Karnovsky's fixative in cacodylate buffer 10% stock

20 ml of 2% paraformaldehyde was mixed with 5 ml of 2.5 % glutaraldehyde, 50 ml of 0.1M cacodylate buffer, 12.5ml of 200mg/ml Calcium Chloride and 12.5 ml of distilled water. The pH was adjusted to 7.2.

2% (w/v) paraformaldehyde

A total volume of 10 ml of 16% formaldehyde is added to 70ml of 1M PBS.

Ethanol

50, 75, 85, 95% absolute ethanol in distilled water and 100%.

2% osmium tetroxide

1 g OsO_4 was dissolved in 50 ml of distilled water

Hexamethyldisilizane- Ethanol

50%, 75%, 85%, 95%, hexamethyldisilizane in absolute ethanol and 100%

Procedure

Scanning electron microscopy was performed at the Electron Microscopy Facility of Cell and Tissue Imaging Core at USC/Norris Comprehensive Cancer Center, University of Southern California Los Angeles. Cells were seeded in a 25 ml flask and allowed to reach 70% confluence before treatment. Immediately following treatment, dishes containing the cells were rinsed twice in PBS and ½ strength karnovsky's fixative for 2h , after which they were rinsed in three changes of 0.1 M sodium cacodylate-buffer, (10 min each), post-fixed with 2% OsO_4 for1 hour and rinse in 0.1 M sodium cacodylate buffer. Cells were later washed in three changes of water and dehydrated with ascending graded ethanol (50, 70, 85, 95 and 100%) as well as infiltrated with 50%, 75%, 85%,95%, hexamethyldisilizane- ethanol. Dishes were air-dried, cut with hot scapel and mounted on aluminum SEM stubs mounted on a stub with silver adhesive (Electron Microscopy Sciences, Hatfield, PA, U.S.A.). The cut sections of the dish were later gold coated in an Electron Microscopy Science Sputter Coater and examined in a JOEL JSM 6390LV Scanning Electron Microscope at 10KV.

Reagents

70% ethanol

70 ml of absolute ethanol was mixed with 30 ml of distilled water

1% Crystal violet Stain

1 g of crystal violet was dissolved in 20 ml of methanol and made up to 100 ml with water.

3.6 TRANSMISSION ELECTRON MICROSCOPY

Principle

Transmission Electron Microscopy (TEM) is an imaging technique that uses electron beam to image a sample. High energy electrons, incident on ultra-thin samples allow for image

resolutions that are on the order of 1-2Å. The high energy electrons (up to 300 kV accelerating voltage) are accelerated nearly to the speed of light. The electron beam behaves like a wave front with wavelength about a million times shorter than light waves. When an electron beam passes through a thin-section specimen of a material, electrons are scattered and sophisticated system of electromagnetic lenses focuses the scattered electrons into an image or a diffraction pattern, or a nano-analytical spectrum, depending on the mode of operation.

Reagents

0.2% Sodium Cacodylate Buffer

42.8g of sodium cacodylate was dissolved in 1 liter of double distilled water. The mixture was stirred until the sodium cacodylate was completely dissolved. The pH was adjusted to 7.2.

½ strength Karnovsky's fixative in cacodylate buffer 10% stock

20 ml of 2% paraformaldehyde was mixed with 5 ml of 2.5% glutaraldehyde, 50 ml of 0.1M cacodylate buffer, 12.5ml of 200mg/ml Calcium Chloride and 12.5 ml of distilled water. The pH was Adjust to 7.2.

15% bovine serum albumin

15 g of bovine serum albumin was dissolved in 100ml distilled water

2% (w/v) paraformaldehyde

A total volume of 10 ml of 16% formaldehyde was added to 70ml of 1M PBS.

2% osmium tetroxide

1 g OsO_4 is dissolved in 50 ml of distilled water

Ethanol

50, 75, 85, 95% absolute ethanol in distilled water and 100%.

Ethanol -propylene oxide

50, 75, 85, 95% propylene oxide in ethanol and 100%.

EPON 812 resin -propylene oxide

50, 75, 85, 95% epon 812 resin in propylene oxide and 100%.

Procedure

Transmission electron microscopy was performed at the Electron Microscopy Facility of Cell and Tissue Imaging Core at USC/Norris Comprehensive Cancer Center, University of Southern

California Los Angeles. Cells were seeded in a 75 ml flask and allowed to reach 70% confluence before treatment. Cells trypsinised and centrifuged at 5000 x g for 5minutes. Cell pellets were washed in three changes of distilled water, gelatinized with 15% bovine serum albumin for 3 hours and dehydrated in 50%, 70%, 85%, 95% and 100% ethanol. Subsequently, pellets were treated with a graded series of ethanol- propylene oxide as well as EPON-propylene oxide. Pellets were covered with EPON overnight and suspended in fresh pure EPON three times for at least three hours and embedded in beam capsules using pure EPON. Polymerization was thermally induced by incubating the samples overnight at 60 °C. Ultrathin sections (70–80 nm) were cut with a microtome diamond knife and mounted on copper grids, stained with uranyl acetate. Sections were observed using a transmission electron microscope (JEOL 2100) operated at 80 kV. Intracellular chromate particles were confirmed by energy-dispersive X-ray analysis (EDX) by Edax Inc. (Mahwah, USA). X- rays beam were focused on the portion of the cytoplasm and nucleus containing chromate particles. The EDX spectra of the elements in the particles were thereafter obtained.

3.7 DETERMINATION OF CELL CYCLE KINETICS

Principle

Measurement of cellular DNA content and the analysis of the cell cycle can be performed by flow cytometry**.** In addition to determining the relative cellular DNA content, flow cytometry also enables the identification of the cell distribution during the various phases of the cell cycle. Four distinct phases could be recognized in a proliferating cell population: the G1-, S- (DNA synthesis phase), G2- and M-phase (mitosis). Usually, a fluorescent dye such as popidium iodide that binds to the DNA is added to a suspension of permeabilized single cells or nuclei.

Popidium iodide binds stoichiometrically to the DNA in a suspension of single cells or nuclei. The stained cells incorporate an amount of dye proportional to the amount of DNA. The stained material is then measured in the flow cytometer and the emitted fluorescent signal yields an electronic pulse with a height (amplitude) proportional to the total fluorescence emission from the cell. The fluorescence data are considered a measurement of the cellular DNA content. Samples are analyzed at rates below 1000 cells per second in order to yield a good signal for discrimination between singlets or doublets

Reagents

70% ethanol

70 ml of absolute ethanol was mixed with 30ml of distilled water

0.05mg/ml of popidium iodide

0.5mg of popidium iodide was dissolved 10 ml of PBS

0.1 mg/mL of DNase-free RNaseA

1mg of RNase was dissolved in 10ml PBS

Procedure

Hundred thousands cells were seeded into 75 ml flask and allowed to grow to 70% confluence. The exponentially growing cells were treated and after treatment, cells were harvested and washed with PBS after a gentle centrifugation at 200 × *g* for 5 minutes. Cells were thoroughly resuspended in 0.5 mL of PBS and fixed in 70% ethanol for at least 2 hours at 4°C. Ethanol-suspended cells were then centrifuged at 200× *g* for 5 minutes and washed twice in PBS to remove residual ethanol. For cell cycle analysis, the pellets were suspended in 1 mL of PBS containing 0.05mg/mL of propidium iodide, 0.1 mg/mL of DNase-free RNase A and incubated in dark at room temperature for 1 hour . Cell cycle profiles were obtained using a FACScan flow cytometer (Becton Dickinson, San Jose, CA) and data were analyzed by ModFit LT software (Verity Software House, Inc., Topsham, ME).

3.8 ASSESSMENT OF CASPASE ACTIVATION

Principle

Caspase activation is an essential event in the apoptotic pathway. Caspase-3 is one of the important "executioner" caspase enzymes that trigger the cleavage of numerous proteins leading to the orderly breakdown of the cell. The assessment of caspase-3 activation is often used as a marker for apoptosis. Glo-apo-tox assay kit from Promega (Madison, WI USA) was used in this study. The Glo-apo-tox assay kit uses a luminogenic caspase-3/7 substrate that contains the tetrapeptide sequence DEVD, in a reagent optimized for caspase activity, luciferase activity and cell lysis. Addition of the Caspase-Glo 3/7 Reagent results in cell lysis, followed by caspase cleavage of the substrate and generation of luminescent signal produced by luciferase (Figure 3.2). Luminescence is proportional to the amount of caspase activity present. In addition, the assay kits also simultaneously measures viability and cytotoxicity within the same assay well. This involves two proteases. The live-cell protease activity is restricted to intact viable cells and

is measured using a fluorogenic, cell-permeant, peptide substrate (glycylphenylalanyl-aminofluorocoumarin; GF-AFC). The substrate enters intact cells where it is cleaved by the live-cell protease activity to generate a fluorescent signal proportional to the number of living cells. In contrast, the live-cell protease becomes dormant when there is damage to the cell membrane and leakage of cell content into the surrounding culture medium.

A second, fluorogenic cell-impermeant peptide substrate (bis-alanylalanyl-phenylalanyl-rhodamine 110; bis-AAF-R110) is used to measure dead-cell protease activity that is released from cells that have lost membrane integrity (Figure 1). Bis-AAF-R110 is not cell-permeant, therefore no signal would be generated in intact, viable cells. The live- and dead-cell proteases produce different products, AFC and R110, which have different excitation and emission spectra, allowing them to be detected simultaneously.

Reagent

Glo-apo-tox assay assay kit

Glo-apo-tox assay triplet assay kit from Promega (Madison, WI USA)

Procedure

The assays were carried out according to manufacturer's instruction**.** 15,000 logarithmic growing cells were seeded per well in 96-well plate , opaque-walled tissue culture plates with clear bottoms. Cells were treated and after the treatment, 20µl of Viability/Cytotoxicity Reagent containing both GF-AFC and bis-AAF-R110 substrate were added to all the wells, mixed briefly by orbital shaking at 300–500rpm for ~30 seconds and incubated for 60 minutes at 37°C. Fluorescence were measured at 400Ex/500Em and 485 Ex/520Em for viability and cytotoxicity respectively. 100µl of Caspase- Glo® 3/7 Reagent was added to all wells, mixed and incubated for 60 minutes at 25°C and luminescence measurement were read. Luminescence is proportional to the activity of caspase.

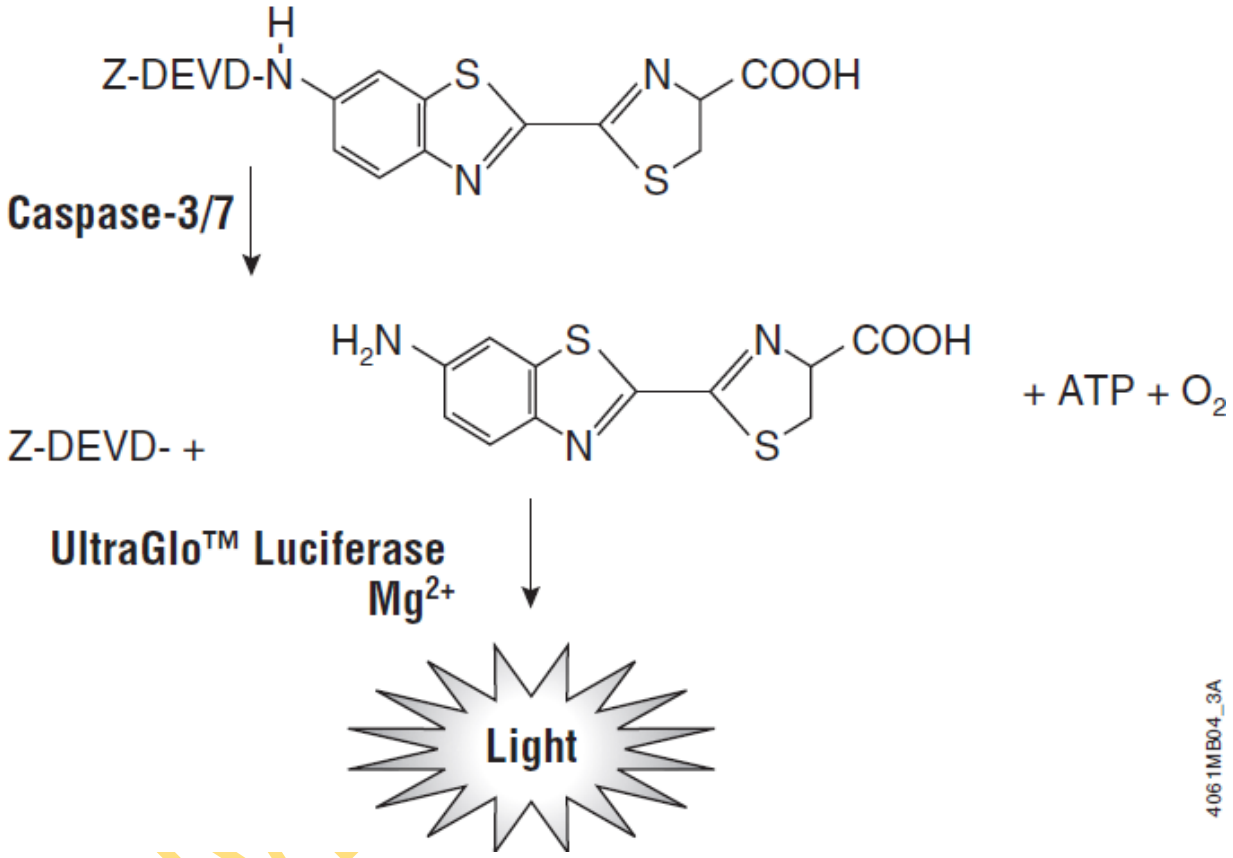

Fig ure 3.2: Caspase-3/7 cleavage of the luminogenic substrate containing the DEVD substrate. Aminoluciferin is released after caspase cleavage, resulting in the luciferase reaction and the production of light **(**Promega, 2012)

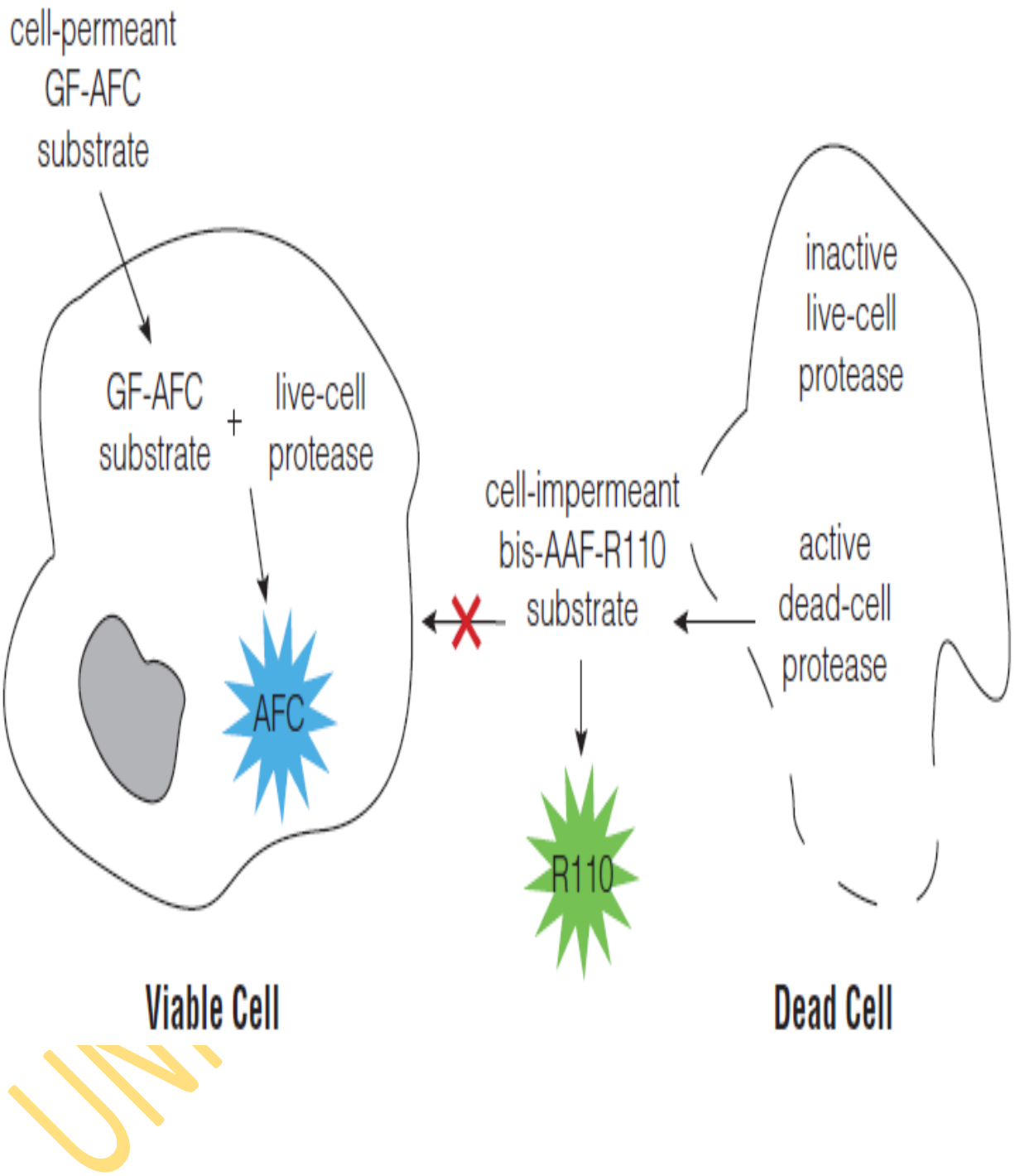

Figure 3.3: Principle of the Viability /Cytotoxicity Assay. The GF-AFC Substrate can enter live cells where it is cleaved by the live-cell protease to release AFC. The bis-AAF-R110 Substrate cannot enter live cells but instead can be cleaved by the dead-cell protease to release R110. **(**Promega, 2012)

3.9 ASSESSMENT OF APOPTOSIS AND NECROSIS

Principle

Cells were double stained the with acridine orange (AO) and propidium iodide (PI) and scored for apoptosis and necrosis as described by Ciapetti *et al*., 2002 with slight modification. AO and PI are intercalating nucleic acid-specific fluorochromes which emit green and orange fluorescence, respectively, when they are bound to DNA. Of the two, only AO can cross the plasma membrane of viable and early apoptotic cells. PI will only interact with the DNA of cells with damaged cell membrane. Therefore, viable cells are identified as green, while apoptotic cells were identified by their green nuclei with evident membrane blebbing or dense orange nuclei indicating DNA condensation. Necrotic cell have intact orange nuclei and sometimes with vacuoles. The assay provides a useful simultaneous quantitative evaluation for necrosis and apoptosis.

Reagents

Acridine Orange Stain

0.20 mg of acridine orange was dissolved in 20ml of PBS

Popidium Iodide Stain

0.20 mg of popidium iodide was dissolved in 20ml of PBS

Procedure

Cell death in CH310T ½ cells was quantified using propidium iodide (PI) and acridine orange (AO) double-staining according to standard procedures and examined under fluorescence microscope (EVOS). Briefly 15,000 cells were cultured in slide chambers. Cells were allowed to attach overnight and treated. After treatment, cells were rinsed with phosphate buffered saline (PBS) and resuspended in BME. 15µl of fluorescent dyes containing AO (10 μgml^{-1}) and PI (10μgml^{-1}) were later added to each chamber and slides were observed with an inverted EVOS UV-fluorescence microscope equipped with a digital camera (Advanced Microscopy Group, Bothell, WA) within 30min before the fluorescent color starts to fade. The percentages apoptotic and necrotic cells were determined in >200 cells.

3.10 ASSESSMENT OF INDUCTION OF AUTOPHAGY

Principle

An investigation on the third form of cell death, autophagy was also carried out. This was monitored by imaging the distribution of LC3B protein in the cytoplasm. The LC3B protein plays a critical role in autophagy. Normally, this protein resides in the cytosol, but following cleavage and lipidation with phosphatidyl ethanolamine, LC3B associates with the phagophore. This localization can be used as a general marker for autophagic membranes (Figure.3.3).

Premo Autophagy Sensors (LC3B-FP) BacMam 2.0 from Molecular Probes (Eugene, OR) was used in this work. The Premo™ Autophagy Sensor combines the selectivity of an LC3B-fluorescent protein (FP) chimera with the transduction efficiency of the BacMam 2.0 technology. BacMam reagents (insect Baculovirus with a Mammalian promoter) are safe to handle (Biosafety Level 1) because they are non-replicating in mammalian cells. They are also non-cytotoxic and ready- to-use. Unlike other expression vectors, BacMam reagents enable titratable and reproducible expression and offer high co-transduction efficiency. Multiple BacMam reagents can therefore be readily used in the same cell. Recent improvements made to the BacMam system, BacMam 2.0, enable efficient transduction in a wider variety of cells, including neurons and neural stem cells (NSCs). The two-step protocol for imaging autophagy involves simply adding the BacMam LC3B-FP to the cells and incubating them overnight for protein expression

Reagent

Premo Autophagy Sensors (LC3B-FP) BacMam 2.0 Assay Kit

Premo Autophagy Sensors (LC3B-FP) BacMam 2.0 Assay Kit from Molecular Probes (Eugene, OR) was used in assessing the extent of autophagy.

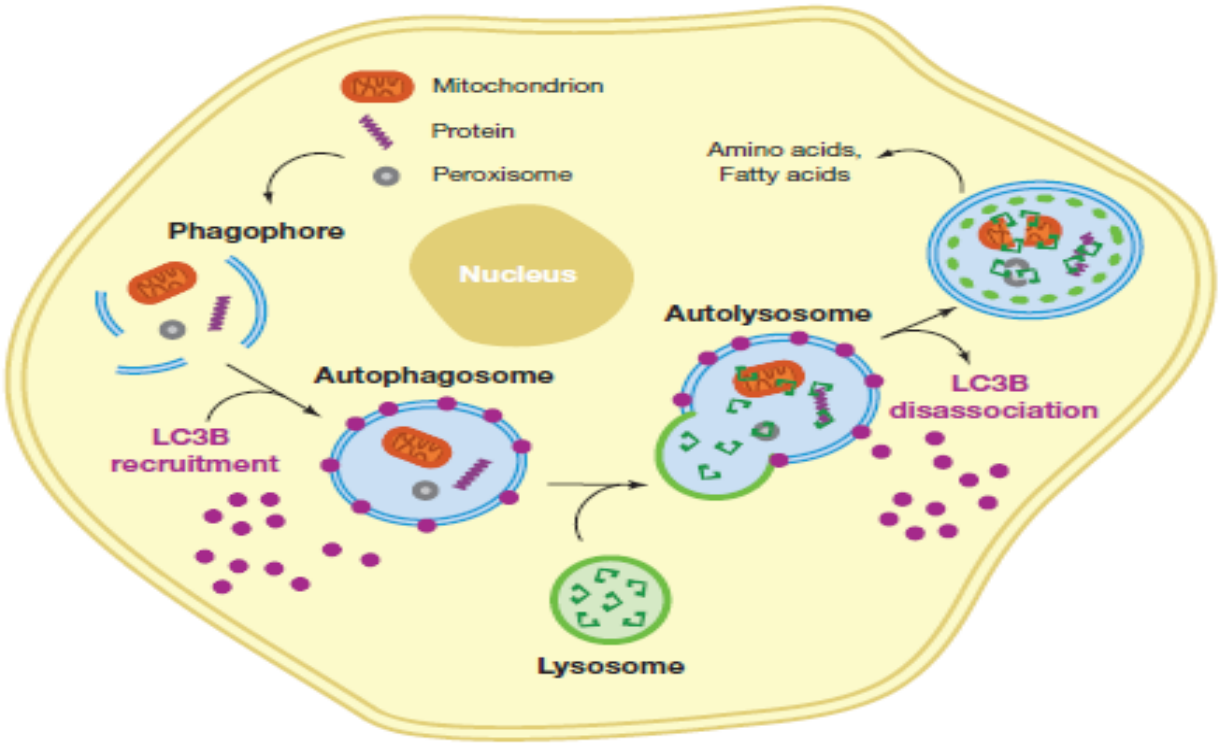

Figure 3.4 Schematic depiction of the autophagy pathway in a eukaryotic cell (Molecular Probes, 2010)

d

Procedure

Ten thousand logarithm growing cells were placed in a 4 slide chamber and allowed to adhere overnight. Cells were later transduced with the LC3B protein for 24 hours in order to allow the expression of the LC3B protein. Thereafter, cells were treated and slides were observed with an inverted EVOS UV-fluorescence microscope equipped with a digital camera (Advanced Microscopy Group, Bothell, WA). The number of cells expressing LC3B-GFP puncta in 10 fields (>100 cells) were scored and expressed as a percentage of the total cells in the test and control groups.

3.11 ASSESSMENT OF ACTIN DISRUPTION

Principle

The actin filaments are the major component responsible for the maintenance of global cell shape in fibroblast (Ujihara *et al*, 2008). Actin plays diverse role in cell growth, maintenance of cell polarity and morphology, locomotion and signal transduction. The transmission electron microscopy (TEM) observations that chromate exposure led to disruption of cytoskeleton informed the decision to stain cells with actin specific dye, TRITC phalloidin. Rhodamine phalloidin is the most widely used F-actin stain. It is a bicyclic peptide that is isolated from mushroom, *Amanita phalloides* toxin conjugated to the orange-fluorescent dye, tetra methylrhodamine (TRITC). It is commonly used in cellular imaging to specifically label F-actin in fixed cells, permeabilized cells, and cell-free experiments. The red fluorescent probe binds to F-actin with nanomolar affinity and very photostable. It binds in a stoichiometric ratio of about one phallotoxin per actin subunit in both muscle and nonmuscle cells.

Reagents

3.7% formaldehyde

3.7 ml of formaldehyde was made up 100ml with PBS

Phalliodin Stain

0.5 mg of tetramethylrhodamine (TRITC) phalloidin was dissolved in 100 ml

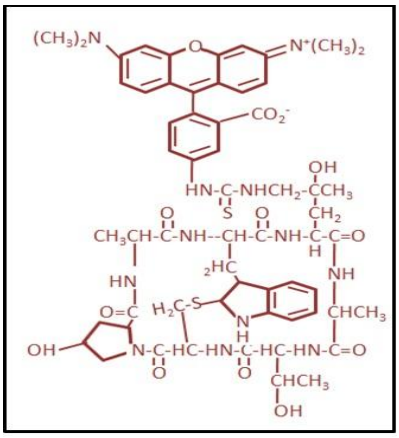

Figure 3.5: Rhodamine Phalloidin

Procedure

Hundred thousand log phase cells were seeded into Lab-Tek II chamber slides and allowed to adhere overnight. Cells treated were and following treatment, cells were washed with phosphate buffered saline and fixed for 5 minutes in 3.7% formaldehyde solution in PBS. Subsequently, cells were washed three times in PBS and stained with a 50 µg/ml fluorescent phalloidin conjugate solution for 90 minutes at room temperature. Cells were later washed several times with PBS to remove unbound phalloidin conjugate. Cells were later observed with an inverted EVOS UV-fluorescence microscope and images captured with a digital camera (Advanced Microscopy Group, Bothell, WA). Images were loaded into Cell Profiler, a cell image analysis software, and then subjected to a "pipeline" of steps that were meant to calculate the mean intensity of the image. The pipeline begins by loading images with the appropriate names (Load Images) and converting them to grayscale (ColorToGray). The software then uses the Sobel method to detect "edges" within the image, providing boundaries for intensity calculation (EnhanceEdges). Next, a threshold is applied to the grayscale, bounded image, converting all pixels to either black or white (ApplyThreshold). Finally, the software measures the mean intensity of the image, and stores it in a spreadsheet.

3.12 MORPHOLOGICAL TRANSFORMATION ASSAY

Assay for the incidence of focus formation was carried out following the method of Nesnow *et al*., 1980.

Principle

Exposure of cells to chemical carcinogen and other cancer causing agent can altered the growth control mechanism of normal cells into neoplastic transformed ones (Figure 3.5). *In vitro* cell transformation is the induction of phenotypic alterations in cultured cells that are characteristic of tumourigenic cells (Kakunaga and Kamasaki *et al.*, 1985). Transformed cells with the characteristics of malignant cells have the ability to induce tumours in susceptible animals. These new characteristics include:

I. Proliferation at higher rate and production of foci (discrete focal area of growth) on a dense monolayer of normal cells
II. Anchorage independent i.e. transformed cells form colonies or grow in soft agar where as normal cells do not
III. Transformed cells formed tumors after injection into susceptible animals

Reagents

Normal saline

0.9 g of NaCl was dissolved in 100 ml of distilled water.

Giemsa stain

Five grams of Giemsa powder was dissolved in 1ml of ethanol before diluting in 50 mls of distilled water.

Procedure

The 10T½ cells were grown to 70% confluence, trypsinized and seeded into 60-mm dishes in 5 ml medium at 2,000cells per dish. Twenty dishes were plated per concentration. Five days post seeding, cells were treated and the medium was then changed after treatment. The medium was subsequently changed once a week for 6 weeks. At the end of the sixth week of the transformation assay, the dishes were rinsed with 0.9% NaCl saline, fixed with methanol, stained with Giemsa and scored for foci under a dissecting microscope, according to standards methods (Reznikoff *et al*, l973b; Landolph and Heidelberger, l979; Miura *et al*., l987; Patierno *et al.*, l988; Landolph, l994).

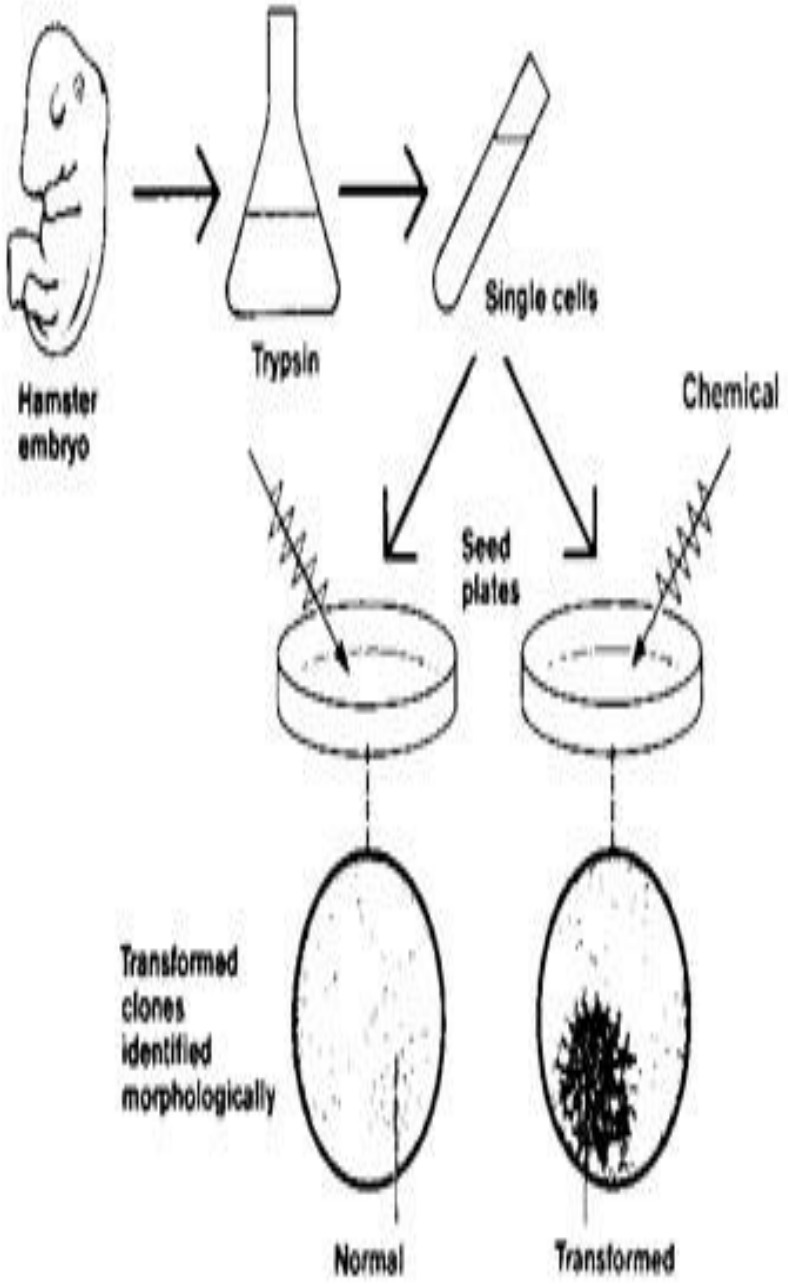

Figure 3.6: Morphological Transformation Assay *In-vitro* (Hall and Hei, 1986)

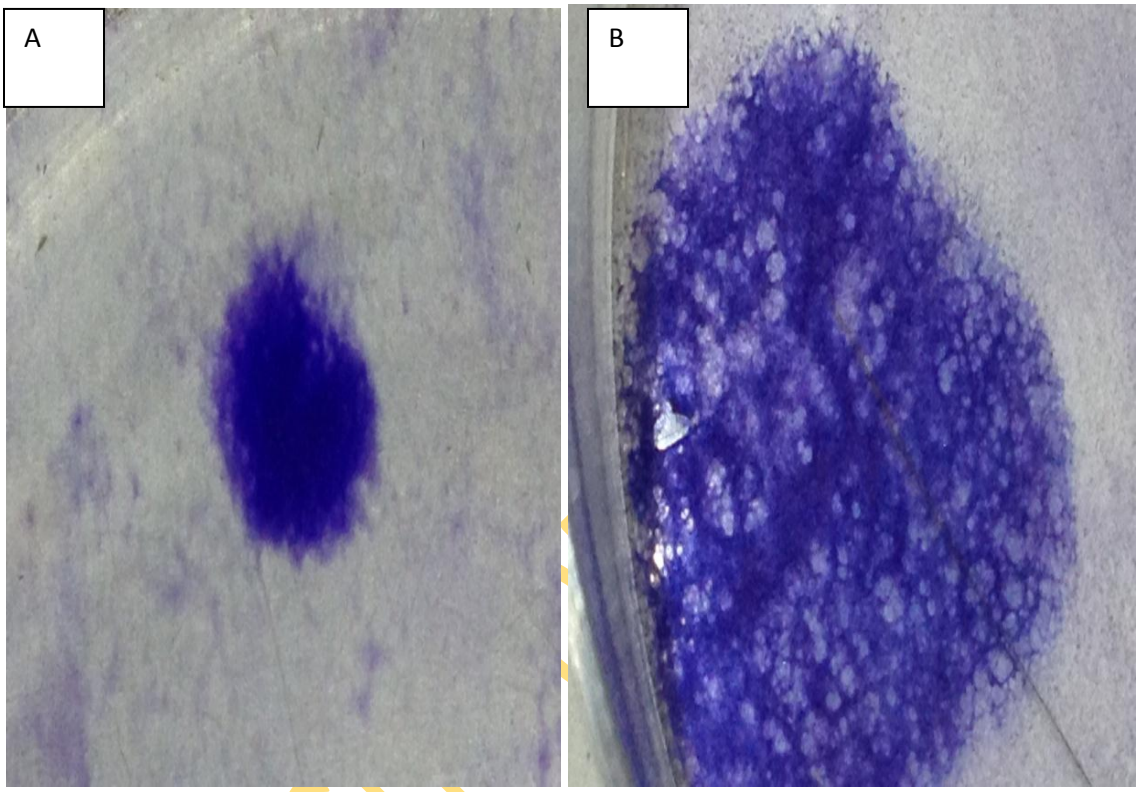

Figure 3.7: Type II (a) and Type III foci (b) observed in 10 T½ cells treated with hexavalent chromate compounds

3.13 DETERMINATION OF THE EXPRESSION OF APOTOSIS, AUTOPHAGY AND NECROSIS RELATED GENES

Principle

RT^2 Profiler PCR Array is employed in the monitoring the expression profile of cell death related genes. Real-time RT-PCR is a reliable and very sensitive method for gene expression analysis. The method is very dynamic and it is used in the quantification of both rare and abundant genes in biological samples. RT^2 Profiler PCR arrays take advantage of the combination of real-time PCR performance and the ability of microarrays to detect the expression of many genes simultaneously. RT^2 Profiler PCR Arrays are designed to analyze a panel of genes related to a disease state or biological pathway. The arrays are provided in 96 or 384-well plates with microfluidic chips. 96-well plates contain primer assays for 84 pathway or disease-focused genes and 12 other housekeeping and control genes.

Reagents

RNeasy Mini Kit (Qiagen,Valencia, CA)

PrimeScript™ RT Master Mix from Takara (Frederick, MD)

SYBR® Premix Ex Taq II (Tli RNaseH Plus)

Procedure

One hundred thousand log phase growing cells were seeded in a 75 ml flask and cultured to 70% confluence before cells were harvested by trypsinisation. The harvested cells was then subjected to centrifugation at 5000 x g for 5minutes. Total RNA was prepared from the cell pellet using triazol and purification was carried out with RNeasy Mini Kit (Qiagen,Valencia, CA) according to the manufacturer's instructions. Complimentary DNA (cDNA) was then produced with 0.5µg of RNA template for each sample using the PrimeScript™ RT Master Mix from Takara (Frederick, MD) following the manufacturer's instruction. To complete the reaction, samples were incubated for 15 minutes at 37 ^{0} C, 5 secs at 85 ^{0} C and then 4^0 C until samples were stored at -80^0 C. The cDNA obtained was used with SYBR® Premix Ex Taq II (Tli RNaseH Plus) from Takara for RT PCR profiling in 96-well Cell Death RT^2 Profiler PCR arrays (PAMM 212Z from Qiagen). The PCR mixture contains 2.75ml SYBR® Premix Ex Taq II (2X), 0.44ml cDNA, 0.11 ml ROX Reference Dye (50X) and 17 ml sterile distilled water. 50µl of reaction mixture was then dispensed into each well and relative quantification of RNA was

determined by real time PCR using an Applied Biosystems 7300 Real Time PCR System and analyzed with 7300 System SDS software v 1.3.1. Each sample was subjected to 40 cycles with an initial incubation of 50° C for 2 min. followed by 90° C for 10 min and then 40 cycles of 95° C followed by 1 minute of 60° C. A manual Ct threshold of 0.0500 was used for all samples and the sample baseline was obtained from cycles 3 through 15. Data were analysed based on ΔΔCt (manual) method using the RT^2 Profiler PCR Arrays Data Analysis soft ware version 3.5 on Qiagen's website: http://pcrdataanalysis.sabiosciences.com/pcr/arrayanalysis.php. For each gene, fold-changes were calculated as difference in gene expression between control and treated the cells or the transformed cell line.

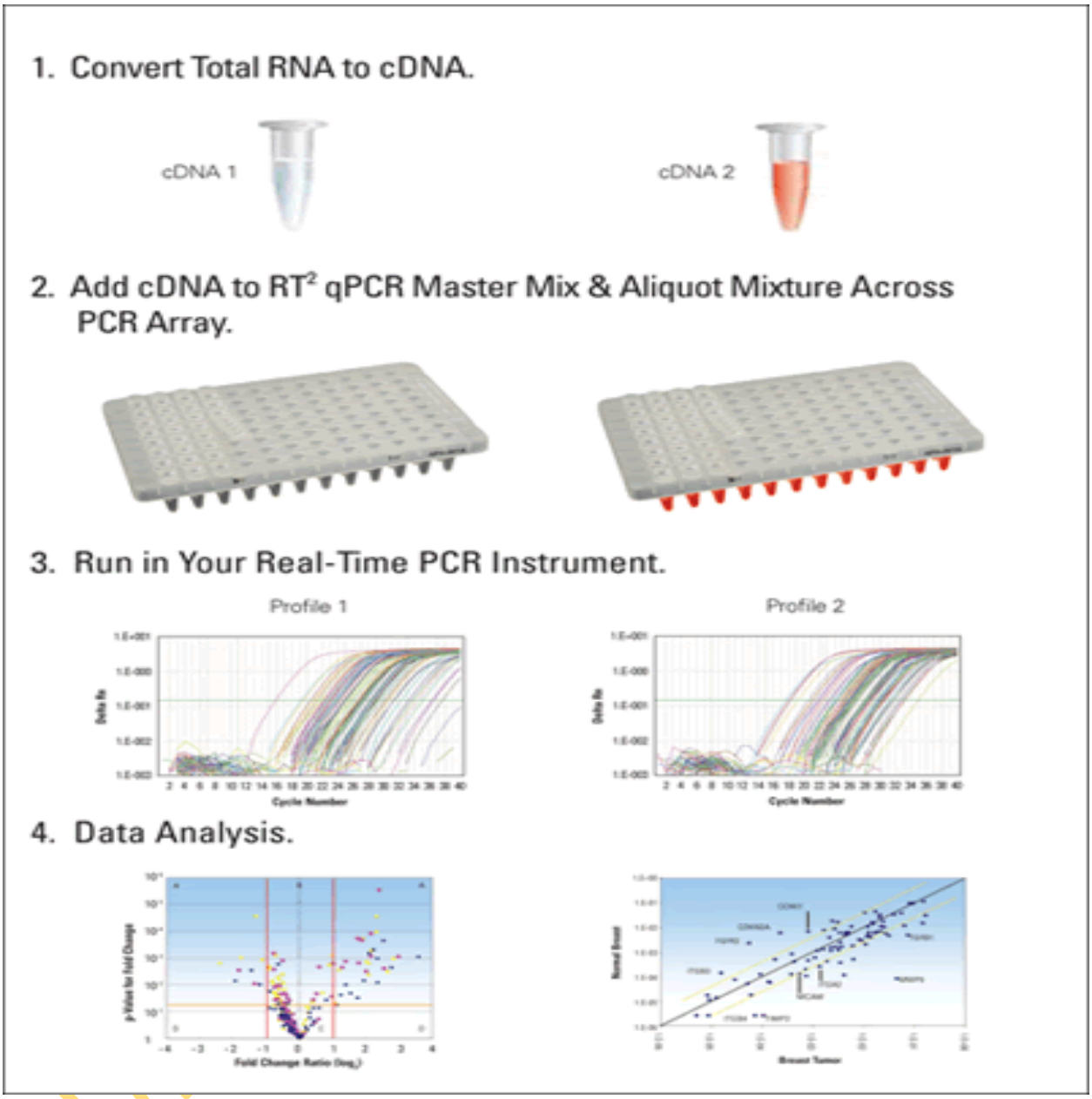

Figure 3.8: Protocol Chart of RT-PCR Array (Qiagen, 2012)

3.14 MICRONUCLEUS ASAY

The frequency of micronuclei formation was determined by the method of Schmid *et al*., 1975.

Principle

A micronucleus (MN) is a small extra nucleus separated from the main one, generated during cellular division by late chromosomes or by chromosome fragments, due to its association with chromosomal aberrations. The mouse MN assay is the most widely used and best validated in vivo test for genotoxicity (Mavournin *et al.*, 1990; Morita *et al.*, 1997). The *in vivo* MN assay has become increasingly accepted as the model of choice for evaluating the genotoxic potential of chemicals and /or radiation. Micronucleus test is a more sensitive and statistically reliable technique when compared with chromosome aberrations test since the former comprises a significantly greater number of analyzed cells. The advantage of the MN test is in its ability to detect both clastogenic and aneugenic effects (Fenech, 2000). Recently, MN assay has been widely used in monitoring genetic damage in different tissue and cell types (Celik *et al*., 2005; Bonassi *et al*., 2007). The work of Schmid, 1973 led to an increasing and now almost universal selection of the polychromatic erythrocyte (PCE) as the cell choice. PCEs are very abundant, easily recognizable and the product of recent cell divisions. The protocol depends on the understanding of the behavior of the cells being studied. Several aspects of the biology of PCE have been insufficiently appreciated in the past. Enucleation of the matured erythrocyte takes place about 6 hours after mitosis, also young erythrocytes (PCEs) do not lose their ribosome for approximately 24hours after enucleation (Rifkind, 1976), and they stain a basophilic blue grey colour with Giemsa-stain. The PCEs are cells that have recently undergone DNA synthesis and mitosis. They are therefore easily distinguished by their color from any other cells on the slide. The PCEs are also somewhat larger and tend to have more diffused boundaries than the red blood cells (RBC).The erythrocytes are the only mammalian cells lacking a nucleus, a feature that makes a micronucleus obvious when present. MN assay is regarded as an important biomarker to predict the relative risk of cancer in upper aero-digestive tract (Bloching *et al.*, 2000).

Reagents

70% Methanol

70 ml of methanol was added into 30 ml distilled water. It was used to fix the slide.

10% Giemsa solution

5 g of Giemsa powder was dissolved in 1ml of ethanol before diluting in 50 ml of distilled water.

1:1 May Grunewald stain

20 ml of May-Grunewald stain was mixed with 20 ml distilled water

Procedure

The laboratory mice were sacrificed and femur was surgically extracted from each mouse. The epiphyses were removed; each of the femurs was flushed with 1ml of Fetal Bovine Serum (FBS) into an ependorff tube with syringe, and mixed thoroughly through tapping of the ependorff tube for proper dispersion of the cells. The samples were spun in a table centrifuge at 2000 rpm for 5mins, after which the supernatant was aspirated with syringe and needle while the pellet was re-suspended in 1 ml of FBS mixed properly and centrifuged again for 5 minutes in a table centrifuge at 2000 rpm. This process was repeated twice. Finally, a viscous suspension was obtained**.** The viscous suspension were dropped on a clean slide and smeared. Four slides were prepared for each mouse. The slides were allowed to dry completely on a slide tray after which each slide was fixed with 70% methanol and allowed to dry completely at room temperature. Each slide was placed in a coupling jar containing May-Greunwald stain for 3-4 minutes, and transferred immediately into another coupling jar containing May-Greunwald and distilled water in ratio 1: 1 for another 3-4 minutes. The slides were removed and rinsed in distilled water and allowed to dry completely. The slides were then stained in 10 % Giemsa for 4-5 minutes, rinsed and allowed to dry completely.

3.15 PREPARATION OF SERUM

The blood samples collected were transferred into pre-labeled heparinized bottles to prevent coagulation and centrifuged at 2,000g for 20 minutes. The clear supernatants obtained were decanted and used immediately for the determination of plasma enzymes activity or stored at –20 ^{0}C until required.

3.16. DETERMINATION OF ALANINE AMINOTRANSFERASE (ALT) AND ASPARTATE AMINO TRANSFERASE (AST) ACTIVITIES

Principle

Alanine aminotransferase (ALT) and Aspartate aminotransferase (AST) are among the most sensitive test employed in the detection of acute liver damage .The increase in the activities of ALT and AST in plasma is indicative of liver damage and dysfunction. Thus, the enzymes are routinely used as markers of hepatic injury. The elevation of the ALT and AST may be due alteration in the permeability of liver membrane, which may lead to the leakage of these enzymes from the liver cytosol into the blood stream and disturbance in the biosynthesis of these enzymes.

The transaminases were determined according to the method of Reitman and Frankel, 1957. ALT was measured by monitoring the concentration of pyruvate hydrazone formed with 2, 4-dinitrophenylhydrazine, while AST was measured by monitoring the concentration of oxaloacetate hydrazone formed with 2,4- dinitrophenylhydrazine

Reagents

Alanine aminotransferase (ALT) and aspartate aminotransferace (AST) assay Kits

Randox alanine aminotransferase (ALT) and aspartate aminotransferace (AST) assay kits from Raandox (Randox Laboratories Ltd, UK) were used in this work

0.4 M NaOH

16 g of sodium hydroxide (BDH, England) pellets was dissolved in little distilled water and the solution made up to 1000 ml final volume.

Procedure

The levels of ALT and AST activity in the plasma was determined using the ALT kits (Randox Laboratories Ltd, UK) and following the method described by Reitman and Frankel (1957). 0.1ml of the sample was mixed with 5ml of Solution 1(Buffer; Phosphate buffer, L- Alanine or L- Aspartate and α-Oxoglutarate) and incubated for exactly 30 minutes at 37 ^{0}C. Thereafter, 0.5ml of Solution 2 (2, 4-dinitrophenylhydrazine) was added, mixed and allowed to stand for exactly 20 mins at 20-25 ^{0}C. 5.0 ml of NaOH was added and the absorbance of the sample was read against the reagent blank at 546 nm after 5 minutes.

3.17 PREPARATION OF LIVER HOMOGENATE

Reagent

Homogenising buffer (Tris HCl buffer)

3.9 g of Tris HCl in 5.75 g of KCl in distilled water and made up to 500 ml. The pH was adjusted to 7.4.

Procedure

The liver of each mouse was weighed and macerated in 10 times the volume of the actual weight of the liver using homogenate buffer (Tris buffer). The homogenate were spun for 10 minute at 10,000 rpm using a cold centrifuge. The supernant was collected and use for the determination of malondialdehyde and reduced glutathione (GSH) as well as catalase activity

3.18 DETERMINATION OF MALONDIALDEHYDE

Principle

Malondialdehyde (MDA) is used as a biomarker of oxidative stress because it is an end-product of lipid peroxidation and its levels indicate the degree of lipid peroxidation (Grotto *et al.*, 2007). In this work, lipid peroxidation was determined using the method described by Esterbauer and Cheeseman, 1990. This method was based on the reaction between 2-thiobarbituric acid (TBA) and malondialdehyde, an end product of lipid peroxide during peroxidation. On heating at acidic pH, the product is a pink complex which absorbs maximally at 532nm and extractable into organic solvents such as butanol. Malondialdehyde (MDA) is often used to calibrate this test and thus the results are expressed as the amount of free MDA produced.

Reagents

0.67% 2-Thiobarbituric acid

0.675g of 2-thiobarbituric acid was dissolved in 100 ml distilled water.

20% Trichloroacetic acid

Twenty grams of trichloroacetic acid was dissolved in 100 ml of distilled water.

Procedure

The extent of lipid peroxidation in terms of thiobarbituric acid reactive substances (TBARS) formation was measured by mixing 0.5 ml of the tissue supernatant with 1 ml TCA (20%) and 2 ml TBA (0.67%) then heated for 1 hour at 100°C. After cooling, the precipitate was removed by centrifugation. The absorbance of the sample was measured at 535 nm.

Lipid peroxidation, in unit/mg protein was computed with a molar extinction coefficient of 1.56 x 10^5 M/cm

$$\text{MDA (unit/mg protein)} = \frac{\text{Absorbance}}{\text{Molar extinction x mg protein}}$$

3.19 PROTEIN DETERMINATION

Principle

The concentration of protein in the liver homogenate was determined by Biuret method as described by Weichselbaun (1946). Protein forms a coloured complex with cupric ions in an alkaline solution. The biuret reaction is a general one for the estimation of proteins, and it provides a relatively accurate measurement of serum protein. Compounds with two or more polypeptide bonds form dark blue-purple color in the presence of biuret reagent, which is characteristic of all proteins in the complex. The polypeptide specific biuret reaction occurs almost equally per given weight of all pure soluble proteins, since proteins are amino acids linked together by consecutive peptide bond. Proteins are about the only compound found in nature that has the polypeptide character required for biuiret assay. Thus, the biuret assay is remarkedly specific for protein. The dark blue colouration is apparently caused by the co-ordination complex of the copper atom and four nitrogen atoms, two from each of two peptide chains.

10% NaOH

50g of sodium hydroxide (BDH, England) pellets was dissolved in little distilled water and the solution made up to 500 ml final volume.

Buiret reagent

1.5 g of copper sulphate was mixed with 6.0g of potassium sodium tartrate and dissolved in 500 ml of distilled water in a 1 liter standard volumetric flask. With constant shaking, 1 g of potassium iodide and 300 ml of 10% sodium hydroxide was added and then made up to 1 liter with distilled water.

Stock bovine serum albumin (BSA) solution

2.5 g of BSA was dissolved in 100 ml of distilled water to give a stock of 2.5 mg/ml.

Preparation Standard Curve

Serial dilutions of stock BSA solutions were made by using varying concentrations. Biuret reagent was added to each diluted protein standard solution (stock BSA) and the mixture was allowed to stand at room temperature for 30mins before reading. The absorbances of the solutions were the read at 550 nm and a graph of absorbance against BSA Concentration (mg/ml) was then plotted.

Determination of Protein Concentration in Sample

Each homogenate sample were diluted twenty times, 1.5ml of the biuret reagent was added to 1ml of each diluted sample and allowed to stand for 30min at room temperature after which the absorbance was read at 550 nm

Table 3.1: Standard curve for protein determination

Test tube in duplicate	Blank	0.125	0.25	0.50	1.00	1.50	2.00	2.50	
Standard BSA (2.5mg/ml) mg	-	0.05	0.10	0.20	0.40	0.60	0.80	1.00	-
Saline (ml)	1.00	0.95	0.90	0.80	0.60	0.40	0.20	-	-
Sample (ml)	-	-	-	-	-	-	-	-	1.00
Biuret reagent (ml)	1.50	All	(T	U	B	E	S	)	
Total volume (ml)	2.50	All	(T	U	B	E	S	)	

Each test tube was mixed and allowed to stand at room temperature for 30 minutes.

The absorbance was thereafter measured at 550 nm.

3.20 ESTIMATION OF CATALASE ACTIVITY

Principle

Catalase is an important first line antioxidant defense enzyme and its main function is the conversion of hydrogen peroxide to water. Catalase activity was determined according to the method of Aebi, 1983 by monitoring the decomposition of H_2O_2 as indicated by the decrease in the absorbance at 240 nm. The difference in the absorbance per unit time is a measure of the catalase activity

$$2H_2O_2 \xrightarrow{\text{Catalase}} 2H_2O + O_2$$

Reagents

30 mM Hydrogen peroxide

6µl of H_2O_2 was completed to 2 ml with phosphate buffer pH 7.0

Phosphate Buffer pH 7.0

The phosphate was prepared by dissolving 3.58 g of $Na_2HPO_4.12H_2O$ and 1.19 g of $NaH_2PO_2.2H_2O$ in distilled water and made to 900 ml. The pH was adjusted to 7.0, and distilled water was then added to make up to 1 liter.

Procedure

0.1 ml of the supernatant fraction of the homogenate was mixed with 1.9 ml of the phosphate buffer, pH 7.0 in a quartz spectrophotometer cuvette. The reaction was started by adding 1 ml of hydrogen peroxide (H_2O_2) to the cuvette. The absorbance of the sample was read against distilled water immediately at zero time (A0) and was read again after 30 second (A30) at 240 nm.

Catalase activity was expressed as µmol/ wet weight of the liver. Catalase activity was calculated by using the equation below:

$$\text{Catalase activity} = \frac{K}{T} \times \frac{10}{\text{g fresh tissue}} \times \frac{\log A_0}{A_1}$$

K = constant = 2.3

T = time

A_0 = absorbance of the sample at zero time

A_1= absorbance of the sample at 30 secs

3.21 ESTIMATION OF REDUCED GLUTATHIONE (GSH)

Principle

Glutathione is also an important antioxidant compound responsible for maintaining intracellular redox homeostasis. Reduced glutathione (GSH) scavenges hydroxyl radical and singlet oxygen directly, detoxifying hydrogen peroxide and lipid peroxides by the catalytic action of glutathione peroxidase. Therefore, the level of the enzyme is altered during oxidative stress. The method of Beutler *et al*., 1963 was used in estimating the level of reduced glutathione in liver supernatants. This method is based upon the development of relative stable (yellow) colour when 5, 5-dithiobis 2-nitrobenzoic acid, (DTNB) is added to liver supernatant. The chromophoric product resulting from the reaction of Ellman's reagent with reduced glutathione, 2-nitro-5-thiobenzoic acid possess a molar absorption at 412nm. Reduced GSH is proportional to the absorbance at 412nm.

Reagents

Reduced Glutathione (GSH)

0.04g of GSH was dissolved in 100ml of phosphate buffer.

Ellman's Reagent

0.04g of 5, 5-dithiobis 2-nitrobenzoic acid (DTNB) was dissolved in 100ml of 0.1M phosphate buffer pH 7.4

Precipitating Agent

4% sulfosalicyclic acid ($C_6H_6O_6S.2H_20$) was prepared by dissolving 4g of sulfosalicyclic acid in 100ml of distilled water.

Phosphate Buffer pH 7.0

3.58g of $Na_2HPO_4.12H_2O$ and 1.19g of $NaH_2PO_2.2H_2O$ were dissolved in distilled water and made to 900ml at the pH 7.0. The pH was adjusted to 7.0, and distilled water was then added to make up to 1 liter.

Procedure

0.75 ml of the homogenate was deproteinized by the addition of 0.75 ml of 4% sulfosalicyclic acid. The mixture was spun at 14000g for 15 minute at 4°C. 0.5 ml of the supernatant was added to 4.5 ml of Ellman's reagent. A blank was prepared by adding 0.4 ml of phosphate buffer with 0.1 ml of sulfosalicyclic acid. From this stock, 0.3ml of the diluted precipitating agent was taken and 4.5ml of Ellman's reagent was added. Reduced glutathione, concentration is proportional to the absorbance at 412nm.

3.22 ESTIMATION OF GLUTATHIONE-S-TRANSFERASE ACTIVITY

Principle

Glutathione–S–transferase activity was assayed spectro- photometrically using 1-chloro-2-4-dinitrobenzene (CDNB) and glutathione as described by Habig *et al*. (1974). This method is based on the fact that all known glutathione –S- transferase demonstrate a relatively high activity with 1-Chloro -2,4-dintrobenzene (CDNB) as the second substrate. Consequently, the conventional assay for glutathione –S- transferase activity utilizes 1-Chloro-2,4-dintrobenzene as substrate. Conjugation of the substrate with reduced glutathione (GSH) shifts the absorption maximum shifts to a longer wavelength. The absorption increase at the new wavelength (340nm) provides a direct measurement of the enzymatic reaction.

Reagents

GSH 40 mM

0.123 g of GSH was dissolved in 10 ml distilled water.

CDNB 8 mM

0.162 g of CDNB was dissolved in 10 ml ethanol 2.5%.

Phosphate buffer pH 6.5

1.375 g of KH_2PO_4 was dissolved in 100 ml of distilled water

1.799 g of Na_2HPO_4 was dissolved in 100 ml of distilled water

The buffer was then made by mixing 68.2 ml KH_2PO_4 solution with 31.8 ml Na_2 PO_4 solution

0.33 N HCl

3 ml of HCl was mixed with 100 ml of distilled H_2O.

Procedure:

1 ml of homogenate was centrifuged for 3 min at 3000 rpm then 0.5 ml of supernatant was taken and diluted 1: 400 with distilled water. The following additions were done:

Reagent	Sample (µl)	Blank (µl)
Sample	500	500
GSH	250	250
CDNB	250	250
Buffer	1000	1000
HCl	-	3000

Then, all tubes were incubated for 1 hour at 30^0 C, followed by addition of 3 ml HCl to the sample. The absorbance was measured at wave length 340 nm for each samples its blank.

Calculation

$$\text{GST activity} = \frac{\text{O.D.Sample - BlankO.D.}}{9.6} \times \frac{1}{\text{mg Protein}}$$

= M mol / min / mg Protein.

Where 9.6 mM cm^{-1} is the extension coefficient of 1- Chloro-2,4-dinitrobenzene.

3.23 STATISTICAL ANALYSIS

Data were presented as mean and standard error of the mean. They were analysed by one-way analysis of variance (ANOVA) using the 17^{th} version of SPSS while differences between test and control groups were examined using Student's t- test. $p < 0.05$ was considered to be the level of significance.

CHAPTER FOUR

EXPERIMENTS AND RESULTS

4.1 EXPERIMENT 1: EFFECT OF ASCORBATE OR DEHYDROASCORBATE ON LEAD CHROMATE CYTOTOXICITY

INTRODUCTION

Ascorbate is the dominant biological reducing agent required for reductive activation of the toxicity and carcinogenic activity of Cr (VI) in vivo. In addition, Cr (VI) is usually present in the micromolar range when humans are exposed to it occupationally, whereas ascorbate is present at concentrations in the millimolar range under physiological conditions in humans. Inadequate or lack of ascorbate in culture has been suggested to result in low mutation and morphological transformation in chromate treated cells (Holmes *et al*, 2008). Therefore, in order to reproduce *in vitro* the conditions in mammalian cells *in vivo*, it is important to supplement cell culture medium with ascorbate.

PROCEDURE

Cells were cultured and seeded as previously described under "Materials and Methods" (Section 3.3., Page 78-79). Seeded cells were treated 24 hours later with 100µl of various concentrations of ascorbate or dehydroascorbate alone or with 25 µl of 1.62µg/ml lead chromate for 48 hours. The concentrations of ascorbate tested were 0.00625 mM, 0.0125 mM, 0.025 mM, 0.05 mM, 0.1mM, 0.25mM and 0.375 mM. For dehydroascorbate, the same concentrations were used as for ascorbate in addition to 0.5 mM. Control dishes were left untreated or were alternatively treated with 100µl phosphate buffer saline (PBS), 25µl acetone, 100µl PBS and 25µl acetone, or 1.62 µg/ml lead chromate. The medium was changed after treatment, but ascorbate or dehydroascorbate was again added at the same concentrations and volumes, with which the dishes were initially treated. Ten days post-seeding, dishes were fixed and stained as described earlier (Section 3.3., Page 78-79). Colonies containing 20 or more cells were counted and averaged in the five dishes. Relative survival was determined as a percentage of survival of cells.

RESULTS

The effect of ascorbate on the survival of CH310T½ treated with $PbCrO_4$ is shown in Figure 4.1. The blue line shows the effect of ascorbate alone on the survival of 10T½ cells based on the average results of 3 experiments. The highest concentration of ascorbate that is non-cytotoxic was found to be 0.025 mM. Curiously, concentrations less than 0.025 mM, such as 0.0125 mM and 0.00625 mM appeared to cause some slight but measurable cytotoxicity. Above 0.025 mM, concentrations of 0.05 mM, 0.10 mM, 0.25 mM, and 0.375 mM reduced the survival of 10T½ cells in a dose-dependent manner, from a survival fraction of 1.0 to survival fractions of 0.82, 0.70, 0.30, and 0.10, respectively. The green rectangles show the survival fractions of CH310T½ cells after they were treated with 1.62 µg/ml of $PbCrO_4$, which reduced the survival fraction of 10T½ cells from 1.0 down to 0.70 (70%). The red line shows the effect of ascorbate on the survival of CH310T½ cells treated with $PbCrO_4$. The hypothesis in this experiment was that ascorbate inside cells would activate chromium (VI) compounds to become toxic to cells. The data can only be analysed up to concentrations of 0.025 mM ascorbate, since ascorbate itself becomes cytotoxic at higher concentrations. It was observed that at the lowest three concentrations of ascorbate (0.025 mM, 0.0125 mM, and 0.00625 mM), the survival fraction of cells treated with ascorbate and lead chromate decreased from 0.70 in cells treated with lead chromate only, down to 0.50, 0.45, and 0.55, respectively, in cells treated with these concentrations of ascorbate. Therefore, these three concentrations of ascorbate did decrease the survival of CH310T½ cells below that observed in cells treated with lead chromate only. This was consistent with our hypothesis; however, the decrease in cell survival was not dose-dependent with the ascorbate concentrations.

Next, the effect of dehydro-ascorbate on the survival of CH310T½ cells treated with $PbCrO_4$ was studied. As shown in Figure 4.2, treatment of CH310T½ cells with 1.62 µg/ml lead chromate reduced the survival of CH310T½ cells from 1.0 to 0.72. Dehydro-ascorbate was not cytotoxic up to a concentration of 0.05 mM. When dehydro-ascorbate was added to cells treated with lead chromate, it first decreased the cytotoxicity of lead chromate from 0.72 down to 0.40 at a concentration of 0.00625 mM of dehydro-ascorbate, i. e., this caused a pro-oxidant effect. Interestingly, higher concentrations of dehydro-ascorbate of 0.0125 and 0.0250 mM of dehydro-ascorbate actually increased the survival fraction of CH310T½ cells to 0.50 and to 0.65,

respectively. This suggests that the initial reductive toxic effect becomes reversed at higher dehydro-ascorbate concentration. To demonstrate a dose-response dependent toxicity, there was need to lower the concentrations of dehydro-ascorbate, below 0.00625 mM dehydro-ascorbate, In the same vein, there was also need to repeat this experiment with concentrations of ascorbate between 0.0025 and 0.025 mM, to determine whether these concentrations of ascorbate can cause an anti-oxidant effect on the cytotoxicity of lead chromate, i. e., whether these concentrations reduce the cytotoxicity of lead chromate. To achieve this, the experimental set up was altered and the concentration of both ascorbate and dehydroascorbate were lowered as shown in appendix 1 (Table A1)

The effect of lower concentrations of ascorbate on the survival of CH310T½ cells treated with $PbCrO_4$ is shown in Figure 4.3. Figure 4.3 shows that when 1.62 µg/ml $PbCrO_4$ was added to CH310T½ cells, it was cytotoxic as before, and reduced the survival fraction of CH310T½ cells to 0.70. Next, when ascorbate concentrations between 0.0025 to 0.025 mM were added to cells treated with non-cytotoxic concentrations of ascorbate, the survival fraction of the cells decreases to 0.40 as the concentration of ascorbate was increased from 0.0025 mM to 0.0125 mM, indicating a pro-oxidant effect. As the ascorbate concentration was increased from0.015 mM to 0.02 mM, the survival fraction actually increased to 0.70, indicating an anti-oxidant effect.

The effect of lower concentrations of dehydroascorbate on the survival of CH310T½ cells treated with $PbCrO_4$ is shown in Figure 4.4. In Figure 4.4, it can be seen that 1.62 µg/ml lead chromate reduced again the survival of CH310T½ cells from 1.0 to 0.70. Adding dehydro-ascorbate at concentrations from 0.00025 mM to 0.002 mM further decreased the survival of lead chromate-treated cells down to 0.45, indicating a pro-oxidant effect. Further increase in the concentration of dehydro-ascorbate to 0.003 and 0.004 mM increased the survival fraction back up to 0.50 and 0.70, conveying an anti-oxidant effect (Figure 4.4). Hence, again, it appeared that low concentrations of dehydro-ascorbate (0.00025 mM to 0.002 mM) increased the cytotoxicity of lead chromate, but increasing the concentrations of dehydro-ascorbate back up to 0.003 and 0.004 reversed the enhancement of the cytotoxicity (Figure 4.4).

Conclusion

Beyond 25 µM, ascorbate is cytotoxic to CH310T½. In addition, ascorbate or its oxidized form dehydroascorbate plays a paradoxical role in the toxicity of lead chromate. At low concentration ≤ 12.5 µM ascorbate or ≤ 2 µM dehydroascorbate), they act as proxidant by increasing the toxicity of lead chromate. In contrast at higher concentration (15-20 µM ascorbate and 3-4 µM dehydroascorbate), they act as anti-oxidant by deactivating lead chromate and decreasing its toxicity.

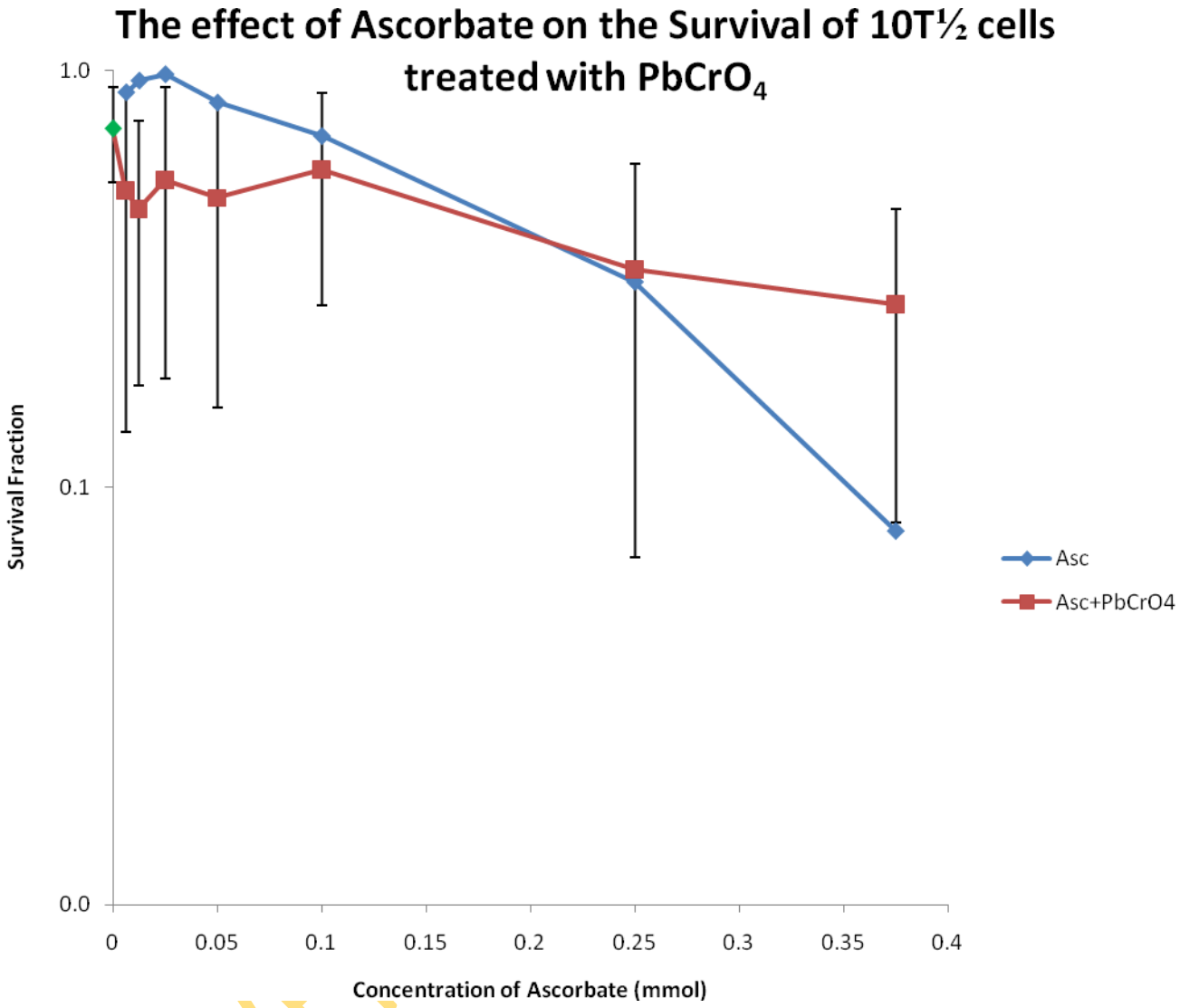

Figure 4.1: Survival curve of 10T½ cells treated with $PbCrO_4$ in the presence of ascorbate. 10T½ were treated simultaneously with suspension of $PbCrO_4$ and ascorbate for48h. Blue line represents the survival curve of 10T½ cells treated with the higher concentrations of ascorbate alone while the red line represents the survival curve of the cells treated simultaneously with $PbCrO_4$ and the same concentrations of ascorbate.The green rectangle on the y-axis represents the survival of the cells with with 1.62 µg/ml $PbCrO_4$ alone.

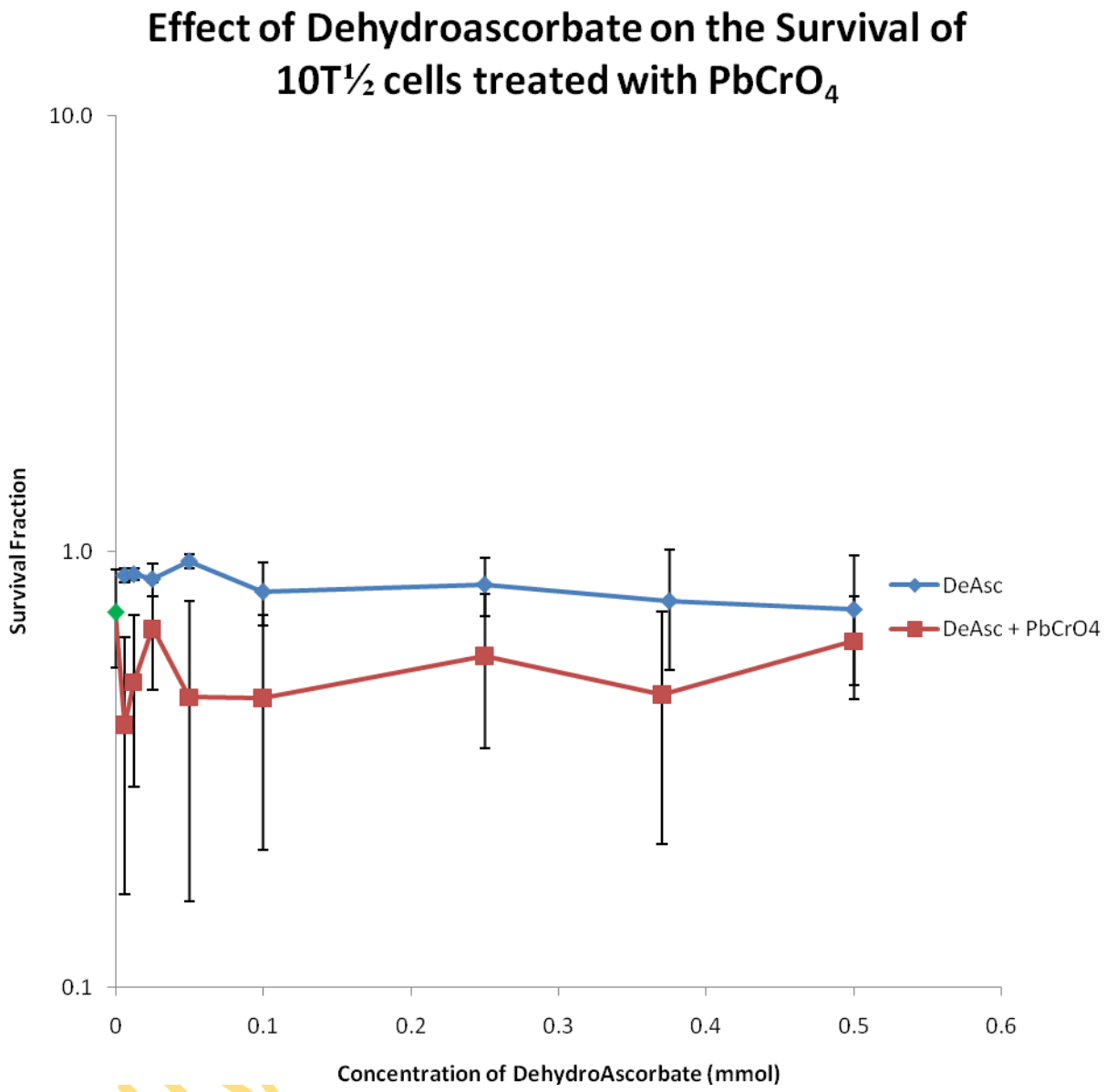

Figure 4.2: Survival curve of 10T½ cells treated with $PbCrO_4$ in the presence of ascorbate. CH310T½ cells were treated simultaneously with suspension of $PbCrO_4$ and dehydroascorbate for 48h. Blue line represents the survival curve of 10T½ cells treated with the higher concentrations of dehydroascorbate alone while the red line represents the survival curve of the cells treated simultaneously with $PbCrO_4$ and the same concentrations of dehyroascorbate.The green rectangle on the y-axis represents the survival of the cells with 1.62 µg/ml $PbCrO_4$ alone.

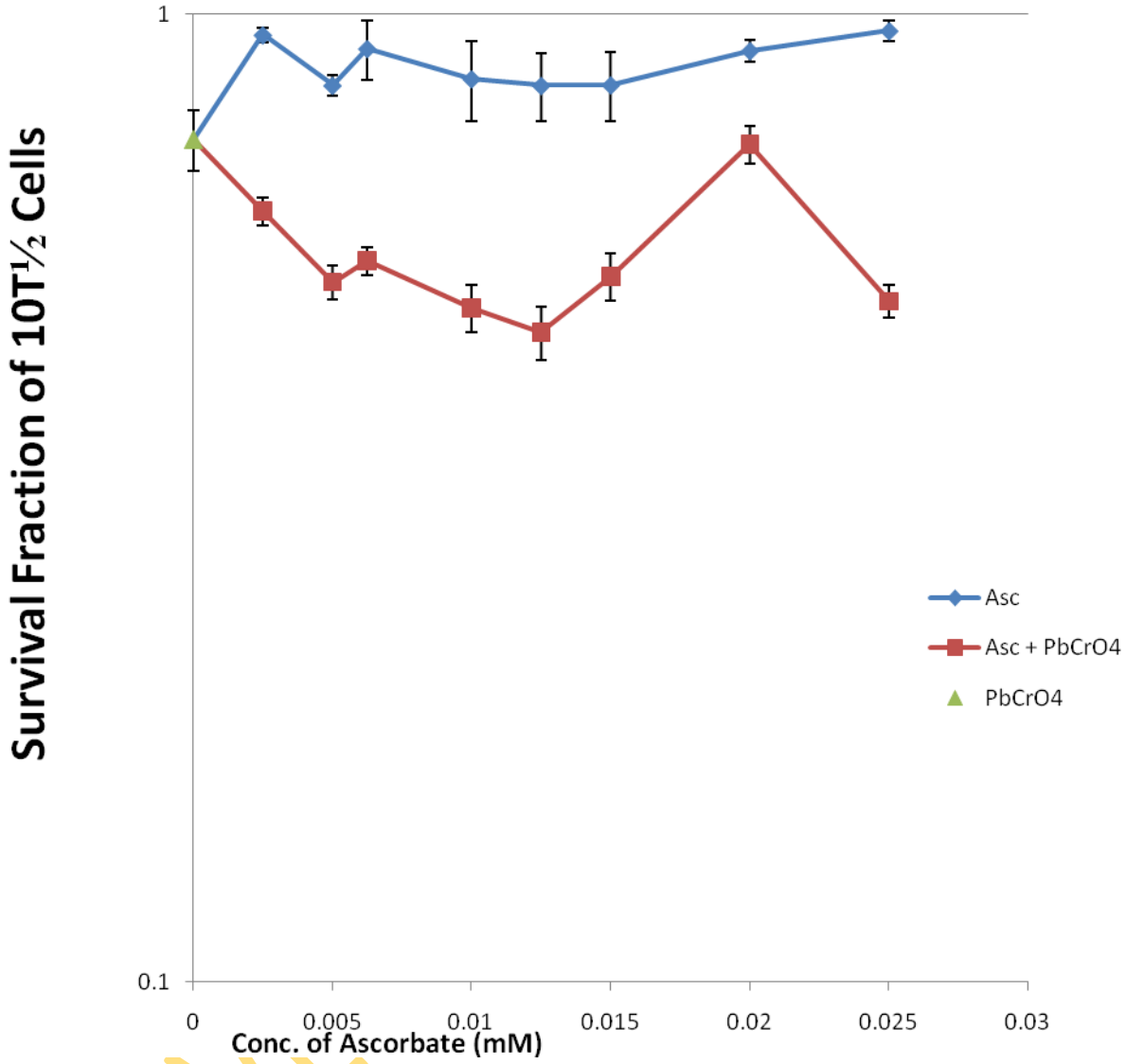

Figure 4.3: Effect of ascorbate on the survival of 10T½ cells treated with $PbCrO_4$ for 48hrs**.** Blue line represents the survival curve of 10T½ cells treated with the lower concentrations of ascorbate alone, while the red line represents the survival curve of the cells treated simultaneously with $PbCrO_4$ and the same concentrations of ascorbate.The green triangle on the y-axis represents the survival of the cells with treated with 1.62 µg/ml $PbCrO_4$ alone.

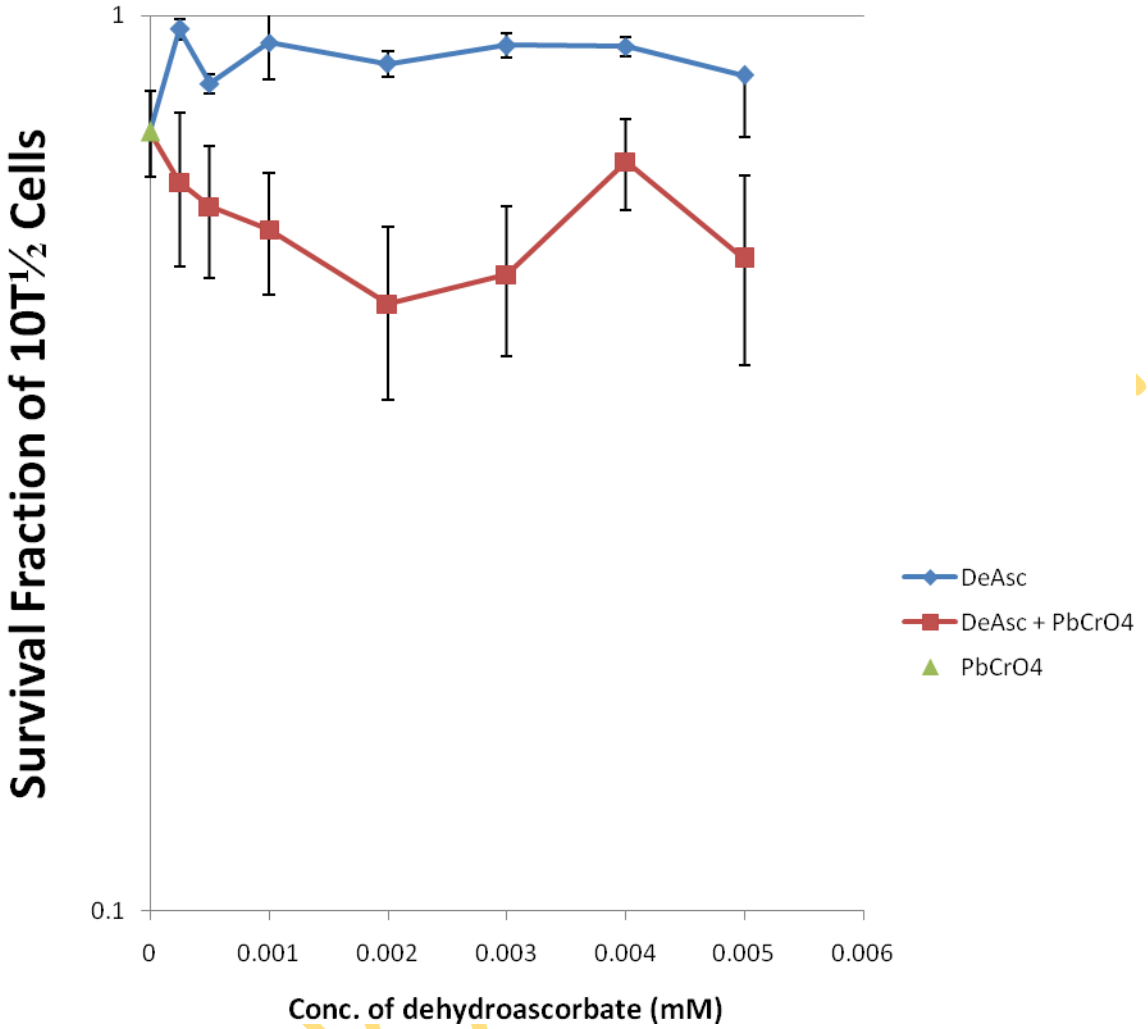

Figure 4.4: Effect of dehydroascorbate on the survival of 10T½ cells treated with $PbCrO_4$ for 48hrs. Blue line represents the survival curve of 10T½ cells treated with the lower concentrations of dehydroascorbate alone, while the red line represents the survival curve of the cells treated simultaneously with $PbCrO_4$ and the same concentrations of dehyroascorbate. The green triangle on the y-axis represents the survival of the cells treated with 1.62 µg/ml of $PbCrO_4$ alone.

4.2 EXPERIMENT 2: THE EFFECT OF PARTICLE SIZE ON THE CYTOTOXICITY BY $PbCrO_4$, $BaCrO_4$ and $SrCrO_4$ USING CLONOGENIC ASSAY

INTRODUCTION

Workers in various chromate related industries are exposed to different particles sizes of particulate chromate. For instance, a spray painter is occupationally exposed to particulate chromate with reduced particle size when compared to that of a household painter. This in turn may affect the toxicity inherent from exposure to hexavalent chromate by two different workers. In addition, earlier work by Patierno *et al.* (1989) ascribed the weak transformation of CH310T1/2 mouse embryonic fibroblast by lead chromate to large particle size that limits its phagocytic uptake. However, comparative work with different particle size of chromate was not done. Moreover, the effect of particle size on the toxicity of particulate chromate VI compounds has not yet been investigated. In this experiment, the effect of particle size on the cytotoxicity of three insoluble chromate compounds to cultured CH310T½ mouse embryo cells was investigated. CH310T½ cells were exposed to both small (average particle size is ≤ 3 µm) and large particles (average particle size is ≤ 8 µm) of lead chromate ($PbCrO_4$), Barium chromate ($BaCrO_4$), and strontium chromate ($SrCrO_4$) at concentrations ranging from 0.125 to 10 µg /ml for 48 hours.

PROCEDURE

20 mg of each insoluble chromate compound was sonicated in 10 ml acetone, using a Braun Sonic Ultra Sonicator set at 150 watts for either 5, 10, or 20 minutes. The sonicated compounds and a control, containing an equal amount of unsonicated insoluble chromate compound in 10 ml acetone, were subsequently processed for electron microscopy. Twenty-five microliter of each insoluble chromate compound was briefly suspended in acetone and deposited on formvar-coated copper grid. The acetone was allowed to evaporate, and the grid was mounted on a stub. This was later gold coated in an Electron Microscopy Science Sputter Coater and examined in a JOEL JSM 6390LV Scanning Electron Microscope at 10KV. The particle diameter as observed with a JOEL JSM 6390LV Scanning Electron Microscope as measured with the Image J software for image processing and analysis. Briefly, Images from the electron microscope were loaded into ImageJ, an open-sourced image-processing software. The line tool was used to

generate measurements of particle size along each particle's longest axis, giving values in raw pixels from the image. The line tool was also used to measure the image's scale bar, creating a unit conversion factor to change the units from pixels to microns. The CH310T½ cells were later exposed to the sonicated (small) and unsonicated (large) chromate compounds.

The cells were thereafter seeded at 200 cells per 60 cell culture dish, five dishes per concentration of toxin studied, according to the plating efficiency protocol described earlier under "Materials and Methods" (Section 3.3., Page 78-79) . Twenty-four hours later, cells were treated with either unsonicated or sonicated insoluble chromate compounds. The concentrations of insoluble chromate compounds tested were between 0.5 µg/ml and 10 µg/ml. After 48 hours of exposure to toxin, the medium was changed, and cells were cultured for an additional 8 days without toxin. On the 10^{th} day, the medium was removed and the cells were rinsed once with isotonic phosphate-buffered saline. Cells were then fixed, stained and colonies counted as previously described (Section 3.3., Page 79-80)

RESULTS

Lead chromate particles were sonicated for 0, 5, 10 or 20 minutes. It was noted that the unsonicated particles of lead chromate were mostly in large particles aggregates < 8 µm in diameter. In previous work from the laboratory of Landolph, the particle size of unsonicated lead chromate particles as measured by light scattering was noted to be around 80 µm (Landolph, J. R., unpublished data). However, in this study using electron microscopy, it was observed that the size of particles of the compounds decreased with increasing time of sonication (Figure 4.5). After 5 minutes of sonication, approximately 50% of the particles had diameters < 8 um (Figure 4.5B). After 10 minutes of sonication, the average particles were 4.81 µm (Figures 4.5C and 4.6). After 20 minutes of sonication, the average particle sizes of the particles of lead chromate were lowered to 2.59 µm (Figures 4.5D and 4.6). In addition, more of the $PbCrO_4$ particles went into suspension as the time of sonication was increased from 5 minutes to 10 minutes to 20 minutes. Based on this observation, lead chromate and the other insoluble chromate compounds used for the determination of the effect of particle size on cytotoxicity to CH310T½ cells were sonicated for 20 minutes. The mean particle size of $BaCrO_4$ sonicated for 20 mins was 1.79 µm as compared to 2.19 µm for the unsonicated form (Figures 4.7. and 4.8). The mean particle size

of sonicated $PbCrO_4$ (2.59 µm) and $BaCrO_4$ (1.79 µm) as well as unsonicated $BaCrO_4$ (2.19 µm) are within the size range predicted for deposition in the bronchial tree where chromium-induced cancers usually occur (IARC, 1990).

The cytotoxicity of large particles (unsonicated) $PbCrO_4$ was first examined over a wide range of concentrations 0.5µg/ml to 10µg/ml. Treatment of CH310T½ cells with unsonicated $PbCrO_4$ at concentrations of 0.5, 1.0, 1.62, 2.5 5.0, 7.5 and 10µg/ml resulted in a dose-dependent cytotoxicity and survival fractions of 0.87, 0.82, 0.71, 0.66, 0.08%, 0.04% and 0%, respectively (Figure 4.9). To compare the effect of particle size reduction on the cytotoxicity of lead chromate, CH310T½ cells were next treated with small particles (sonicated) of $PbCrO_4$ at the same concentrations as the unsonicated particles. The dose-response relationship for cytotoxicity induced by sonicated lead chromate is presented in Figure 4.9. Treatment of 10T½ cells with sonicated particles of lead chromate reduced their survival at all doses in a dose-dependent manner. Sonicated lead chromate exposure led to survival fractions of 0.50, 0.40, 0.40, 0, 0, and 0 in cells exposed to 0.5, 1.0, 1.62,2.5, 5, 7.5, and 10 µg/ml respectively of lead chromate. The effect of particle size of lead chromate on the survival of 10T ½ cells, in comparison to that of the unsonicated lead chromate is shown in Figure 4.9. The results suggest that the smaller the lead chromate particles are in suspension, the higher their cytotoxicity to CH310T½ cells. The toxicity parameters obtained for both sonicated and unsonicated $PbCrO_4$ is summarized below in Table 4.1

Next, the clonogenicity and the survival of 10T½ cells exposed to different concentrations of the large particles of $BaCrO_4$ was assessed.The results are expressed as survival fraction of the no addition control, as shown in Figure 4.10. The 10T½ cells showed dose-dependent reduction survival after treatment with increasing concentrations of $BaCrO_4$. Specifically, it resulted in 0.88, 0.47., 0.40, 0.38, 0.12%, 0%, 0%, and 0% clonogenic survival after treatment with 0.5, 1.0, 2.5, 5.0, 7.5 and 10.0 µg/ml $BaCrO_4$ respectively. Next, cells were treated with small (sonicated) $BaCrO_4$ to test the hypothesis that reduced particles size of $BaCrO_4$ will reduce its clonogenic survival and enhance its cytotoxicity.

The dose-response relationship for cytotoxicity induced by sonicated barium chromate is presented in Figure 4.10. Treatment of 10T½ cells with sonicated particles of barium chromate

reduced their survival at all doses in a dose-dependent manner. Sonicated barium chromate exposure led to survival fractions of 0.43, 0.26, 0.23, 0.14, 0.08and 0.04 in cells exposed to 0.5, 1.0, 2.5, 5, 7.5, and 10 µg/ml of barium chromate, respectively. Over all, the effect of smaller particles of $BaCrO_4$ on its cytotoxicity was noticeable at lower concentrations. The toxicity parameters obtained for both sonicated and unsonicated $BaCrO_4$ is summarized in Table 4.2.

The survival fraction of 10T ½ cells treated with different concentrations of unsonicated $SrCrO_4$ is presented in Figure 4.11 Treatment of 10T½ cells with unsonicated $SrCrO_4$ at concentrations of 0.125, 0.25, 0.5, 1.0, 2.5 and 5.0µg/ml resulted in a dose-dependent cytotoxicity and survival fractions of 0.74, 0.62, 0.37, 0.21, 0.03, and 0, respectively (Figure 4.11). Similarly, treatment of CH310T½ cells with sonicated $SrCrO_4$ at concentrations of 0.125, 0.25, 0.5, 1.0, 2.5 and 5.0µg/ml resulted in a dose-dependent cytotoxicity and survival fractions of 0.70, 0.56, 0.42, 0.14, 0.07, 0, and 0, respectively (Figure 4.11). When the survival curve of the sonicated $SrCrO_4$ was compared with the corresponding unsonicated form, the difference in cytotoxic effect was only apparent at higher doses (Figure 4.11). The toxicity parameters obtained for both sonicated and unsonicated $SrCrO_4$ is summarized in Table 4.3.

CONCLUSION

Both the large and small forms of all the three hexavalent chromate induced dose dependent cytotoxicity in 10T½ cells .Generally, the order of toxicity of the hexavalent chromate compounds to 10T½ cells is: $PbCrO_4$<$BaCrO_4$ <$SrCrO_4$. In addition the cytotoxicity of insoluble chromate compounds is enhanced by reduction of their particle size. The concentration at which enhancement was observed was however different in the three chromate compounds. The cytotoxic effect was enhanced in cells treated with the reduced $PbCrO_4$ particle size at all the tested concentrations. The effect of reduced particles of $BaCrO_4$ on its cytotoxicity was noticeable at lower concentrations, while the effect of reduced particle size on $SrCrO_4$ toxicity in cultured CH310T½ cells was only apparent at higher concentration.

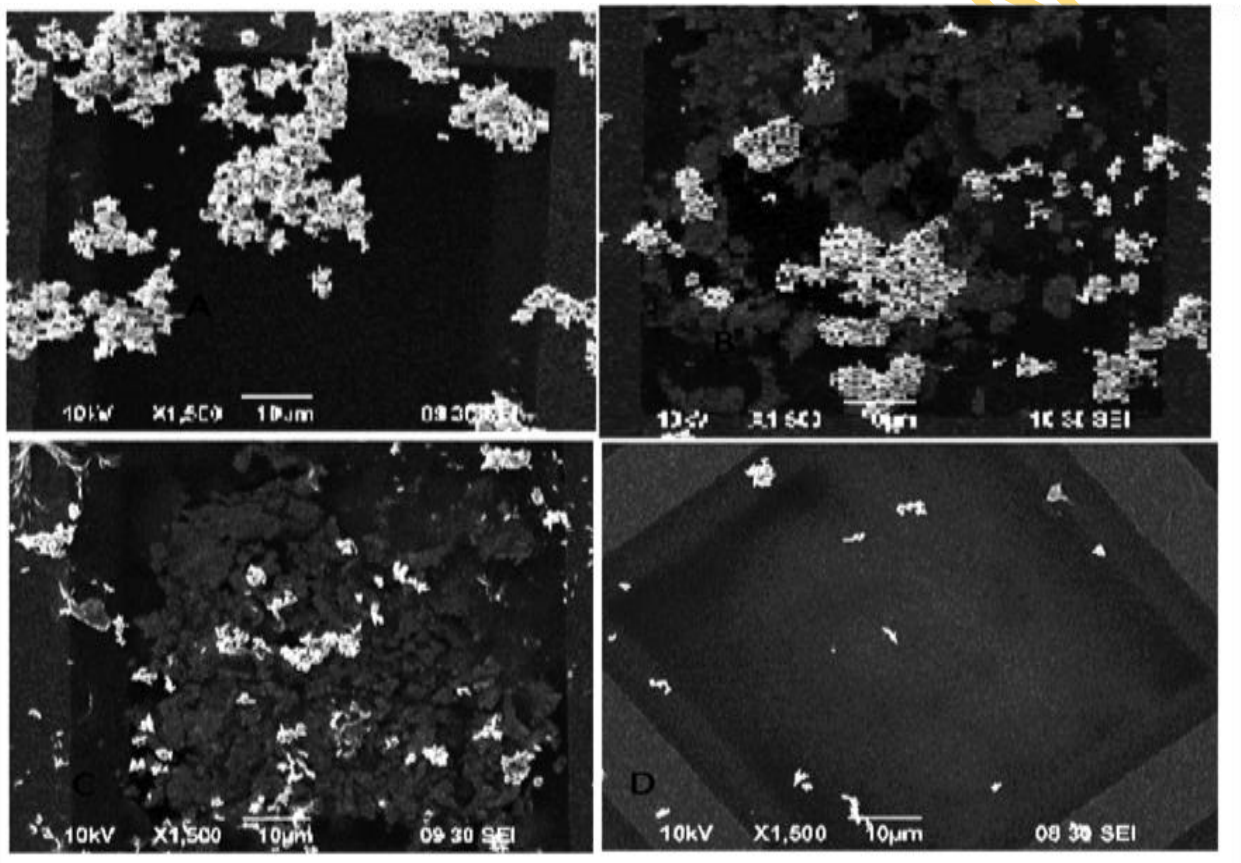

Figure 4.5: Electron micrographs showing the effect of time of sonicaion on the size of lead chromate particles. (A) Unsonicated $PbCrO_4$; (B) $PbCrO_4$ particles sonicated for 5 minutes; (C) $PbCrO_4$ particles sonicated for 10 minutes; (D) $PbCrO_4$ particles sonicated for 20 minutes

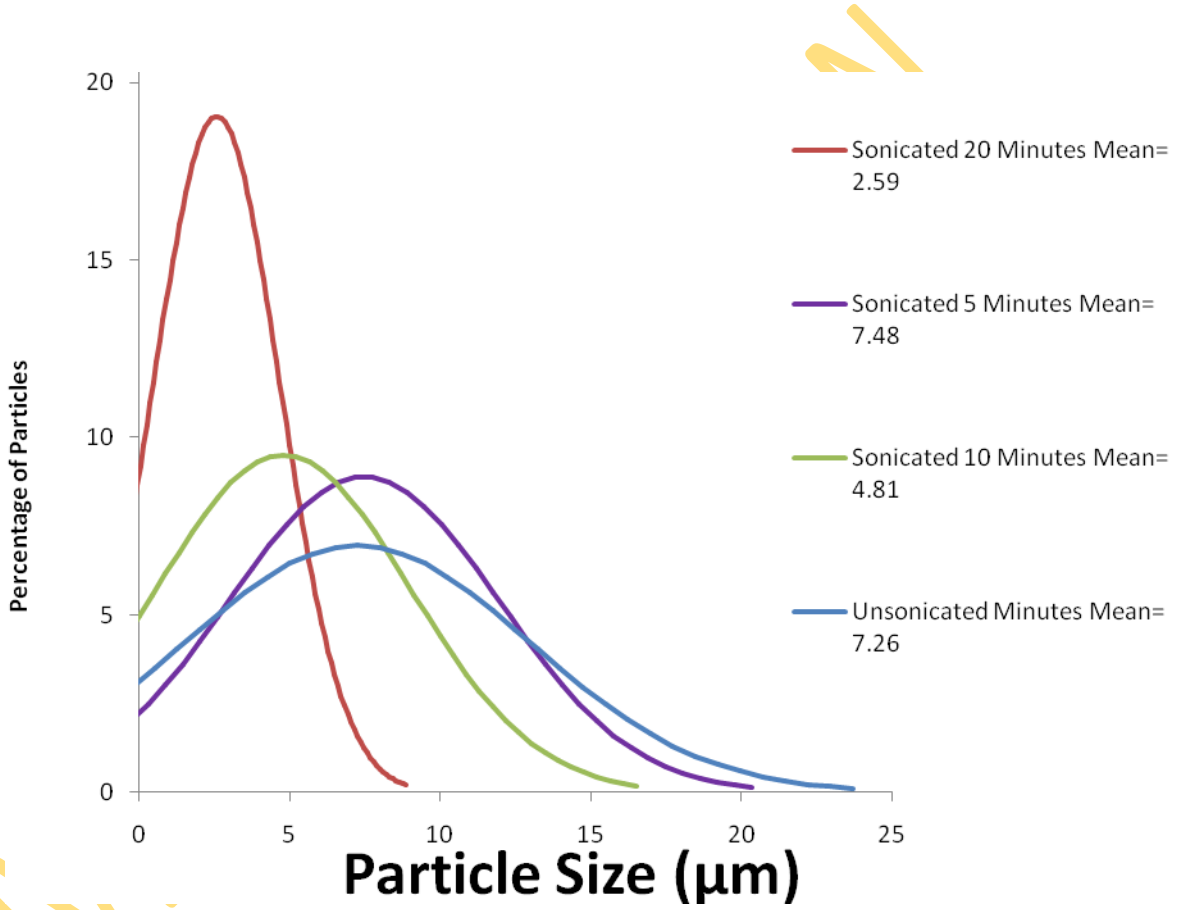

Figure 4.6: Comparison of particle size distribution of lead chromate sonicated for 5minutes, 10 minutes and 20 minutes in a Braun Sonic Ultra Sonicator. The sizes of the particles as observed with a JOEL JSM 6390LV Scanning Electron Microscope as measured with the Image J software for image processing and analysis. The red, purple, green and blue curves represent the particle size distribution of lead chromate sonicated for 20, 10, 5 and 0 minutes respectively.

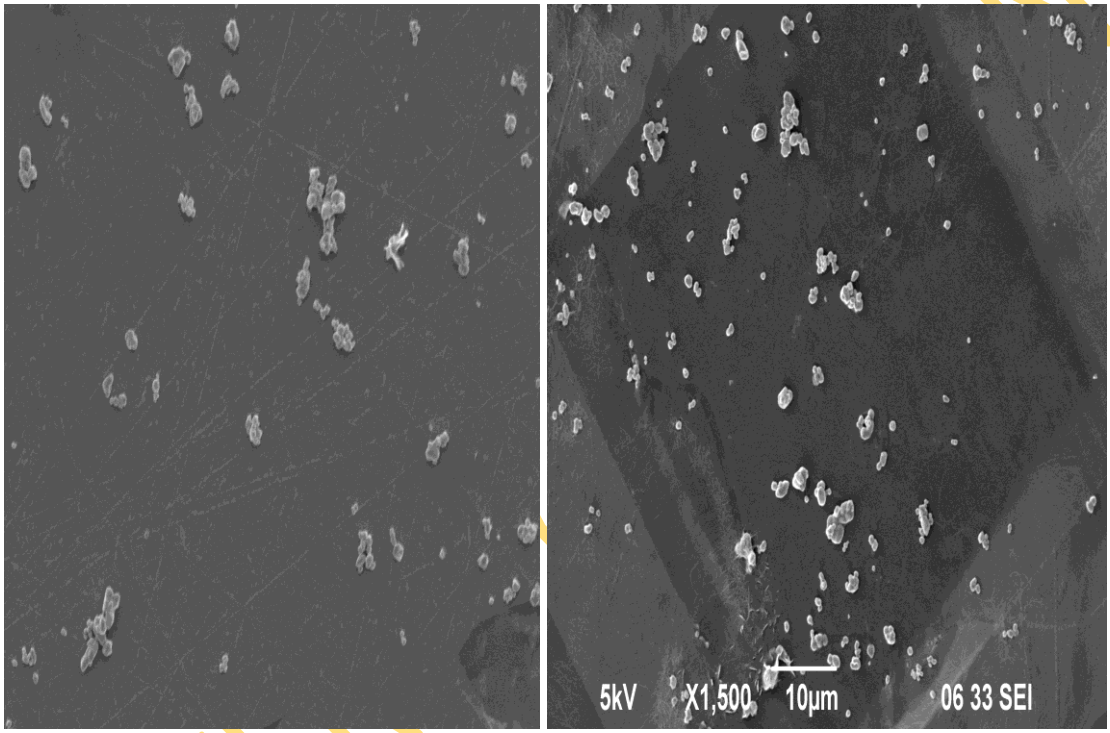

Figure 4.7: Electron micrographs showing the effect of sonication on $BaCrO_4$ particles. (A) Unsonicated $BaCrO_4$; (B) $BaCrO_4$ sonicated for 20 minutes.

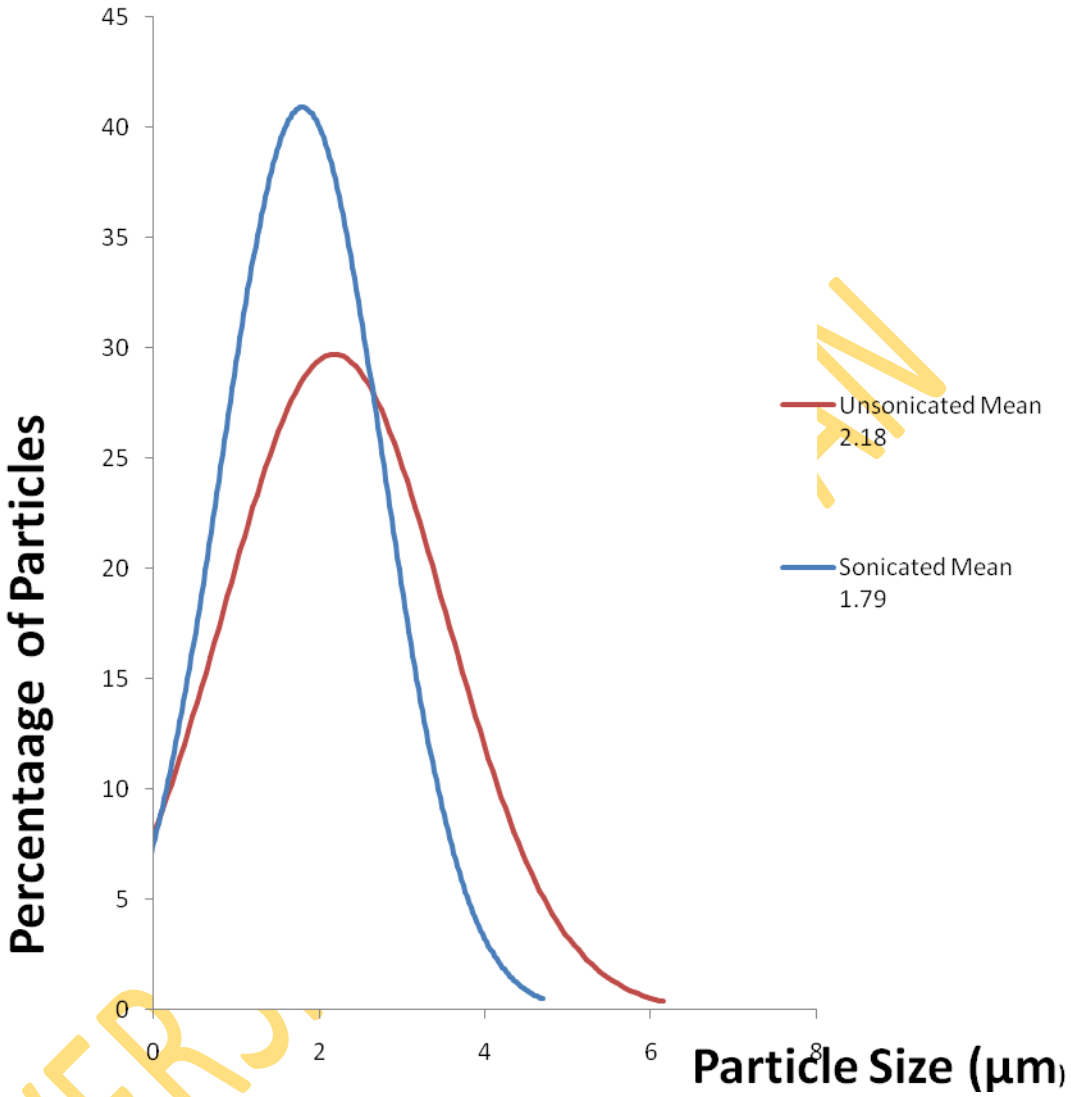

Figure 4.8: Comparison of particle size distribution of barium chromate sonicated for 0 and 20 minutes in a Braun Sonic Ultra Sonicator. The sizes of the particles as observed with a JOEL JSM 6390LV Scanning Electron Microscope and measured with the Image J software for image processing and analysis. The red and blue curves represent the particle size distribution of barium chromate sonicated for 0 and 20 minutes respectively.

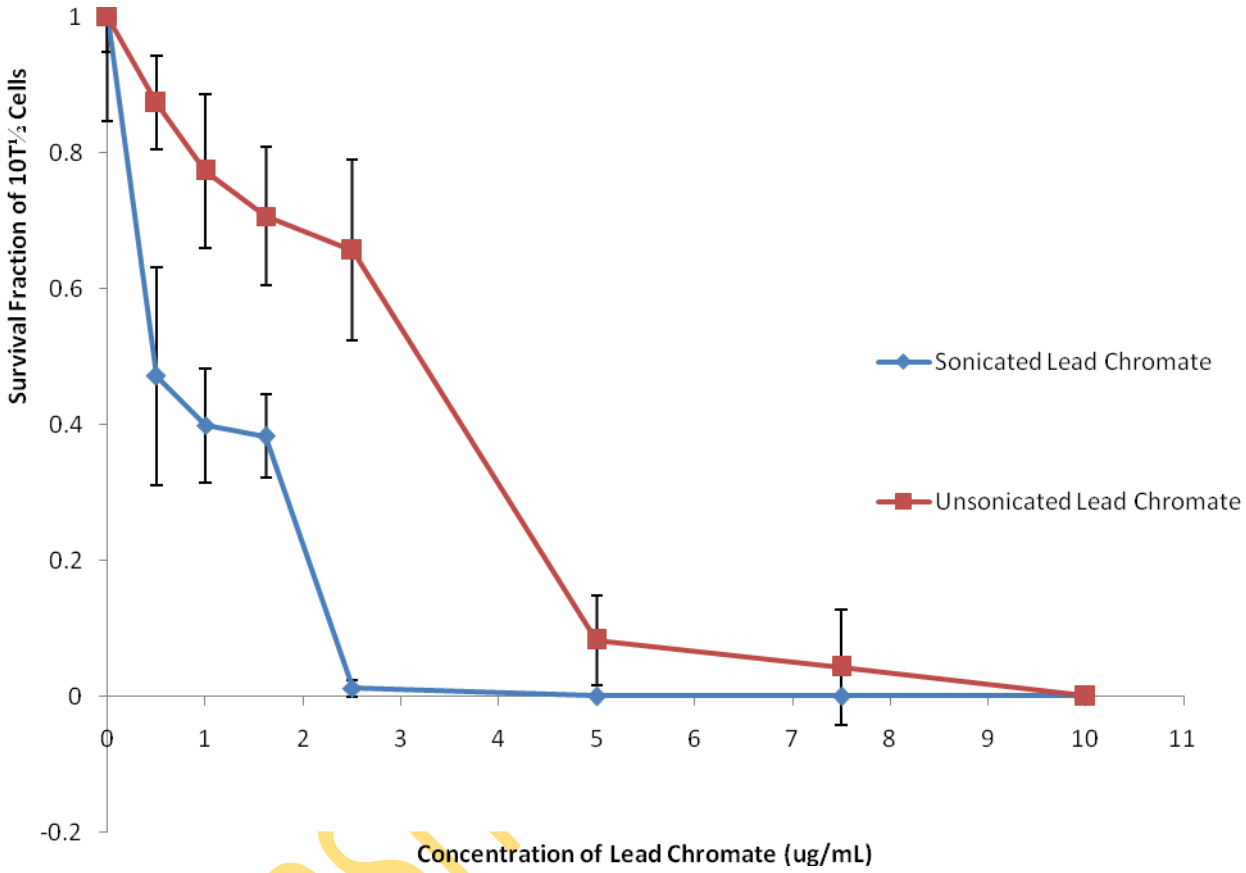

Figure 4.9: Survival fraction curve for CH310T½ cells treated with small and large particles of $PbCrO_4$ for 48hrs. The blue line represents the survival curve of CH310T½ treated with sonicated (small particles) $PbCrO_4$, while the red line represents the survival curve of the cells treated with unsonicated (large particles) $PbCrO_4$.

Table 4.1: Toxicity Parameters of Large and Small particles of $PbCrO_4$ in CH310T ½ cells

$PbCrO_4$ Form	**LC_{50}**	**LC_{37}**	**K**
Large	3.16	3.75	0.27
Small	0.47	1.65	0.64

LC_{50} is the concentration of $PbCrO_4$ that provoked a 50% survival

LC_{37} is the concentration of $PbCrO_4$ that caused a 37% survival

$K = 1/ LC_{37}$

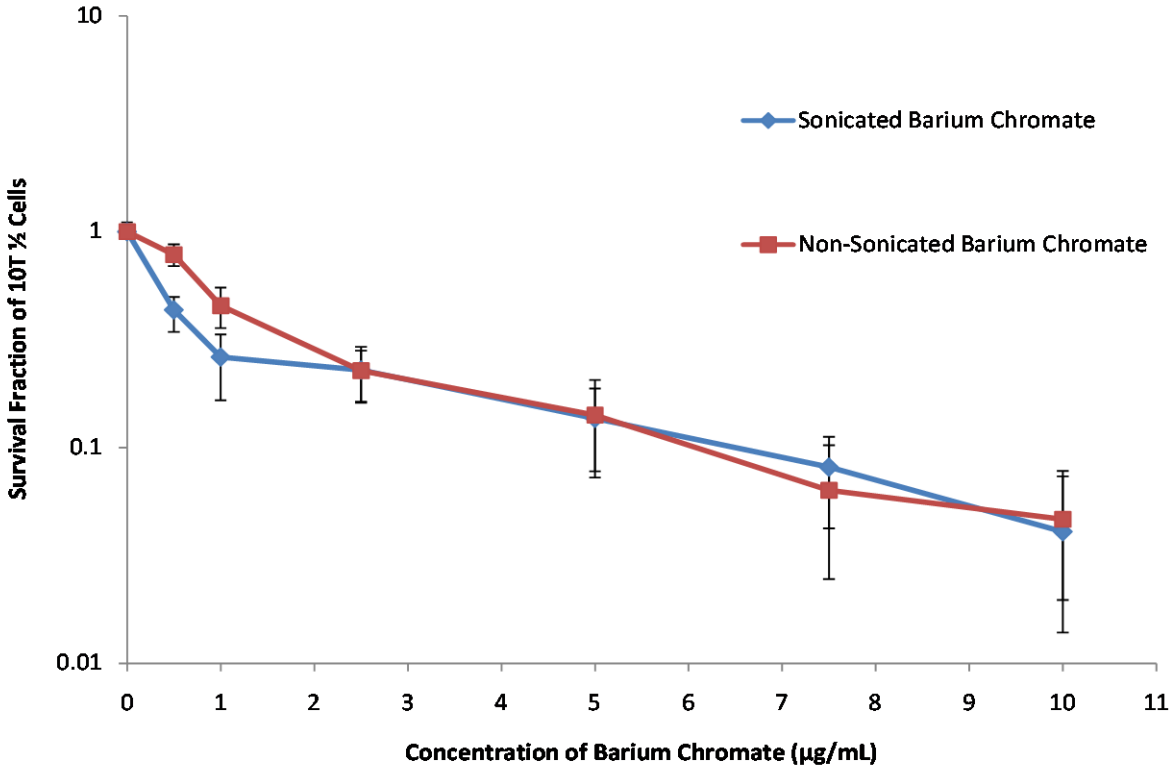

particles of $BaCrO_4$ for 48hrs. The blue line represents the survival curve of CH310T½ treated with sonicated (small particles) $BaCrO_4$, while the red line represents the survival curve of the cells treated with the unsonicated (large particles) $PbCrO_4$.

Table 4.2: **Toxicity Parameters of Large and Small particles of $BaCrO_4$ in CH310T½ cells**

$BaCrO_4$ Form	**LC_{50}**	**LC_{37}**	**K**
Unsonicated $BaCrO_4$	0.93	1.56	0.64
Sonicated $BaCrO_4$	0.43	0.69	1.45

LC_{50} is the concentration of $BaCrO_4$ that provoked a 50% survival

LC_{37} is the concentration of $BaCrO_4$ that caused a 37% survival

$K = 1/ LC_{37}$

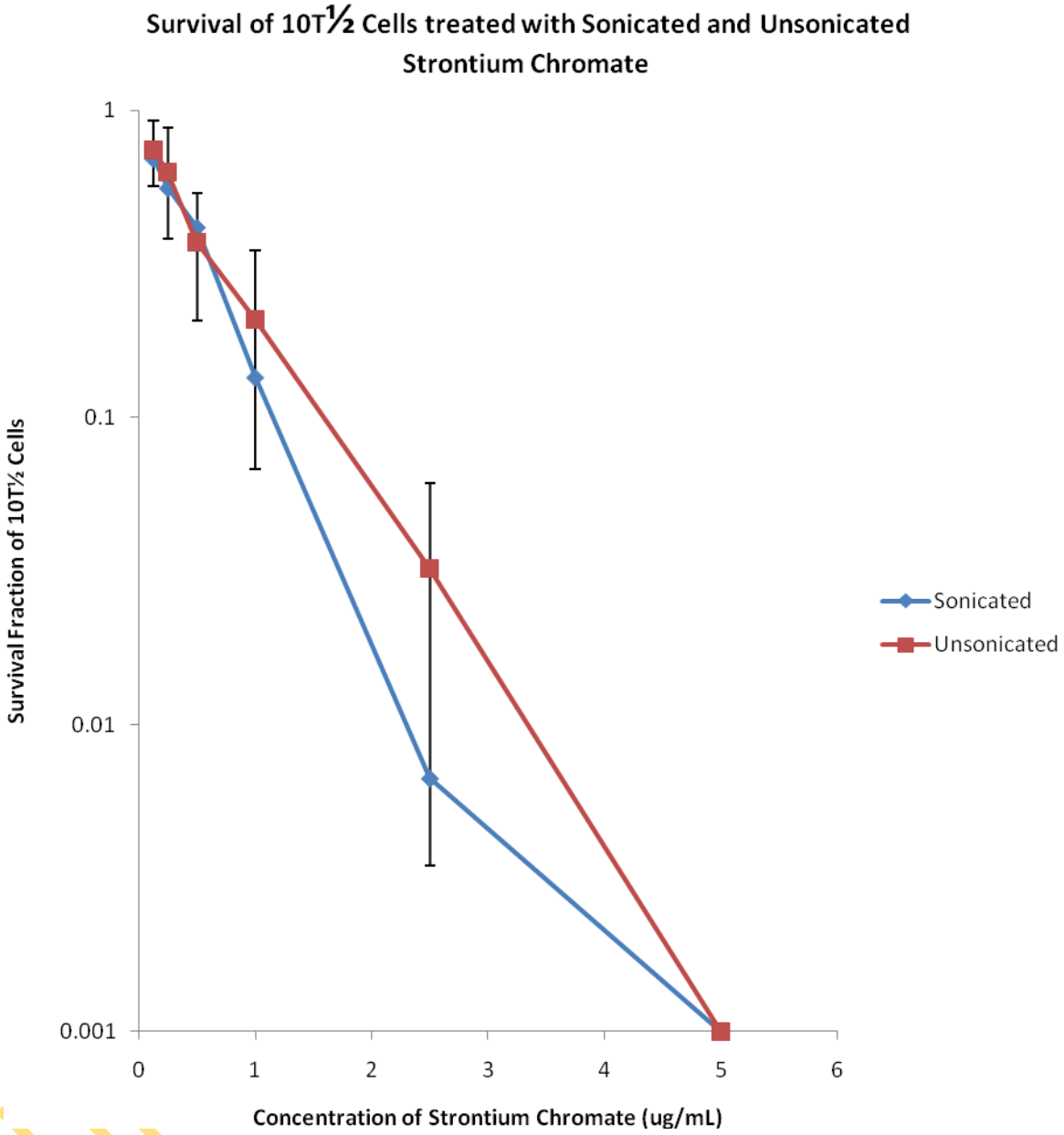

Figure 4.11: Cytotoxicity of sonicated and unsonicated $SrCrO_4$ in 10T½ cells. Exposure of cells to the sonicated particles of $SrCrO_4$ decreased the survival of 10T½ cells at higher concentrations. The blue line represents the survival curve of CH310T½ treated with sonicated (small particles) $SrCrO_4$, while the red line represents the survival curve of the cells treated with unsonicated (large particles) $SrCrO_4$.

Table 4.3: Toxicity Parameters of Unsonicated and Sonicated $SrCrO_4$ in CH310T½ cells

$SrCrO_4$ Form	**LC_{50}**	**LC_{37}**	**K**
Unsonicated	0.37	0.58	2.00
Sonicated	0.35	0.50	1.72

LC_{50} is the concentration of $SrCrO_4$ that provoked a 50% survival

LC_{37} is the concentration of $SrCrO_4$ that caused a 37% survival

$K = 1/ LC_{37}$

4.3 EXPERIMENT 3: PHAGOCYTIC UPTAKE OF $PbCrO_4$, $BaCrO_4$ AND $SrCrO_4$ BY CH310T ½ CELLS

INTRODUCTION

Phagocytic uptake studies was embarked on in order to correlate cytotoxicity of the different insoluble chromate VI with uptake of the particles of the insoluble chromate (VI) compounds in CH310T½ cells.

PROCEDURE

Brifely, 10T½ cells were seeded at 2,000 cells in 60 mm dishes and treated after 24 hours with either sonicated (small particles) or the unsonicated (large particles) form of $PbCrO_4$ or $BaCrO_4$ or $SrCrO_4$ for 2 days. Following 48 hours of exposure, cells were fixed, stained and examined with a light microscope as earlier described under "Materials and Methods" (Section 3.4, P0[-[']]p0ikm k,m u8ijijyhh6y65ttgvrfc dxdcxzage79-80).

RESULT

Phagocytosis has been suggested to be an important means of internalization of insoluble chromate compounds (Patierno *et al.*, 1988). This experiment was therefore an attempted to quantify the internalized chromate (VI) particles and study the morphological features of treated cells by using light microscopy. However, it was difficult to differentiate attached particles from internalised particles by light microscopy.

Light microscopy of the cells exposed to lead chromate revealed that cells were apparently dividing as evidenced by the presence of two nuclei and colony forming ability of the cells especially at the lower doses i.e. 0.5 and 1.0µg/ml (Figure 4.12a and b). At 2.5 and 5.0µg/ml cells were observed to have diminished in size and irregular in shape (Figure 4.12C and E). At these concentrations some cells appeared with condensed cytoplasm, while others appear with vacuolation, cytoplasmic expansion Figure 31C-E. At concentrations greater than 5µg/ml, cells were scarcely seen and cells with condensed cells predominated tissue culture dish Figure 31 (F and G). This may indicate that higher concentration of lead chromate induced growth arrest, while at lower concentration growth is inhibited. Similar observations were made for barium chromate and strontium chromate. However shriveled cells with condensed cytoplasm dominated the dish at 2.5 and 5 µg/ml. For strontium chromate that is relatively much more soluble than the

other two chromate compounds, cells with condensed cytoplasm predominate at 1.0 and 2.5 µg/ml, while cells were scarcely seen at 5 µg/ml. Thus, confirming the earlier observation that strontium chromate is more toxic than barium chromate and lead chromate in CH310T½cells.

Interestingly, some treated cells were observed to have lost their nucleus or gradually pushing it out with a corresponding increase in cytoplasmic space (Figure 4.12E). Similarly, vacuolation appeared to be a common feature in cells exposed to the hexavalent chromate compounds. Therefore, the frequency of anucleation and vacuolation was assessed in treated and control cells. The frequency of anucleation and vacuolation was determined in 100 cells. The percentage of anucleated and vacuolated cells in CH310T½ cells treated with lead chromate, barium chromate and strontium chromate are presented in Figure 4.13 and 4.14 respectively. The percentage vacuolated and anucleated cells increased as the concentration of the insoluble chromates were increased. Under our experimental conditions, barium chromate caused the highest frequency of anucleation, followed by lead chromate (Figure 4.13). Strontium chromate induced the least anucleation. The increasing order of vacuolation of CH310T1/2 cells by the chromates compounds was: $SrCrO_4$<. $BaCrO_4$ <$PbCrO_4$

It was difficult to differentiate attached particles from internalised particles by light microscopy. Therefore, it was impossible to quantify cells with internalised particles in cells exposed to different concentration of the 3 chromate compounds using light microscopy. The percentage of cells with internalised particles were however, scored in thick sections of cells treated with lead chromate and barium chromate over a 48h period (Figure 4.15 and Table 4.5). Lead chromate and barium chromate were very insoluble and a lot of the particles were retained 48h after treatment, whereas $SrCrO_4$ was relatively soluble. The intracellular uptake of the chromate compounds was clearly evident as early as 6h after treatment and throughout the duration of the experiment. Sometimes particles were found in vacuoles and at other times they were found independent of the vacuole. For both compound, the percentage of cells with internalized particles increases as the time of exposure (Table 4.4). Thus, cellular uptake of $PbCrO_4$ and $BaCrO_4$ and invariably their toxicities were time-dependent. In addition, exposed cells showed morphological features of apoptosis as evidenced by blebbing of the membrane, cell shrinkage, condensation of nuclei material and formation of apoptotic bodies (Figure 4.15C). Similarly, morphological signs of necrotic cell death were observed at the three different time of exposure

in this study as revealed by extensive vacuolization (Figure 4.15D) and expulsion of the nucleus (Figure 4.15E)

CONCLUSION

The chromate (VI) particles are internalized by CH310T½ cells and the nature of cell death in treated cell is a mixture of apoptosis and necrosis. Inaddition, hexavalent chromate treatment led to anucleation in CH310T½ cells.

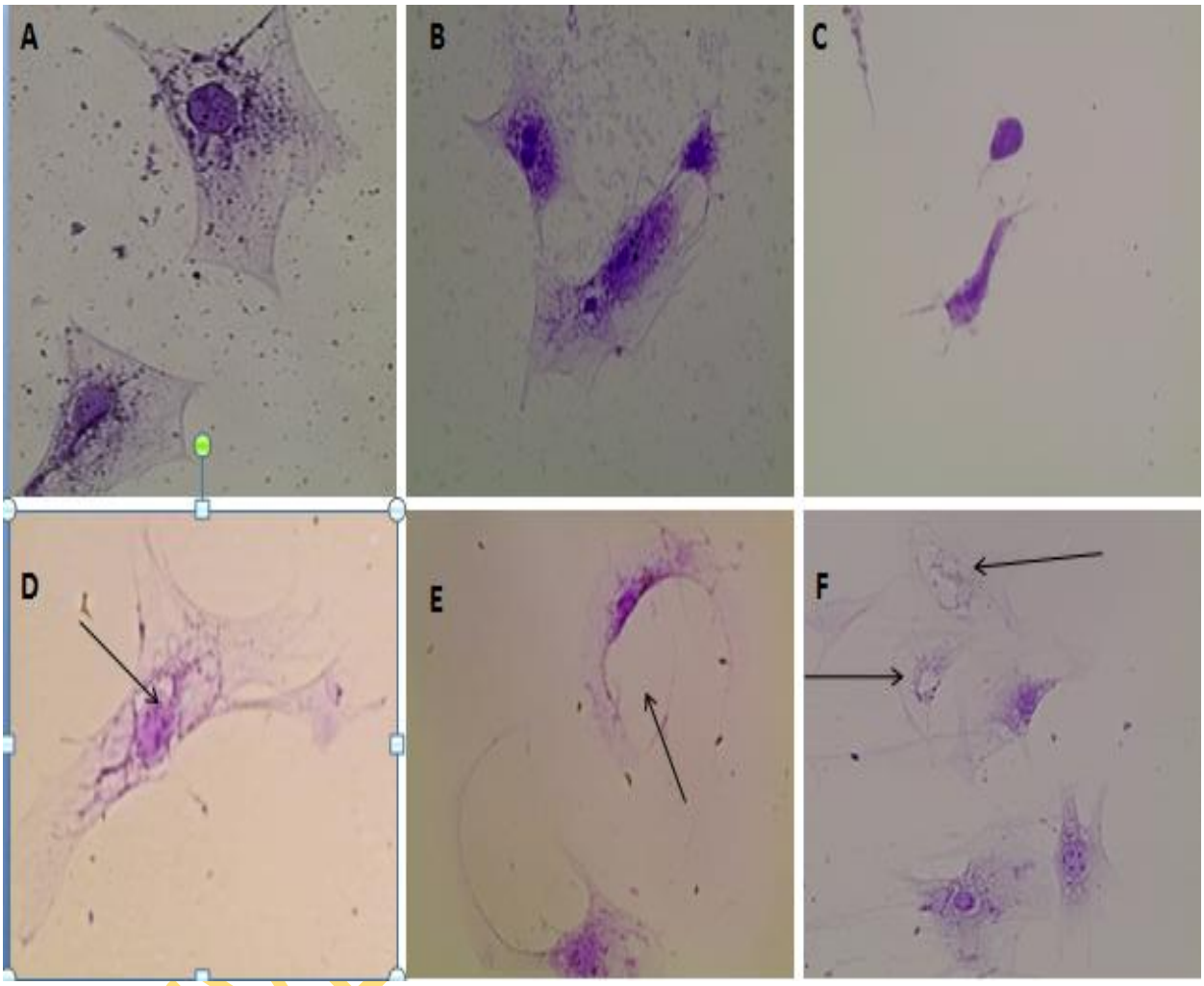

Figure 4.12: Micrographs showing the effect of insoluble chromate treatment on 10T ½ cells. (A) Control cells with normal cellular structure and morphology (B) Dividing cells even after chromate treatment(C) Condensed cells (D) A vacuolated cell (arrow) (E) Distorted cells (arrow) (F) Anucleated cells (arrow) X 40

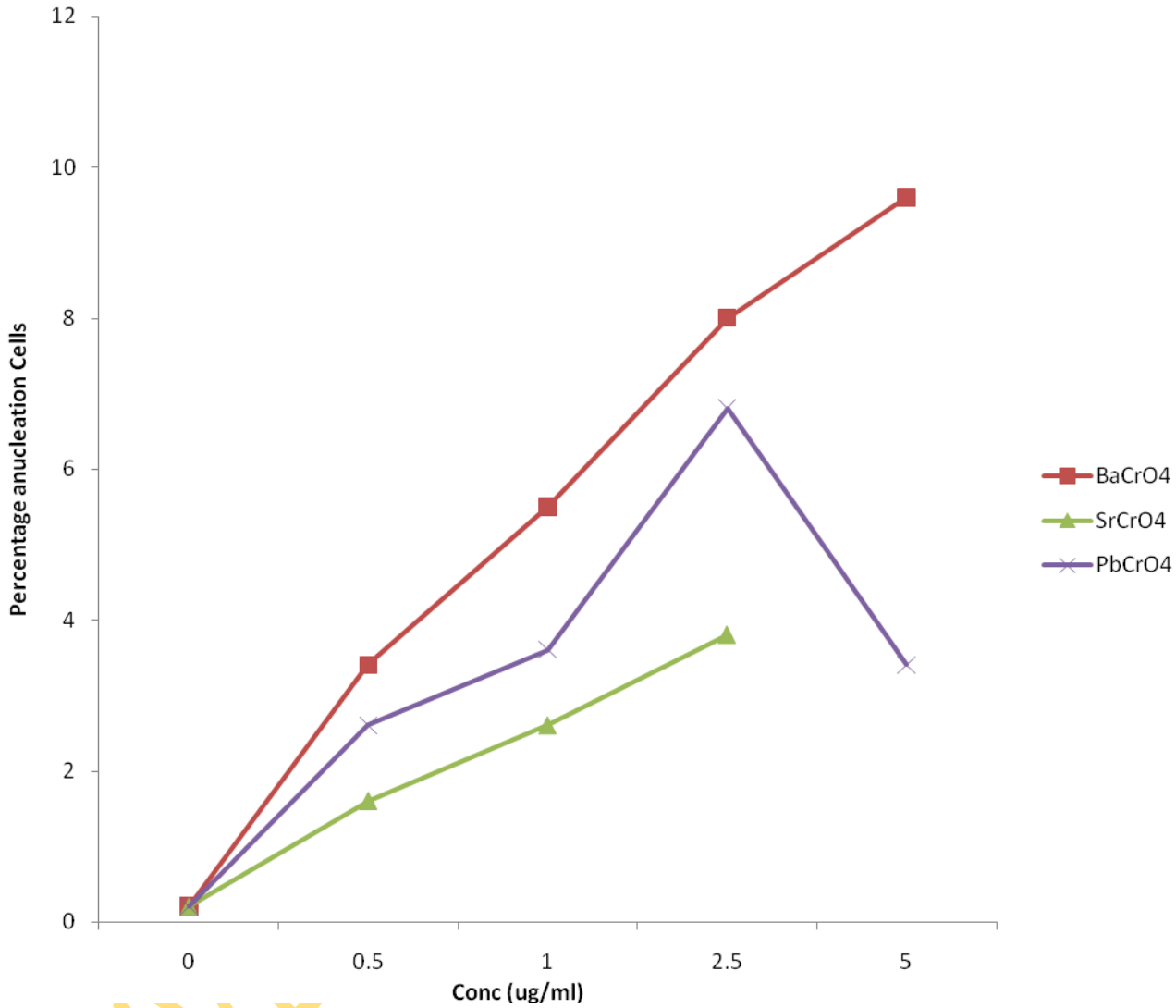

Figure 4.13: Assessment of anucleation in the log phase CH310T½ cells exposed to $PbCrO_4$ or $BaCrO_4$ or $SrCrO_4$ for 48h. The red, green and purples represent the percentage of anucleated cells observed in cells treated $BaCrO_4$, $PbCrO_4$ and $SrCrO_4$ respectively.

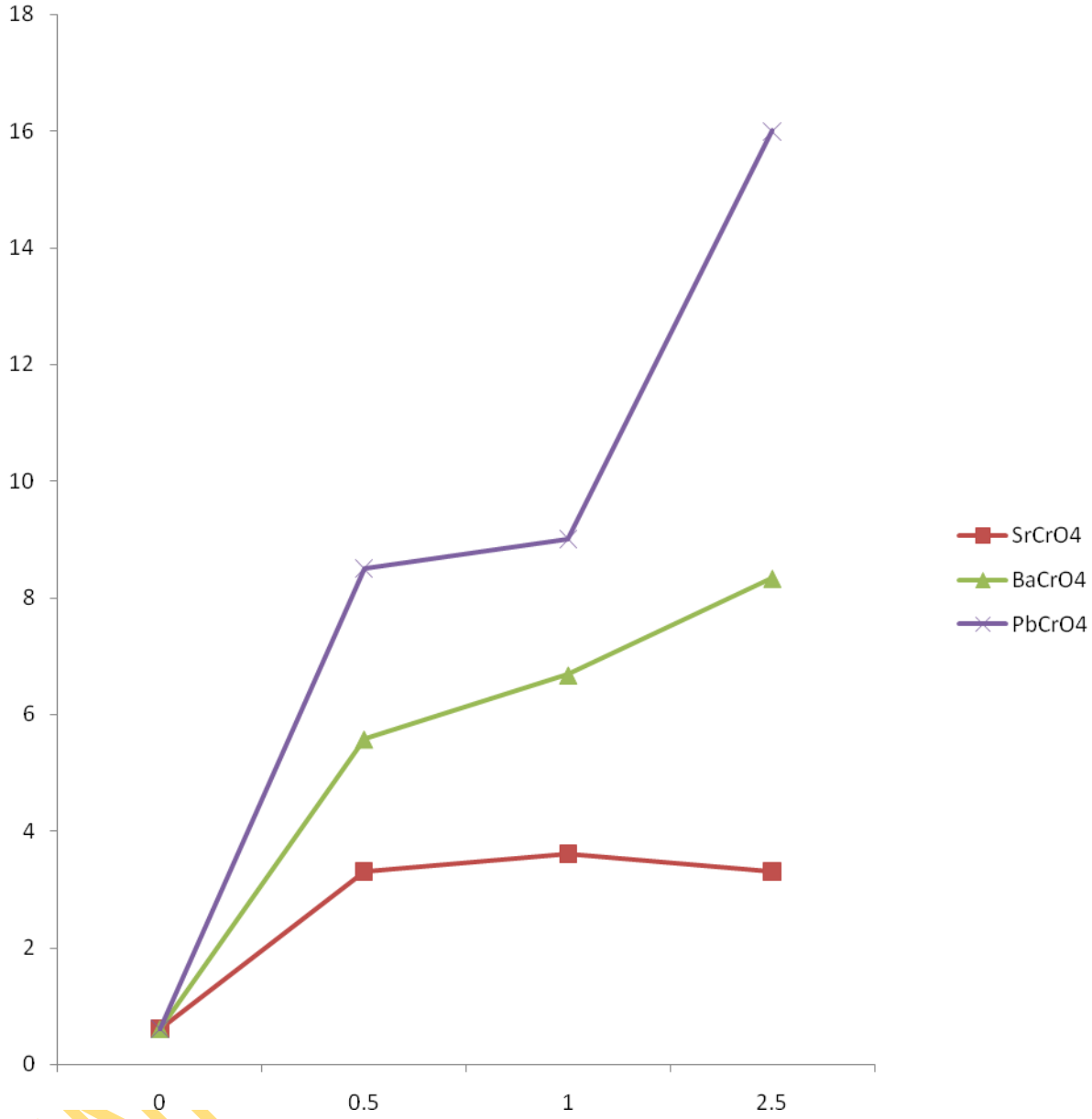

Figure 4.14: Formation of phagocytic vacuoles by CH310T½ cells in the log phase growth exposed to $PbCrO_4$ or $BaCrO_4$ or $SrCrO_4$ for 48h. The red, green and purples represent the percentage of vacuolated cells observed in cells treated $SrCrO_4$, $BaCrO_4$ and $PbCrO_4$ respectively.

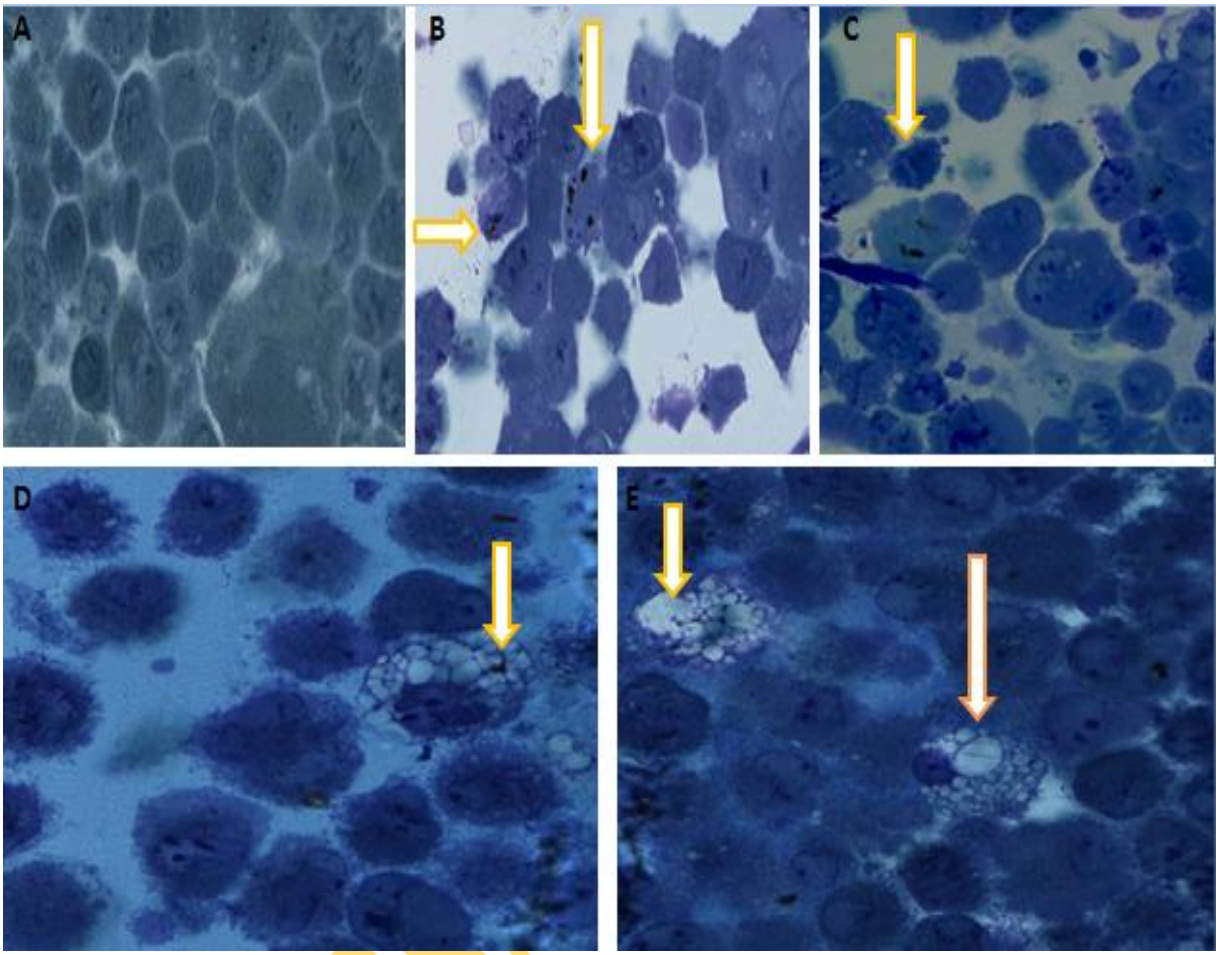

Figure 4.15: The Thick section (1µm) from chromate treated 10T ½ cells. (A) Control cells (B) Cells with internalised particles (arrow) (C) An apopotic cell with blebb (arrow) (D) A vacuolated cell (arrow) (E) Anucleated cells (arrow) X 10^3

Table 4.4: Percentage cells with internalized particles in cells exposed to $PbCrO_4$ or $BaCrO_4$ for 6- 48h. 4 thick sections were scored for cells with internalised particles

.

Exposure Time (h)	**% cells with Internalised $PbCrO_4$ particles**	**% cells with Internalised $BaCrO_4$ particles**
0	0	0
6	10.36 ± 2.61	16.04 ± 6.59
24	12.85 ± 2.36	16.23 ± 0.74
48	21.13 ± 7.12	24.99 ± 3.45

4.4 EXPERIMENT4: SCANNING ELECTRON MICROSCOPY OF CH310T ½ TREATED WITH $PbCrO_4$, $BaCrO_4$ AND $SrCrO_4$

INTRODUCTION

Scanning electron microscope (SEM) was done in order to visualize damage to cell membrane of treated cells. This may also give information about the toxicity of chromate compounds and mode of cell death.

PROCEDURE

About 500,000 logarithmic growing cells were seeded in 25ml dishes and allowed to adhere overnight before treatment with 2.5 µg/ml $PbCrO_4$ or 2.5µg/ml $BaCrO_4$ or 1.0ug/ ml $SrCrO_4$ for 6h or 12h or 24h or 48 h. Immediately following treatment dishes containing the cells were prepared for scanning electron microscopy as earlier described under "Materials and Methods" (Section 3.8, Page 80-82).

RESULTS

The SEM images obtained from the cell cultures (Figure 4.16) showed that the chromate particles pierce through membrane (Figure 4.16B) and had clear effect on the membrane integrity after 6h of lead chromate exposure, whereas untreated cells retained their membrane structure (Figure 4.16). Exposed cells showed cellular flattening, membrane blebs, formation of filopodia and blisters as well as formation apoptotic bodies, which are hallmarks of cells undergoing apoptotic cell death (Figure 4.16B and C). The degree of appearance of the above mentioned morphological features of apoptosis continued to increase in tissue culture exposed to lead chromate for 24h (Figure 4.16C). It was further exacerbated in cells exposed for 48h (Figure 4.16C and D). Similarly, cells with necrotic morphology were observed in some cells as early as 6h after lead chromate exposure. This was characterized by evident vacuolation (Figure 4.16D), which is suggestive of loss of membrane activity as well as permeability. Furthermore, cracks that led to the visibility and protrusion of the nucleus were also observed in some cells (Figure 4.16C).

CONCLUSION

The chromate (VI) particles were internalized by CH310T½cells and the nature of cell death in treated cell is a mixture of apoptosis and necrosis.

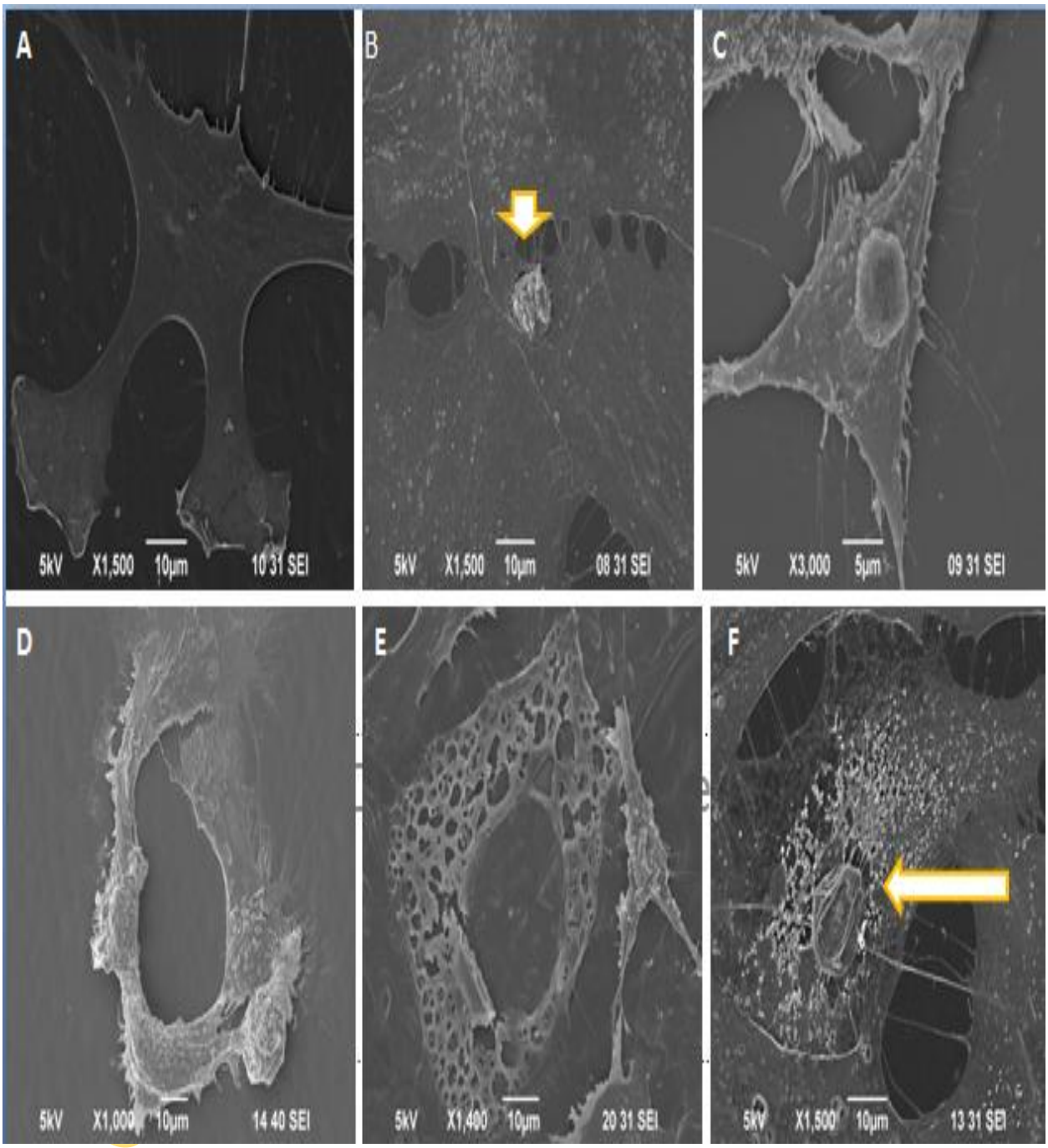

Figure 4.16: SEM micrograph of cells treated with $PbCrO_4$ for 0h (A), 6h (B) and (C), 24h (D) and 48h (E & F). Arrow head chromate particles been internalized by 10T½ cells, while arrow indicate an exposed nucleus in treated cell. X 1.5 X 10^3

4.5 EXPERIMENT 5: TRANSMISSION ELECTRON MICROSCOPY OF CH3 10T ½ CELLS TREATED WITH $PbCrO_4$, $BaCrO_4$ and $SrCrO_4$

INTRODUCTION

Transmission Electron Microscopy (TEM) provides information on the mode entry of the insoluble chromate (VI) into the cell. Additionally, TEM provides mechanism information on the mode cell death. Furthermore, the effect of the three chromate (VI) compounds on cellular ultra structures was also studied using TEM.

PROCEDURE

About 100,000 logarithmic growing cells were seeded in 75ml flask and allowed to adhere, and cultured until 70% confluence before treatment with 2.5 µg/ml $PbCrO_4$ or 2.5µg/ml $BaCrO_4$ or 1.0ug/ ml $SrCrO_4$ for 6h or 12h or 24h or 48 h. The control was left untreated.Immediately following treatment, cells were harvested and processed for transmission electron microscopy as earlier described under "Materials and Methods" (Section 3.8, Page 82-83).

RESULTS

The uptake of the insoluble chromate compounds may be required before their intracellular fate and toxic effect could be studied. Phagocytosis has been suggested a mechanism by which insoluble chromate enter different cells including fibroblast (Patierno *et al.*, 1988). The intracellular localisation of the chromate compounds was evaluated from the images of CH310T½ cells exposed to lead chromate, barium chromate and strontium chromate during a 48-h period. The TEM image illustrating the series of step involved in the uptake of the chromate compounds are shown in Figure 4.17. The uptake sequence in CH310T½ cells was a stepwise process in which the insoluble chromates compounds were first attached to the cell surface and subsequently internalised by vesicle-mediated phagocytosis. After attaching to the external side of the cell (Figure 4.17), the invagination of the cell membrane began at the areas of contact (arrow in Figure 4.17) to form an endosomal structure that finally progressed to the cell interior with some of its volume occupied by the endocytosed chromate particles (arrow head in Figure 4.17).

Chromates particle were seen inside the cells as early as 2 hours after treatment with the chromate compounds. Chromates particles were seen with or without phagocytic vacuoles in the cytoplasm as early as 2hrs after treatment and the internalization of chromate compounds was

time dependent (Figure 4.18). The particles were confirmed inside the cells using X-ray diffraction (Fig 4.19). The X-ray diffraction spectrum shown in Figure 4.19A was targeted at a lead chromate particle present in the cytoplasm, while that of Figure 4.19B was targeted at a lead chromate particle present in the nucleus. Both Cr and Pb ions were detected in both organelles, implying that both ions were released by the dissolution of lead chromate particles. Alternatively, scanning electron micrograph of the particles taken before treatment was compared with phagocytosed particles in the TEM images (Figure 4.20). Chromate particles were seen in other organelles such as endoplasmic recticulum and mitochondria (Figure 4.21)

In addition, TEM was used to investigate whether exposure of the three chromate compounds would lead to changes in subcellular organelles, organelles structure and organization in CH310T½ cells (Figure 4.22-4.32 and in Table 4.5- 4.7). The control cells were normal with irregular nuclei with intact nuclear membrane and several endoplamic recticulum. The cells contained several mitochondria with visible cristae. They were also filled with several rough endoplasmic reticulum (rER) as well as polyribosomes indicative active protein synthesis typical of fibroblast (Figure 4.21A, 4.22A and 4.23A). In contrast, the toxic effects the chromate compounds appear to affect several cellular organelles including nucleus, mitochondria, rER, lysosome, cytoskeleton etc (Figure 4.21-.28). The toxicity of $PbCrO_4$, $BaCrO_4$ and $SrCrO_4$ to different organelles in cells exposed to the compounds as compared to the control over a period of 48hrs is summarized in Table 4.5. 4.6 and 4.7 respectively. Furthermore, TEM confirmed that nature of cell death in treated cells was mixed because prominent features of the three main mode of cell death: autophagy, apoptosis and necrosis were also observed at higher frequency in chromate (VI) treated cells (Figure 4.29-31)

CONCLUSION

TEM confirmed that the mode of entry of the insoluble chromate particles into CH310T½ cells is by phagocytosis. The internalised insoluble chromate particles caused alteration and toxicity to several subcellular organelles, which may eventually lead to cell death. The nature of cell death observed in cells exposed to the three chromate compounds is mixed: apoptosis, necrosis and autophagy.

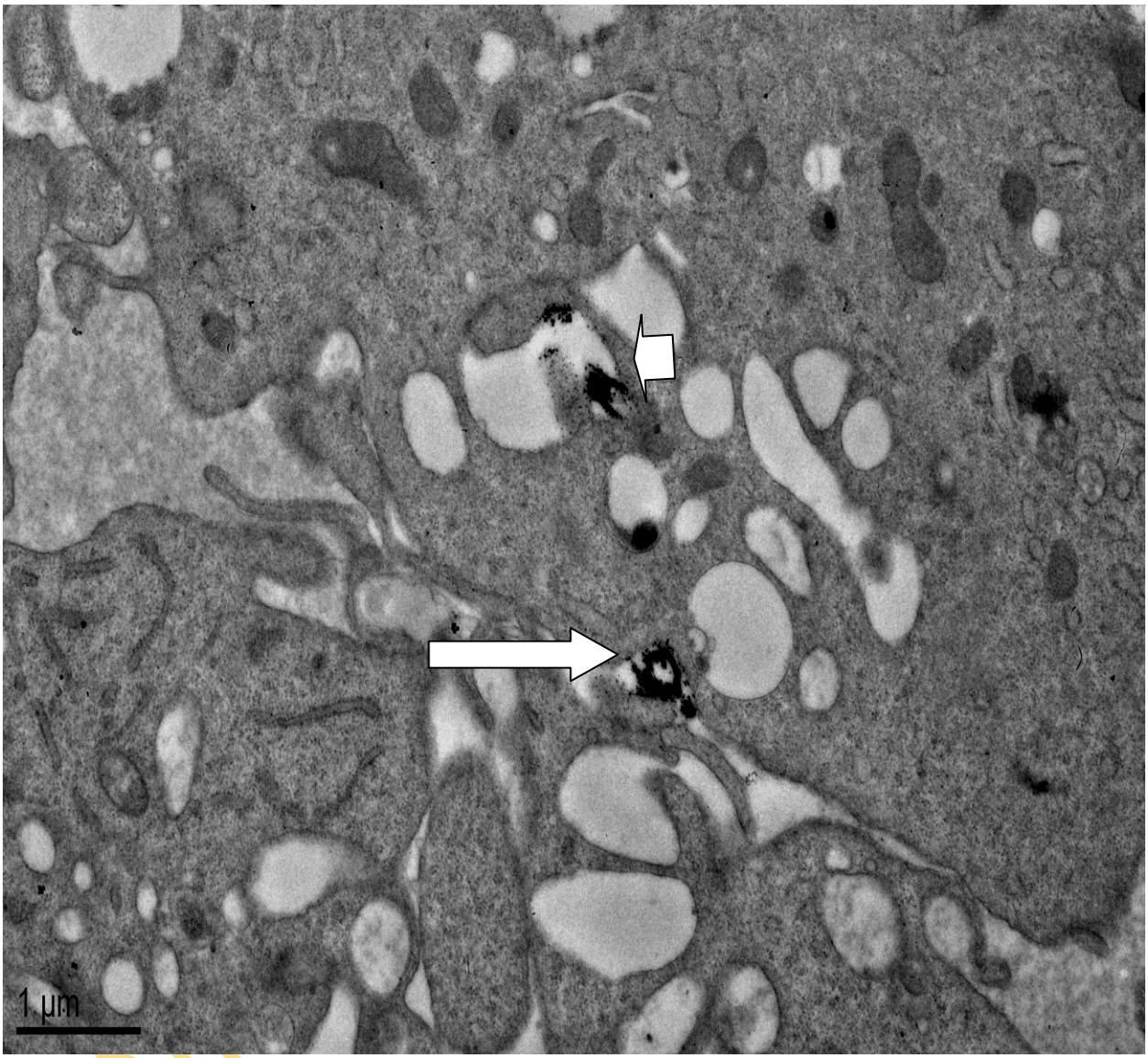

Figure.4.17: TEM images of 10T½ cells showing phagocytic uptake of $PbCrO_4$. The presence of $PbCrO_4$ bound to the cell surface and invagination of the cell membrane can be seen (arrow). Arrow head show phagosome with $PbCrO_4$ particle inside. X 2.5 X 10^3

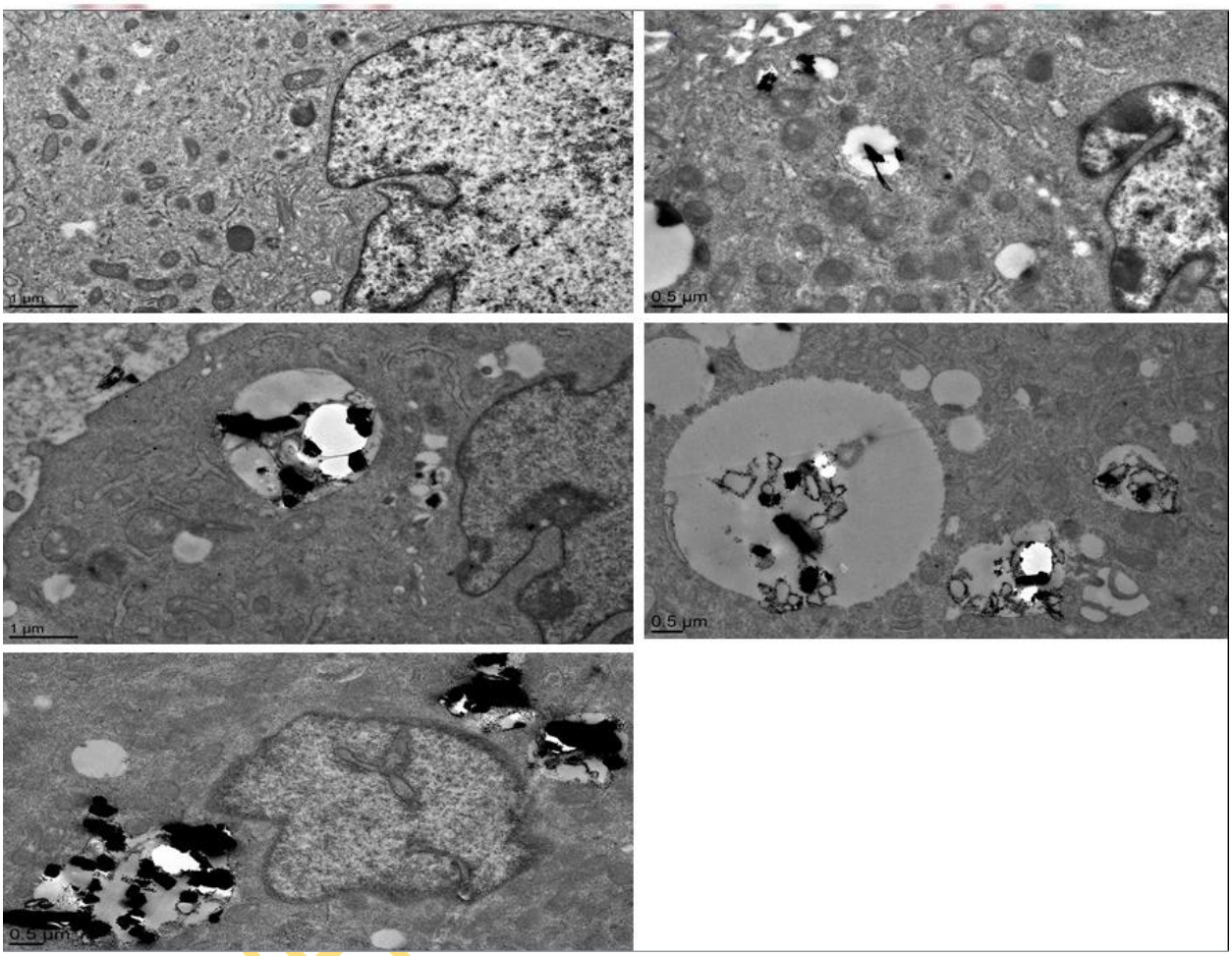

Figure 4.18: Time dependent increase in internalization of lead chromate. (A) Control (B-E) Cells were treated with $PbCrO_4$ for 2h, 6h, 24h and 48hrs respectively. X 2.5 X 10^3

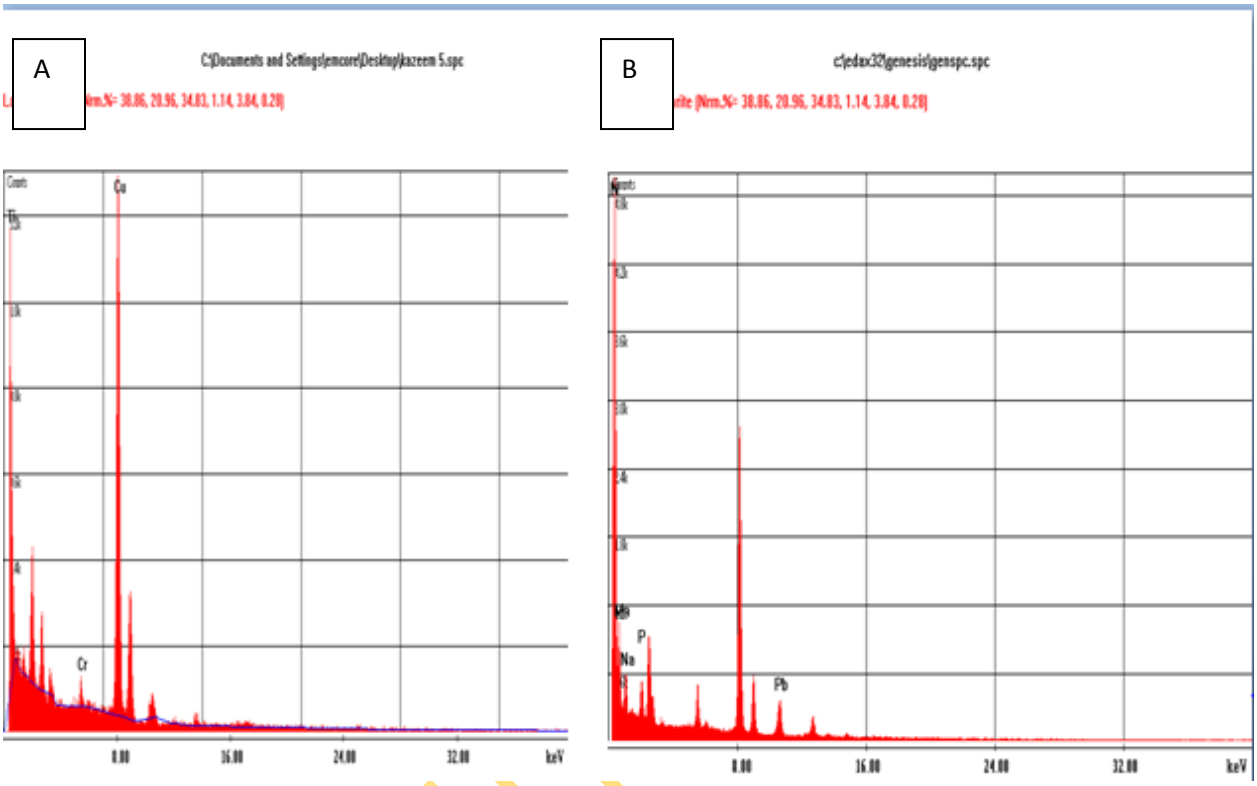

Figure 4.19: Energy Dispersive X-rays (EDX) analysis of $PbCrO_4$ treated 10 T1/2 cells. EDX spectra of the lead chromate found in the cytoplasm (A) and nucleus (B).

Figure 4.20: Phagocytosed $SrCrO_4$ particles in the cytoplasm of CH310T½ cells (A) X 2500 and SEM picture of the $SrCrO_4$ particles used in this study (B) 1.5 X 10^3.
Big arrow in A shows $SrCrO_4$ particles in the cytoplasm of the treated cells.
The slim arrow in B shows the same particle before being exposed to the cells.

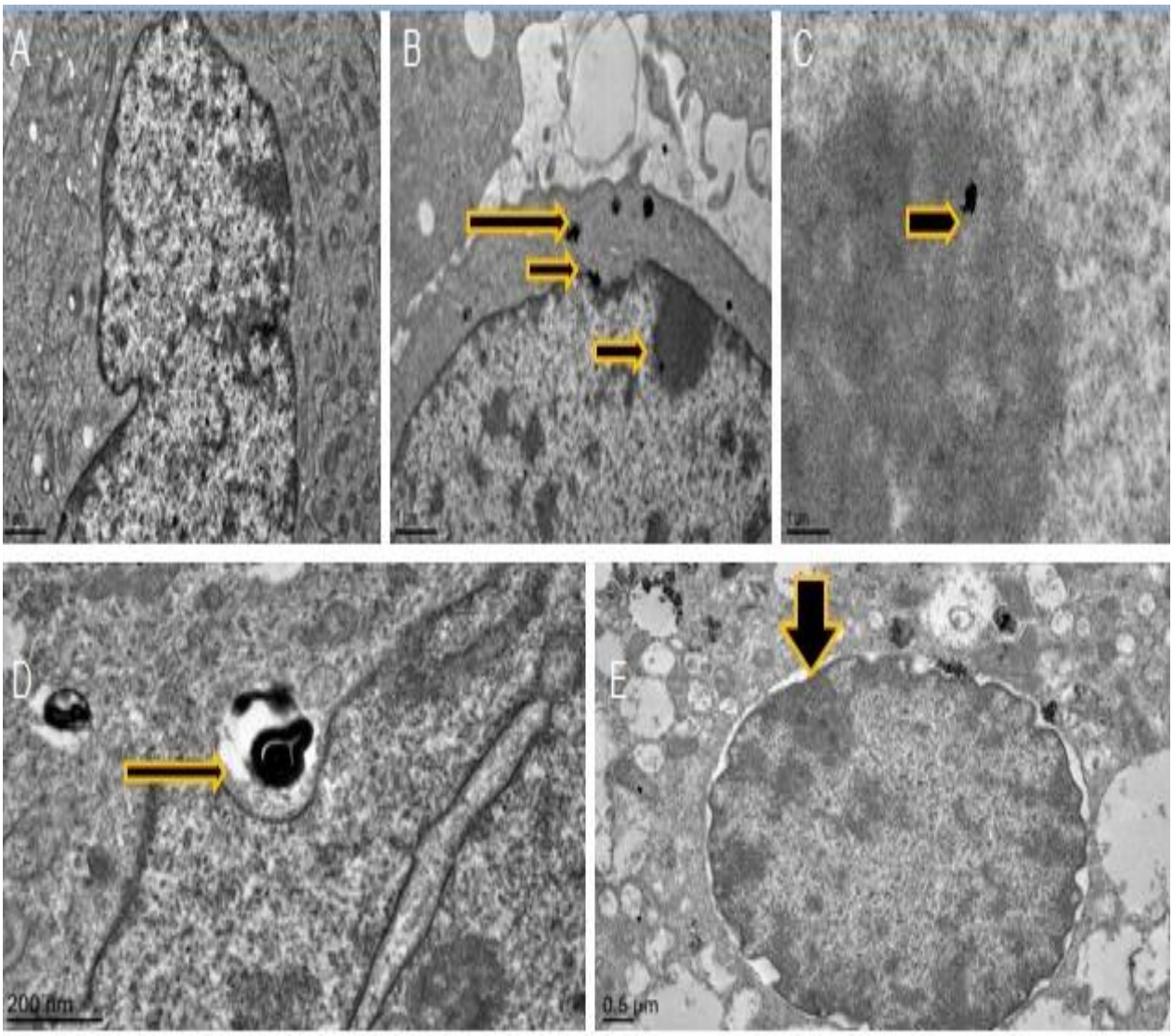

Figure 4.21: The hexavalent chromate particles in the cytoplasm and nucleus. (A) Untreated CH310T1/2 cells with normal intracellular structures (B) Phagocytosed chromate particles in cytoplasm, on nuclear membrane and in the nucleus(C) Chromate particle in the nucleus (D) Invagination of the nuclear membrane caused by an approaching particles, which may results in the particle being vescularised into the nucleus (E) Dilation of nuclear membrane in cell exposed to the insoluble chromate [A, B ,D and E X 2.5 X 10^3 , C 1.0 X 10^3]

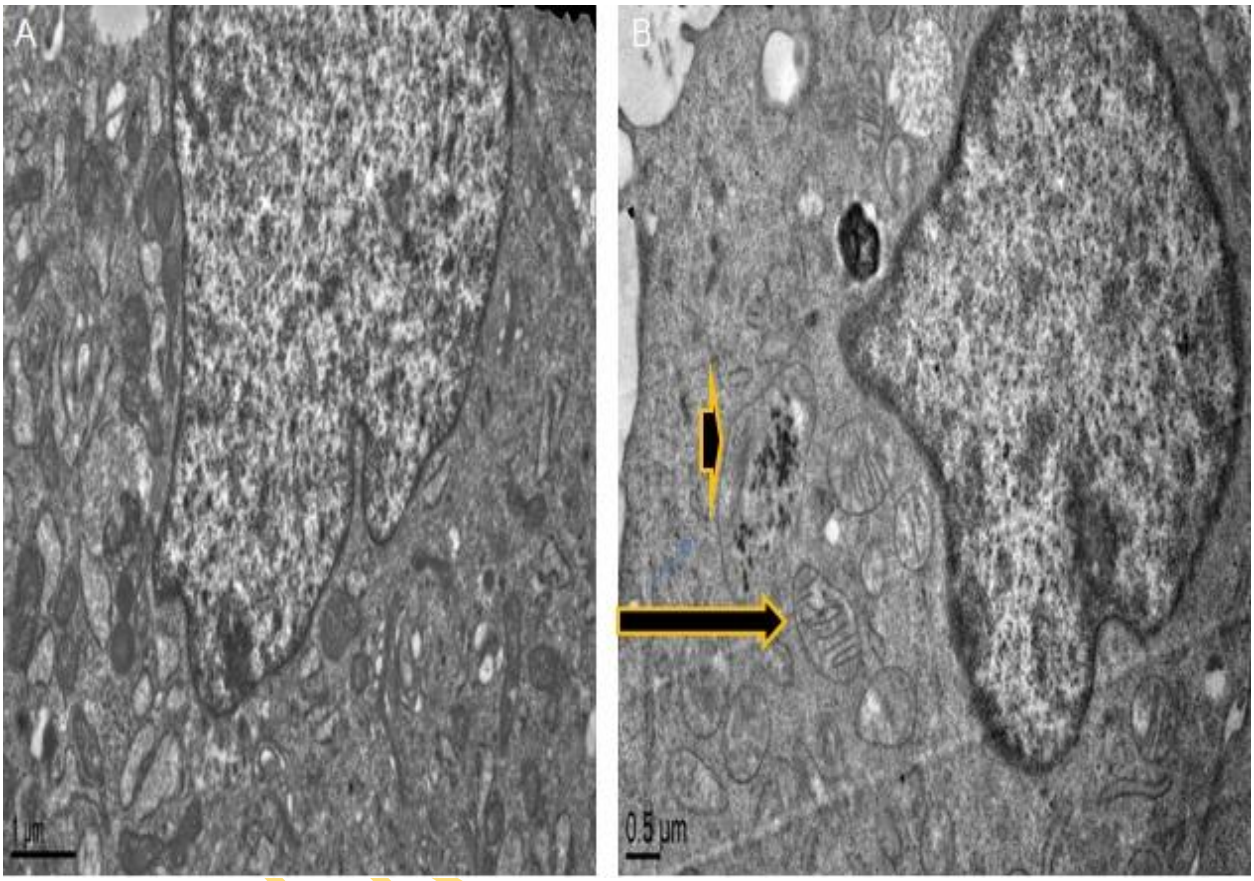

Figure 4.22: The effect of chromate treatment on the mitochondria ultrastructure. (A) Control cells with normal mitochondria architecture. (B) Treated cells showing dilated cristae (arrow) and condensed mitochondria (arrow head) X 2.5 X 10^3

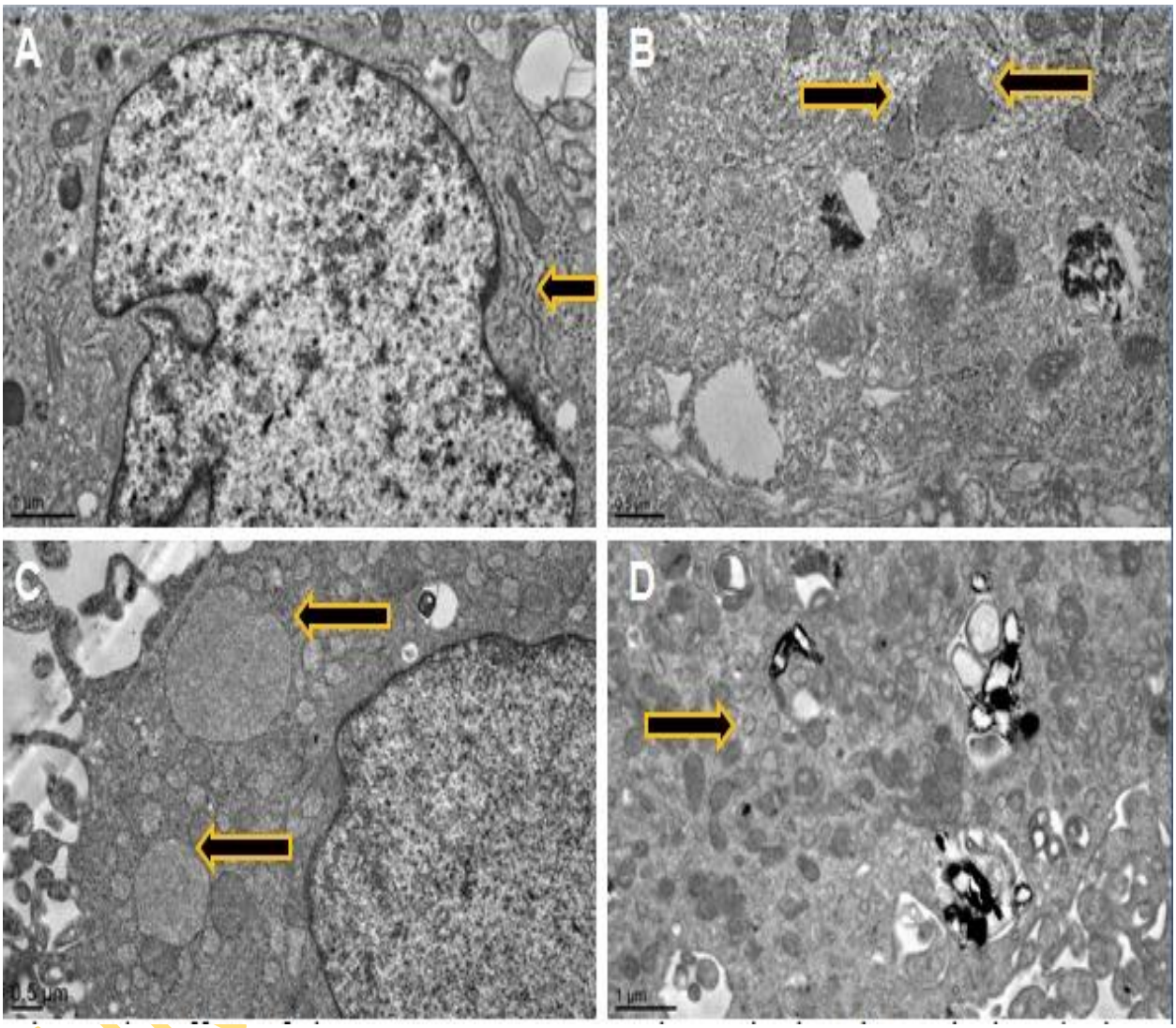

Figure 4.23: The effect of chromate treatment on the endoplasmic recticulum (ER). Control with normal ER (arrow in A). Chromate treated cells showed dialated ER (arrow in B), swollen ER (arrow in C) and shortened ER (arrow in D). X 2.5 X 10^3

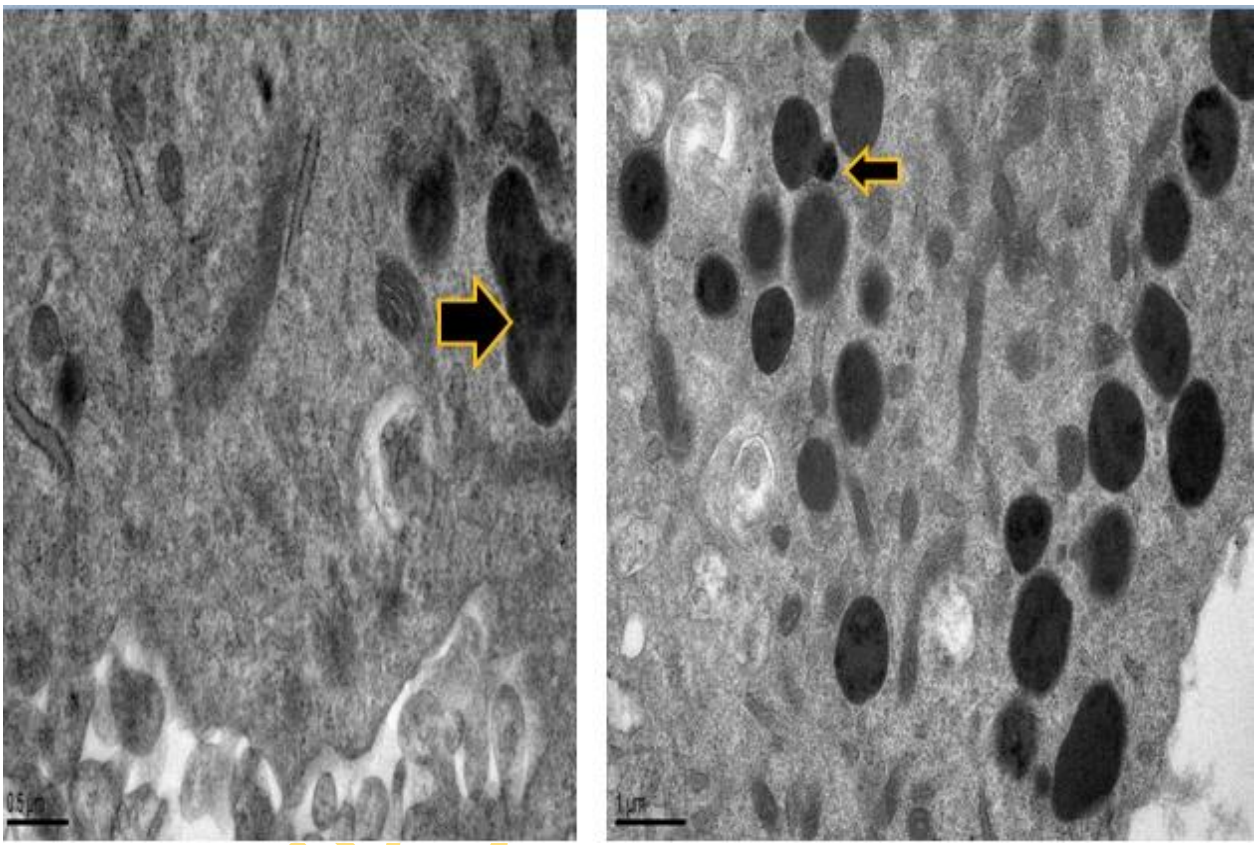

Figure 4.24: The effect of hexavalent chromate treatment on lysosome in CH310T½ cells. The distorted (arrows in A and B) and high number of lysosomes (B) in chromate treated cell X 2.5 X 10^3.

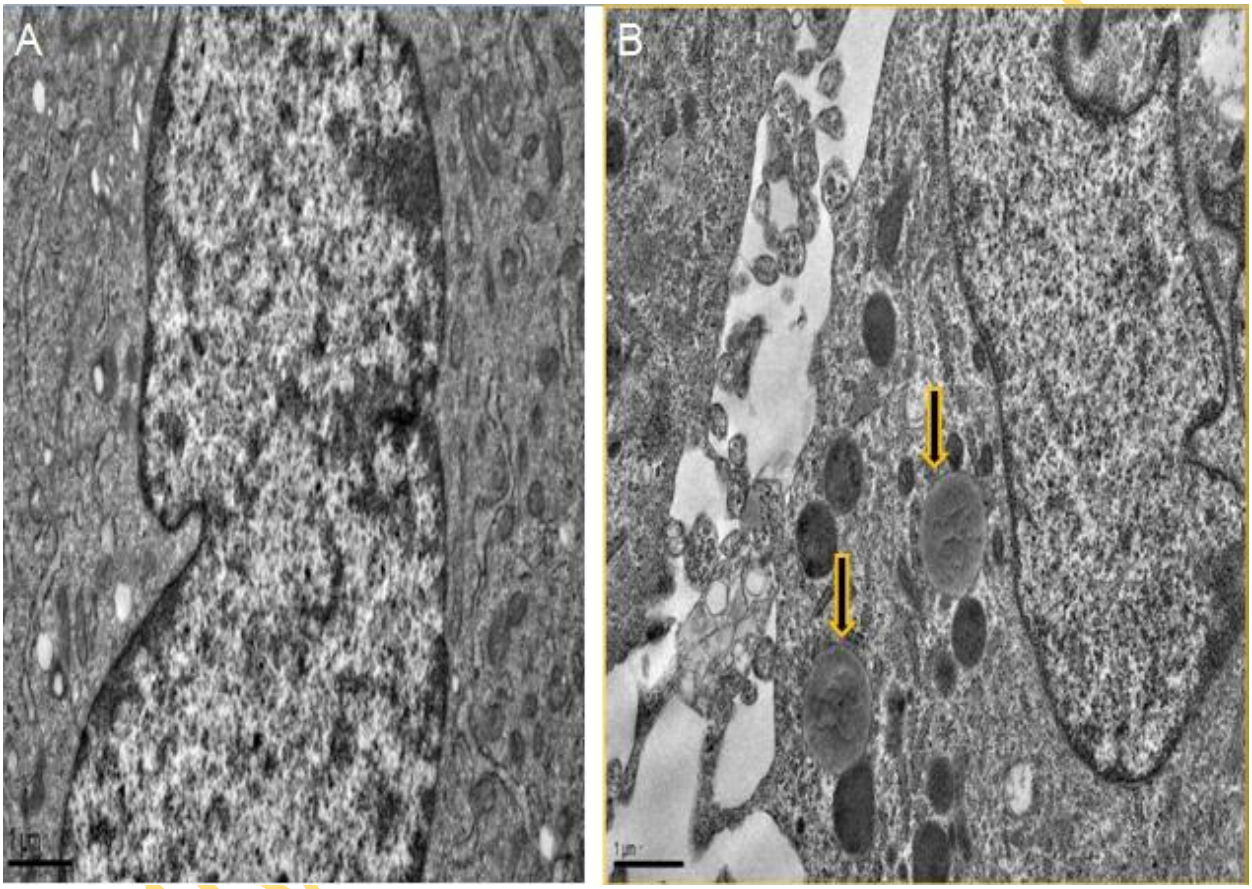

Figure 4.25: Chromate treatment led to the formation of lipid droplet (arrow in B) as compared to the untreated control (A) X 2.5 X 10^3

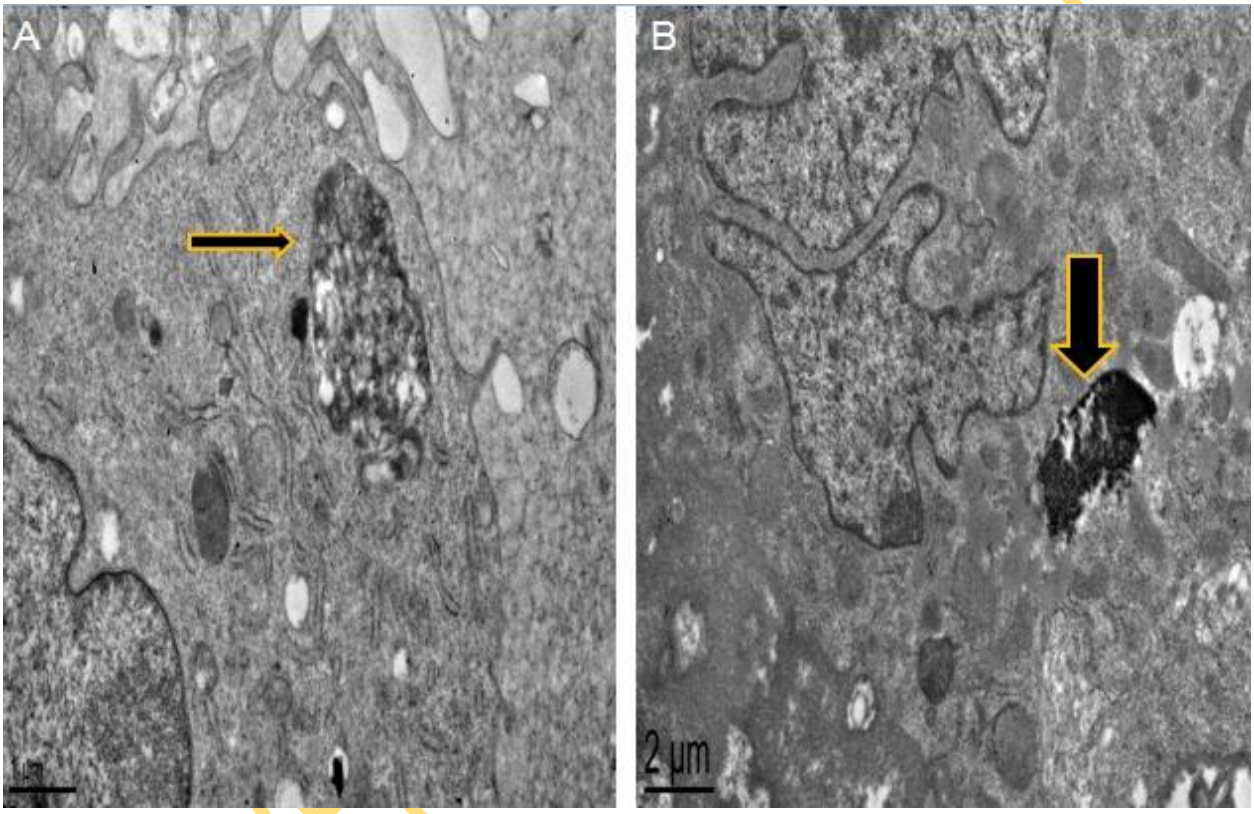

Figure 4.26: Focal degeneration (arrows) was frequently observed in chromate treated cells X25 X 10^3

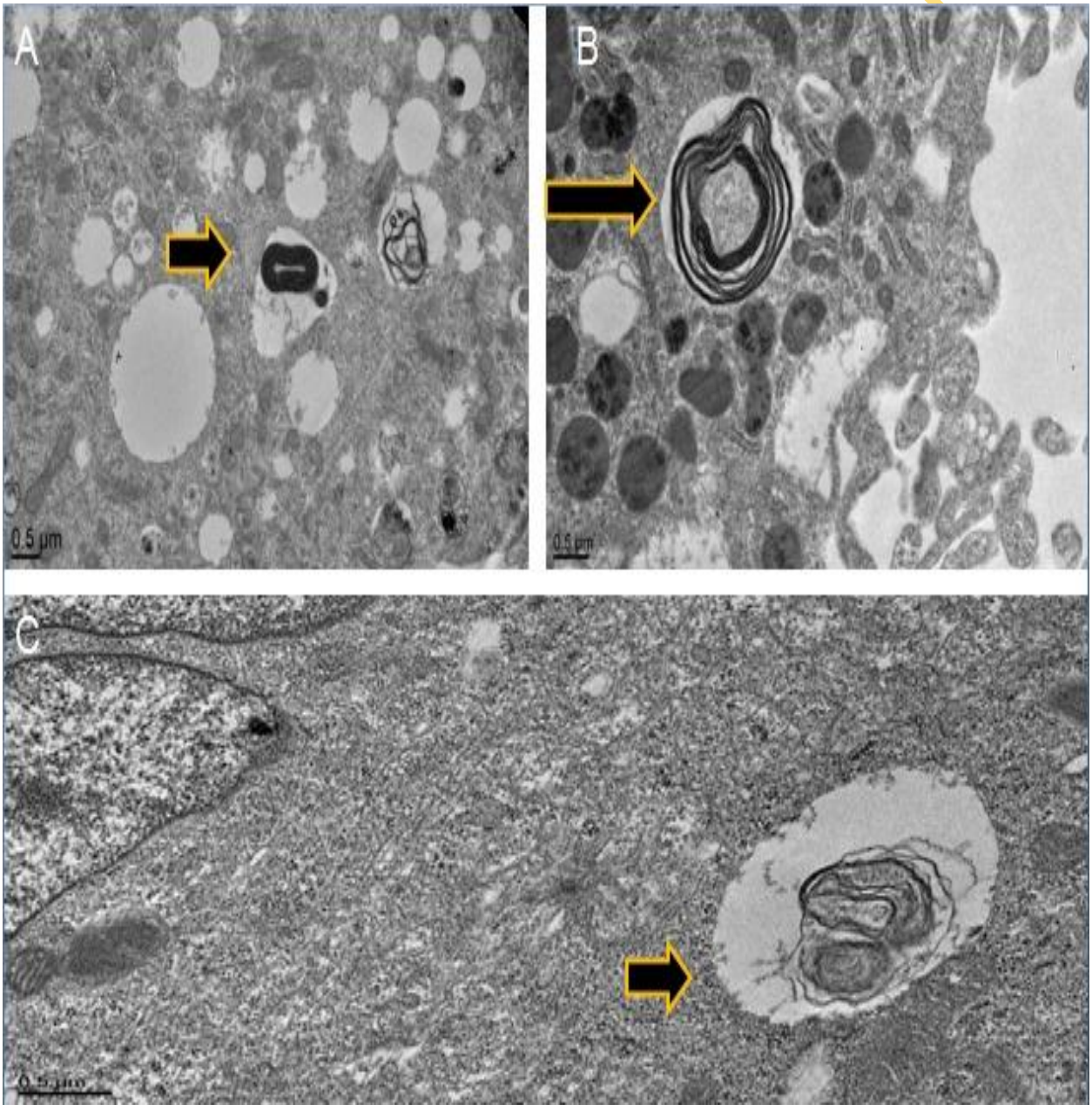

Figure 4.27: Different forms of myelin figures (arrows) observed in chromate treated cells X 2.5 X 10^3

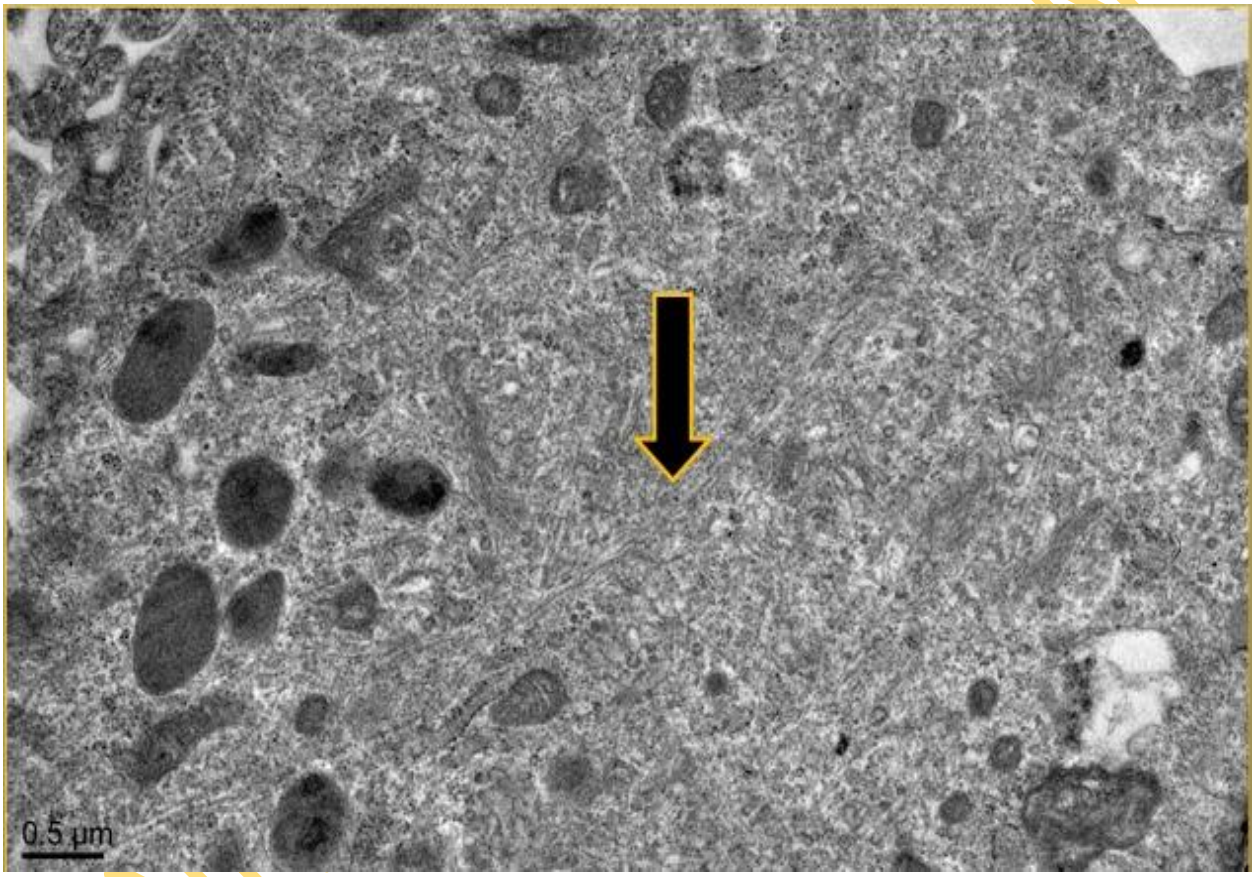

Figure 4.28: Disruption of cytoskeletal structure (arrow) in chromate treated cells X 2.5 X10^4

Table 4.5: Alteration in ultrastructures of 10T ½ cells treated with $PbCrO_4$

Effect	Control	6h	24h	48h
Irregular Shaped Nuclei	+++	+++	+++	+++
Dilated Nuclear Membrane	–	–	++	++
Dilation of rER	+	+++	+++	+++
Shortened ER	+	+++	+++	+++
Swollen ER	+	++	++	+++
Smaller Mitochondria	+	+	+	++
Mitochondria Granules	–	–	+++	++
Large no of Lysosome	+	+	+	++
Distorted Lysosome	+	+	+	++
Lipid Droplet	–	–	+++	++
Focal Degredation	–	+++	+++	+++
Large Vacuoles	+	+++	+++	+++
Myelin Figures	++	++	+++	+++
Autophagic Vacuoles	++	+++	+++	+++
Disruption of cytoskeleton	–	–	++	++

Absent (-), occurred rarely (+), occurred occasionally (++), occurred often (+++).

Table 4.6: Alteration in ultrastructures of 10T ½ cells treated with $BaCrO_4$

Effect	Control	6h	24h	48h
Irregular Shaped Nuclei	+++	+++	+++	+++
Dilated Nuclear Membrane	–	+	++	++
Dilation of rER	+	++	++	+++
Short ER	+	++	++	++
Swollen ER	+	–	–	–
Smaller Mitochondria	+	++	++	++
Mitochondria Granules	–	–	+	++
Large no of Lysosome	+	+++	+++	+++
Distorted Lysosome	+	+++	+++	+++
Lipid Droplet	–	++	+++	+++
Focal Degredation	–	++	++	+++
Large Vacuoles	+	++	+++	+++
Myelin Figures	++	+++	+++	+++
Autophagic Vacuoles	++	+++	+++	+++
Disruption of cytoskeleton	–	–	+++	++

Absent (-), occurred rarely (+), occurred occasionally (++), occurred often (+++).

Table 4.7: Alteration in ultrastructures of 10T ½ cells treated with $SrCrO_4$

Effect	**Control**	**24h**	**48h**
Irregular Shaped Nuclei	+++	+++	+++
Dilated Nuclear Membrane	–	–	–
Dilation of rER	+	+++	+++
Shortened ER	++	++	++
Swollen ER	+	++	+
Smaller Mitochondria	+	+	++
Mitochondria Granules	–	+	+
Large no of Lysosome	–	+++	+++
Distorted Lysosome	+	+++	+++
Lipid Droplet	–	+++	+++
Focal Degredation	–	+++	+++
Large Vacuoles	+	+++	+++
Myelin Figures	++	+++	+++
Autophagic Vacuoles	++	+++	+++
Disruption of cytoskeleton	–	+++	+++

Absent (-), occurred rarely (+), occurred occasionally (++), occurred often (+++).

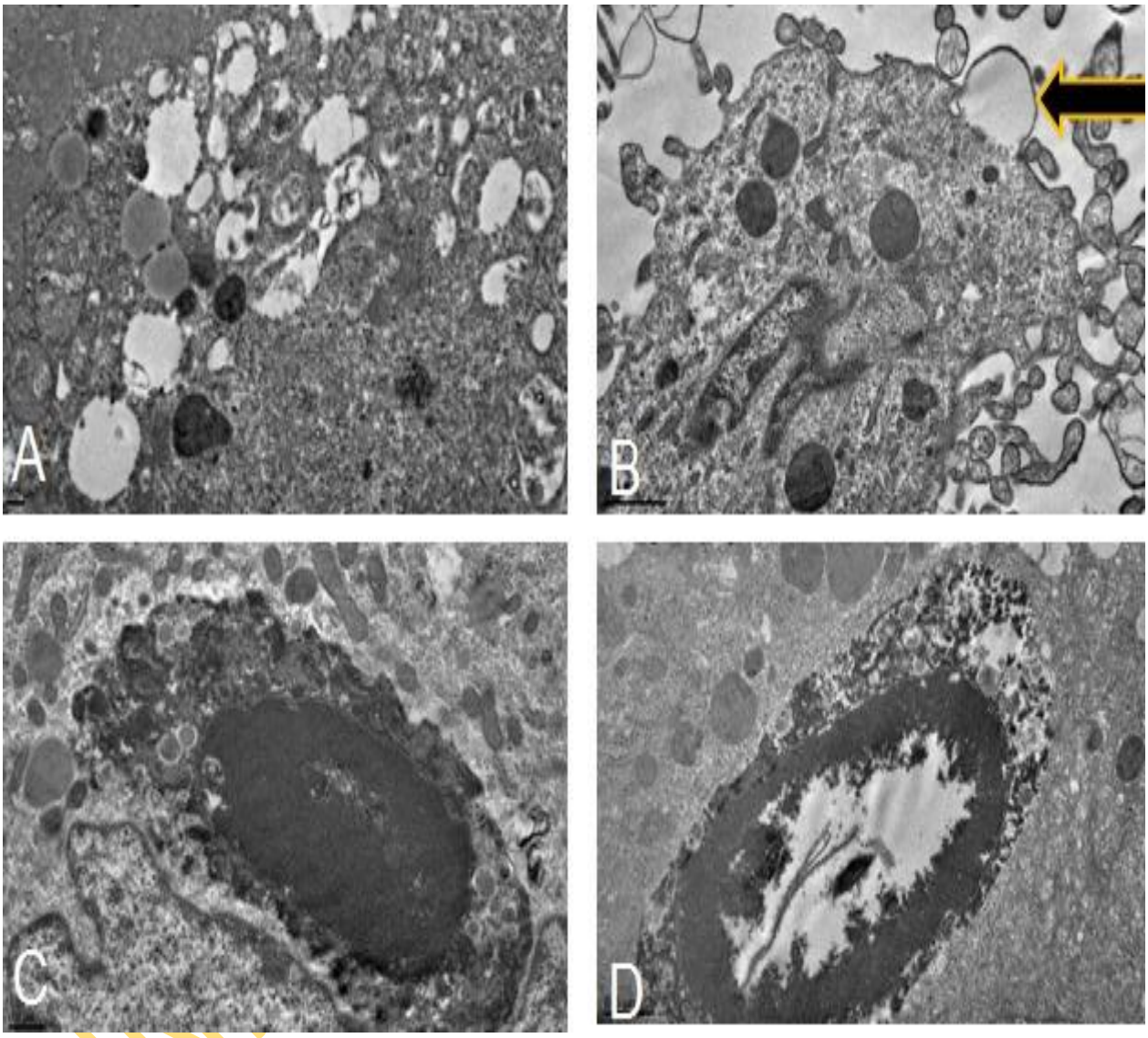

Figure 4.29: Typical features of necrosis observed in the chromate treated cells. Vacuolated cell (A). Disruption of the cell membrane (arrow in B). Condensation of the membrane (C) and dissolution of the condensed nuclear material materials karyolysis (D) X 2.5 X 10^3.

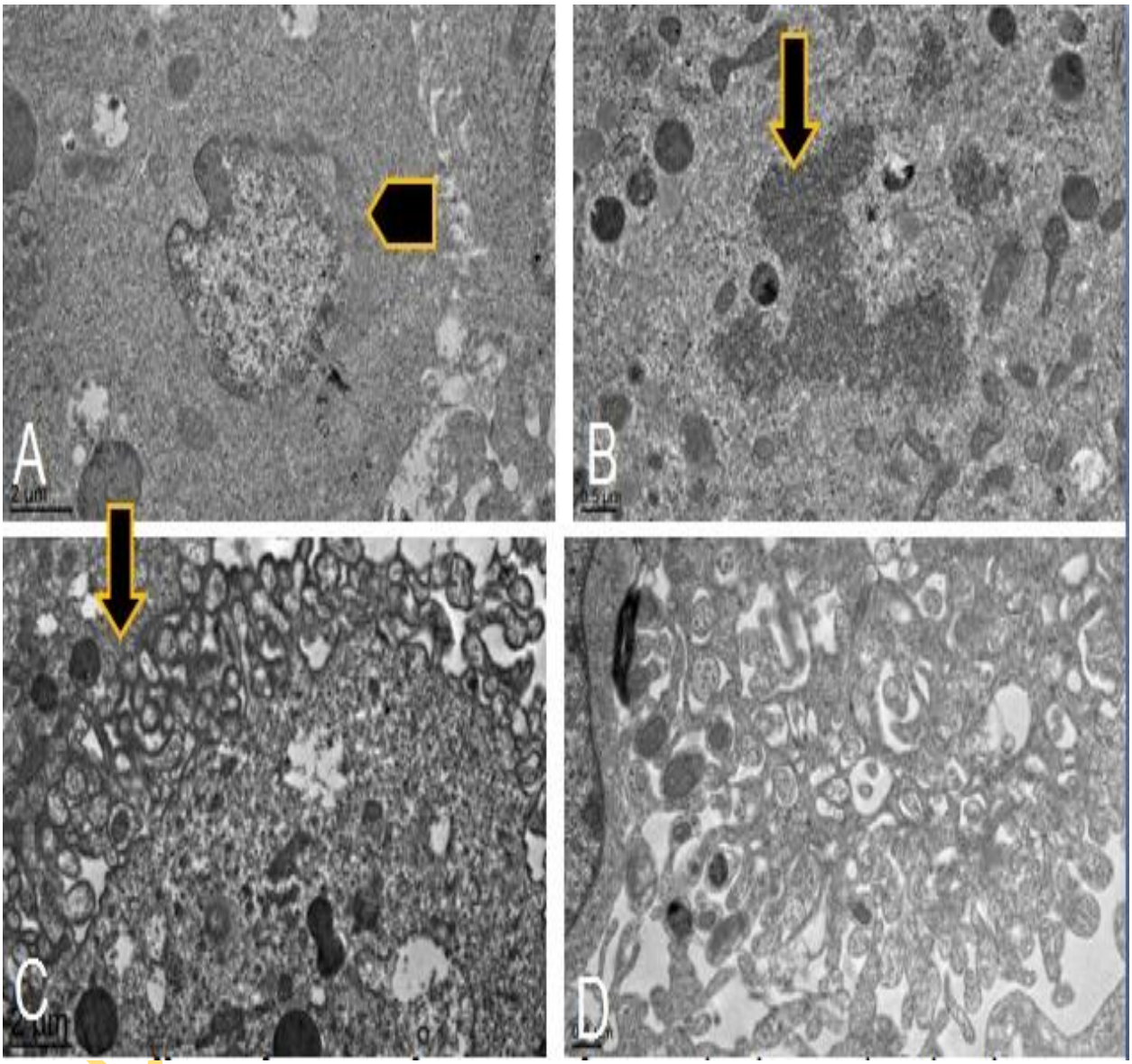

Figure 4.30: Different features of apoptosis frequently observed in the chromate treated cells. Partial dissolution of nuclear membrane (arrow in A). Complete dissolution of the nuclear membrane and nuclear fragmentation (B). An apoptosing cell with blebbs (C). A dying cell with apopotic bodies (D) X 2.5 X 10^3

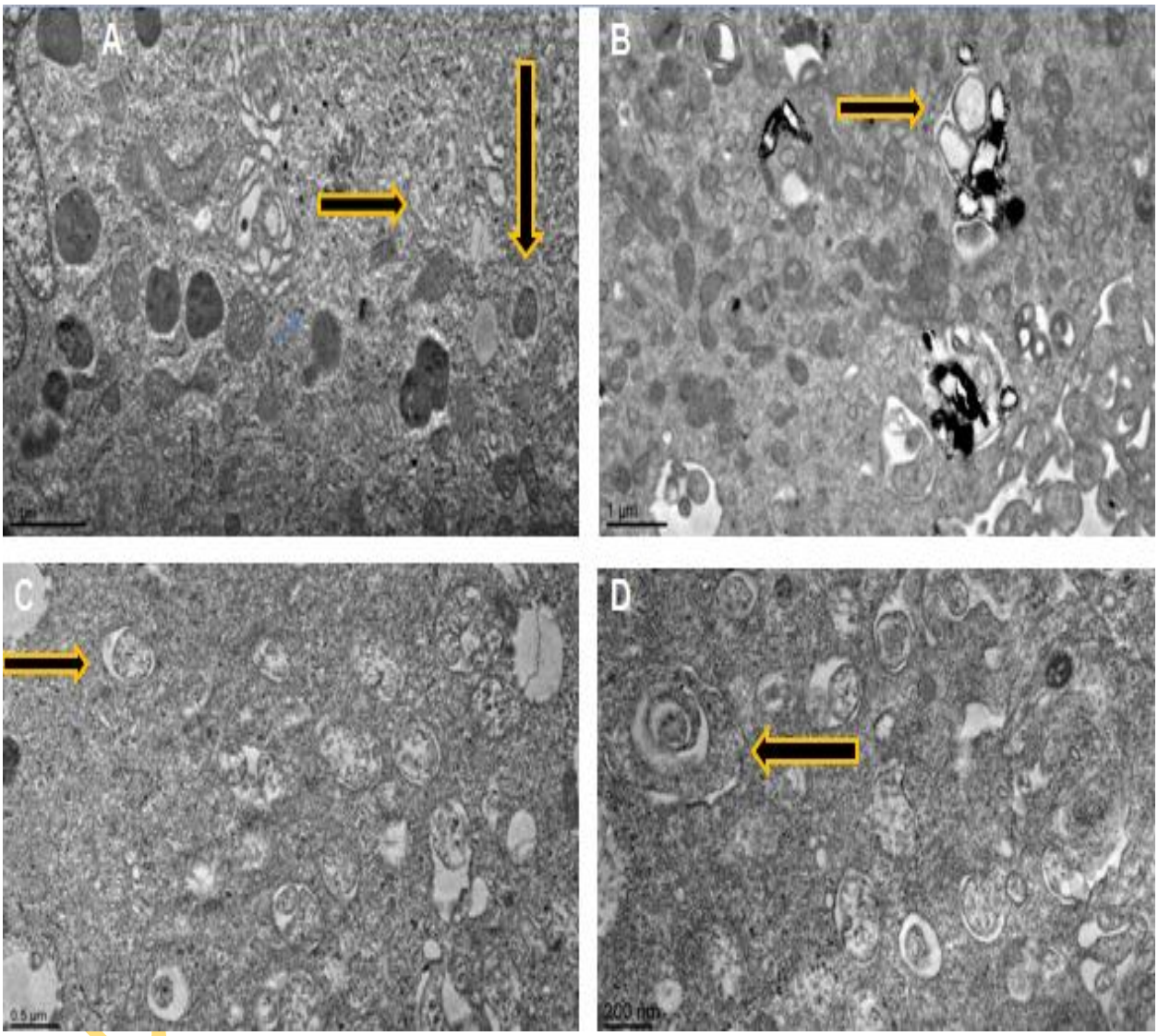

Figure 4.31: Autophagic features observed in the chromate treated cells. Note the presence of cytoplasmic content with double (A-C) or multiples membranes (D). Arrows indicate autophagic vacuole. X 2.5 X 10^3

4.6 EXPERIMENT 6: CELL CYCLE DISTRIBUTION OF CH3 10T ½ CELLS EXPOSED TO $PbCrO_4$, $BaCrO_4$ AND $SrCrO_4$

INTRODUCTION

Chromate (VI) exposure induces DNA lesion formation and therefore exposure to the chromate should cause cells to pause in at least one of the phases of the cell cycle while the damage is assessed and/or repaired. More importantly, all the three hexavalent chromate compounds ($PbCrO_4$, $BaCrO_4$ and $SrCrO_4$), altered the growth of CH310 T ½ cells under the experimental conditions as evidenced by the decreased plating efficiency and survival of exposed cells. More over, the different microscopic techniques also showed the chromate compounds altered the growth pattern of exposed cells. Cell cycle kinetics studies was done to determine whether the growth suppression by the compounds was due induction of cell death and / or activation of cell cycle arrest

PROCEDURE

About 5000,000 exponentially growing CH310T ½ cells were treated with between 0- 4.0 ug/ml lead chromate, barium chromate and strontium chromate for 48 hours.Controls were either untreated or were exposed to 2.5 µg/ml vinblastine. At the end of the treatment, cells were fixed, stained and observed in a flow cytometer as previously described under "Materials and Methods" (Section 3.10, Page83-84).

RESULTS

The result of chromate treatment on cell cycle progression in actively dividing CH310 T½ cells as determined by flow cytometry is presented in Table 4.8-10. In this work, obvious cell cycle progression differences was observed between control cells and the treated cells depending on the specific hexavalent chromate (VI) compounds.

The effect of lead chromate treatment on cell cycle kinetics is shown in Table 4.9. Upon lead chromate treatment, cells showed a dose dependent increase and decrease in hypodiploid or Sub G0 and G0/G1 cells population respectively when compared with the control. Treatment of cells with 1-4 µg/ml lead chromate also resulted in between 3.8-50% increase in G2/M cell population when compared with the control. Similarly, there was a 7.9 % increase in S-phase cell population

after exposure to 1.0 µg/ml lead chromate. However, exposure to higher concentrations of 2.5 and 4.0 µg/ ml resulted in 45.45 and 39.77% decline respectively in S-phase cell population.

A quantification of cells in G0/G1, S, and G2/M phase of the cell cycle after treatment with the barium chromate for 48h showed accumulation of the cells at G2/M and S-phase cells when compared with the control (Table 4.10). In addition, there was significant ($P < 0.05$) increase in population of Sub G0 cells and a decrease in the population of G0/G1 cells when compared with the control.

The progression of cells through the cell cycle was analysed at 48h post strontium chromate treatment by flow cytometry (Table 4.11). A dose-dependent delay in the progression of cells through the S-phase and G2/GM cells was observed at 48h post- strontium chromate treatment when compared with control cells (Table 4.11.). Similarly, there was an increase in Sub G0 cells in the strontium chromate treatment groups when compared with the control. Conversely, there was dose dependent decreased in cell population in G0/G1 when compared with control.

CONCLUSION

Collectively these observations suggest that cells treated with the hexavalent chromate compounds are arrested at G2/M and S-phase with corresponding decrease in G0/G1 cells as well as increase in cells undergoing cell death as evident by the increase in Sub G0 cells when compared with the control.

Table 4.8: Effect of $PbCrO_4$ treatment on cell cycle kinetics of CH310 T ½ cell.

Treatment	Hypodiploid (%)	G0/G1 (%)	S (%)	G2/M (%)
Control	6.65± 0.92	83.6± 1.91 * **	3.70± 0.00	5.30± 0.78**
2.5 µg/ml Vinblastine	5.2± 0.57	87.4± 0.35*	2.65±0.070	1.0 0.142
1.0 µg/ml $PbCrO_4$	16.15 ± 6.01	70.75± 9.98 * **	4.75± 1.55	7.85 ± 1.76 **
2.5 µg/ml $PbCrO_4$	21.45 ± 4.31 * **	70.25 ± 3.18 * **	2.40 ± 0.42	5.45 ± 0.64 **
4.0 µg/ml $PbCrO_4$	39.20 ± 8.20* **	50.60 ± 6.22* *	2.65 ± 0.07	6.45 ± 1.63 **

Values with the same superscript are not significant are not significant at 5% level.whereas values with different superscript are significantly different ($p < 0.05$) from one another.

Table 4.9: Effect of $BaCrO_4$ treatment on cell cycle kinetics of CH310 T ½ cell.

Treatment	Hypodiploid (%)	G0/G1 (%)	S (%)	G2/M (%)
Control	6.65± 0.92	83.6± 1.91 * **	3.70± 0.00 **	5.30± 0.78
2.5 µg/ml Vinblastine	5.2± 0.57	87.4± 0.35*	2.65±0.070 **	4.30 ± 0.142
1.0 µg/ml BaCrO4	8.1± 0.14 *	78.2± 0.57* **	4.95 ±0.21* **	8.40± 0.28 *
2.5 µg/ml BaCrO4	31.4± 2.23* **	55.8 ± 1.98* **	4.60± 0.28* **	6.2± 0.00
4.0 µg/ml BaCrO4	22.1± 0.28* **	63.25± 0.35* **	6.40±0.57* **	7.95± 0.78 *

Values with the same superscript are not significant are not significant at 5% level.whereas values with different superscript are significantly different ($p < 0.05$) from one another.

Table 4.10: Effect of $SrCrO_4$ treatment on cell cycle kinetics of CH310T ½ cells**.**

Treatment	Hypodiploid (%)	G0/G1 (%)	S (%)	G2/M (%)
Control	6.65± 0.92	83.6± 1.91 **	3.70± 0.00	5.30± 0.78
2.5 µg/ml Vinblastine	5.20± 0.57	87.4± 0.35*	2.65±0.070	4.30 ± 0.142
1.0 µg/ml BaCrO4	11.1 0± 0.28 * **	78.95 ± 0.70 * **	2.75 ± 1.20	5.95 ± 0.35
2.5 µg/ml BaCrO4	12.85 ± 0.78 * **	74.75 ± 0.64* **	4.75 ± 1.49	6.90 ± 0.42
4.0 µg/ml BaCrO4	11.90 ± 2.54* **	70.10 ± 0.14 * **	7.05 ± 0.35 * **	10.30 ± 1.98 * **

Values with the same superscript are not significant at 5% level, whereas values with different superscript are significantly different ($p<0.05$) from one another.

4.7 EXPERIMENT 7: ASSESSMENT OF CASPASE ACTIVATION AND CYTOTOXICITY IN CH310T ½ CELLS EXPOSED TO $PbCrO_4$, $BaCrO_4$ and $SrCrO_4$

INTRODUCTION

A major finding in the earlier studies reported in this work is that hexavalent chromate induced apoptosis in the treated. This experimental was therefore undertaken to correlate the microscopy result with the induction of caspase 3/7 activity in treated cells. Caspase-3/7 plays a central role in both intrinsic and apoptosis extrinsic pathways. Assessment of caspase-3/7 activation is therefore a biochemical marker of choice for the detection of programmed cell death both *in vitro* and *in vivo* and it has already been chosen to image (noncardiac) apoptosis in various models (Bullok *et al.*, 2000; Maxwell *et al.*, 2009*;* Zhang *et al.*, 2009*)*

PROCEDURE

15,000 logarithmic growing cells were seeded per well in 96-well plate , opaque-walled tissue culture plates with clear bottoms and treated with between 0- 4.0µg/ml $PbCrO_4$, $BaCrO_4$ and $SrCrO_4$ for 48 hours. After the treatment, Caspase activation and cytotoxicity in the control and treated cells were determined as earlier described under "Materials and Methods" (Section 3.8, Page 84-87).

RESULT

The effect $PbCrO_4$, $BaCrO_4$ and $SrCrO_4$ on caspase activity, cytotoxicity and viability in cells treated for 48 hrs are presented in figures 4.32-4.34 respectively. Exposure to all the chromate (VI) compounds resulted in a dose dependent increase in cytotoxicity coupled with a dose dependent decrease in viability (Figure 4.32- 34). Similarly, treatment of CH310T½ cells with the chromate compounds led to a higher caspase 3/7 activity when compared with the control. Capase 3/7 activity was observed to be dose dependent in the cell treated with both $PbCrO_4$ and $BaCrO_4$, while it was not dose-dependent in cells treated with $SrCrO_4$ (Figure 4.32- 34).

CONCLUSION

The results of this experiment support earlier observations that the chromate compounds induce cytotoxicity via both apoptosis and necrosis. In addition, the induction of apoptosis in CH310T½cells is caspase 3/7 dependent under our experimental conditions.

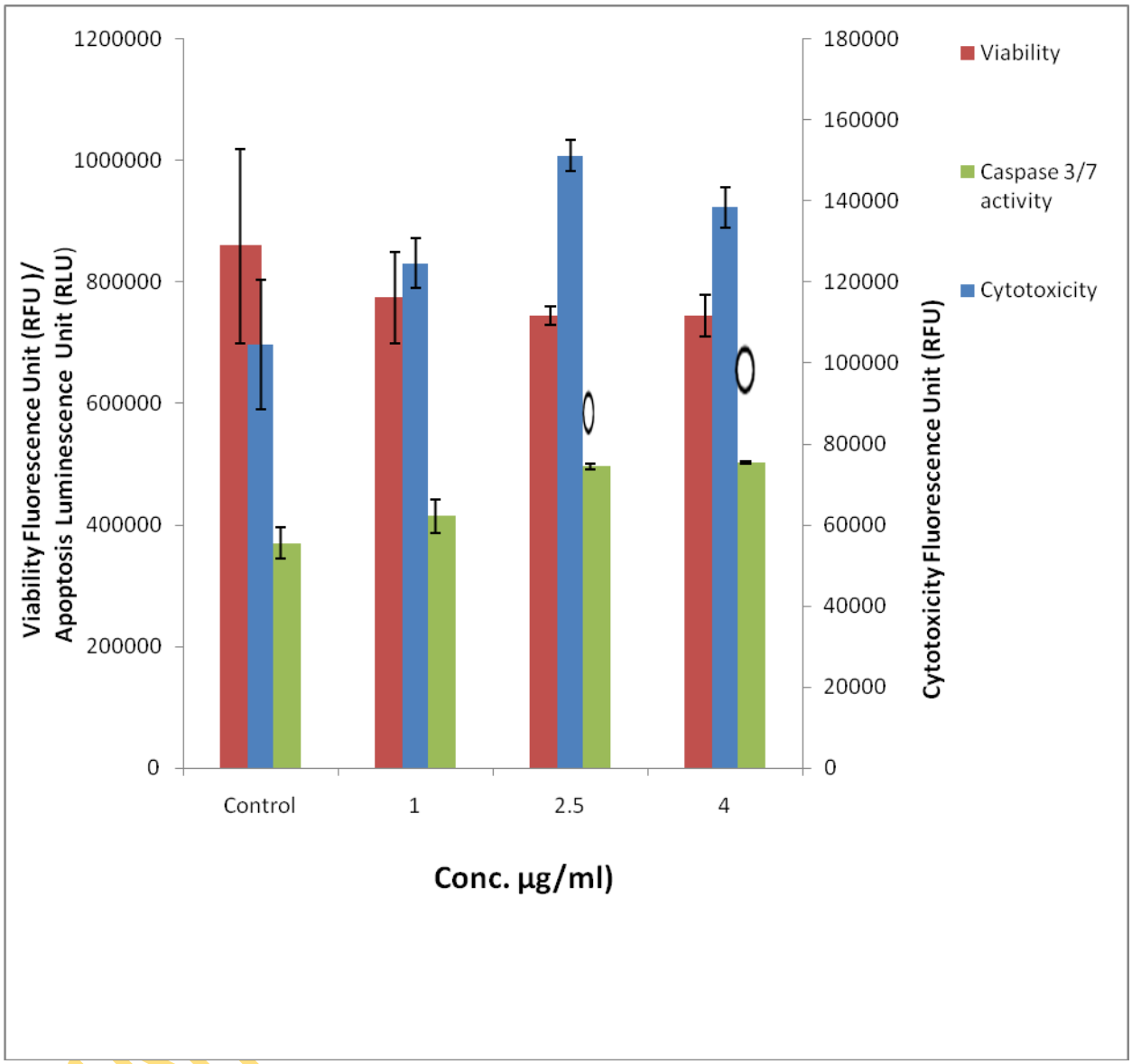

Figure 4.32: The effect of $PbCrO_4$ treatment on viability, capase 3/7 activity and cytotoxicity to cultured CH310T½ cells.

*Significantly different from the control

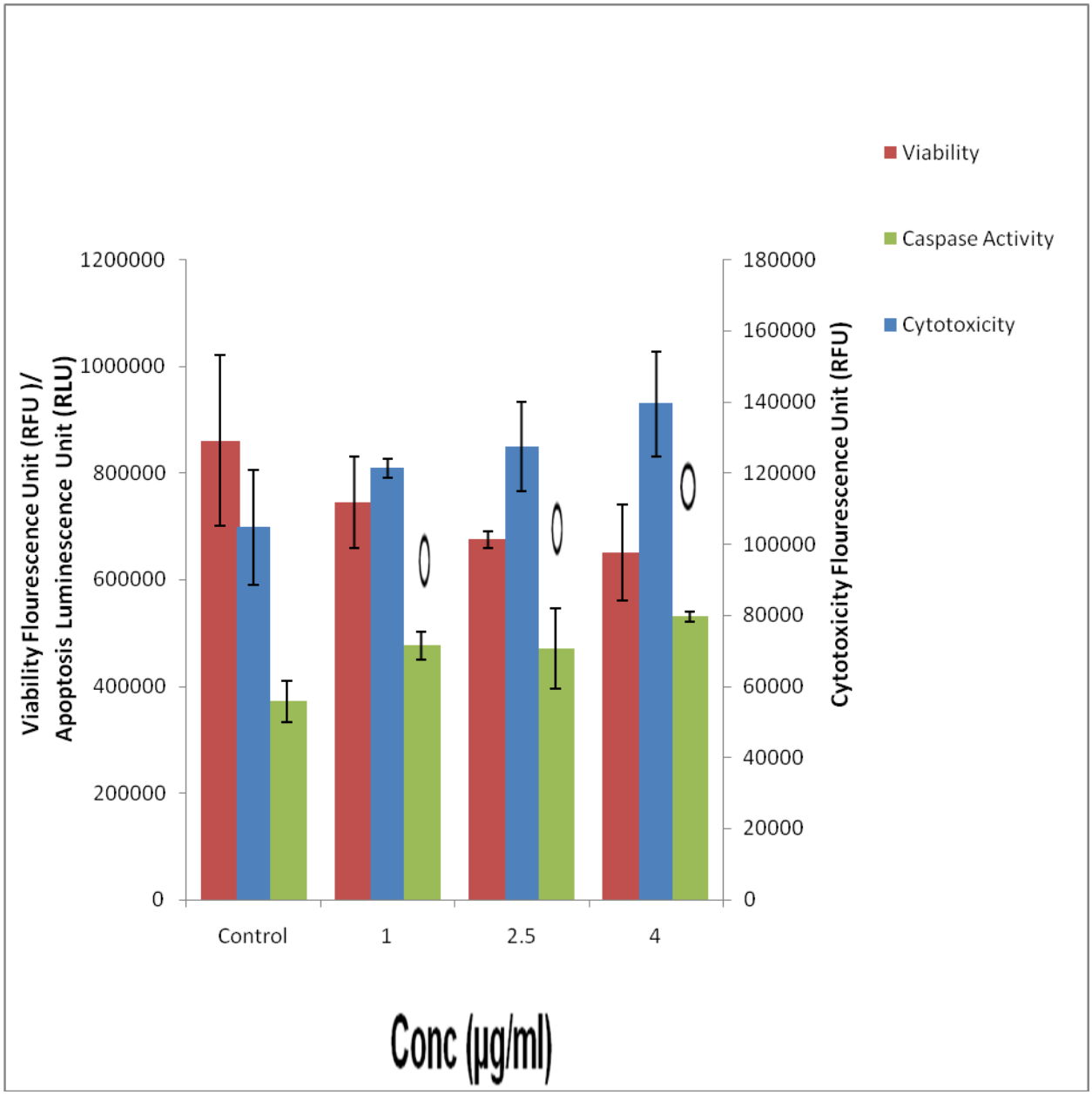

Figure 4.33: The effect of $BaCrO_4$ treatment on viability, capase 3/7 activity and cytotoxicity to cultured CH310T½cells.

*Significantly different from the control

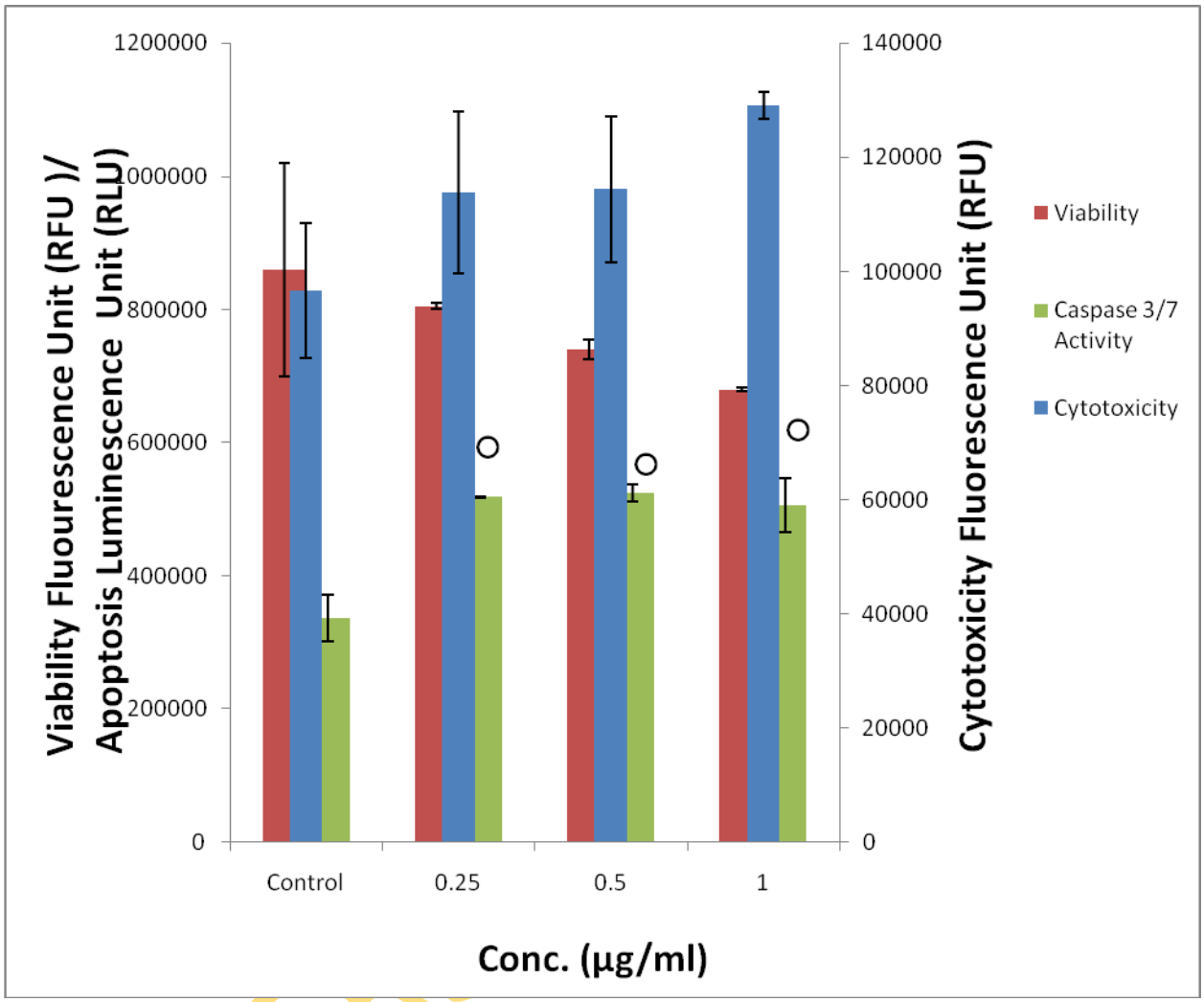

Figure 4.34: The effect of $SrCrO_4$ treatment on viability, capase 3/7 activity and cytotoxicity to CH310T½ cells.

*Significantly different from the control

4.8 EXPERIMENT8: QUANTITATIVE ASSESSMENT OF THE EXTENT OF APOPTOSIS AND NECROSIS IN CH3 10T ½ CELLS EXPOSED TO $PbCrO_4$, $BaCrO_4$ and $SrCrO_4$

INTRODUCTION

Nature of cell death observed in the chromate (VI) treated cells was mixed. There is no biochemical marker available that could unambiguously differentiate between necrotic and apoptotic cell death (Berghe *et al.,* 2013).Therefore, the extent of apoptosis and necrosis was determined by fluorescent microscopy in cells treated with between 0.25-4.0µg/ml $PbCrO_4$, $BaCrO_4$ and $SrCrO_4$ for 48 hours. Flourescent microscopy is a powerful method that allows the visualization of the multiple morphological features that occur during apoptosis and necrosis.Visualisation of apoptic and necrotic cell death makes fluorescent microscopy a more reliable method for the simultaneous assessment of the degree of apoptosis and necrosis occurring in cultured cells

PROCEDURE

Fifteen thousand cells were seeded in slide chambers. Cells were allowed to attach overnight and treated with 0- 4.0µg/ml $PbCrO_4$, $BaCrO_4$ and $SrCrO_4$ for 48 hours. The cells were subsequently stained with propidium iodide and acridine orange, as well as observed with an EVOS UV-fluorescence microscope as previously described under "Materials and Methods" (Section 3.12, Page 88).

RESULTS

The percentage of cells undergoing apoptosis and necrosis in cells treated with $PbCrO_4$, $BaCrO_4$ and $SrCrO_4$ are presented in Fig. 4.35- 37. The percentage apoptotic cells rose from 13.47% in control to 51.67% in cells treated with 1.0 µg/ ml $PbCrO_4$ while it decreased to 48.23% and 42.57 % respectively in the 2.5 µg/ ml and 4.0 µg/ ml treatment groups (Fig. 4.35). On the other hand, the percentage necrotic cells increased to 44.5 % in the 2.5 µg/ ml treatment group from 3.44% in control. The value subsequently decreased to 32.08% in cells treated with 4.0 µg/ ml $PbCrO_4$ (Fig. 4.35). This indicates that more cells die by apoptosis than necrosis at all the test doses of $PbCrO_4$.

The induction of apoptosis and necrosis in CH310T½ cells treated with $BaCrO_4$ is shown in Figure 4.36. Treatment of the cells with $BaCrO_4$ increased the percentage cells with apoptotic features from 13.47% in control to 48.12% in cells treated with 2.5 µg/ ml $BaCrO_4$, but it decreased to 38.78% in cells exposed to 4.0 µg/ ml $BaCrO_4$. Treatment of 10T ½ with 1.0 – 4.0 µg/ ml barium chromate resulted in a dose- dependent 31.38 to 46.38 % increase in necrotic cells as compared with 3.44% in control.

The degree of apoptosis and necrosis in cells treated with $SrCrO_4$ was similar to those observed in $BaCrO_4$ (Figure 4.37). $SrCrO_4$ treatment caused a marked rise ($p < 0.05$) in the percentage apoptotic cells from 13.53% in control to 47.42% and 47.47% in cells treated with 0.25 and 0.5 µg/ ml (Figure 4.37). However, the percentage apoptotic cells decreased to 33.53% in cells treated with 1.0µg/ ml $SrCrO_4$. Similarly, exposure of the cells to 0.25, 0.5 and 1.0 µg/ ml $SrCrO_4$ significantly ($p < 0.05$) increased the percentage necrotic cells to 32.86%, 41.73% and 55.76 % respectively from 3.44 % in control (Figure 4.37). Overall, cells die by apoptosis at lower concentrations while cell death is mainly a necrotic at higher concentrations for both $BaCrO_4$ and $SrCrO_4$ treated cells.

CONCLUSION

The result obtained in this experiment confirmed that the nature of cell death in the cells exposed to the three chromate compounds is mixed. Overall, more cells died by apoptosis at all the tested concentrations of $PbCrO_4$ and lower concentrations of $BaCrO_4$ and $SrCrO_4$. However, more cells died via necrosis at higher concentrations of both $BaCrO_4$ and $SrCrO_4$ under our experimental conditions.

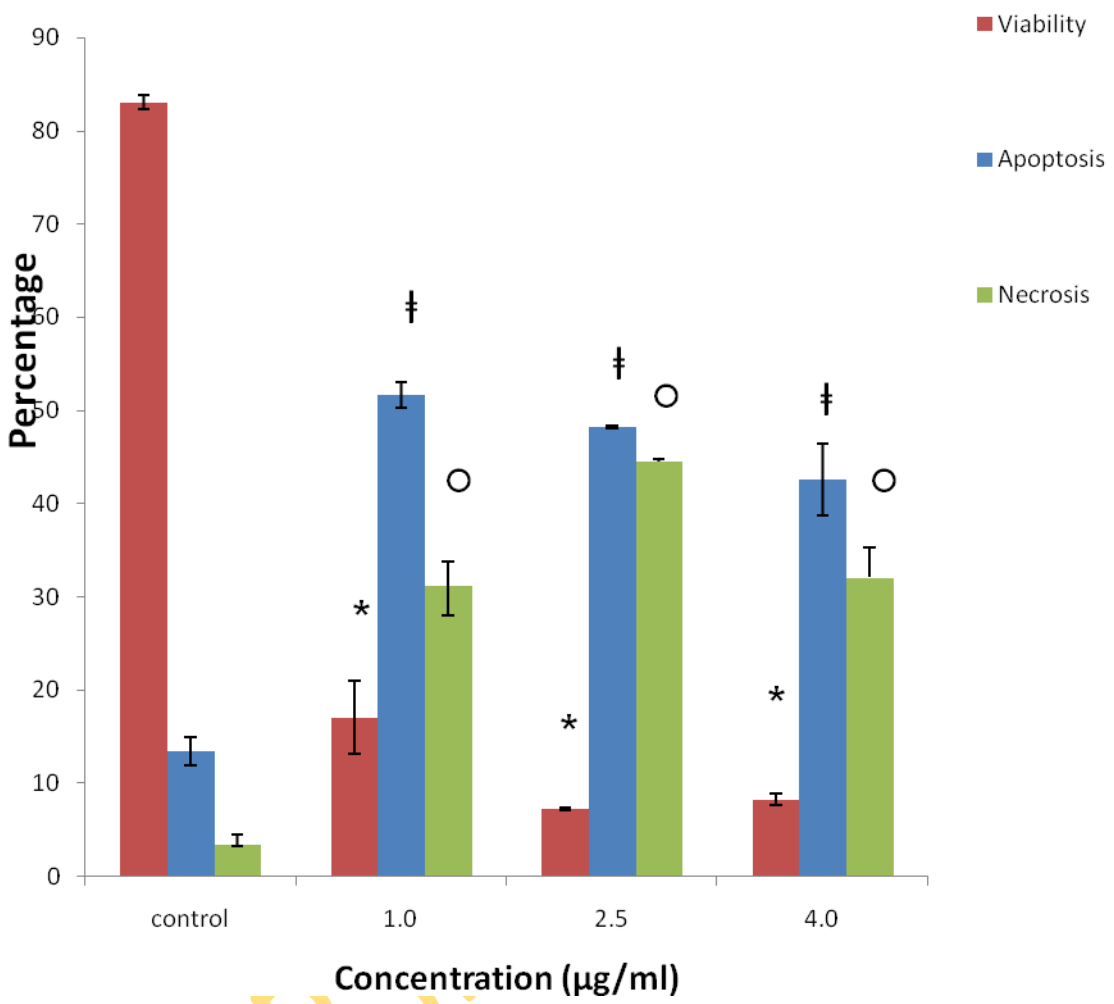

Figure 4.35: The percentage apoptotic and necrotic cells in 10 CH310T1/2 cells treated with $PbCrO_4$ for 48 hours.

* ǂand o are significantly different ($p < 0.05$) from the control.

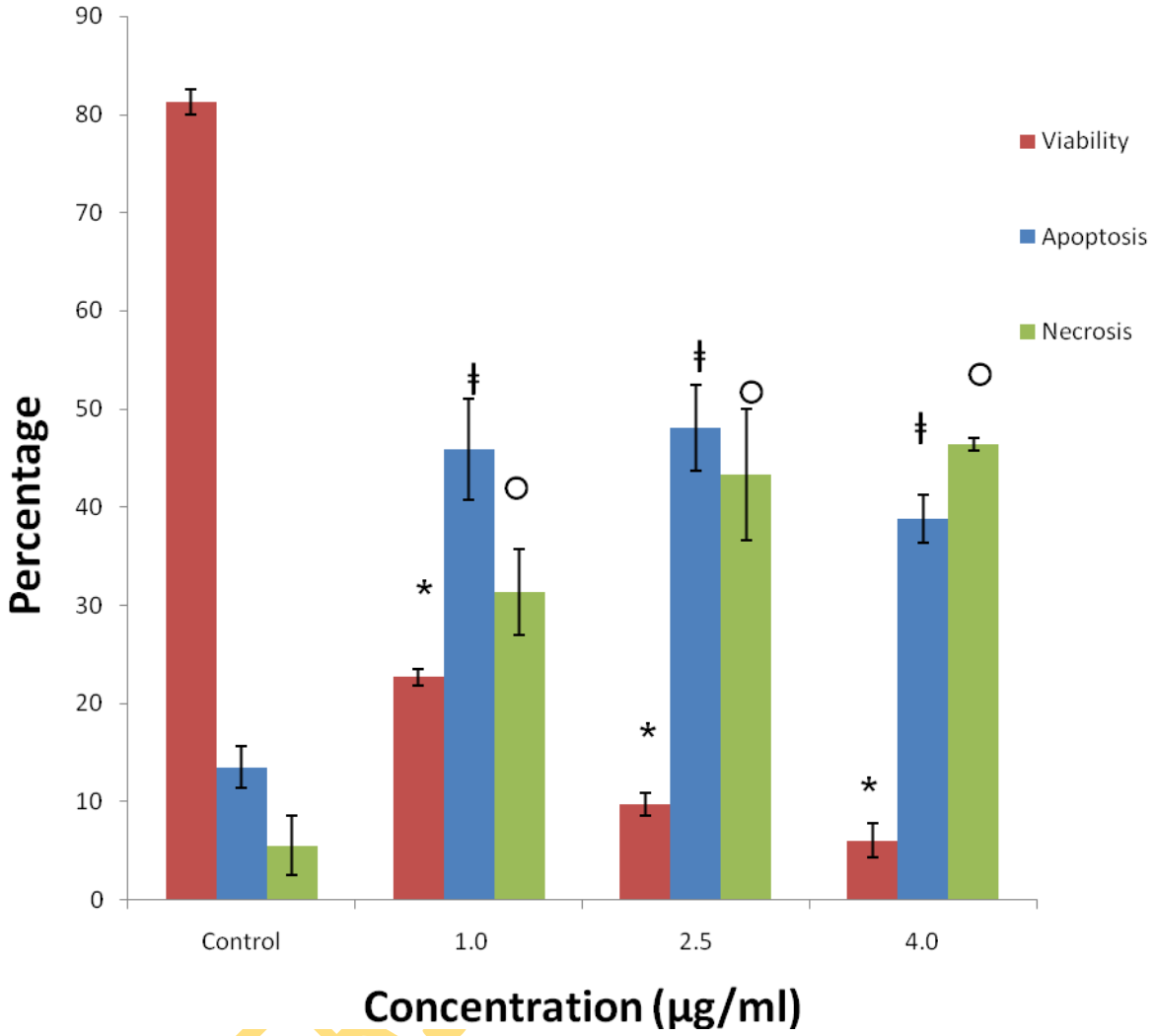

Figure 4.36: The percentage apoptotic and necrotic cells in CH310T1/2 cells treated with $BaCrO_4$ for 48 hours.

*‡and o are significantly different ($p < 0.05$) from the control.

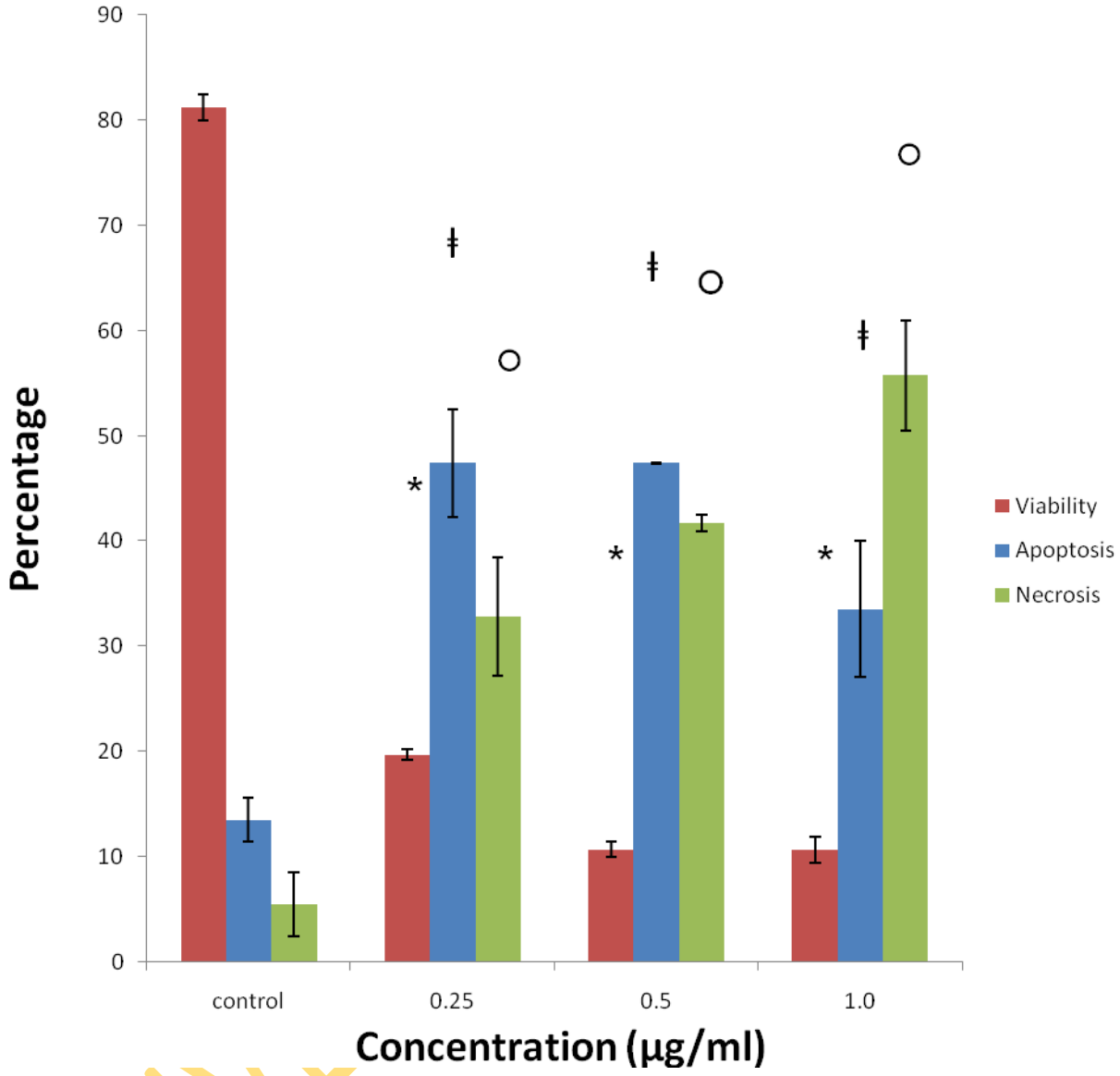

Figure 4.37: The percentage apoptotic and necrotic cells in CH310T½ cells treated with $SrCrO_4$ for 48 hours.

*ǂand o are significantly different ($p < 0.05$) from the control

4.9 EXPERIMENT 9: ASSESSMENT OF INDUCTION OF AUTOPHAGY IN CHROMATE TREATED CELLS

INTRODUCTION

Since the earlier microscopic observation revealed that the nature of cell death in treated was mixed i.e. apoptosis, necrosis and autophagy. An investigation on the third major form of cell death, autophagy was also carried out to assess the extent of autophagy in cell treated at different concentration and at different time.

PROCEDURE

Ten thousand logarithm going cells were placed in a 4 slide chamber and allowed to adhere overnight. Cells were later transduced with the LC3B protein for 24 hours in order to allow the expression of the LC3B protein. Cells were treated with between 0- 4.0µg/ml $PbCrO_4$, $BaCrO_4$ and $SrCrO_4$ for 16 hours. The reagent kit was added and slides were observed with an inverted EVOS UV-fluorescence microscope as initially described under "Materials and Methods" (Section 3.15, page 89-91).

RESULT

The lead chromate induced the formation of autophagic puncta in the cytoplasm of CH310T½ cells is presented in Figure 4.38A. Similarly, barium chromate and strontium chromate induced apparent formation of autophagic puncta in the cytoplasm of treated cells whereas, less formation of the puncta were observed in control cells (Figure4.39). Quantitatively,
15.7 ± 3.7 % of cells treated with 1 µg/ml lead chromate showed LC3B-GFP autophagic puncta, 14.15 ±1.65 % punctuated cells were observed in the 2.5µg/ml lead chromate treatment and 15.25± 1.45 % of such cells were seen with 4.0 µg/ml lead chromate treatment , whereas 12.9 ± 0.4 % of control cells exhibited autophagic puncta in the control

The induction of autophagy decreased as the concentration of barium chromate increased (Figure 4.40). The percentage cell expressing the LC3B-GFP puncta after barium chromate treatment decreased from 18.8 ± 3.40 % to 14.0 ± 3.48 % as the concentration of barium chromate was increased from the 1.0 µg/ml to 4.0 µg/ml (Figure 4.40). However, strontium

chromate treatment provoked a dose dependent increased in the induction of autophagy as evidenced by the rise in percentage cell expressing the LC3B-GFP puncta from 12.9 ± 0.4 % to 31.14 ± 0.5 % as the concentration of strontium chromate was increased from 0µg/ml to 4 µg/ml (Figure 4.41).

The time dependent induction of autophagy in CH310T½ cells treated with 2.5 µg/ml lead chromate or barium chromate or 0.5 µg/ml strontium chromate was analysed by the transmission electron microscopy. Transmission electron microscopy is gold standard for detecting autophagic compartments in animal cells. The total number of autophagosome and autolysosomes (Figure 4.38B) found in each cell were scored in 40 electro micrographs for the test and control groups. As shown in Table 4.11-13, more autophagic vacuoles were observed in the chromate–treated CH310T½ cells when comapared to the control. In addition, autophagosomes and autolysosomes were more frequently observed in chromate treated cells. Exposure of the cells to 2.5 µg/ml of either $PbCrO_4$ or $BaCrO_4$ also resulted in a time dependent increase in total autophagic vacuoles. The observed total autophagic vacuoles in the $SrCrO_4$ treated cells rose to about 116 % in the 24 hours treatment and later decreased to about 58% after 48 hours (Table 4.14)

CONCLUSION

Exposure to the three chromate compounds ($PbCrO_4$, $BaCrO_4$ and $SrCrO_4$) caused an increase in the induction of autophagy. This however, varied in the three chromate compounds. The induction of autophagy was dose dependent and significant ($p< 0.05$) in the $SrCrO_4$ treated cells, but was not dose dependent and significant in cells treated with $PbCrO_4$ and $BaCrO_4$. In contrast, there was a time dependent increase in the induction of autophagy in cells treated with $PbCrO_4$ and $BaCrO_4$, while those treated with $SrCrO_4$ did not show time dependence under our experimental conditions.

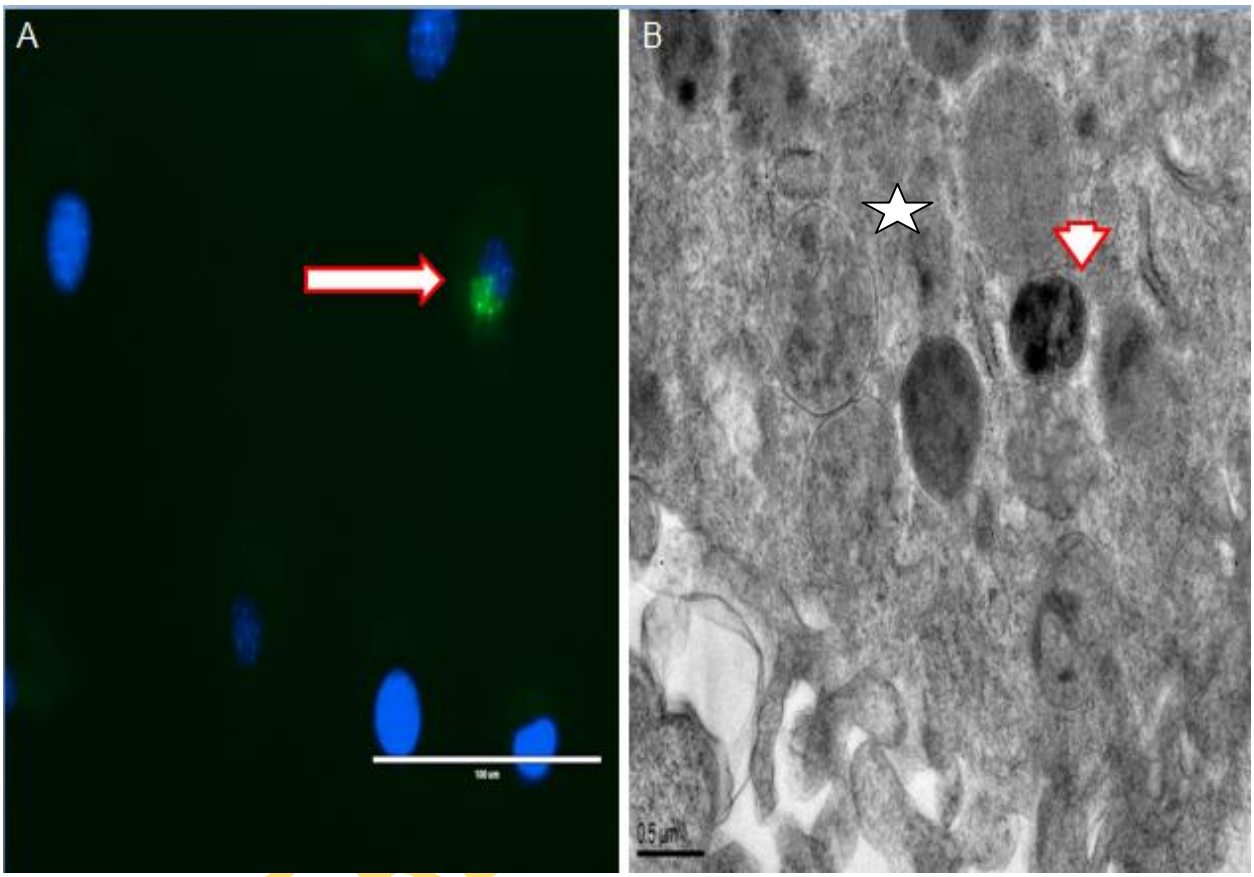

Figure 4.38: Induction of autophagy in hexavalent chromate treated cells. (A) Cell with autophagic puncta X 400 and (B) autophagosme and autolysosome (star and arrow head) X 2500

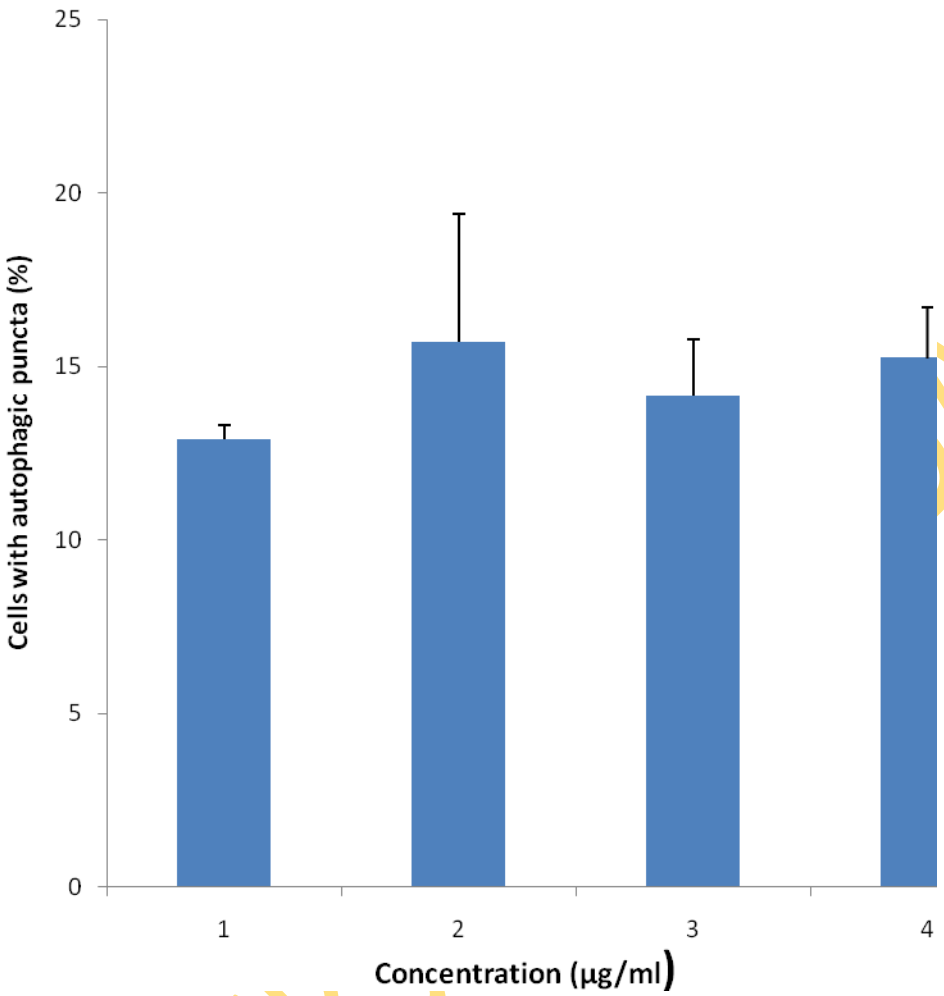

Figure 4.39: Percentage cell expressing the LC3B-GFP puncta after BacMam LC3B-GFP transduction in CH310T ½ cells exposed to $PbCrO_4$

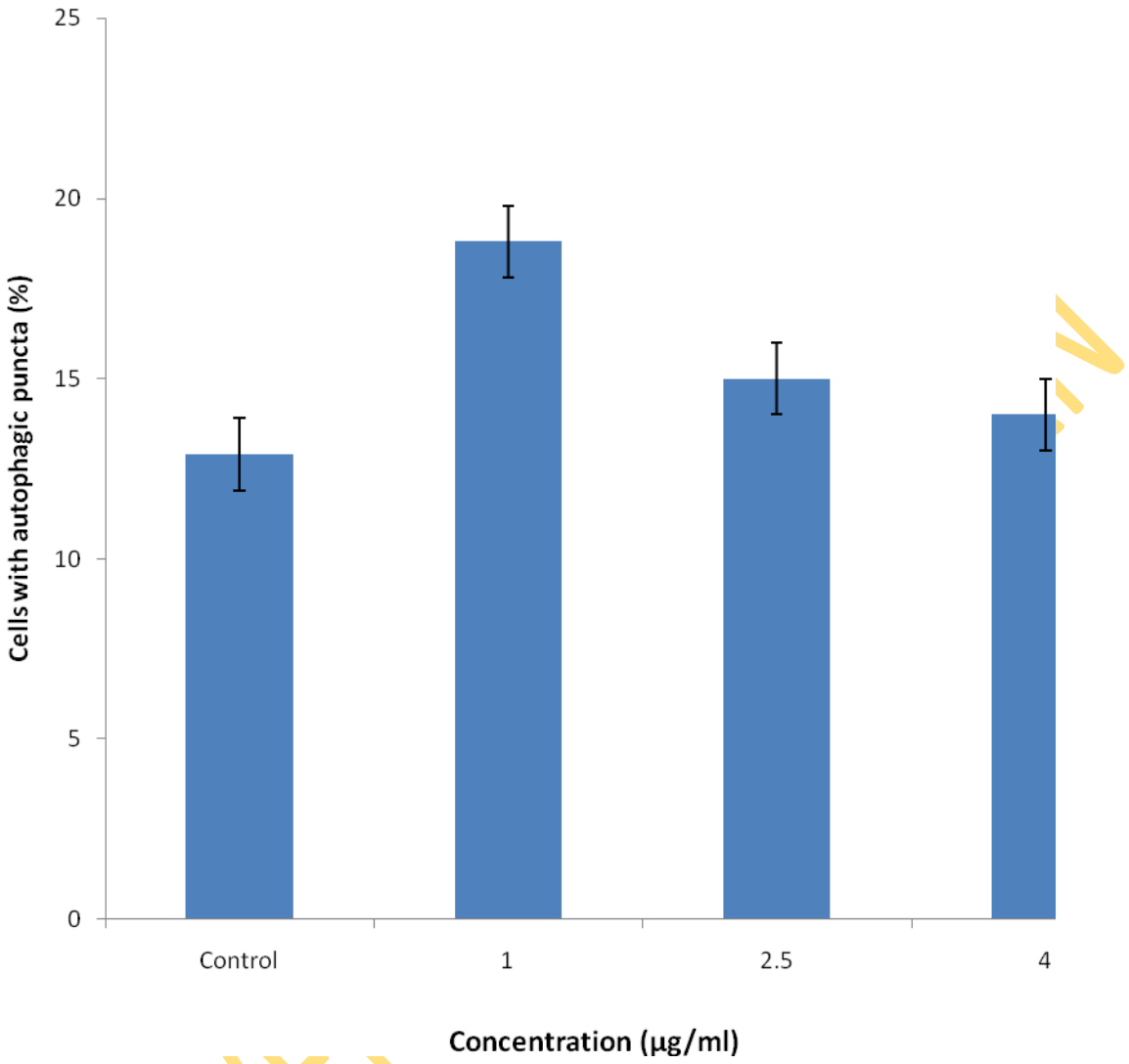

Figure 4.40: Percentage cell expressing LC3B-GFP puncta after BacMam LC3B-GFP transduction in CH310T½ cells exposed to $BaCrO_4$.

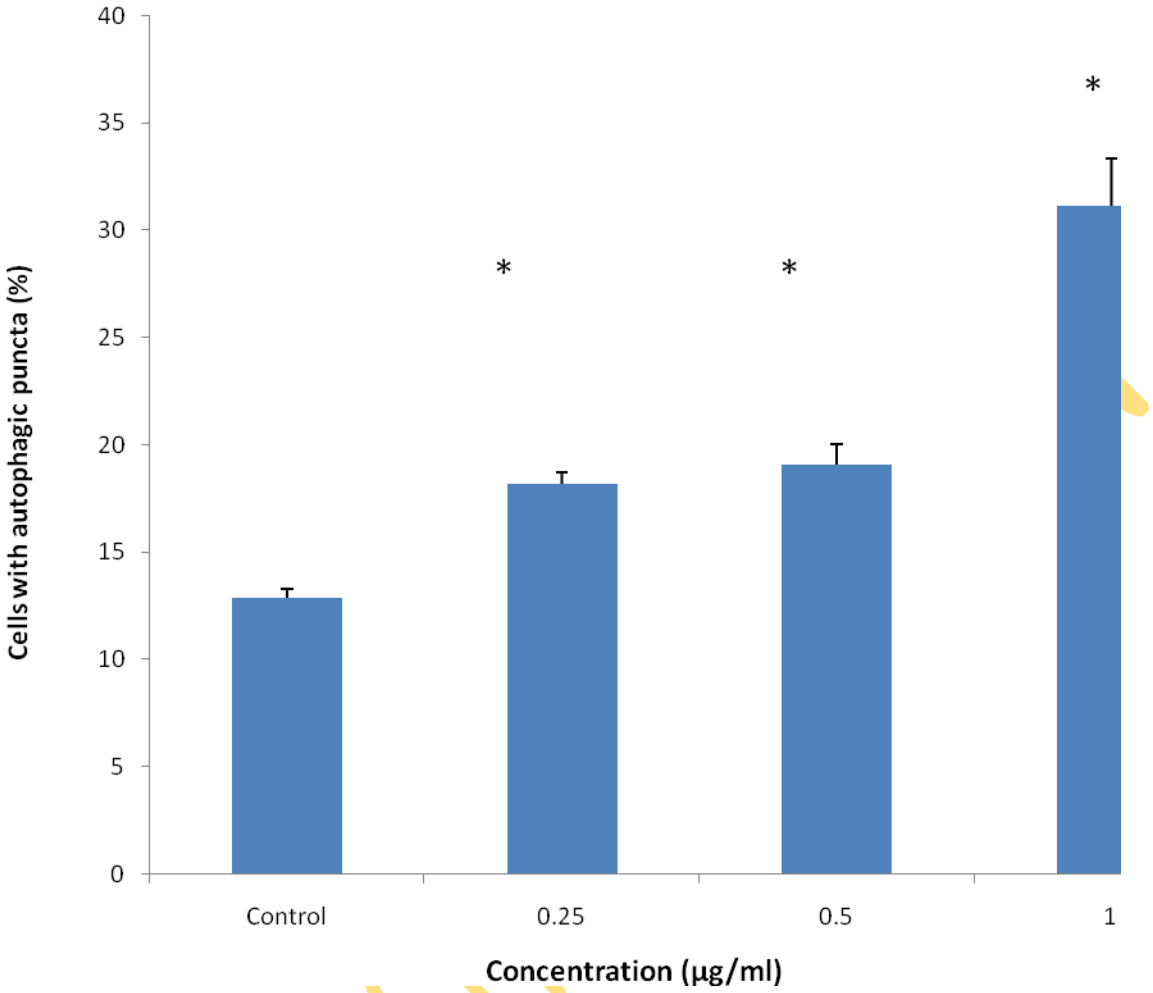

Figure 4.41: Percentage cell expressing LC3B-GFP puncta after BacMam LC3B-GFP transduction in CH310T ½ cells exposed to $SrCrO_4$.

*Significantly different ($p < 0.05$) from the control.

Table 4.11: Autophagic vacuoles observed in cells exposed to lead chromate

Treatment	No. of Autophagosome	No. of Autolysosome	Total Autophagic Vacuoles
Control	12	19	31
6h	9	34	43
24h	16	42	58
48h	29	48	77

Table 4.12: Autophagic vacuoles observed in cells treated with Barium Chromate

Treatment	No. of Autophagosome	No. of Autolysosome	Total Autophagic Vacuoles
Control	12	19	31
6h	9	30	39
24h	27	26	53
48h	22	35	57

Table 4.13: Autophagic vacuoles observed in cells exposed to Strontium chromate

Treatment	No. of Autophagosome	No. of Autolysosome	Total Autophagic Vacuoles
Control	12	19	31
24h	33	34	67
48h	20	29	49

EXPERIMENT 10: ASSESSMENT OF ACTIN DISRUPTION IN CH310T ½ CELLS EXPOSED TO $PbCrO_4$, $BaCrO_4$ AND $SrCrO_4$

INTRODUCTION

The actin filaments are the major component responsible for the maintenance of global cell shape in fibroblast (Ujihara *et al*, 2008). Actin plays diverse role in cell growth, maintenance of cell polarity and morphology, locomotion and signal transduction. Transmission Electron Microscopy (TEM) observations that chromate exposure led to disruption of cytoskeleton informed the decision to stain cells with actin specific dye, TRITC phalloidin. Staining of cells with phalloidin allows visualization of disturbance in actin filament architecture. In addition, phalloidin binds stoichiometrically to actin present in cells. It is therefore exploited in cellular imaging to generate quantitative data by measuring the actin fluorescent intensity.

PROCEDURE

Ten thousand log phase cells were seeded into Lab-Tek II chamber slides and allowed to adhere overnight. Cells treated with between 0 and 4.0µg/ml $PbCrO_4$, $BaCrO_4$ and $SrCrO_4$ for 48 hours. Following treatment, cells were stained, fixed and observed with the EVOS fluorescent microscope as previously described under "Materials and Methods" (Section 3.14, Page 91-92).

RESULTS

Exposure of cells to the chromate compounds resulted in dramatic change in cell structure when compared with the control (Figure 4.42).The uniform distribution of the actin filament in control cells (Figure 4.42A) disappeared after hexavalent chromate treatment (Figure 42B-D). In treated cells, the actin aggregated in some areas, whereas it absent in some areas. This may be responsible for the change in cell shapes shape observed in treated cells (Figure 4.42B -D). Many cells with round/oval configuration (indicative of apoptosing cells) and those with folded configuration (indicative of remodel cells) were also observed in the chromate exposed cells (Figure 4.42C - D). In addition, a dose and time dependent increase in disruption of actin was observed in the $PbCrO_4$ treated cells (Figure 4.43). Similar observations were made for $BaCrO_4$ and $SrCrO_4$ treated cells.

Furthermore, the effect of hexavalent chromate on the fluorescent intensity of actin filament in CH310T ½ cells is shown in Figure 4.44-5. Treatment of the cells with $PbCrO_4$ and $BaCrO_4$

resulted in a dose and time dependent decrease in actin intensity (Figure 4.44-5). There was also a decrease in actin fluorescence intensity in strontium chromate treated cells when compared with the control. The decrease in intensity was however, not dose dependent (Figure 4.45 and 4.46).

The staining of the cells with TRITC phallodin stain also gave an insight into the possible mechanism of anucleation and transformation of CH310T½ cells. (Figure 4. 47):

(i) Treatment of the cells with the insoluble chromate led to induction of stress fibers (1)

(ii) Over time, the stress fiber were disrupted and the nucleus of the cell may be thrown out (2 and 2b)

(iii) Cells may be induced to fold probably to protect the nucleus from the toxicity of chromate compounds (3 and 4).

(iv) In the process, some of the cells are incorrectly folded and the nucleus may be thrown out of the cells (5)

(v) The folded cells (4) may eventually become the transformed cell population in the chromate treated cells since change in cell shape is central to carcinogenesis.

(vi)

CONCLUSION

The hexavalent chromate compounds caused disruption of actin filament and reduction of actin intensity in CH310T½ cells.

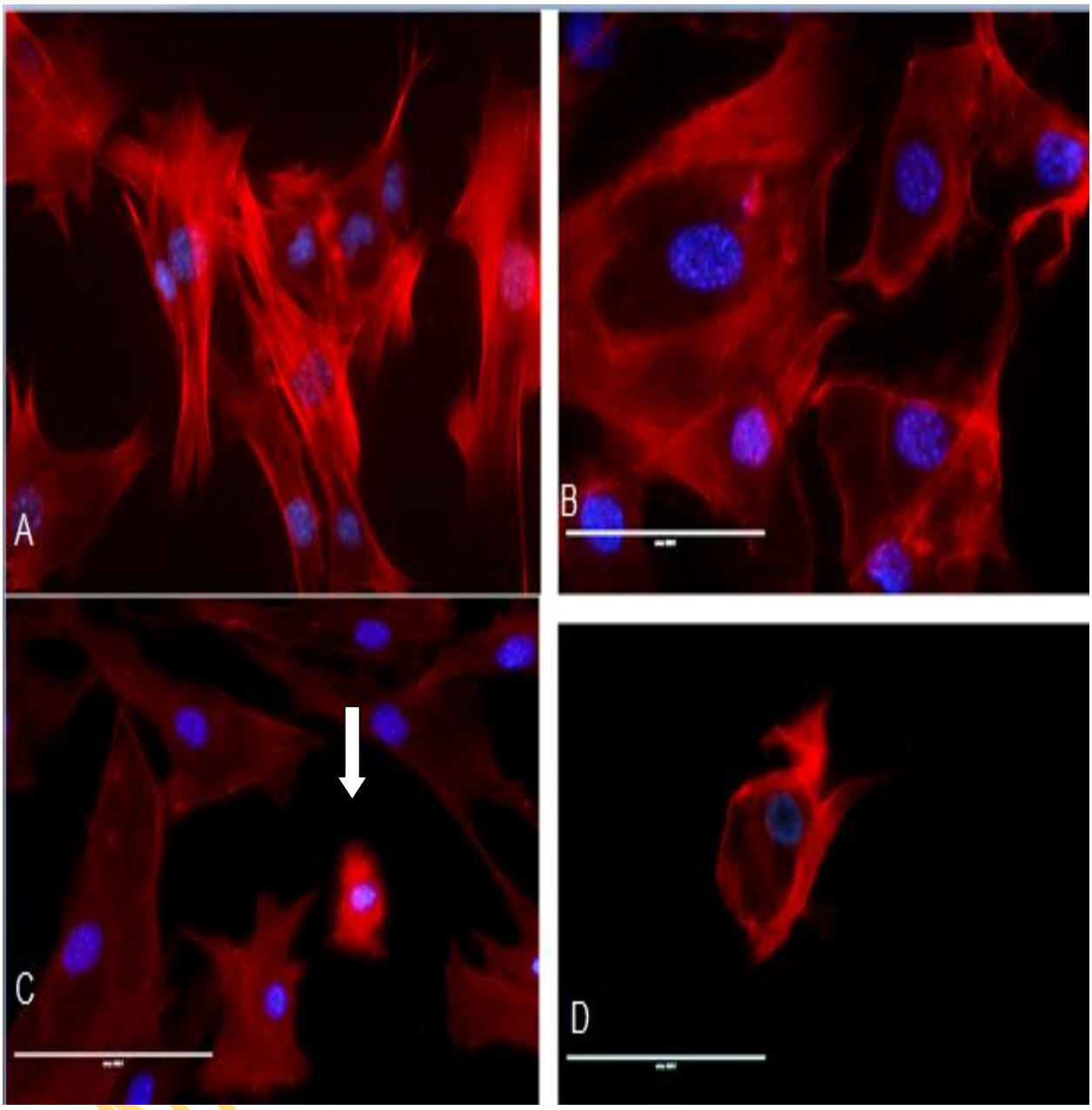

Figure 4.42: The effect of hexavalent chromate treatment on actin filament in CH310T 1/2 cells (A) Contol cells (B) treated cells with with distrupted actin fibre (C) apoptosing cell (arrow). (D) Reshaped cell in exposed cells. X400

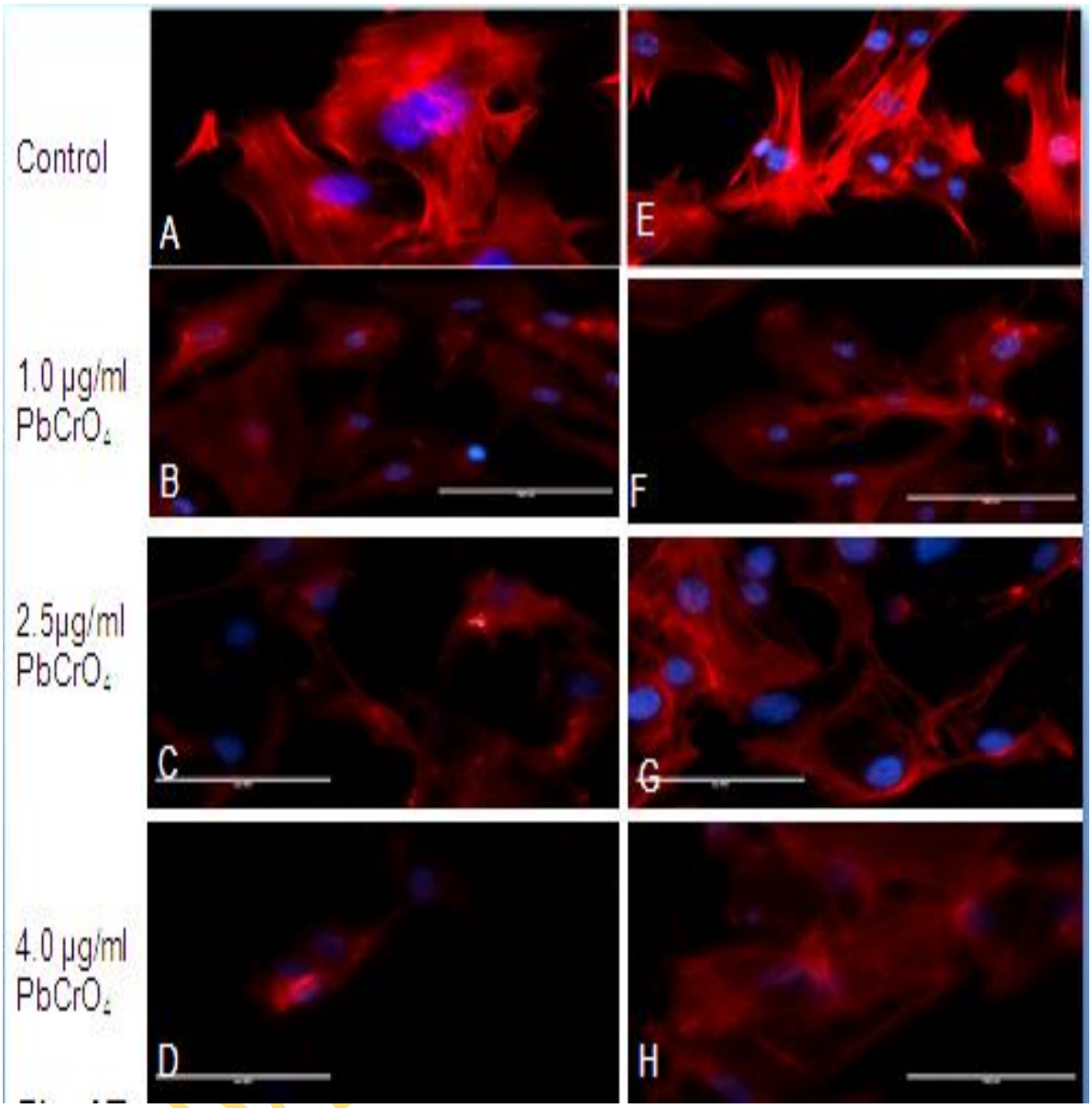

Figure 4.43 : Reduction of actin flourescence intensity and disruption actin fibre by $PbCrO_4$ X 400

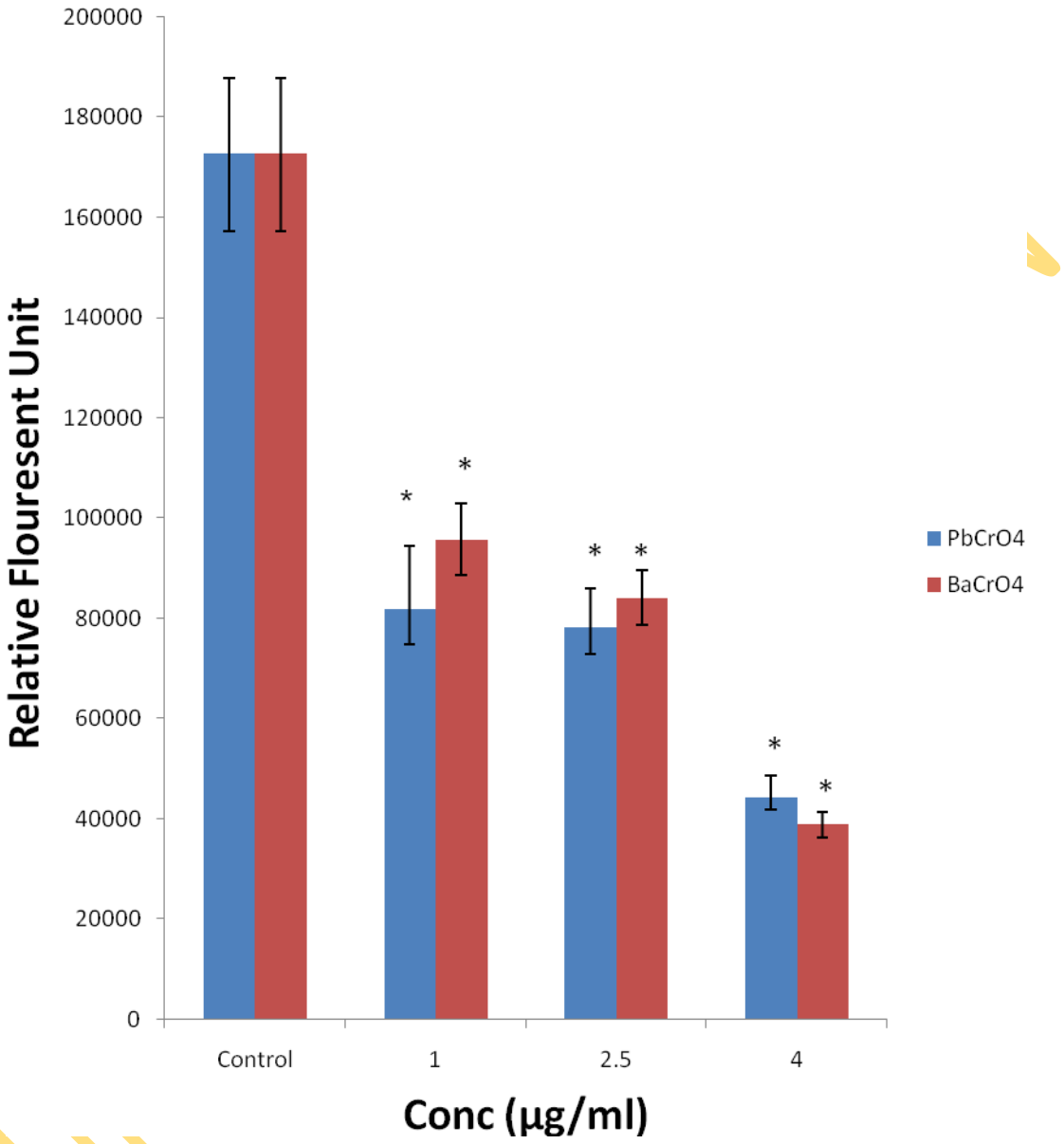

Figure. 4.44: Dose dependent decrease in the relative TRITC-phalloidin fluorescence in $PbCrO_4$ and $BaCrO_4$ treated cells.

*Significantly different ($p < 0.05$) from the control.

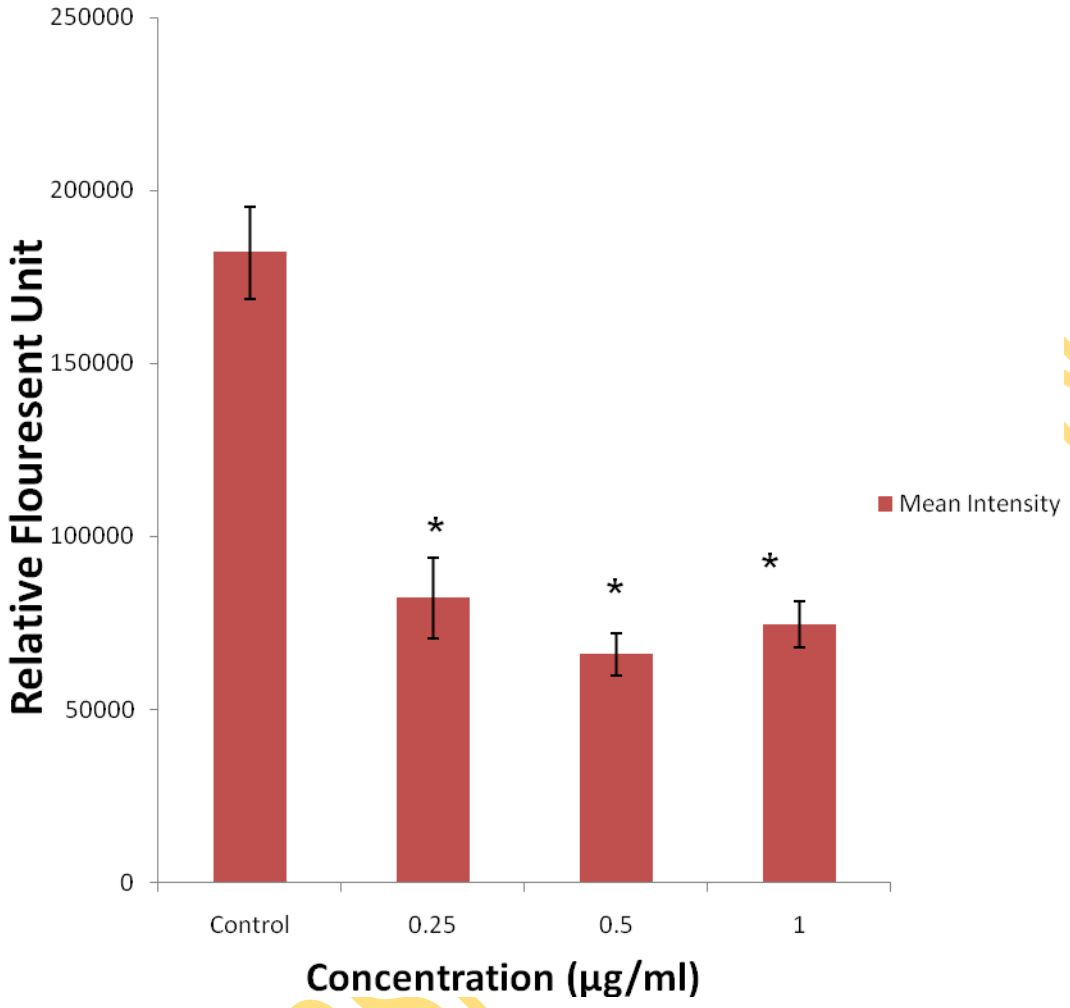

Figure 4.45: Dose dependent decrease in the relative TRITC-phalloidin flourescence in $SrCrO_4$ treated cells.

*Significantly different ($p < 0.05$) from the control.

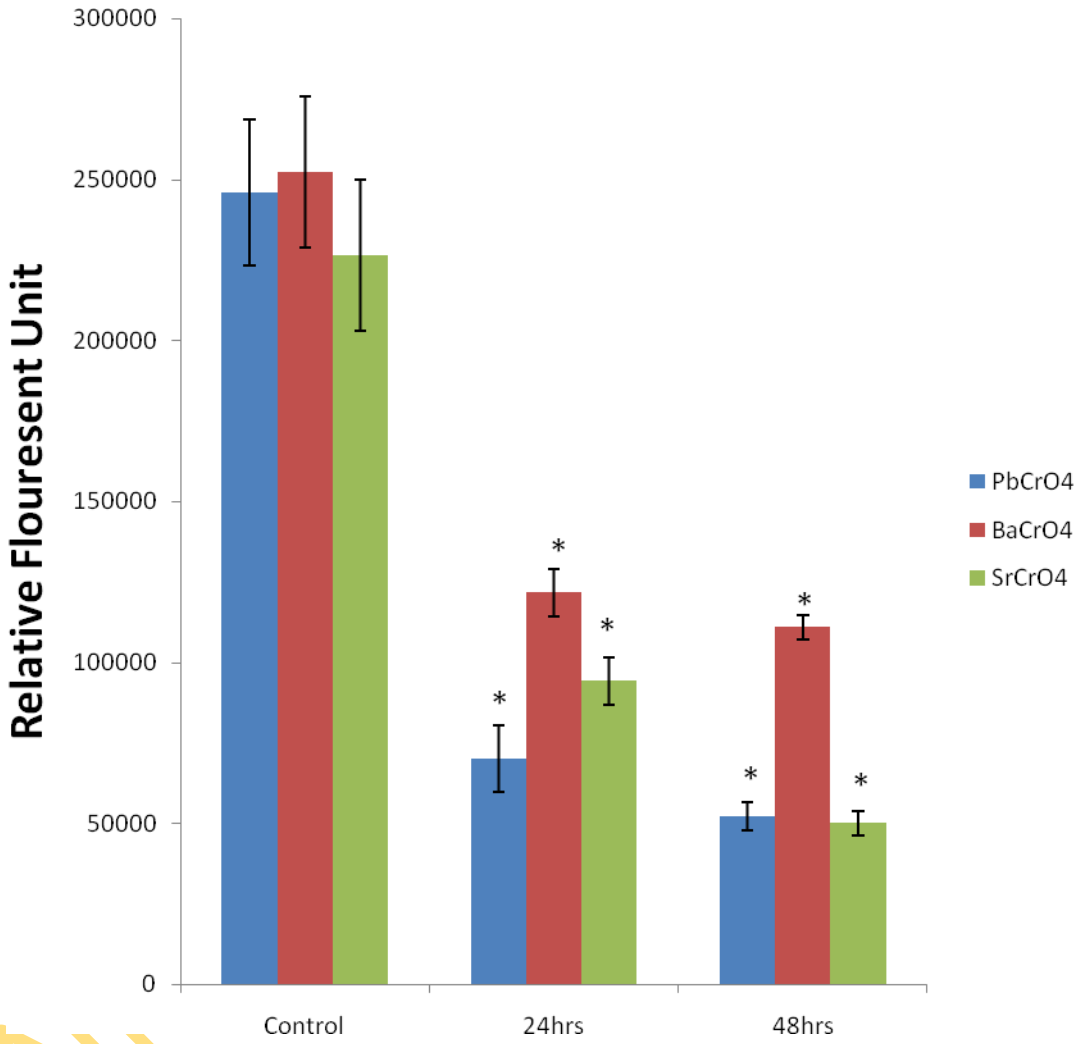

Figure 4.46: Time dependent decrease in the relative TRITC-phalloidin flourescence of $PbCrO_4$, $BaCrO_4$ and $SrCrO_4$ treated cells. The cells were exposed to 2.5µg/ml $PbCrO_4$ and $BaCrO_4$, while the concentration of $SrCrO_4$ used was 0.5µ g/ml.

*Significantly different ($p < 0.05$) from the control

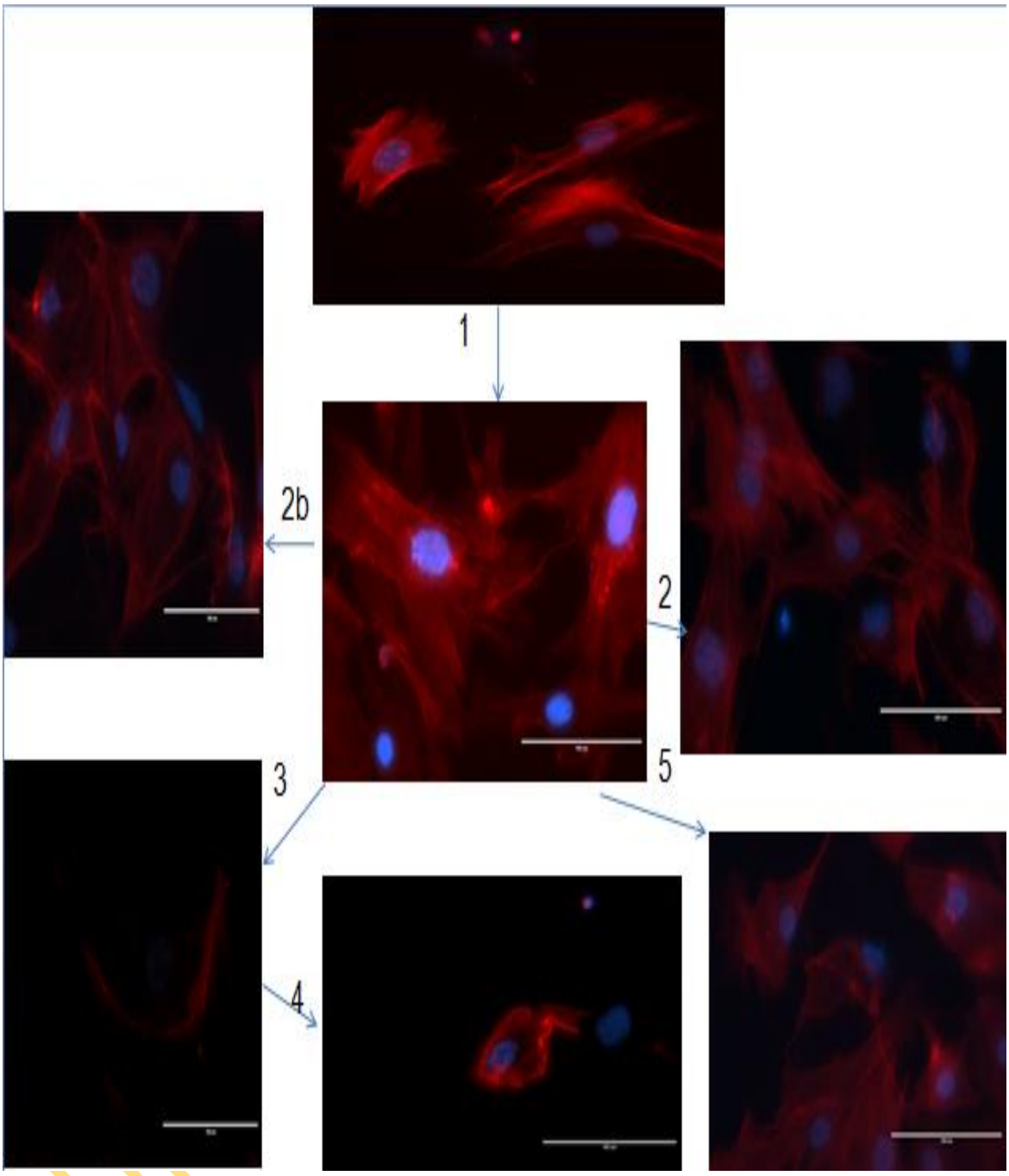

Figure 4.48: Possible mechanisim of anucleation and cell remodelling in CH310T½ cells treated with hexavalent chromate compounds X 40

4.11 EXPERIMENT 11: ASSAY FOR MORPHOLOGICAL TRANSFORMATION INDUCED BY $PbCrO_4$, $BaCrO_4$ and $SrCrO_4$

INTRODUCTION

Despite the overwhelming evidences from epidemiological and animal studies concerning the strong potency of insoluble hexavalent chromates as human carcinogen, effort to establish the carcinogenesis of hexavalent chromate compounds in vitro has only yielded limited success. For instance, Patierno *et al.*, 1988 reported that $PbCrO_4$ induced a weak morphological transformation in CH310T½ cells. The weak transformation was ascribed to a number of factors including particle size that limits its uptake (Patierno *et al.*, 1988). Therefore the yield of transformation by $PbCrO_4$, $BaCrO_4$ and $SrCrO_4$ with small particles were compared their corresponding large particle forms.

PROCEDURE

CH310T½ cells were grown to 80% confluence, trypsinised and seeded into 60 mm dishes in 5 ml medium at 2,000 cells per dish. 20 dishes were plated per concentration. Five days post seeding, cells were treated with 0-4.0 µg/ml of $PbCrO_4$ or $BaCrO_4$ and $SrCrO_4$ for 48 hrs. Control cells were exposed to 1 µg/ml of 3-methyl cholanthrene (MCA) or left untreated. The medium was then replaced with medium lacking the chromate compounds, and then the medium was changed once a week for 6 weeks. At the end of the sixth week, the dishes were rinsed with 0.9% NaCl saline, fixed with methanol, stained with Giemsa and scored for both type I and type II foci (Figure 3.6)using a dissecting microscope as previously described under "Materials and Methods" (Section 3.15, Page92-94).

RESULTS

In this experiment the modified transformation assay procedure of Nesnow *et al*., 1980 was employed. In this assay, CH310T½ cells were seeded and cultured for 5days before they were exposed to the small (sonicated) and large (unsonnicated) particles of $PbCrO_4$, $BaCrO_4$ and $SrCrO_4$ for 48 hours . The rationale behind the protocol is based on the assumption that by seeding cells and waiting until five days later, more total cells will be at risk. In addition more cells will be in the S-phase of the cell cycle, where they are most vulnerable to attack by chemical carcinogens. The method has been shown to increase the sensitivity and yield of

transformation by chemical carcinogens (Miura *et al.*, 1989; Patierno *et al.*, 1988; Nesnow, *et al.*, 1980). The yield of foci by the small and large particles of $PbCrO_4$ is shown in table 4.14. As shown in table 4.14, the positive control in this experiment 3-methyl cholanthrene (MCA) induced about 23 folds increase in the yield of total foci when compared with vehicle control. Treatment of CH310T½ cells with different concentrations of the large $PbCrO_4$ led to between 0-3.0 folds increase in foci yield when compared with the control. However, the total yield of transformation with the highest dose of sonicated $PbCrO_4$ was 0.6, while none was observed at the lower doses. This implies that, under our experimental conditions, reduced particle size of $PbCrO_4$ reduced the morphological transformation caused by $PbCrO_4$.

The yield of foci by the small and large particles of $BaCrO_4$ is shown in Table 4.15. The total foci yield observed in cells exposed to small particles of $BaCrO_4$ was between 3.4 to 5.1 folds higher than that of the control (Table 4.15). The yield of total foci was also dose dependent in treated cells. No foci was observed when cell were treated with 1.0 and 2.5 µg/ml of the large $BaCrO_4$ particles, but the 4.0 µg/ml $BaCrO_4$ treatment led to 2.2 folds increase in total foci when compared with control. Thus, reduced particle size of $BaCrO_4$ increased the yield of transformation in CH310T½ cells under this experimental set up. Similarly, treatment of cells with $SrCrO_4$ resulted in between 1.5 folds and 4.8 folds increase in total foci formation. However, the total yield of foci was not dose dependent (Table 4.16).

CONCLUSION

Overall, all the 3 chromate compounds (under one condition or the other) increased the frequency of morphological transformation in CH310T½ cells when compared with the contol. However, the yield of transformation was at least 5 times less than that of MCA.Thus, indicating that the chromate compounds were not as strong as MCA in inducing morphological transformation in CH310T½ cells.

Table 4.14: The yield of foci in CH310T1/2 cells treated Small (S) and Large(L) particles of $PbCrO_4$

Treatment	Type II Foci*	Type III Foci*	TOTAL Foci*
NA	0.6	0	0.6
Ace	1.3	0	1.3
1 µg/ml MCA	18.8	11.6	30.4
1.0 µg/ml S $PbCrO_4$	0	0	0
2.5 µg/ml S $PbCrO_4$	0	0	0
4.0 µg/ml S $PbCrO_4$	0	0.6	0.6
1.0 µg/ml L $PbCrO_4$	2.2	0	2.2
2..5 µg/ml L $PbCrO_4$	3.8	0	3.2
4.0 µg/ml L $PbCrO_4$	0	0	0

*The number of foci has been normalized to a total 20 dishes

Table 4.15: The yield of foci in CH310T1/2 cells treated Small (S) and Large (L) particles of $BaCrO_4$

Treatment	Type II Foci*	Type III Foci*	TOTAL Foci*
NA	0.6	0	0.6
Ace	1.3	0	1.3
1 µg/ml MCA	18.8	11.6	30.4
1.0 µg/ml S $BaCrO_4$	4.4	0	4.4
2.5 µg/ml S $BaCrO_4$	4.4	2.2	6.6
4.0 µg/ml S $BaCrO_4$	6.6	0	6.6
1.0 µg/ml L $BaCrO_4$	0	0	0
2..5 µg/ml L $BaCrO_4$	0	0	0
4.0 µg/ml L $BaCrO_4$	2.9	0	2.9

* The number of foci has been normalized to a total 20 dishes

Table 4.16: The yield of foci in CH310T1/2 cells treated with small particles of $SrCrO_4$

Treatment	Type II Foci*	Type III Foci*	TOTAL Foci*
NA	0.6	0	0.6
Ace	1.3	0	1.3
1 µg/ml MCA	18.8	11.6	30.4
0.25 µg/ml $SrCrO_4$	6.3	0	6.3
0.5 µg/ml $SrCrO_4$	2	0	2
10 µg/ml $SrCrO_4$	4.2	1.1	6.3

* The number of foci has been normalized to a total 20 dishes

4.12 EXPERIMENT 12: EXPRESSION OF APOTOSIS, AUTOPHAGY AND NECROSIS GENE IN $PbCrO_4$, $BaCrO_4$ and $SrCrO_4$ TREATED CELLS

INTRODUCTION

Cell death gene expression studies were carried out to complement the earlier observations that the nature of cell death is mixed. At the molecular level, changes in cell death signaling are critical alterations that contribute to cytotoxicity and cellular transformation.

PROCEDURE

One hundred thousand log phase growing 10T½ cells or $PbCr_3$ were seeded in 75 ml flasks and allowed to reach 70% confluence. The 10T½ cells were treated with 2.5µg/ml $PbCrO_4$ or $BaCrO_4$ for 48 hours, while the control and $PbCr_3$ were left untreated. The total RNA from the the harvested control and treated cells as well as the transformed, $PbCr_3$ cells was isolated, cDNA was synthesized and the expression profile of cell death related genes was determined as previously described under "Materials and Methods" (Section 3.16, Page 96-98).

RESULTS

To gain more insight into the mechanisms underlying the mixed form of cell death earlier observed in chromate treated cells, the expression of 84 apoptosis, necrosis and autophagy related genes were monitored in treated and control cells. Differential expression of these genes in normal and $PbCrO_4$ transformed cell line, $PbCr_3$ were also studied. The results obtained for cells treated with $PbCrO_4$ are presented in Figure 4.48-51. A positive value indicates gene up-regulation, while a negative value indicates gene down-regulation. As shown in Figure 4.48, $PbCrO_4$ treatment resulted in the up regulation of 10 out of the monitored 25 pro-apoptotic genes including Bax, Casp3, Casp9 and Gadd45a, but Fas was down regulated. Out of the 11 anti-apoptotic genes monitored, $PbCrO_4$ exposure resulted in the up regulation of 4 anti-apoptotic genes including Akt1and Xiap, but the prominent anti-apoptotic genes, BCl-2 genes was down regulated (Figure 4.49). Nine autophagy related genes including Akt1, Pik3c3 and Nfkb1 out the 34 monitored were up-regulated by at least 4 folds, while 5 autophagy genes including Atg 5 and Atg 12 were down regulated (Figure 4.50). Out of the 24 necrotic genes that were monitored, 9 including Galnt 5 and Foxil were over expressed in cells exposed to $PbCrO_4$ (Figure 4.51)

The expression profile of proapoptotic, antiapoptotic, autophagic and necrotic genes after exposure of CH310T½ cells to 2.5 µg/ml $BaCrO_4$ is presented in Figure 4.52- 4.55 respectively. The expression of Bcl 2/11, Casp7, Dffa, Spata 2,and Tnfrsf1a out of the 25 proapoptotic genes monitored were up regulated by at least 4 folds in cell treated with $BaCrO_4$ for 48hrs (Figure 4.52). For the antiapoptotic genes, Akt 1, BCl2/1, Birc 3, and Casp 2 were all over expressed by at least 4 folds, while Traf 2 was down regulated (Figure 4.53). Autophagy related genes including Akt 1, Atg3, BCl2/11, Nfkb1 and Snca were upregulated in the $BaCrO_4$ exposed cells, while Atg12 and Igf1 were down regulated (Figure 4.54). A total of 7 genes associated with necrosis including Ccdc 103, Foxi1, Galnt 5, Hspbap1, Spata, Tem 57 and Tnfrs1a were up regulated in CH310T½ cells exposed to $BaCrO_4$ for 48 hours (Figure 4.55). The result may be a confirmation of the observation earlier made at the cellular level that the nature of cell death in chromate treated cell is mixed.

Next, the differential cell death gene expression analysis between the untreated (normal) CH310T½ cells and $PbCrO_4$ transformed cell line, $PbCr_3$ was carried out using the RT^2cell death profiler array. The folds changes in expression of proapoptotic, antiapoptotic, autophagic and necrotic genes results are presented in Figure 56-59. The experiment revealed changes in the expression pattern of cell death genes in the transformed cell. Although some proapoptotic genes like BCl2/11, Casp 3, Casp 6, Gadd 45a, Spata2 , cyld and Fas were up regulated, major proapoptotic genes such as Bax, Casp7, Casp 9, Nol 3 and Sycp 2 were down regulated (Figure 4. 56) . Among the antiapoptosis genes tested, Bcl 2, Birc 3, Igf1r, mcl 1, Tnfrsf 11b and Traf 2 were all up regulated (Figure 4.57). Only Akt 1 was down regulated in the transformed cell line (Figure 4.57). In the case of autophagy related genes, a total of 15 genes including App, Atg12, Atg16l1, Atg3, Atg5, Atg7, Bcl2, Becn1 , Casp3, Ctsb , Fas , Gaa, Irgm1, Mapk8 and Ulk1 that participate in autophagy were up regulated in the transformed cells line, PbCr3, while Akt was down regulated (Figure 4.58). For the necrosis genes, an increased expression was observed for Cyld, Dennd4a, Mcl 1, Spata 2, Tmem 57 and Txnl4b (Figure 4.59). However, Sycp2 and Hspbap 1 were both down regulated in the transformed cells.

CONCLUSION

The simultaneous alteration in expression of apoptosis, autophagy and necrosis related genes confirmed earlier observation at the cellular level that the nature of cell death in CH310T½ treated with the chromate compounds is mixed. In addition, up regulation of antiapoptotic and autophagy genes as well as down regulation of proapoptotic genes may be responsible for the survival of the chromate transformed cells. Therefore, chemotherapy targeted against both apoptosis and autophagy may be useful in the treatment of hexavalent chromate related tumours.

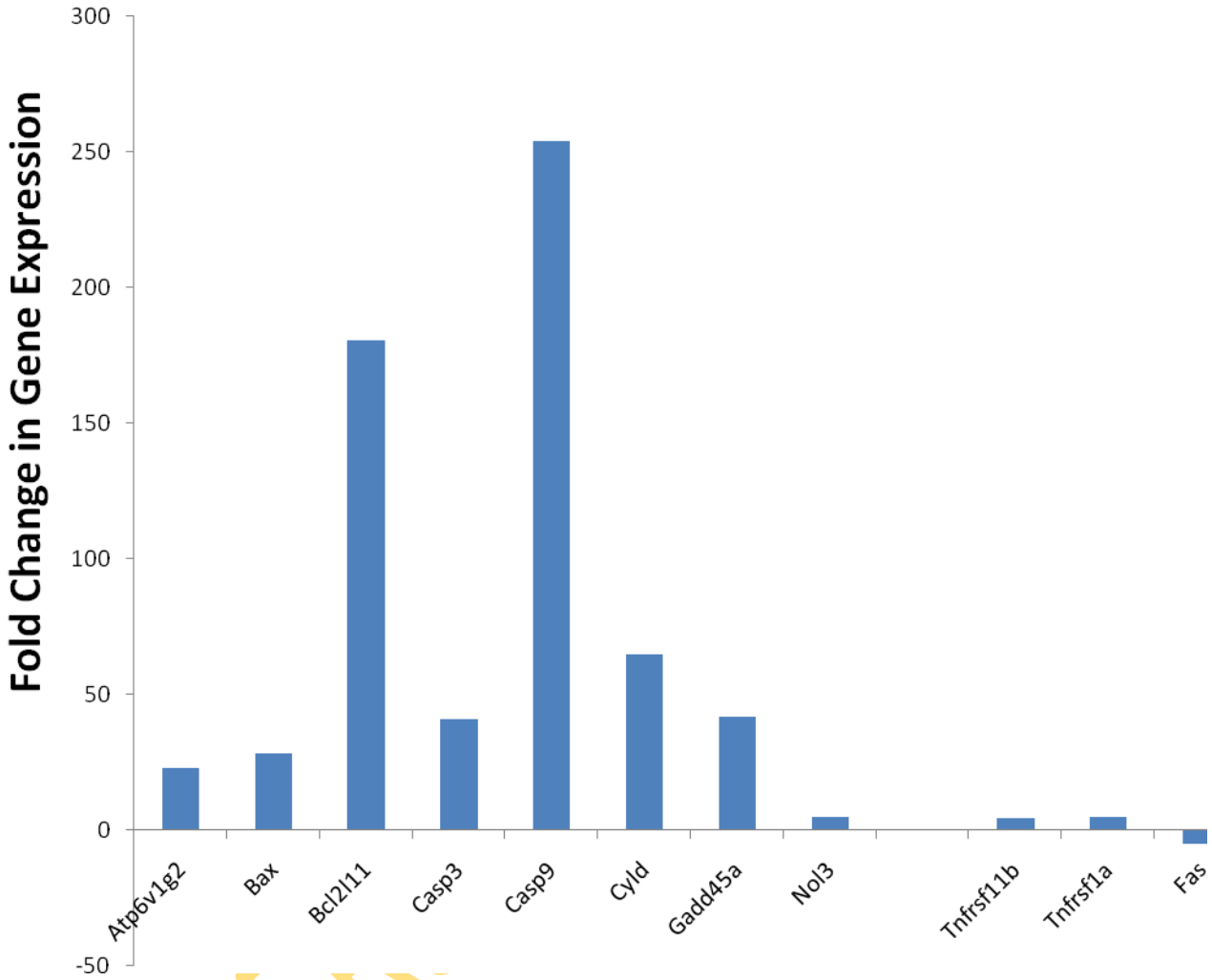

Figure 4.48: Fold change in apoptosis related genes after exposure of CH310T½ cells to 2.5 µg/ml $PbCrO_4$. Data were normalised with GADPH and ActinB

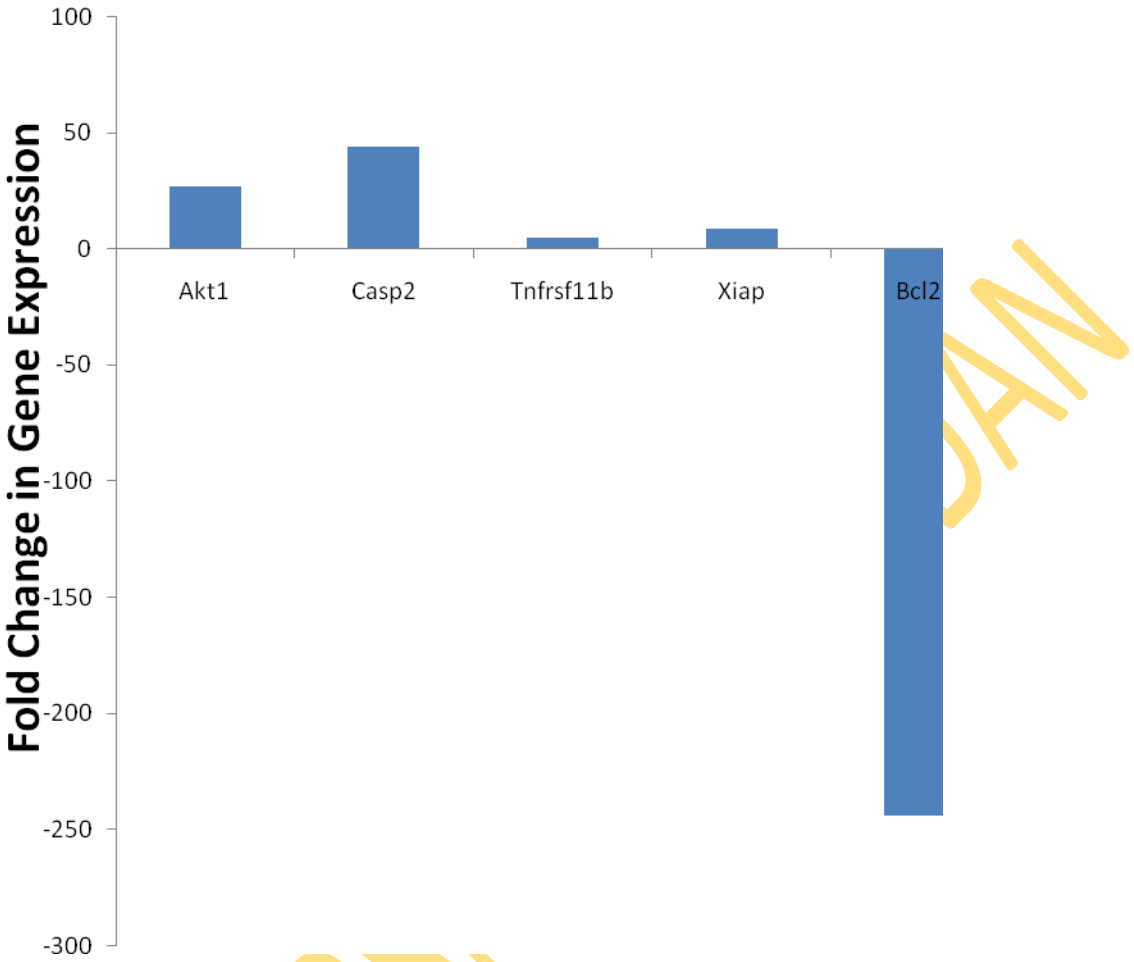

Figure 4.49: Fold change in anti-apoptotic gene expressions after treatment of CH310T½ cells to 2.5 µg/ml $PbCrO_4$ .Data were normalised with GADPH and ActinB

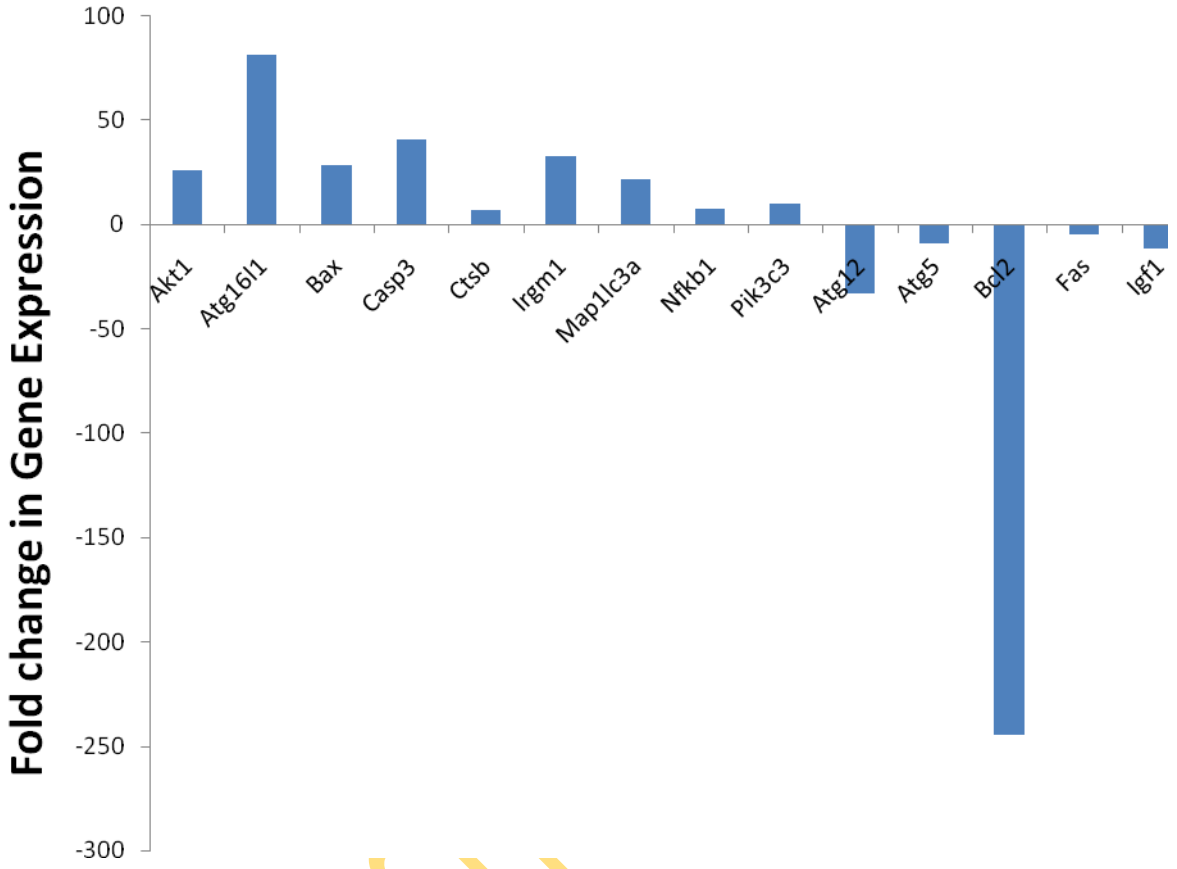

Figure 4.50: Differential changes in the expression of autophagic related genes after treatment of CH310T½ cells to 2.5 µg/ml $PbCrO_4$. Data were normalised with GADPH and Actin B

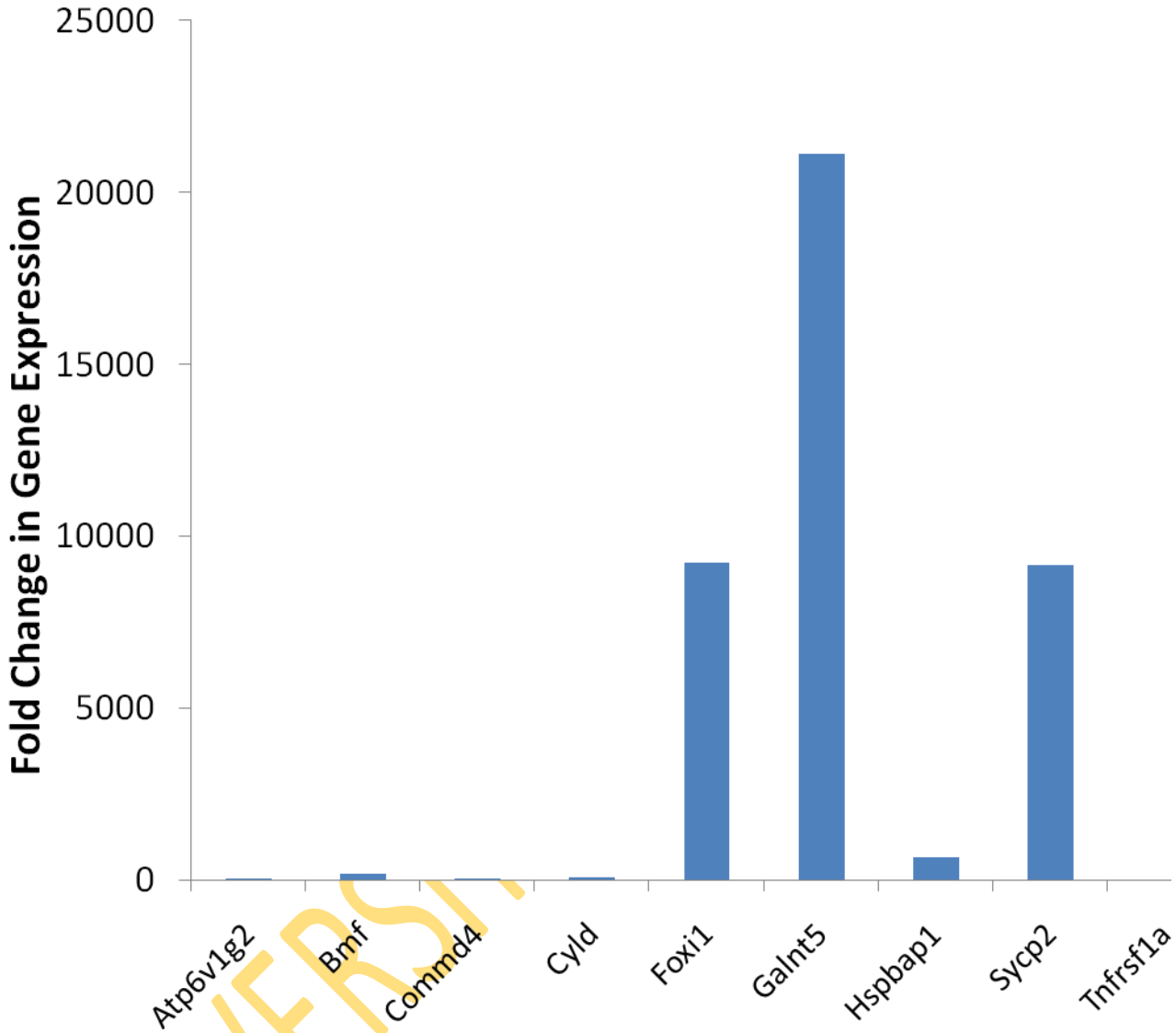

Figure 4.51: Differential Expression of genes associated with necrosis after exposure of CH310T ½ cells to 2.5 µg/ml $PbCrO_4$. Data were normalised with GADPH and Actin B.

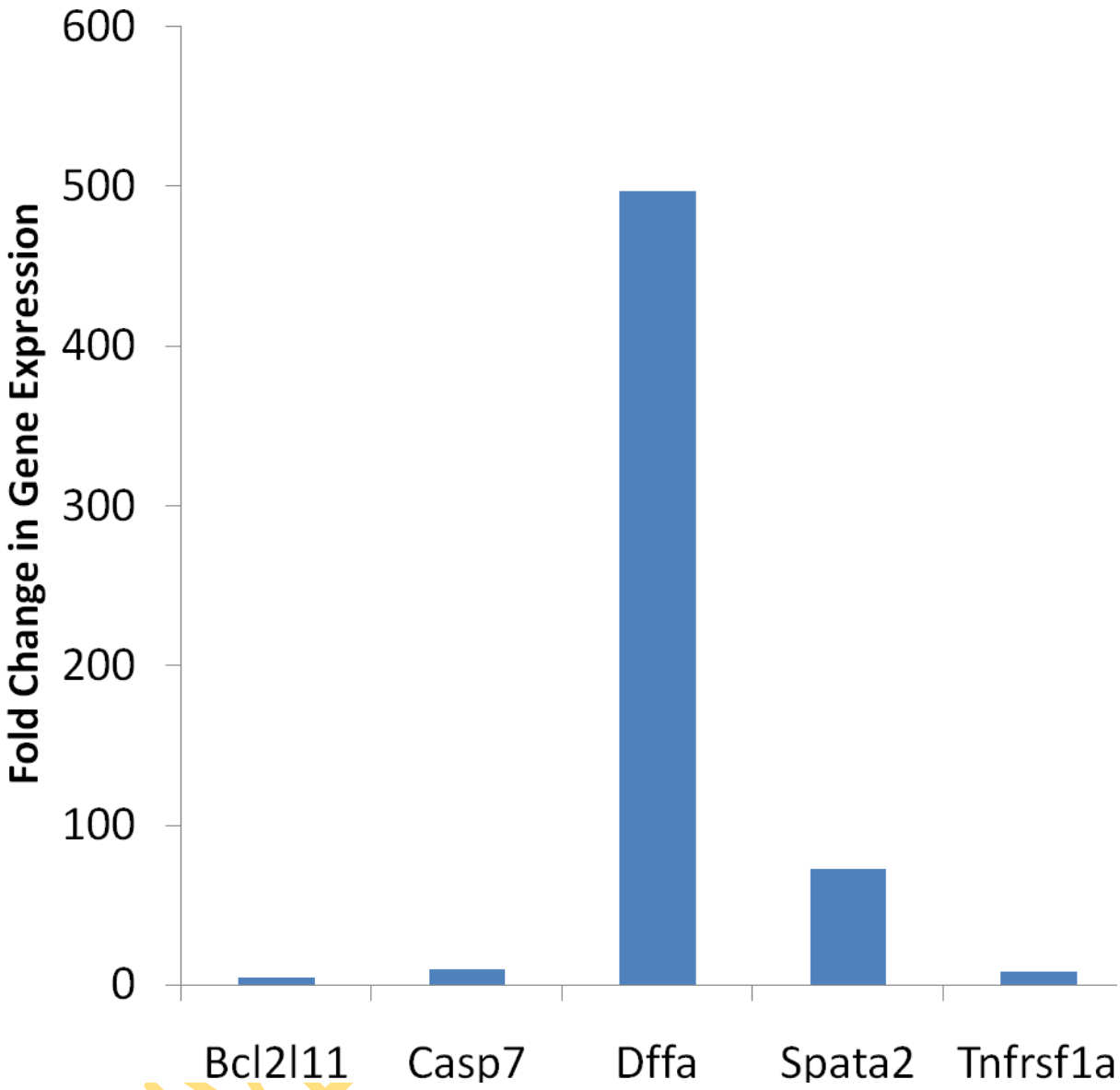

Figure 4.52: Fold increase in proapoptotic genes after treatment of CH310T½ cells with 2.5 µg/ml $BaCrO_4$. Data were normalised with GADPH and Actin B.

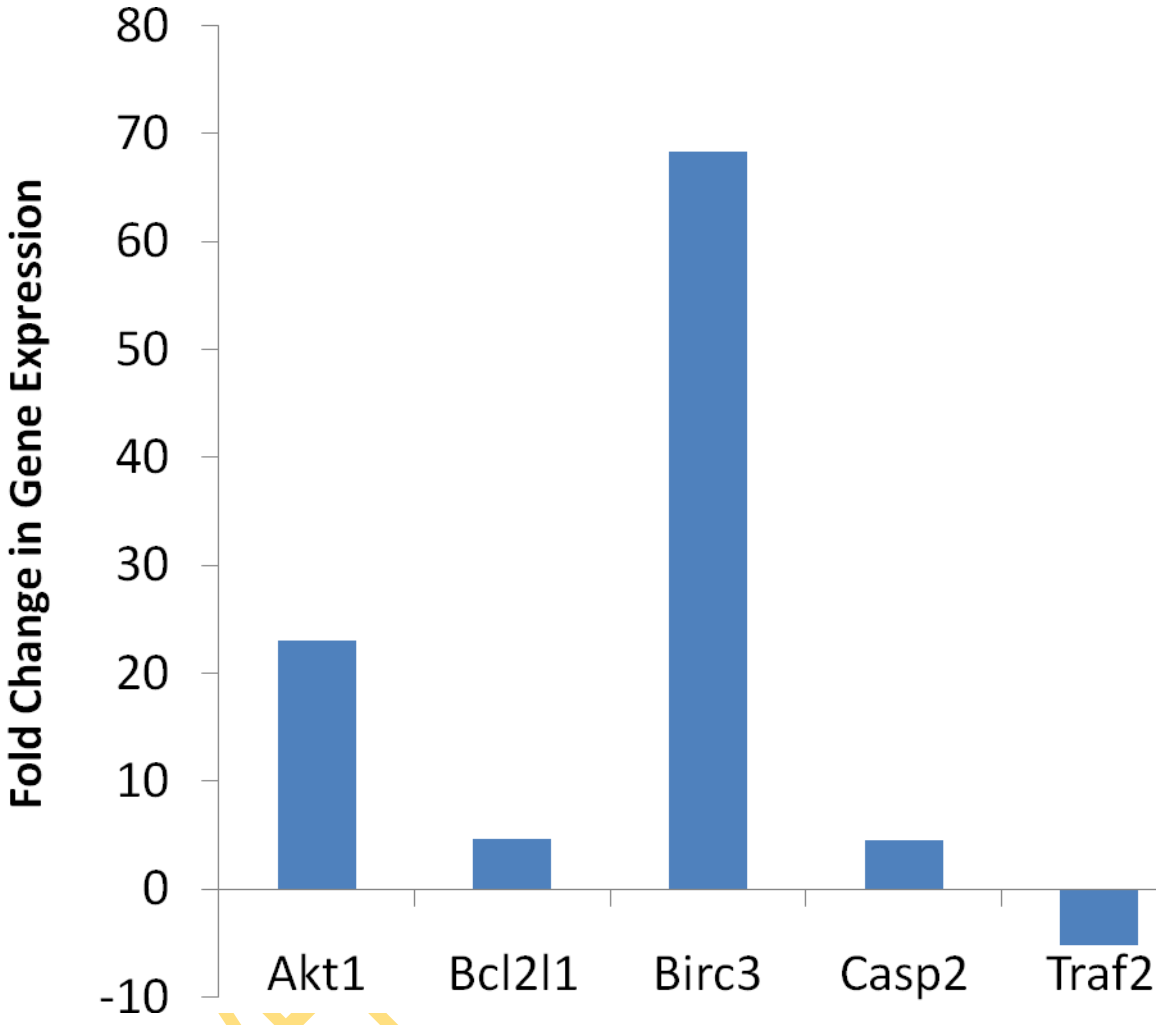

Figure 4.53: Fold change in anti -apoptotic gene expression after treatment of CH310T½ cells with 2.5 µg/ml $BaCrO_4$. Data were normalised with GADPH and Actin B

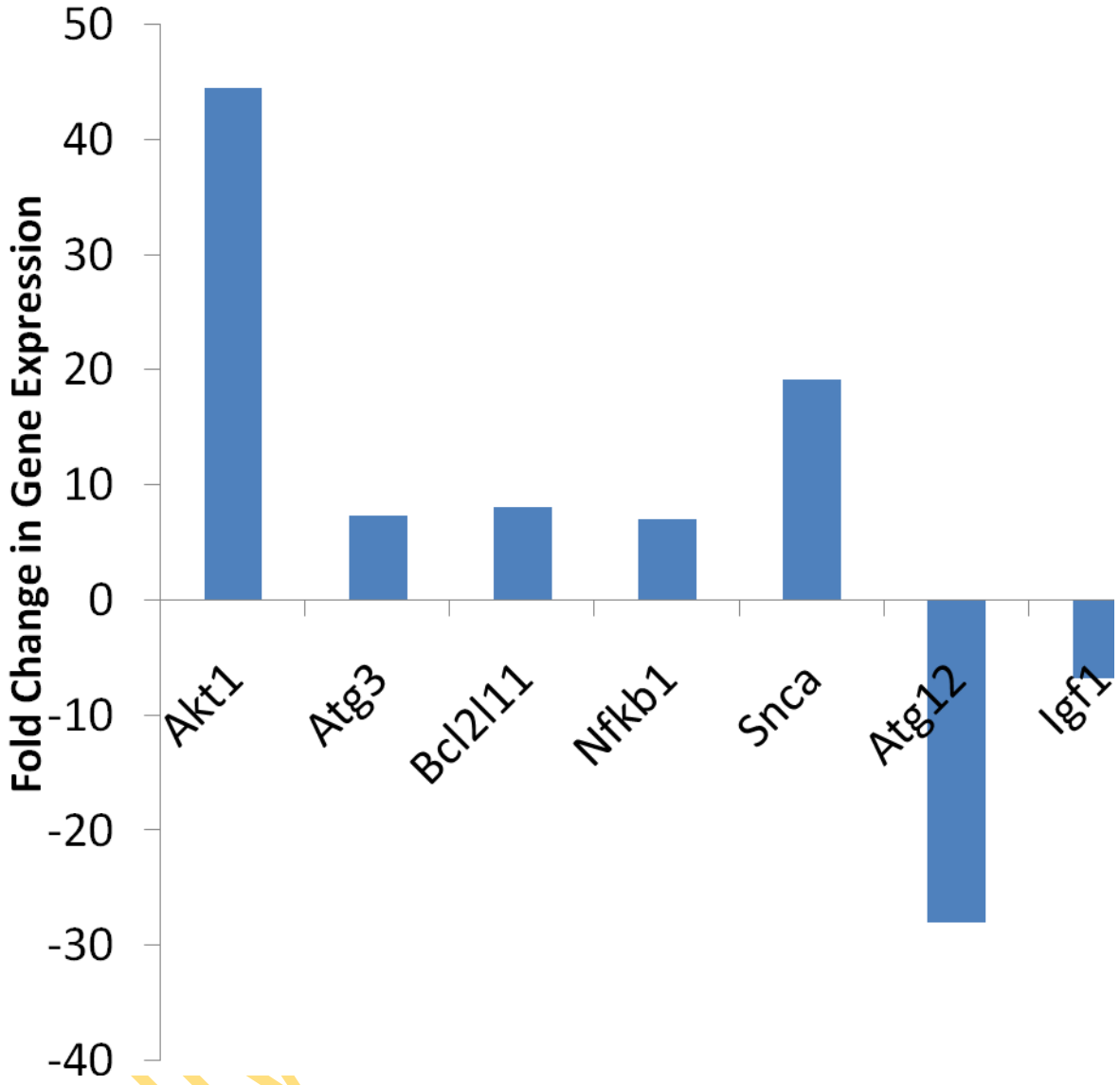

Figure 4.54: Fold change in autophagic related gene expression profile after exposure of CH310 T½ cells to 2.5 µg/ml $BaCrO_4$. Data were normalised with GADPH and Actin B

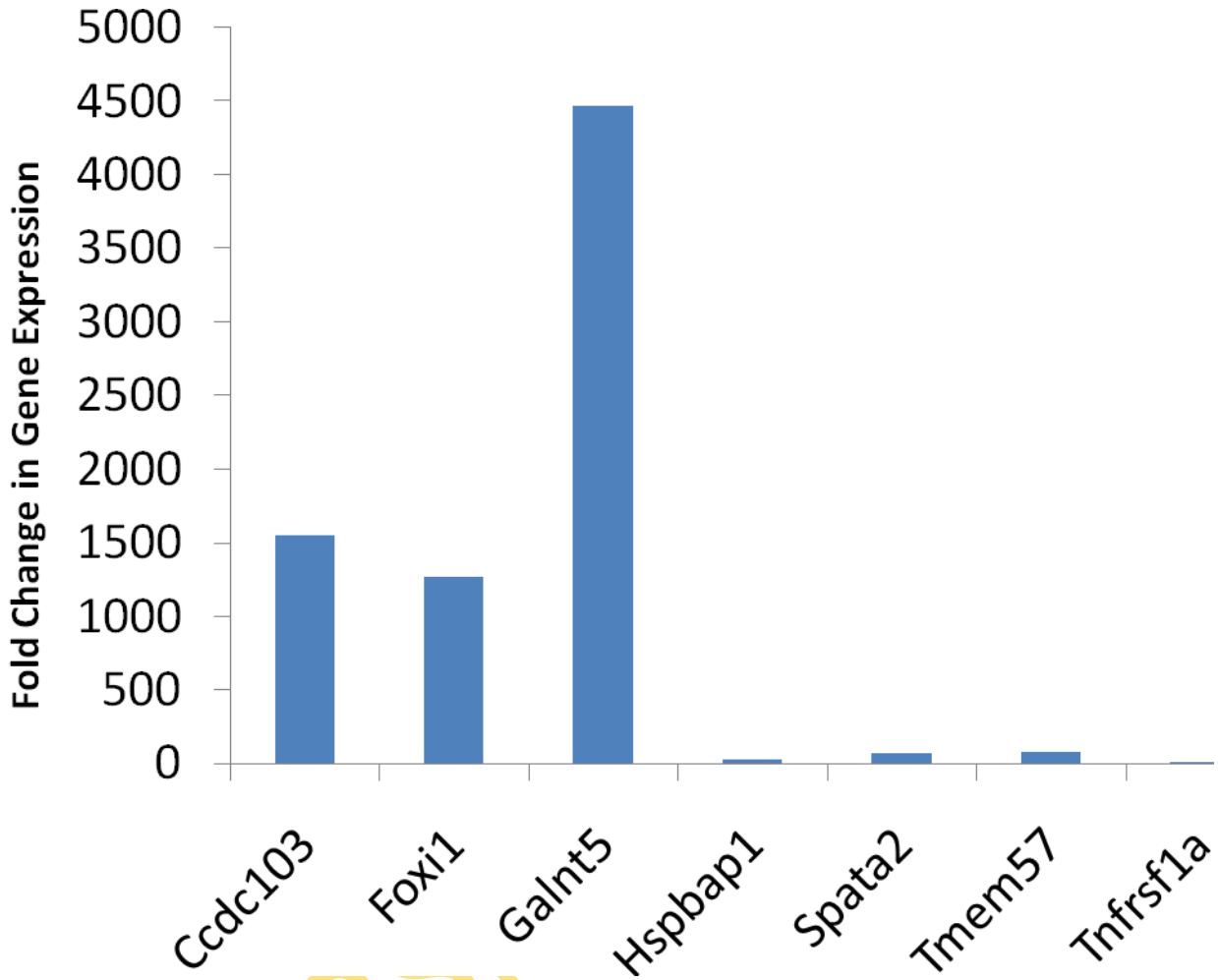

Figure 4.55: Fold change in expression of genes that regulate necrosis after $BaCrO_4$ exposure. Data were normalised with GADPH and Actin B.

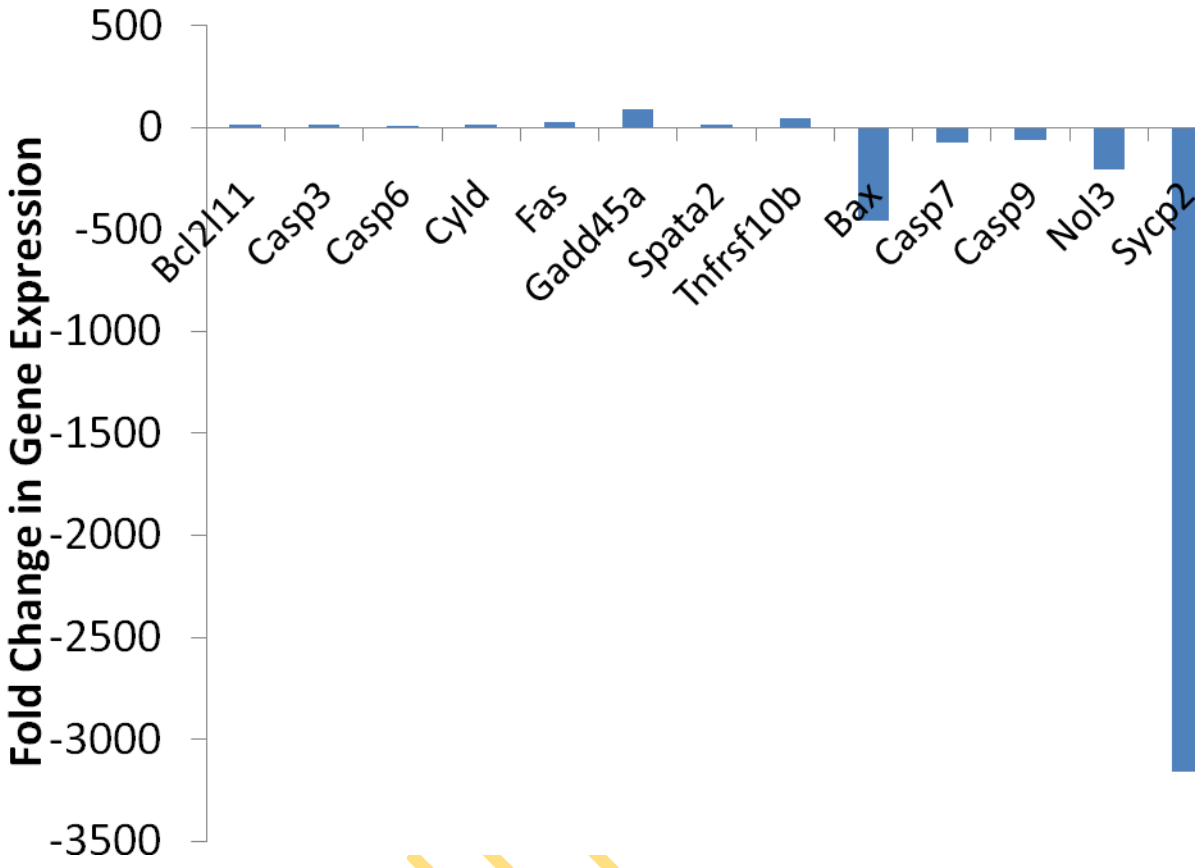

Figure 4.56: Fold changes in genes that regulate apoptosis in $PbCrO_4$ transformed cell line, $PbCr_3$. Data were normalised with GADPH.

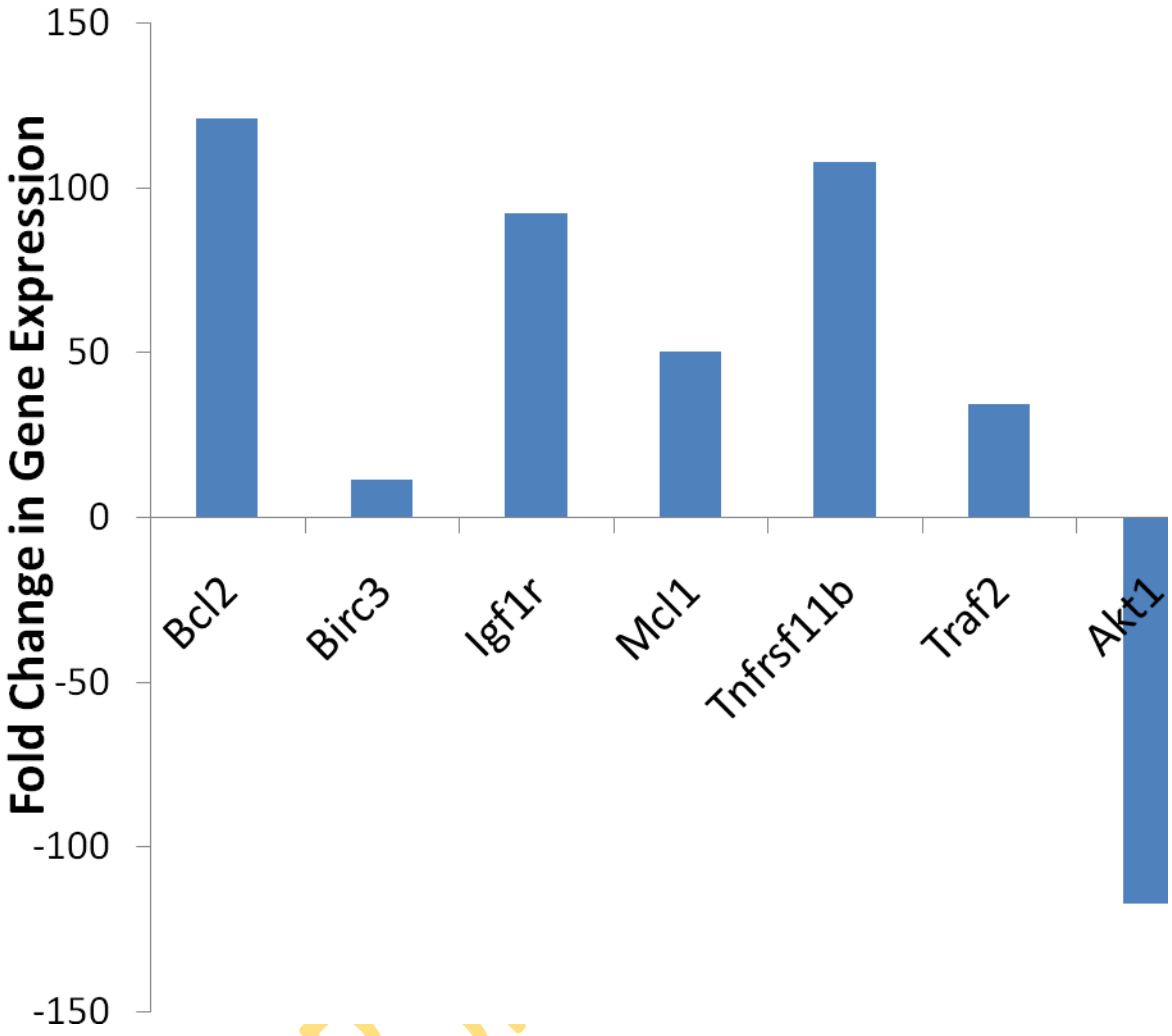

Figure 4.57: Fold changes in anti-apoptotic genes in $PbCrO_4$ transformed cell line, $PbCr_3$ Data were normalised with GADPH.

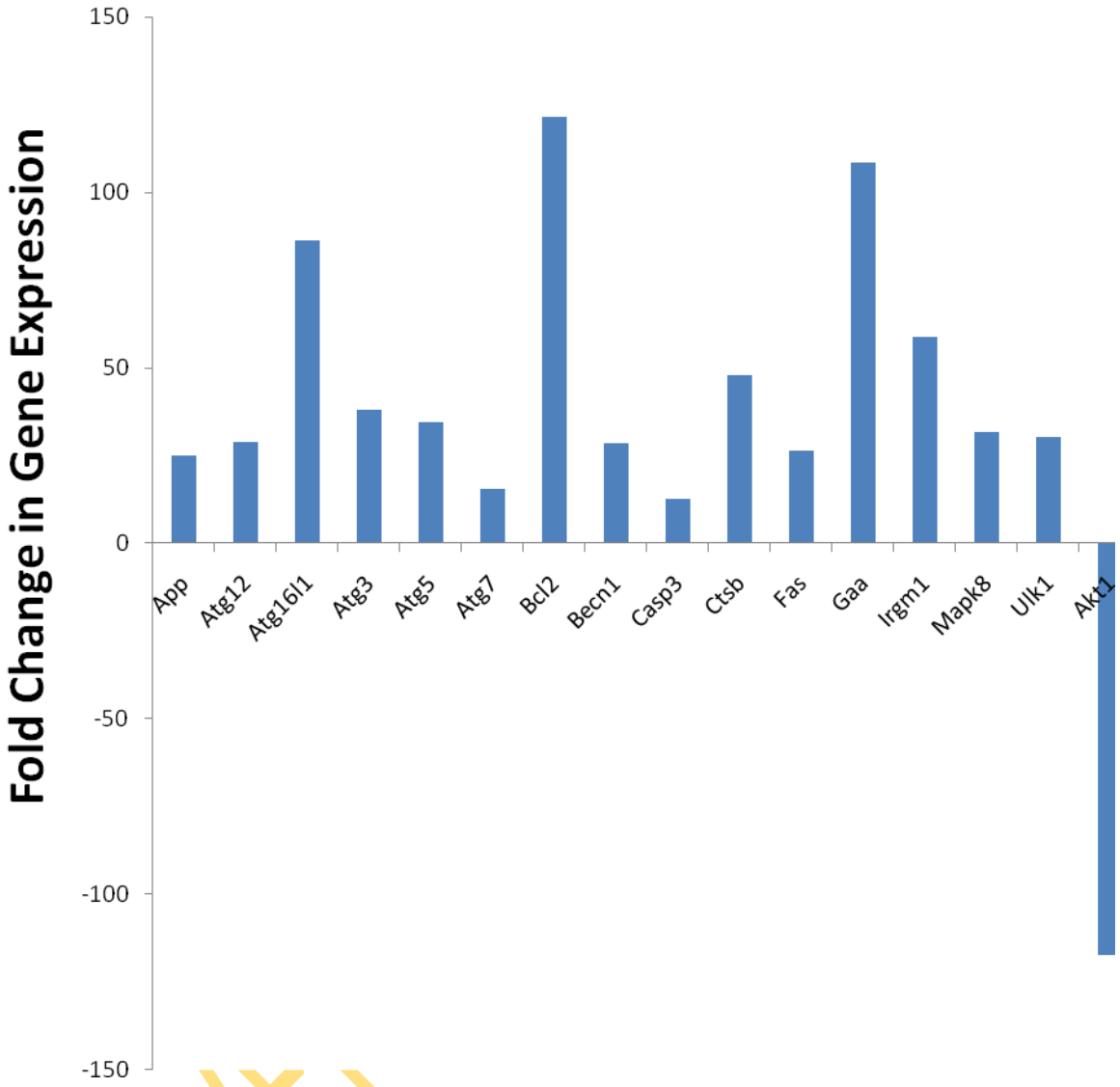

Figure 4.58: Expression profile of autophagy related genes in $PbCrO_4$ transformed cell line, $PbCr_3$. Data were normalised with GADPH.

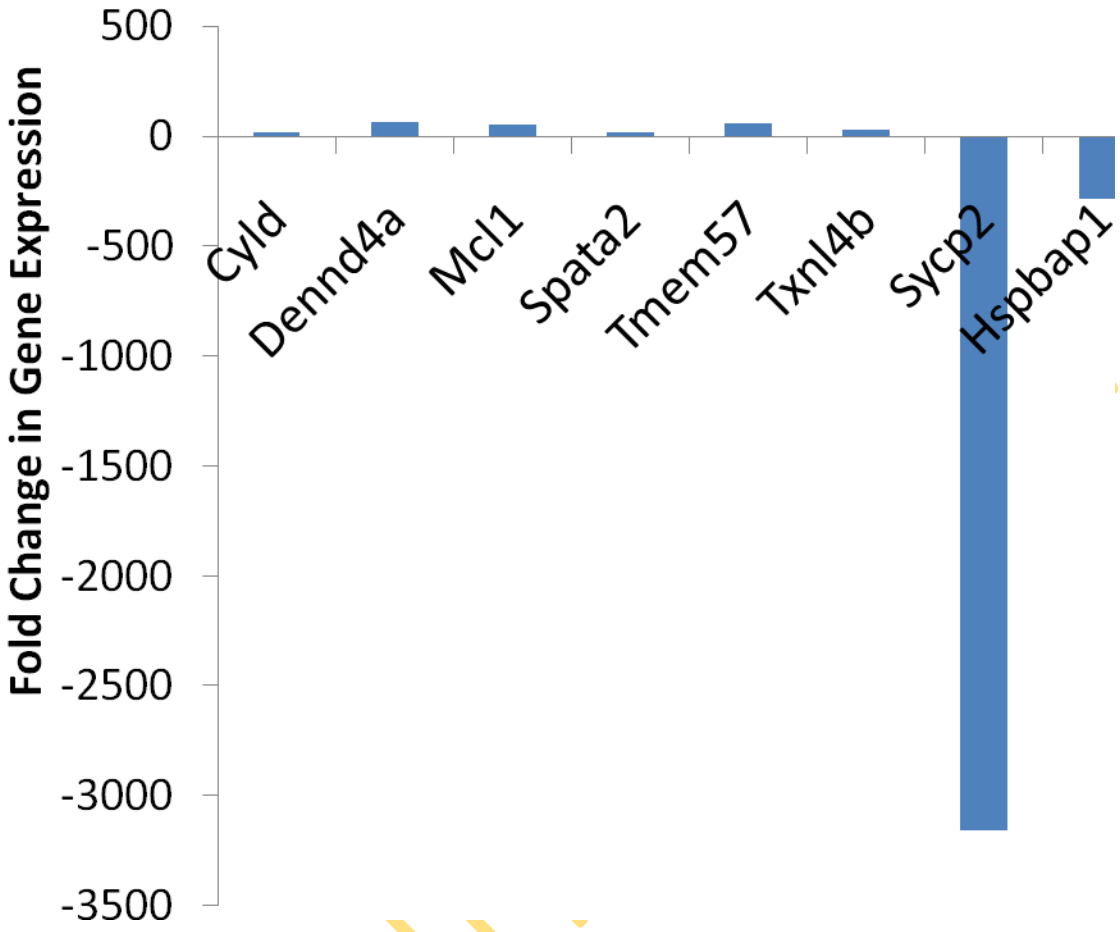

Figure 4.59: Fold changes in genes that control necrosis in $PbCrO_4$ transformed cell line, $PbCr_3$ Data were normalised with GADPH.

4.13 EXPERIMENT 13: THE EFFECT OF SODIUM ARSENITE AND METHANOL EXTRACT OF *RAUVOLFIA VOMITORIA* ON THE TOXICITY OF POTASSIUM DICHROMATE IN MICE

INTRODUCTION

The toxicity of hexavalent chromate compounds have been described in several *in vivo* and *in vitro* works. However, chromate toxicities are complicated by co-exposure with other environmental toxicant like cigarette smoke, UV and other heavy metals (Salnikow and Zhitkovich, 2008). Co-exposure to chromate and arsenic is common in drinking water, beverages and some fungicides (Maduabuchi *et al*, 2007). There is dearth of information on the toxicity inherent from the co-exposure to both metals in vivo. A prime focus of this *in vivo* work was to investigate the cytomodulation of chromate (VI) toxicities by sodium asrenite in mice. Moreover, there is no safe and effective antidote for preventing or treating chromate (VI) and arsenic toxicities. To address this problem, this part of the thesis also examines the usefulnes *Rauvolfia vomitora* (RV), a medicinal plant used traditionally in treating tumour related problems in the modulation of chromate (VI) and arsenic toxicities.Specifically, the toxicological markers evaluated in test and control animal include the frequency of formation of micronucleated polychromatic erythrocytes, serum activities of AST and ALT and hepatic oxidative stress markers such as malondialdehyde, catalase, reduced glutathione and glutathione – S- transferase

PROCEDURE

Test and control mice were housed and treated as described under "Materials and Methods" (Section 3.1, Page 76 and Section 3.2, Page 76-77). Twenty-four hours after the last treatment, the animals were sacrificed and the frequency of micronucleated polychromatic erythrocytes (mPCEs) was monitored in bone marrow cells (Section 3.14, Page 99-100) while aspartate aminotransferase (AST) and alanine aminotransferase (ALT) activities were assessed in the serum (Section 3.15, Page 101; Section 3.16, Page101-102). Malondialdehyde (MDA) and Hepatic glutathione (GSH) levels as well as catalase (CAT) and glutathione-S-transferase (GST) activities were also monitored in the liver homogenate. (Sections 3.17-3.22, Page 102-109)

RESULTS

The effect of mice pretreated with methanol extract of *Rauvolfia vomitora* (RV) on the clastogenicity of potassium dichromate ($K_2Cr_2O_7$) and sodium arsenite ($NaAsO_2$) alone and in

combination as evaluated by the frequency of formation of micronucleated polychromatic erythrocytes is shown in Table 4.17.

$K_2Cr_2O_7$ and $NaAsO_2$ significantly induced mPCEs formation in the bone marrow cells by about 11 and 14 folds respectively as compared with the negative control group ($P< 0.05$) in both cases (Table 4.17, groups I, III, IV). Furthermore, co-administration of $K_2Cr_2O_7$ and $NaAsO_2$ markedly induced mPCEs formation by about 23 folds as compared with the negative control group (Table 4.17, groups I, V). When compared with the groups administered $K_2Cr_2O_7$ and $NaAsO_2$, the induction observed in the co-treatment group was about 2.1 and 1.6 folds respectively (Table 4.17, groups III, IV , V). Treatment with RV alone resulted in a 2 folds increase when compared with the control (Table 4.17, groups I, II). Combination of RV with $K_2Cr_2O_7$ or $NaAsO_2$ and their combination led to about 6 folds, 6 folds and 8 folds increase respectively in mPCEs formation as compared with the control (Table 4.17, groups VI , VII , VIII).

The data for the serum activities of ALT and AST in the treated and control mice are presented in table 4.18. From the data, $K_2Cr_2O_7$ induced the serum activity of ALT (237%) and AST (63.65%) respectively as compared with the negative control group (Table 2, groups I and III). $NaAsO_2$ induced the activity of ALT by 260%, while AST was increased by 73.73% as compared with the negative control (Table 2, groups I and IV). Simultaneous feeding of both $K_2Cr_2O_7$ and $NaAsO_2$ further induced the serum activities of ALT by 428% while AST was increased by 135.21% when compared with the mice given distilled water only (Table 4.16, groups I, V). The increase in the serum ALT and AST activities observed in the mice pretreated with RV before being exposed to $K_2Cr_2O_7$ was about 210% and 49.84% respectively as compared with the negative control. Pretreatment of mice with RV before $NaAsO_2$ administration resulted in 233% and 77% increase in ALT and AST activities respectively when compared with the control. The activities of ALT and AST in mice exposed to $K_2Cr_2O_7$ and $NaAsO_2$ after pretreatment with RV were increased by 393% and 110% (Table 4.16, groups I, V).

The effect of methanol extract RV on glutathione –S-Transferase (GST) and catalase (CAT) activities as well as reduced glutathione (GSH) and malondialdehyde (MDA) levels in mice treated with $K_2Cr_2O_7$ and / or $NaAsO_2$ are shown in Table 4.19. Animals treated with $K_2Cr_2O_7$

or $NaAsO_2$ individually recorded mean liver GST activities that were decreased by 62% and 45% respectively when compared to the mean value obtained for the negative control mice treated with distilled water alone. Co-treatment with $K_2Cr_2O_7$ and $NaAsO_2$ further aggravated the toxicity as evidence by the 67% decrease in GST activity. RV treatment ameilorated the toxicity as seen by the 41%, 35% and 41% decrease in GST activity in animals pretreated with RV before exposure to $K_2Cr_2O_7$, $NaAsO_2$ and the combination of the two compounds respectively. Similarly, GSH levels dropped by 43% and 45% in the mice exposed to $K_2Cr_2O_7$ and $NaAsO_2$ as compared with the negative control. Combination of the two compounds resulted in a 66% depletion of GSH levels. Pretreatment with extract of RV resulted in a 25%, 29% and 25% decrease in GSH levels in animal exposed to $K_2Cr_2O_7$, $NaAsO_2$ and the combination of the compounds respectively.

The levels of MDA in liver homogenate was elevated by 36 % and 23 % in animals administered $K_2Cr_2O_7$ and $NaAsO_2$ respectively as compared to the negative control. Co-treatment with the two compounds marginally increased it to 37%. Pretreatment with RV reduced it to 3%, 4% and 3% respectively in animal exposed to $K_2Cr_2O_7$, $NaAsO_2$ and the combination of the compounds. The activities of catalase CAT were induced by 93 % and 96 % in mice exposed $K_2Cr_2O_7$ and $NaAsO_2$ respectively as compared to the negative control. Catalase activities were further increased by 292% in the co-exposure group, while RV pre treatment reduced it to 43%, 47% and 108% respectively in mice exposed to $K_2Cr_2O_7$, $NaAsO_2$ and the combination of the compounds

CONCLUSION

Both potassium dichromate and sodium arsenite are toxic and may induce the formation of micronuclei, hepatic damage and oxidative stress in Swiss albino mice. Co-exposure to both metal salts exacerbated the induction of micronuclei, hepatic injury and oxidative stress in exposed mice. Methanol extracts of *Rauvolfia vomitora* cytomodulated the toxicity of potassium dichromate and sodium arsenite by reducing the frequency of micronuclei formation, hepatic damage and oxidative stress.

Table 4.17 : Frequency of micronucleated polychromatic erythrocytes (mPCEs) in polychromatic erythrocytes in of test and control animals.

Group	Treatment	mPCEs/1000 PCEs
1	Distilled Water	0.25 ± 0.25^{a}
2.	275mg/kg bd.wt. Rauvolfia Vomitora (RV)	0.50 ± 0.28^{a}
3.	2.5mg/kg bd.wt Sodium Arsenite (SA) only	3.50 ± 0.28^{b}
4.	12 mg/kg body weight of $K_2Cr_2O_7$ only	2.75 ± 0.25^{b}
5.	SA+ $K_2Cr_2O_7$	5.75 ± 0.25^{c}
6.	RV + SA	1.5 ± 0.28^{d}
7.	RV + $K_2Cr_2O_7$	1.5 ± 0.29^{d}
8	RV + SA +$K_2Cr_2O_7$	2.0 ± 0.40^{d}

Table 4.18: Serum alanine amino transferase (SALT) and serum aspartate amino transferase (SAST) in test and control animals.

Group	SALT (U/L)	SAST (U/L)
1	24.25± 1.61[a]	44.08 ± 0.90[a]
2.	24.25 ± 0.47[a]	50.26 ± 0.34[b]
3.	87.45 ± 1.18	76.58 ± 0.46[c]
4.	81.79 ± 0.90[b]	72.11 ± 1.07[c]
5.	128.01 ± 1. 41[c]	103.68 ± 1.14[d]
6.	80.80 ± 0.86[b]	78.68 ± 1.37[c]
7.	75.18 ± 0.47[d]	66.05 ± 0.26[e]
8	119.66 ± 1.10[e]	92.63 ± 0.21[f]

Values with the same superscript are not significant at 5% level, whereas values with different superscript are significantly different ($p<0.05$) from one another

Table 4.19: Oxidative stress parameters in test and control animals.

S/N	GSH (µ mol/mg Prt)	GST (µmol/min/mg Prt)	CATALASE (µmol/ sec/ g wet tissue)	MDA (ɪmol/mgPrt)
1	51.15± 1.99^{a}	161.85 ± 2.74^{a}	2.25±0.09^{a}	63.09 ± 3.74^{a}
2	52.35 ± 1.64^{a}	175.02 ± 3.42^{a}	2.51± 0.04^{a}	65.07 ± 1.40^{a}
3	27.82 ± 0.26^{b}	62.55 ± 3.63^{b}	4.42 ± 0.11^{b}	77.69 ±3.73^{b}
4	28.85± 2.64^{b}	87.63 ±1.03^{c}	4.36 ± 0.02^{b}	85.98 ± 1.35^{c}
5	17.29± 0.07^{c}	53.38 ± 1.21^{d}	8.84 ± 0.04^{c}	86.71 ± 2.04^{c}
6	35.81 ± 1.17^{d}	95.00 ± 2.20^{e}	3.31 ± 0.21^{d}	65.98 ±1.07^{a}
7	38.13± 2.06^{d}	103.76 ± 1.80^{e}	3.23 ± 0.23^{d}	65.23 ± 0.44^{a}
8.	38.29 ± 0.44^{d}	94.23 ± 1.77^{e}	4.68 ± 0.50^{b}	65.23 ± 0.40 ^{a}

Values with the same superscript are not significant at 5% level, whereas values with different superscript are significantly different (p<0.05) from one another.

CHAPTER FIVE

5.1 DISCUSSION

In this work, the role of ascorbate and its oxidized form, dehydroascorbate as well as particle size in the cytotoxicity and transformation induced by $PbCrO_4$, $BaCrO_4$ and $SrCrO_4$ were studied in CH310T½. The effect of the selected hexavalent chromate exposure on cell morphology and ultra structures were also evaluated. In addition, the cellular and molecular mechanism of cytotoxicity and transformation were assessed in the same cell line. Furthermore, the cytomodulation of the toxicity of potassium chromate ($K_2Cr_2O_7$) by sodium arsenite ($NaAsO_2$) and methanol extract of *Rauvolfia vomitora* (RV) was assessed *in vivo* using swiss albino mice.

The role of ascorbate in the toxicity of chromate is controversial. Several studies have shown that vitamin C could protect against hexavalent chromate cytotoxicity and clastogenicity, while others have shown that it either does not affect chromate (VI) toxicity or may even exacerbate hexavalent chromate toxicity. For instance, Xie et *al.* (2004) reported that ascorbate blocked the clastogenicity of lead chromate in WTHBF-6 cells. Pretreating cells with ascorbate was also shown to reduce chromate-induced alkali labile sites, clastogenic effects, apoptotic effects and overall cytotoxicity, but had no effect on chromium-DNA adduct levels (Blankenship *et al.*, 1997; Sugiyama *et al.*, 1991). However, Shi *et al.* (1991) reported that ascorbate increased DNA double strand breaks when co-exposed with Cr (VI). More recently, it was shown that ascorbate increased clonogenic lethality and apoptosis of Cr (VI) in IMR90 human lung fibroblast and H460 epithelia cells (Reynolds and Zhitkovich, 2007). Carlisle showed that ascorbate has no effect on chromate (VI) induced apoptosis or clonogenic survival in HLF cells. In the present study, both activation and deactivation of lead chromate toxicity were observed. Treatment of cells with 1.62µg/ml of $PbCrO_4$ and ≤ 12.5 µM ascorbate or ≤ 2 µM dehydroascorbate reduced the survival fraction of $PbCrO_4$ from 0.70 to about 0.40, while simultaneous treatment of the cells with $PbCrO_4$ and 15-20 µM ascorbate or 3-4 µM dehydroascorbate reversed it back to about 0.70 (Figure 4.3 and 4.4). The results may have provided explanation for the proxidant and antioxidant activities of ascorbate in the toxicity chromate (VI) observed in aforementioned studies and thus indicating a paradoxical role for ascorbate and dehydroascorbate in the toxicity of chromate (VI) compounds. The data also suggest that ascorbate and dehydroascorbate availability could be very important in determining the toxicity or otherwise of hexavalent

chromate. Indeed, the result of this study is in agreement with the work of Poljsak *et al.* (2005), who showed in- situ using electron spin resonance (ESR) that the ratio of ascorbate: chromate (VI) could also affect the overall action of ascorbate. A low ratio of asc: Cr (VI) [low asc, high Cr(VI)] promotes the production of the transient and toxic chromate (V), which gives an overall pro-oxidative activity (Poljsak, *et al*., 2005). Conversely a high ratio of ascorbate: Cr (VI) promotes the production of the relatively less toxic chromate (IV) that may confer anti-oxidation (Poljsak *et al*., 2005). In addition, the antioxidant activities of ascorbate or dehydroascorbate observed in this study may be a result of extracellular reduction of chromate (VI) to (III). Chromate (III) is almost impervious to the cell membrane and thus its intracellular uptake is limited.

The greater surface area of the small particles of the chromate (VI) compounds especially for lead chromate may be responsible for the increased cytotoxicity observed in treated cells (Figure 4.9-11). The greater surface would facilate dissolution and increased the number of phagocytosed particles, which in turn may increase cytotoxicity. Increased phagotosis of nickel compounds have been correlated with cytotoxicity (Miura *et al*, 1989).

Light microscopy and scanning electron microscopy (SEM) evaluations of hexavalent chromate treated cells treated cells revealed that chromate compounds were internalized and the integrity of the cell membrane was compromised (Figure 4.12- 4.16). The relative increase in particle internalization with time, suggest that cytotoxicity of the hexavalent compounds is dependent on exposure time. Chromate (VI) treatment resulted in vacuolation, cellular flattening, membrane blebbing and cell shortening, which may be related to loss of cell to cell contact or condensation indicating possible necrosis or apoptosis (Evan *et al.*, 1995; Evan et *al.*, 1992; Mills *et al.*, 1992; Ghadially, 1988). Furthermore, the results obtained in this study (Figure 4.12E and 4.13) extend previous observation on hexavalent chromate toxicity in CH310T½ cells to include anucleation. Although the three chromate compounds induced anucleation of CH310T½ cells, the highest induction was found with $BaCrO_4$ (Figure 4.13). Anucleation could be beneficial in the treatment of cancer. Cancer cells may be induced to undergo enucleation. The advantage of this process is that the cells lose their nucleus and hence the emergence of resistance is very unlikely (Guddati,

2012). Anucleation may be particularly effective against cancer stem cells which may be resistant to conventional modes of therapy (Guddati, 2012).

The transmission electron microscopy (TEM) confirmed that the hexavalent chromate compounds were internalized by phagocytotosis (Figure 4.17). The detection of Cr and Pb ions in the cytoplasm and nucleus of treated cells (Figure 4.19) suggested that ions were released by either intracellular or extracellular dissolution before being transferred to the sub cellular structure. Similar result was obtained in HSAE cells exposed to $PbCrO_4$ (Singh *et al.*, 1999). In contrast, previous studies using Chinese hamster ovary (CHO) and WTHBF-6 indicated that lead chromate particles do not dissolve inside cells (Xie *et al.*, 2004; Wise *et al.*, 1993; Elias *et al.*, 1989). Thus, suggesting that the mode of internalization of chromate particles may be cell type specific.

The TEM also showed that the internalization of the chromate (VI) compounds affects cellular ultrastructures (Fig. 4.21-4.28 and Tables 4.4-4.7). Cytoplasmic injury, including distortion of organelles such as lysosome and endoplasmic recticulum, mitochondria, focal degeneration and disruption of cytoskeletal organization were observed following treatment with $PbCrO_4$, $BaCrO_4$ and $SrCrO_4$ (Figure 4.21 -4.28). Damage to the nucleus such as nuclear condensation and dilation of the nuclear envelope observed in this study may stall the reproductive machinery of the treated cells and this may ultimately lead to terminal growth and cell death. Injury to the mitochondria may lead to dysregulation of mitochondria controlled functions, such as apoptosis and energy metabolism. Damage to the endoplasmic recticulum including dialation of the endoplasmic reticulum observed in this study may be indicative of E.R stress. Similar observations were made in $CD34^+$ HSPC cultures obtained from umbilical cord blood that were exposed for 48 h to 0.1µ M- 10 µ M potassium chromate (Gioacchino *et al.*, 2008).

The increase in the number lysosome observed in the chromate treated cells (Figure 4.24) may be indicative of the necessity to get rid of the chromate and other toxic substances generated during metabolism in the cells. In addition, the distortion of lysosomal morphology observed in the treated cells may suggest lysosomal dysfunction. This has a profound impact on cell homeostasis, resulting in pathological conditions (Boya *et al.*, 2012). Specifically, damage to the

lysosomal membrane results in the release of its contents into the cytoplasm and thus, inducing indiscriminate degradation of cellular components (Boya *et al.*, 2012). Additionally, massive lysosomal breakdown may induce cytosolic acidification, which in turn can induce cell death by necrosis (Boya *et al.*, 2012).

The induction of lipid droplet observed in the chromate treated cells in this study (Figure 4.25) may be an indication of lipotoxicity in the cells exposed to the chromate compounds. Lipid bodies, consist of a highly hydrophobic core of neutral lipids, mainly triacylglycerols and/or steryl esters, surrounded by a phospholipid monolayer. Lipid droplets also bioaccumulate free fatty acids. Free fatty acids are toxic to the cell because of their protonophoric action(Wojtczak and Schonfeld, 1993) and proapoptotic effect (Listenberger *et al.*, 2003) In contrast, Listenberger *et al.* (2003) showed that that the accumulation of lipd droplet, initially formed by the addition of free fatty acids, can protect against apoptotic cell death by channelling free fatty acids into triglyceride pools. More recently, Barba *et al* (2009) showed *that* lipid dropletprotected against cell death secondary to simulated ischaemia reperfusion by sequestering excess free fatty acids and free Ca^{2+}

The induction of lamellar bodies myelin figures (Figure 4.27) in the chromate treated cells may be a result of phospholipidosis in the treated cells. Lamellar bodies with concentric myelin-like structures are morphological markers of abnormal phospholipid metabolism, phospholipidosis (Ryrfeldt, 2000). Phospholipidosis is characterised by accumulation of the polar phospholipids in cells owing to abnormal lipid metabolism. Abnormalities of phospholipid metabolism may lead to myelin body accumulation, and the whorled membranes represent damaged foci (Song *et al.*, 2011). Accumulation of myelin body could disrupt cell function. Several reports have demonstrated a link between cell damage and phospholipidosis (McCarthy *et al.*, 2004; Mouallem *et al.*, 2007). Thus, the induction of myelin figures after treatment with chromate (VI) compounds in this study may be an indication of toxicity. In addition, phospholipidosis has also been linked to mitochondrial swelling, release of lactate dehydrogenase, activation of caspase-2 and -3, induction of apoptosis, development of necrosis and inflammation (Nonoyama and Fukuda, 2008).

The increase in hypodiploid cells (Sub G0) and corresponding decrease in the population of cell in the G0/G1 cells in the treated cells is an indication of induction of cell death on exposure to the chromate compounds (Table 4.11- 4.13). In particular, the sub-G0 fraction represents cells with fragmented chromosomes and thus usually used as a measure of apoptosis. Cr(VI) compounds have been suggested to induce mitochondrial mediated and caspase-dependent apoptosis in skin epidermal cells through activation of p53 protein that are essentially mediated by reactive oxidants generated by the compounds (Son *et al.,* 2011). The lack of G0/G1 arrest in chromate treated cells in this study is in contrast to the observation Lou *et al*., 2013, that found an increase in G0 phase in human B lymphoblastoid and human lung A549 cells after exposure to lead chromate for 24 hours. Therefore, the effect of chromate (VI) treatment on the activation of cell cycle arrest may be dependent on exposure time and tissue type.The observed increase in the population of G2/M cells in lead chromate treated cell may be an indication of G2/ M arrest. In addition to the G2/M phase arrest , treatment of CH310T½ cells with 1.0 µg/ml of lead chromate induced S-phase arrest, whereas exposure to the higher concentrations of lead chromate stalled DNA synthesis as evidenced by the decreased in the population of S-phase cells after exposure to 2.5 and 4.0 µg/ml lead chromate. Holmes *et al*. (2010) and Xie *et al.* (2009) observed similar decrease in percentage S-phase cells after 24h exposure of human lung fibroblast, WTHBF-6 cells to a similar highly insoluble hexavalent chromate, zinc chromate. However unlike lead chromate, 48 h exposure of CH310T½ cells to barium chromate and strontium chromate in this study prevented cells from entering the G2 phase of the cell cycle, resulting in the accumulation of cells in S phase. In addition, cells were also stalled at G2/M phase of the cell cycle. The arrest of the cells in the S-phase by barium chromate and strontium chromate observed in this study is similar to that observed after $K_2Cr_2O_7$ treatment. For instance, Bakke *et a*l., 1984 demonstrated a prolong S-phase arrest in NHIK 3025 cells treated with between 1–2 µM $K_2Cr_2O_7$. The G2/M and / or S-phase arrest can be caused by DNA damage in the treated cells. Many studies have revealed that exposure to chromate (VI) compounds result in both DNA single or double-strand breaks that are generated in the S and / or G2 phase of the cell cycle (Alderton *et al*., 2004; Bartel *et al*., 2005; Cliby *et al*., 1998). ATM (ataxia telangiectasia mutated) protein, ATR (ataxia telangiectasia mutated- and Rad3-related), Chk2 (Chk is checkpoint kinase) and MRE11 are activated in response to DNA double and single strand breaks (Holmes *et al.,* 2010). Activation of these proteins is thought to be

responsible for G2/M and S arrest observed after Cr (VI) exposure (Holmes *et al.,* 2010). DNA damage usually triggers an arrest in either S or G2 phases of the cell cycle in order to allow cells to repair their genomic damage. Generally, cell arrest in the G2 phase because they are unable to transcribe damaged DNA and make mRNA essential for passage into mitosis. Cells that are successfully repaired progress through the cell cycle. However, if repair is unsuccessful, cell growth may be terminated and consequently, cell death results due to inability to adequately recover transcription. In addition, prolonged arrest usually uncouples cell cycle progression from centrosome duplication. This results in generation of cells with aberrant centrosome numbers (Urbano *et al*., 2008; Xie *et al*, 2005; Doxsey *et al*., 2005; Brito and Rieder, 2006; Ganem *et al.,* 2007). Cells with aberrant centrosome numbers are potentially harmful and may suffer mitotic catastrophe, which may result in the development of malignant aneuploid descendants (Doxsey *et al*., 2005; Brito and Rieder, 2006, Ganem *et al*., 2007). In deed Holmes *et al.* (2010) and others showed that zinc chromate, arsenic and methyl mercury induce centrosome amplification and numerical chromosomal instability (CIN) after G2/M arrest (Holmes *et al.,* 2010; Wise *et al.,* 2006 Ochi, 2002; Taylor *et al.,* 2008). Therefore, suggesting that G2/M and / or S- phase arrest and subsequent centrosome amplification may not only be a common mechanism of chromate carcinogenesis, but may be very important for the induction of cancers by other heavy metals. It is also possible that the observed G2/M arrest in this study might have occurred due of disturbance of mitotic spindle structure. For example Wise *et al.* (2006) demonstrated that lead chromate induced aberrant mitotic figures in WHTBF-6 cells. Holy (2002) in his study of curcumin-induced G2-M arrest in MCF-7 cells also showed that G2-M arrest was associated with problems in mitotic spindle structure, including assembly of aberrant monopolar mitotic spindles that led to impaired segregation of chromosomes and likely represented mitotic arrest

Induction of apoptosis by hexavalent chromate can be caspase dependent or independent depending on cell type. Rudolf and Červinka (2006) reported a caspase 3 dependent activation in human diploid dermal fibroblast exposed to potassium chromate. Similarly, Xiao *et al* (2012) showed that hexavalent chromate targeted mitochondrial respiratory chain complex I to induce reactive oxygen species-dependent caspase-3 activation in L-02 hepatocytes. In addition, mitochondrial-mediated and caspase-dependent apoptosis via reactive oxygen species-mediated p53 activation was also observed in JB6 Cl41 cells treated with hexavalent chromate (Son *et al.,*

2010). However, Hayashi *et al.* (2004) demonstrated a caspase3 independent apoptotic pathway in U937 cell exposed to chromate (VI) compounds. In the present studies, as seen in Figure 4.32-35 , exposure of CH310T½ cells to the hexavalent compounds induced apoptosis via the activation of caspase-3/7. Chromate (VI) caspase dependent cell death is associated with disturbance of energy metabolism and decreased ATP production (Xiao *et al.,* 2012). Thus, simultaneous reduction in viability of cells exposed to the three chromate (VI) compounds in this experiment may be a consequence of interruption of energy metabolism in treated cells. Moreover, the reduction in viability and increased cytotoxicity observed in treated cells is in concert with the clonogeinc assay result, which showed that exposure of cells to hexavalent chromate led to retarded growth and / or cell death in exposed cells.

Although apoptosis is thought to be the main mode of cell death in hexavalent chromate exposed cells, several researchers have noted the existence of some necrotic cells in addition to apoptotic cells in chromate treated cell culture (Bagchi *et al.*, 2001; Singh *et al*., 1999; Blankenship *et al.*, 1997). However, the degree induction of necrosis was not quantified. Therefore in this thesis, hexavalent chromate induced cell death was characterized quantatively in CH310T½ cells by double staining treated cells with acridine and propidium iodide and observing with EVOS fluorescent microscope. Data obtained here in Figure 4.35-4.37 was in agreement with the phase contrast and electron microscopy that showed that the mode of cell death in treated cells was mixed albeit there were some variations in the degree of induction of apoptosis and necrosis amongst the three studied chromate (VI) compounds. While cells die predominantly by apoptosis at all the tested concentration of $PbCrO_4$ (Figure 4.35), the mode of death in cell treated with $BaCrO_4$ and $SrCrO_4$ was predominantly by apoptosis at lower concentrations and necrosis at higher concentration (Figure 4.36-4.37). Simultaneous induction of apoptosis and necrosis has also been observed in Molt-4 cells treated with zinc (Hamatake, 2000). This emphasizes the need to study each hexavalent chromate compound individually, because the carcinogenicity of the chromate may be dependent on the nature of cell death. The observation that the mode of cell death was predominantly apoptotic in $PbCrO_4$ cells was similar to that observed by Singh *et al.* (1999) and Blankenship *et al.* (1997) in HSAE and CHO cells respectively. The induction of apoptosis or necrosis or even both may also be cell line specific and time dependent. For instance, it was reported that exposure of K562 cells to 12. 5µmol of Na_2CrO_4 induced apoptosis,

while it had no effect on HPBM cells (Bagchi *et al.*, 2001). In the same study, an approximately 2.2 folds increase in apoptosis was observed in HPBM cells exposed to the same concentration of Na_2CrO_4 for 48 hours, but caused necrosis in K562 cells under the same condition.

The chromate (VI) compounds induced autophagy was evidenced by the formation GFP-LC3 punta and autophagic vacuoles in the treated cells (Figure 4.38-41 and Table 4.11-13). Induction of autophagy could either be a protective mechanism to enhance cell survival or it may lead to cell death. Autophagy marks damage organelles and proteins for removal and process it into nutrient needed for the survival of cells. Autophagy induction seen in response to the hexavalent chromate compounds may represent a survival mechanism activated to counteract the deleterious effects of endogenous metabolic stress induced by the chromate compounds. However, excessive autophagy may result in cell death. "Self-eating" by autophagy can potentially lead to cell death when cytoplasmic material and cellular organelles are consumed beyond a critical- cell-survival point (Chen and Karantza-Wadsworth, 2009). This raises the possibility that autophagy may also contribute to cytotoxicity. Indeed, it has been demonstrated that down regulation of autophagy resulted in prolong cell survival (Samara *et al.*, 2008; Shimizu *et al.*, 2004; Yu *et al.*,2004). However, several other researchers have shown that inhibition of autophagy under cellular stress conditions reduces cell viability (Degenhardt *et al.*, 2006; Lum *et al.*,2003; Melendez *et al.*,2003) and changes the mode of cell death to either apoptosis (Abedin *et al.*,2007; Boya *et al.*, 2005) or necrosis (Karantza-Wadsworth *et al.*,2007; Degenhardt *et al.*,2006).

The Cr (VI) compounds tested in this study at low concentration (1.0 µg/ml for $PbCrO_4$ and $BaCrO_4$ as well as 0.25 µg/ml for $SrCrO_4$) caused loss of adhesions and induction of actin stress fibres in CH310T½ cells (Figure 4.42). In addition, there was disruption of the F-actin stress fibres coupled with cellular retraction, cell shrinkage and blebbing (Figure 4.42). These effects were more pronounced at higher concentration and increased exposure time (Figure 4.43). These results clearly confirmed and add to other experimental studies performed on dermal fibroblast, kidney epithelial and rat hepatocytes treated with potassium chromate (Rudolf *et al.*, 2005; Gunaratnam and Grant 2004; Dartsch *et al.*, 1998). It has been suggested that Cr (VI) interacts with actin by inhibiting its polymerization (Rudolf *et al.*, 2005). Cr (VI) compounds have also been reported to inhibit protein synthesis in the cytoskeleton, interact with thiol groups and form

complexes with cytoskeletal protein (Rudolp *et al*, 2005; Gunaratnam and Grant, 2002). The disruption of actin filament has reaching effect on the cell. Actin fibres are important for the movement of motor-based organelle and membrane trafficking. Therefore, the disruption of the actin network may contribute to the assorted changes in membrane dynamics and cellular morphology as well as signal transduction. These alterations may eventually lead to cell death or enhanced survival. Ailenberg and Silverman (2003) reported that cytochalsin D disruption of mouse mesangial cells (MMC) caused it to undergo apoptosis, but it promoted cell survival in NIH3T3 cells. Both populations of dying and apparently healthy cells, but with folded morphology were observed in the study. The folded cells may eventually become the transformed cell population in the chromate treated cells. A change in cell shape is pivotal for carcinogenesis. In addition, disruption of the actin filament may also be a consequence of ATP depletion in treated cells (Raman and Atkinson, 1999). ATP depletion channels the cell towards the death pathway. Thus, the reduction in relative fluorescence observed in treated cells (Figure 4.43-6) may be a result of induction of cell death in cells exposed to the hexavalent chromate compounds.

Particulate chromate compounds have been shown to induce neoplastic transformation in rodent cells (Holmes *et al.*, 2008; Costa, 1997) and $PbCrO_4$ is a model for studying the toxicity and carcinogenicity of chromate (VI) compound. The ability of lead chromate to induce transformation has been described in CH310T½ cells (Patierno, 1988). However, the degree of induction was low. Similar to that observation, a low yield of transformation foci in cells treated with the large $PbCrO_4$ particles in this study when compared with 3-methyl cholantrene, (MCA) which serves as the positive control (Table 4.14). Although, Xie *et al.* (2004) posited that lead chromate has higher yield of transformation foci in human epithelial lung BEP2D cells, the study lacks positive control which makes it difficult to make relevant comparison and conclusion. In addition, obvious differences in experimental procedures may also account for the differences in results. For instance, while a total of 500,000 cells were seeded in the work of Xie *et al.* (2004), only 2000 cells were seeded in this study as prescribed by Nesnow *et al.* (1980). The cells used in this study were only cultured for 6 weeks, while Xie *et al.* (2004) cultured the cells until the appearance of the appearance of foci. Furthermore, cells were exposed to $PbCrO_4$ for five days in the procedure adopted by Xie *et al.* (2004), but were only cultured in $PbCrO_4$ for 2 day in this

study. The reduction of the particle size of PbCrO4 further weakened the *in vitro* transformation ability of $PbCrO_4$ under these present experimental conditions. The increase in the number of $PbCrO_4$ particles available for phagocytic uptake may have increased the cytotoxicity, which may have been responsible for the low yield of transformation observed in cell treated with the smaller particles of lead chromate.

The 4.4- 6.6 folds dose dependent yield of foci observed in the cells treated with the smaller particles of $BaCrO_4$ as compared with the 2.2folds yield of foci observed at the highest concentration of $BaCrO_4$ with large particles used in this study (Table 4.15) suggest that smaller particles of $BaCrO_4$ may be more potent in transformation of CH310T½ cells and invariably, inducing cancer in exposed individuals. Generally, a better yield of transformation was achieved with $BaCrO_4$ and $SrCrO_4$ when compared with that of $PbCrO_4$. This suggests that $BaCrO_4$ and $SrCrO_4$ are more potent in transforming CH310T½ cells under this experimental condition Barium chromate has been shown to be more genotoxic than lead chromate in WTHBF-6, human lung cells and thus may account for the higher potency of barium chromate in inducing transformation of CH310T½ cells observed in this study. However, $PbCrO_4$ was shown to be more active than $BaCrO_4$ in inducing transformation of Syrian hamster embryo (SHE) cells (Elias *et al.*, 1989). This may imply that the cell transforming ability of hexavalent chromate compounds may be cell or tissue specific. Overall, the yield of transformation observed for the different forms of the hexavalent chromate compounds was at least 5 times less than that of MCA. Indicating that the chromate compounds are not as strong as MCA in inducing morphological transformation in CH310 T ½ cells. This is inconsistent with epidemiological and *in vivo* carcinogenesis investigations reporting that Cr (VI) compounds are strong carcinogens and mutagens (Nickens *et al.*, 2010). There could be many unknown factors that may justify this phenomenon.

Classifying the gene alterations and analyzing the gene expression patterns of cell death genes would give insight into the molecular mechanisms associated with hexavalent chromate induced cell death. It would also allow the identification of clinically relevant genes that would aid in the development of therapeutics against chromate (VI) related toxicity such as cancer. In this study, using RT^2 PCR cell death profiler array, a number of differentially expressed apoptosis,

autophagy and necrosis related genes associated with hexavalent -mediated toxicity and cell transformation were identified. The induction of apoptosis was evidence by at least 4 folds increase in the expression of 14 proapoptotic genes 48 hours after exposure to $PbCrO_4$ and $BaCrO_4$. The up regulated proapoptic genes include Bax, Bcl2l11, Casp9, Casp3, Casp7, Gadd45a, Atp6v1g2, Bmf Cyld, Nol3, Sycp2, Tnfrsf1a , Dffa and Spata2.

The increase in Bax observed in this study is similar to that observed in rat granulosa cells exposed to $K_2Cr_2O_4$. Translocation of Bax proteins from cytoplasm into mitochondria is essential for the execution of apoptotic cell death in response to oxidative stress and DNA damage (Youle and Strasser, 2008; Ramadan *et al.*, 2005; Melino *et al.*, 2004). Specfically, translocation of BAX protein from the cytosol to the mitochondria leads to release of cytochrome c from the mitochondria into the cytosol and thus, initiate apoptosis. Bax in conjunction with other pro apoptotic proteins may not only promote apoptosis by cleaving and activating caspases, but can also initiate caspase-independent death via channel-forming activity, which could promote the mitochondrial permeability transition or puncture the mitochondrial outer membrane. The up regulation of Casp9, Casp3 and Casp7 observed in this experiment is a confirmation of the earlier observation that chromate (VI) induced apoptosis in CH310T½ cells is caspase dependent. The activation of caspase may be a response to the up regulated Bax in treated cells. Caspases are crucial component of the apoptotic process (Fan *et al.*, 2005). The release of cytochrome *c* from the mitochondria to the cytosol allows the formation of the apoptosome which, in turn, activates effector caspases, that degrades many components of the cells during apoptosis. DNA fragmentation factor A (DFFA) is the substrate for caspase-3 and triggers DNA fragmentation during apoptosis. Therefore, up-regulation of DFFA in this study may be a consequence of caspase-3 activation. DFFA is cleaved by caspase-3 and this in turn triggers both DNA fragmentation and chromatin condensation during apoptosis. Bmf is a pro-apoptotic BH3-only Bcl2 family member that is associated with the actin cytoskeleton-based myosin V motor complex through its interaction with dynein light chain under normal condition (Puthalakath *et al.*, 2001). However, during certain cellular stresses, such as loss of extracellular matrix adhesion (anoikis) or energy crisis or exposure to actin depolymerization drugs, Bmf moves to mitochondria, where it can promote cell death via Bax activation , Bcl-2 inactivation and mitochondrial dysfunction (Moran *et al*, 2013; Cory *et al.*, 2003; Puthalakath *et al.*, 2001). Thus,

corroborating earlier observation that hexavalent chromate compounds caused actin disruption in CH310T½cells and this may responsible the up regulation of Bmf observed in the studies.

The upregulation of the G2/M phase cell cycle arrest check point, GADD 45α (the growth arrest- and damage-inducible protein 45α), in the chromate treated cells may be a response to the DNA damage or oxidation or hypoxia o r other cellular stress condition. It is common knowledge that different types of stress such as DNA damage, oxidation and hypoxia induce cell cycle arrest in order to allow time for DNA repair and thus protecting the organism from the deleterious consequences of mutation. More importantly, the induction of GADD 45α in this present study is a confirmation of the G2/M cell arrest earlier observed in the cells exposed to the three chromate compounds. In addition to G2/M cell arrest, induction of GADD 45α may also be a signaling response resulting in DNA repair, cell survival and senescence, or apoptosis (Creteu, 2009). Up-regulation of GADD 45α and caspase 3 has been reported to cause BJhTERT cells exposed to hexavalent chromate to undergo apoptosis. The up regulation of GADD 45α in this study gives credence to the genotoxic nature of hexavalent chromate compounds. Gadd45 family members are rapidly induced by genotoxic stress agents (Papathanasiou *et al.*, 1989; Fornace *et al.*, 1991; Vairapandi *et al.*, 2002). Also up regulated in the treated cell is Tnfrsf1a. Tnfrsf1a belongs to the tumor necrosis factor receptor superfamily and are pro-apoptotic. TNFR members play diverse biological roles including apoptotic stress response (Locksley *et al.*, 2001; Liu, 2005). In certain cell types, Tnfrst1a mediates cell death, whereas Tnfrst1b acts to enhance TNFR1-mediated cell death (Chan *et al.*, 2000).

Akt1, Casp2 , Xiap and Tnfrsf11b, which are all anti apoptotic genes were also up regulated by at least 4folds, while Bcl2 and Traf 2 were down regulated by about 240 and 5 folds respectively in $PbCrO_4$ and $BaCrO_4$ treated cells. Up regulation of the anti apoptotic in the treated cells may be a reaction to counter the induction of apoptosis caused by the chromate compounds. Under starvation and stress condition in the cell, XIAP proteins is synthesized in order to inhibit both initiator and effector caspase activity (Hoicik *et al.*, 2001). Additionally, increased Akt activity has been associated with in vivo protection against oxidant and mechanical-induced lung injury, tissue protection and repair (Lai *et al.*, 2007; Ray *et al.*, 2003; Lu *et al.*, 2001). Similarly, the activation of Akt by phosphorylation in lung airway epithelium of mouse exposed to a single dose of ZnCrO4 has been shown to be an early response to

genotoxicity (Beaver *et al*, 2009). The down regulation of Bcl-2 and Traf-2 may render the cells susceptible to apoptosis since the suppression of BCl-2 expression has been suggested to accelerate cell death in chromate transformed BEAS cells (Medan *et al*, 2012). In summary, results of the present study suggest that the hexavalent chromate compounds induced apoptosis is mediated via the decreased expression of antiapoptotic and cell survival proteins such as Bcl-2, translocation of BAX proteins from cytosol to the mitochondria, increased mitochondrial membrane permeability, facilitated the release of cytochrome *c*, and activation caspase-3 and 7.

Thirteen (13) autophagy related genes including Atg3, Bcl2, Akt1 Atg16l1, Bax ,Casp3 ,Ctsb, Htt, Irgm1 , Map1lc3a, Nfkb1, Pik3c3 and Snca were up regulated in $PbCrO_4$ and $BaCrO_4$ while Atg12, Atg5, Bcl2, Fas, Igf1 were down regulated in cells treated with the two chromate salts. The up regulation of autophagy related genes in cells treated with the chromate compounds may be a response to metabolic stress or death signal. Cells increased the levels of autophagy to enhance cell survival during stress caused by nutrient and energy provision through lysosomal degradation of cytoplasmic components (Lebovitz *et al.*, 2012). In contrast, elevation of autophagy related genes may be a death signal. 11 necrosis genes including Atp6v1g2, Bmf , Cyld, Sycp2, Tnfrsf1a , Sycp 2, Galnt 5, Cdc 103, Hspbap1, Foxi1 and Spata2 were up regulated in cells treated with the two chromate salts, This indicate that necrosis in addition to apoptosis and autophagy may be involved in the cytotoxicity of the hexavalent chromate compounds. Generally, the result of the cell death gene profiling was in tandem with the earlier microscopic observation that the nature of cell death in the chromate (VI) treated cells was mixed. i.e apoptosis, autophagy and necrosis.

To develop cancer-specific therapeutic approaches, it is important to identify the molecular targets in the cell death pathway that are differentially regulated in normal and tumor cells. For instance, it is well known that a balance of pro- and anti-apoptotic factors determines whether a cell survives or undergoes apoptosis (Igney and Krammer, 2002; Yang et al., 2003). In tumor cells apoptosis can be induced either by activation of molecules upstream of apoptosis signaling or by inhibition of antiapoptotic factors (Mesri *et al*., 2001; Reed, 2001). Similarly, inflammation and unscheduled necrotic cell death are associated with adult cancer formation (Vakkila and Lotze, 2004). Furthermore, autophagy has dual roles in cancer, acting as both a tumor suppressor

by preventing the accumulation of damaged proteins and organelles and as a mechanism of cell survival that can promote the growth of established tumors. Included in this work therefore, is a study to unravel differential expression of cell death genes between lead chromate transformed CH310 T½ cells otherwise named $PbCr_3$ against the normal CH3 10T½. Although there were up regulation of some apoptosis and necrosis related genes such as GADD 45 and Spata 2, key apoptotic genes such as Bax, Casp7, Cas 9,Nol 3 and Sycp2 were all down regulated in $PbCr_3$ cells . Simultaneously, there was at least 10 folds increase in the expression of six anti apoptotic genes including Bcl 2, Birc 3, Igf1, Mcl1, Tnfrsf 11b and Traf2. Many of these genes have been shown to be up regulated in many human cancers and have been reported to confer drug resistance on tumour cells. For example, the up regulation of BCl-2 has been shown to inhibit cell death in cancer cells (Korsmyer, 1999). IGF1R activation protects cells from a variety of apoptosis-inducing agents, including osmotic stress, hypoxia and anti-cancer drugs (Dunn *et al*., 1997, Peretz *et al.,* 2002). IGF1R is frequently overexpressed in tumours, including melanomas, cancers of the colon, pancreas, prostate and kidney (Bohula *et al.,* 2003; Hellawell *et al.,* 2002). Mcl-1 expression is required to maintain viability, promote cell differentiation and oppose proapoptotic stimuli. Mcl-1 is known to promote survival of multiple myeloma and is a target for future therapy of ovarian, prostate, and gastric carcinoma; chronic lymphoid leukemia; sarcoma; cholangiocarcinoma; and multiple myeloma (Gouill *et al,* 2004*).* Thus, down regulation of major apoptosis and necrosis executing genes and up regulation of antiapoptotic genes in this study may be a mechanism by which the transformed cell, PbCr3 continue to grow in cell culture without recourse to death control signal.

In addition, a total of 15 genes including App, Atg12, Atg16l1, Atg3, Atg5, Atg7, Bcl2, Becn1, Casp3, Ctsb, Fas, Gaa, Irgm1, Mapk8 and Ulk1 that participate in autophagy were up regulated in the transformed cells PbCr3, while Akt was down regulated .Up regulation of these genes suggest that continued survival of chromate transformed cells may have driven by autophagy in addition to lack of response to cell death signals. Tumour cells increased the levels of autophagy to buoy cell survival via nutrient and energy provision through lysosomal degradation of cytoplasmic components (Lebovitz *et al.,* 2012). The rise in the expression of autophagy related genes in the transformed cells may also have occurred as a reaction to the increasing metabolic/ energy demand of the transformed $PbCr_3$ cells. Tumor cells activate autophagy in response to cellular stress and /or increased metabolic demands in rapidly proliferating cell (Yang, 2011).

Moreover, several studies have reported that autophagy may be a survival mechanism for tumor cells (Lum *et al.*, 2005; Degenhardt *et al.*, 2006; Amaravadi *et al.*, 2007; Karantza-Wadsworth *et al.*, 2007; Mathew *et al.*, 2007). Like the antiapoptotic genes, many of the over expressed autophagic genes have been implicated in the etiology and progression of several cancers.

Increased Beclin-1 expression has been reported to be a hallmark of autophagy upregulation in advanced tumors and alteration Beclin-1 expression has recently been proposed as a tumor marker and prognostic factor in various malignancies (Lebovitz *et al.*, 2012; Koukourakis *et al.*, 2012). Increased expression of Atg 7 in human MDA-MB-231 cells exposed to Mitoquinone has been shown to confer survival through autophagy activation, while apoptosis was increased in ATG7-deficient cells (Gonzalez *et al.*, 2014). In addition, ATG7 was reported to play an important role in chemoresistance and it has been shown to affect prognosis of breast cancer (Ahn *et al.*, 2013). The serine/threonine kinase UNC-51-like kinase 1 (ULK1) plays an essential role in autophagosome formation and its up-regulation have been shown to be a novel biomarker of poor prognosis in patients with esophageal squamous cell carcinoma (Jiang *et al.*, 2011). Up regulation of MAPK8 gene in this study may be a mechanism by which lead chromate transformed cells protect against TNFSF10/TRAIL-induced apoptosis. Activation MAPK8 activation pathway through TRAF2 and RIPK1 have been shown to block apoptosis in cell lines derived from lung, bladder and prostate tumors (He *et al.*, 2012).

Taken together, down regulation of proapoptotic and necrotic genes as well as over expression of antiapoptotic and autophagy related genes in the lead chromate transformed cells may be a plausible mechanism employed by hexavalent chromate compounds to transform cells and induce cancer. Therefore chemotherapy targeted against these altered genes may be useful in the treatment of hexavalent chromate related tumours.

The results of the *in vivo* geneotoxicity studies showed a ($p < 0.05$) increase in the formation of micronucleated polychromatic erythrocytes (mPCE) in mice injected with potassium dichromate ($K_2Cr_2O_7$) or sodium arsenite (SA) when compared with the negative control. This is in accord with earlier observations (Balakumar *et al.*, 2010; Odunola *et al.*, 2008*; Balansky et al.*, 2000). The observed increase in mPCEs may be an evidence of the clastogenic and carcinogenic potential of potassium dichromate, since a strong association has been established between such increase and the development of cancer in different tissues (Mitelman, 1994). Besides, chromate

(VI) compounds have been reported to cause DNA damage, DNA strand cross-links, DNA-protein cross-links, sister chromatid exchanges and chromosomal aberrations *in vivo* (Luca, 2007). A further increase in mPCEs formation was also observed in the group co-exposed to $K_2Cr_2O_7$ and SA. This suggests that clastogenicity and carcinogenicity of $K_2Cr_2O_7$ could be worsened by simultaneous exposure with SA. Conversely, pretreatment with the methanol extract of RV significantly ($p < 0.05$) reduce the degree mPCEs in the test animal exposed to $K_2Cr_2O_7$ alone and in combination with SA. This is suggestive of beneficial influence of RV against the clastogenicity and carcinogenicity of both metals. The antioxidant and anti-carcinogenic compounds present in the extract of RV may be responsible for the reduced incidence of micronuclei observed in the test mice. ß-carboline alkaloid, alstonine found in the root bark extract of RV has been reported to reduce tumor cell growth in mice inoculated with YC8 lymphoma cells or Ehrlich ascitice cells (Beljanski and Beljanski, 1986). Similarly, it was recently shown that extract of RV effectively inhibit cell growth in the human prostate cancer cell line, LNCaP, in both cell culture and *in vivo* tumor xenograft experimental systems by suppressing growth and cell cycle progression (Bemis *et al.*, 2006).

Alanine aminotransferase (ALT) and Aspartate aminotransferase (AST) are among the most sensitive test employed in the detection of acute liver damage. The result showed that the activity of ALT and AST were greatly increased in the serum of mice exposed to $K_2Cr_2O_7$ or SA alone. Additional increase in the activities of both enzymese was equally encountered in mice co-exposed to both $K_2Cr_2O_7$ and SA. This increase could be as a result of acute liver damaged induced by both $K_2Cr_2O_7$ and SA. The elevation of ALT and AST may be due to alteration in the permeability of liver membrane, which may lead to the leakage of these enzymes from the liver cytosol into the blood stream. Disturbance in the biosynthesis of these enzymes could also account for the rise. In contrast, pretreatment with RV resulted in reduced ALT and AST activities in the group exposed to RV before treatment with the individual or both metals. This reduction suggests that the extract may have hepatoprotective effect against hepatotoxicity induced by the two heavy metals.

The $K_2Cr_2O_7$ and SA-induced lipid peroxidation in this study were demonstrated by the increased MDA levels in mice exposed to the two metals salts when compared to the negative control. This was further complicated in the combined exposure group. Previous studies have found an

association between MDA elevation and exposure to the metals. Bagchi *et al*., 1997 reported that rats fed Cr (VI) orally in water induced hepatic mitochondrial and microsomal lipid peroxidation, as well as enhanced excretion of urinary lipid metabolites including malondialdehyde (Bagchi *et al*., 1995). Recently, Arreola-Mendoza *et al.*, 2006 also showed that lipid peroxidation accompanied Cr (VI) administration in female wistar rats. The enhanced lipid peroxidation observed in this study may be evidence of oxidative stress in liver of mice exposed to $K_2Cr_2O_7$ or SA or combination of both metals. The induction of lipid peroxidation may be due to the formation of hydroxyl radical (HO) through a Fenton/Haber-Weiss reaction, catalysed by the metals . This radical is capable of removing a hydrogen atom from a methylene group of polyunsaturated fatty acids and thus, enhancing lipid peroxidation. This may damage the cell membrane and its physiological functions leading to disturbances in membrane integrity (Gutteridge, 1995). Interestingly, RV pretreatment exerted its inhibitory effect against $K_2Cr_2O_7$ and SA induced lipid peroxidation by the reducing MDA levels in mice pretreated with RV. This indicates that methanol extract of RV under this experimental condition, helped to ameliorate the free radical assault generated by $K_2Cr_2O_7$ and $NaAsO_2$.

Catalase (CAT) is a crucial first line antioxidant defence against oxidative stress caused by ROS. It eliminates hydrogen peroxide, which is a precursor of hydroxyl radical. Hence a decrease in the activity of this cellular antioxidants can lead to an excess availability of H_2O_2 in biological systems, which in turn generate $OH^{\cdot}$ resulting in initiation and propagation of lipid peroxidation. In this study, the activities of CAT increased significantly in the liver of mice exposed to $K_2Cr_2O_7$ and / or SA, while CAT activity decreased following pretreatment with RV. The rise in catalase activity observed in this study may support oxidative stress inducing capacity of $K_2Cr_2O_7$ and SA in biological tissue. The $K_2Cr_2O_7$ and SA intermediates generated during their metabolism were reported to increase hydrogen peroxide production (Kadiiska *et al.*, 1994). Thus, the rise in catalase activity observed in this study may be a response to counter the increased production of hydrogen peroxide in animals exposed to the metal salts. Pretreatment with RV restored the rise in catalase activity induced by $K_2Cr_2O_7$ and SA towards that of the negative control value. This may describe the scavenging properties of the extract of RV against radicals produce as a result of $K_2Cr_2O_7$ and SA ingestion.

Reduced glutathione (GSH) and it conjugating enzyme glutathione –S-transferase (GST) are essential for maintaining cellular integrity. GSH has reducing properties and participates in cellular metabolism. Both GSH and GST are therefore responsible for maintaining the redox status of cells and play important roles in quenching oxy radicals (Rose, 1988). In this study, GSH levels and GST activity decreased significantly in mice injected $K_2Cr_2O_7$ and /or SA. The apparent decrease in GSH level in the liver suggests an overproduction of reactive species which depleted GSH. It has been shown that cysteine conjugate resulting from GSH metabolism can be bioactivated in the kidney by either cysteine β-lyase or the flavin containing monoxygenase to toxic reactive species which can cause nephrotoxicity and other tissue damage (Lash, 2005). The decreased GSH could also account for the marked lipid peroxidation earlier discussed above. However, the free radical inhibiting and oxidative stress relieving ability of methanol extract of RV was evidenced by increased level of GSH in the RV pretreated mice.

CHAPTER SIX

SUMMARY AND CONCLUSION

6.1 Conclusion

In conclusion, the cytotoxicty of hexavalent chromate compounds is particle size and ascorbate dependent. The cytotoxicity might be due to actin disruption, anucleation, cell cycle arrest, micronuclei induction and induction of cell death. Co-exposure of mice to dichromate and sodium arsenite could exacerbate the cytoxicity, while methanol extract of *Rauvolfia vomitora* modulated the cytotoxicity of both potassium dichromate and sodium arsenite.

6.2 Contribution to Knowledge

(i) Toxicity of hexavalent chromate compounds may be dependent on antioxidant (Vit. C) status of the cell i.e. Vit. C deficiency may increase hexavalent chromate toxicity, while its surplus may reduce the toxicity.

(ii) The role of particle size in chromate (VI) toxicity/ carcinogenicity varies among the different hexavalent chromate compounds

(iii) Hexavalent chromate compounds can be used as anucleator. Anucleation is one of the latest promising treatments for cancer

(iv) The mechanism of hexavalent chromate toxicity and carcinogenesis may involves oxidative stress, apoptosis, autophagy, G2/M and S-phase arrest as well as micronuclei induction.

(v) Antiapoptotic and autophagy genes may be promising target for the treatment of chromate related cancers

(vi) Toxicity of hexavalent chromate compounds can be modified by simultaneous exposure with arsenite

(vii) Methanol extract of *Rauvolfia vomitora* has a promising potential in the treatment /management of chromate and arsenic toxicity.

REFERENCES

Abedin, M.J., Wang,D. , McDonnell,M.A., Lehmann,U. and Kelekar, A. 2007. Autophagy delays apoptotic death in breast cancer cells following DNA damage *Cell Death and Differentation* 14: 500–510

Adastra, K.L., Chi, M.M., Riley, J.K. and Moley, K.H. 2011. A differential autophagic response to hyperglycemia in the developing murine embryo. *Reproduction* 141: 607-615

Aebi, H. 1987. Catalase. *Methods of Enzymatic Analysis.* Bergmeyer, H.V. (Ed.), Weinheim: Verlag-Chemie. 273–282.

Agency for Toxic Substances and Disease Registry 2000. Toxicological Profile for Chromium, U.S. Department of Health andHuman Services, Washington, DC.

Ailenberg, M. and Silverman, M. 2003. Cytochalasin D disruption of actin filaments in 3T3 cells produces an anti-apoptotic response by activating gelatinase A extracellularly and initiating intracellular survival signals. *Biochimical et Biophysica Acta* 1593: 249– 258

Alberts, B., Johnson, A., Lewis, J., Raff, M., Roberts, K., Walter, P. 2002. *Molecular Biology of the Cell*, 4th Ed., New York; Garland Science. 401.

Alderton, G.K., Joenje, H., Varon, R., Borglum, A.D., Jeggo, P.A. and O'Driscoll M. 2004. Seckel syndrome exhibits cellular featuresdemonstrating defects in the ATR-signalling pathway *Human Molecular Genetics* 13: 3127–3138.

Akinwumi, K. A., Odunola O. A., Olawale O.T., Dosunmu A. N." Nwajei I.U, Osifeso O.O. and Ajayi J. O.. 2011. Carbon tetrachloride induced hepatotoxicity: protective effect of *Rauvolfia vomitora*. *Journal Scientific Research*: 53-58.

Akpanabiatu, M., Umoh, I. and Edet, E., 2009. Effects of interaction of vitamin A and *Rauwolfia vomitoria* root bark extract on marker enzymes of cardiac diseases. *Indian Journal ClinicalBiochemistry* 24 (3): 241-244.

Amaravadi, R.K., Yu, D., Lum, J.J., Bui, T., Christophorou, M.A., Evan, G.I., Thomas-

Tikhonenko, A., and Thompson, C.B. 2007. Autophagy inhibition enhances therapy-induced apoptosis in a Myc-induced model of lymphoma. *Journal Clinical Investigation* 117**:** 326–336

Amole, O.O., Yemitan, O. K., Oshikoya, K.A., 2009. Anticonvulsant activity of *Rauvolfia Vomitoria* (Afzel). *African Journal of Pharmacy and Pharmacology* 3(6): 319-322

Amole, O.O. and Onabanjo, A.O 1999. Antipyretic effect of *Rauwolfia vomitoria* in rabbits. *Nigerian Journal Natural Product and Medicine* 3: 77-78.

Anand, P., Kunnumakkara, A.B., Sundaram, C., Harikumar, K.B., Tharakan, S.T., Lai, O.S., 2008. Cancer is a preventable disease that requires major lifestyle changes. *Pharmaceutical Research* 25: 2097–116.

Andrew, M. and Wetterhahn, K.E. 1989. Chromium(VI) Toxicity: Uptake, Reduction, and DNA Damage. *International Journal Toxicology* 8 (7): 1275-1283

Annunziato, L., Amoroso, S., Pannaccione, A., Cataldi, M., Pignataro, G., D'Alessio, A., Sirabella, R., Secondo, A., Sibaud, L. and Di Renzo, G.F. 2003. Apoptosis induced in neuronal cells by oxidative stress: role played by caspases and intracellular calcium ions. *Toxicological Letters* 139: 125–133.

Apte, A. D., Tare, V. and Bose, P. 2006. Extent of oxidation of Cr (III) to Cr (VI) under various conditions pertaining to natural environment. *Journal of Hazardous Materials*. 128: 164–174.

Arakawa, H., Wu, F., Costa, M., Rom, W., and Tang, M. S. 2006. Sequence specificity of Cr(III)-DNA adduct formation in the p53 gene: NGG sequences are preferential adduct-forming sites. *Carcinogenesis* 27: 639–645.

Arends, M.J., Morris, R.G. and Wyllie, A.H. 1990. Apoptosis: the role of the endonuclease. *American Journal Pathology*. 136: 593–608.

Arreola-Mendoza, L., Melendez. E., Martin D., Namorado, M.C., Sanchez, E. and Del Razo, L.M. 2006. Alpha-tocopherol protects against the renal damage caused by potassium dichromate. *Toxicology* 218(2-3):237-46.

Ashford, T.P. and Porter, K.R. 1962. Cytoplasmic components in hepatic cell lysosomes. *Journal of Cell Biology* 12: 198– 202.

ATSDR. 2012. Toxicological profile for chromium. Atlanta, GA: U.S. Department of Health and Human Services, Public Health Service, Agency for Toxic Substances and Disease Registry.

ATSDR. 2000. Toxicological profile for chromium(final Report) NTIS Accession No PB2000-108022.Atlanta GA: Agency for Toxicsubstances and Disease Registryp.455

Azad, N., Iyer, A.K. and Wang, L. 2010. Nitric oxide-mediated bcl-2 stabilization potentiates malignant transformation of human lung epithelial cells. *American Journal of Respiratory Cellular and Molecular Biology* 42:578–85.

Bagchi, D., Stohs, S.J., Downs B.W., Bagchi, M., and Preuss, H.G. 2002. Cytotoxicity and oxidative mechanisms of different forms of chromium. *Toxicology* 180: 5–22.

Bagchi, D., Bagchi, M. and Stohs, S. 2001. Chromium (VI)-induced oxidative stress, apoptotic cell death and modulation of p53 tumor suppressor gene. *Molecular Cell. Biochemistry.* 222: 149–158.

Bakke, O., Karin, J. and Eik-Nes, K. 1984. Concentration-dependent effects of potassium dichromate on the cell cycle. *Cytometry* 5(5):482-6.

Balakumar, B.S., Ramanathan, K., Kumaresan, S. and Suresh, R. 2010. DNA damage by sodium arsenite in experimental rats: ameliorative effects of antioxidant vitamins C and E. *Indian Journal of Science and Technol*ogy 3 (3): 322-327.

Balansky, R.M. D'Agostini, F., Izzotti, A. and De Flora, S.M. 2000. Less than additive interaction between cigarette smoke and chromium(VI) in inducing clastogenic damage in rodents. *Carcinogenesis* (9): 1677-82.

Barba, I., Laia, C., Marisol, R., Maribel, M., Esperanza, A. and David, G. 2009. Effect of intracellular lipid droplets on cytosolic Ca^{2+} and cell death during ischaemia–reperfusion injury in cardiomyocytes. *Physiology* 587(6): 1331–1341

Barh, D. 2005. Dietary Phytochemicals: a Promise to Chemoprevention. *Advanced Biotechnology* 8:21-23.

Barns, J.A., Collins, B.W., Dix, D.J. and Allen J.W. 2002. Effects of heat shock protein-70 (HSP) on sodium arsenite induced genetoxicity. *Environmental and Molecular Mutagenesis* 40(4): 236-242.

Barth Sandra, Danielle Glick and Kay F Macleod 2010. Autophagy: assays and artifacts. *Journal of Pathology* 221(2): 117–124.

Baxley, M.N, Hood, R.D, Vedel, G.C, Harison, W.T and Szczech G.M.1981. Prenatal orally administered sodium arsenite in mice. *Bulletin of Environmental Contaminant and Toxicology* 26: 749–756.

Beaver L. M., Stemmy, E. J., Constant, S. L. , Schwartz, A., Little, L. G., Gigley, J. P., Chun, G., Sugden, K. D., Ceryak, S. M. and Patierno S. R. 2009. Lung injury, inflammation and Akt signaling following inhalation of particulate hexavalent Chromium. *Toxicology and Applied Pharmacol*ogy15: 235(1): 47–56.

Bemis, D.L., Capodice, J.L.,Gorrochum P., Katz, A.E., Buttyan, R .2006. Antipostrate Cancer activity of a carboline alkaloid enriched extract from Rauwolfia Vomitoria. *International Journal of Oncology* 29 (5): 1065-1073.

Beljanski, M. and Beljanski, M. 1986. Three alkaloids as selective destroyers of cancer cells in mice. Synergy with classic anticancer drugs, Oncology 43: 198-203.

Bergsten P., Amitai G., Kehrl J., Dhariwal K. R., Klein H. G. and Levine M. .1990. Millimolar

concentrations of ascorbic acid in purified human mononuclear leukocytes. Depletion and reaccumulation. *Journal of Biologial Chemistry* 265: 2584–2587.

Berghe, T. V., Sasker, G., Vera, G., Yves, D., Dmitri, V. K., Nozomi, T. and Peter V. 2013. Determination of apoptotic and necrotic cell death in vitro and in vivo. *Methods* 61:117–129.

Berghe W. V. 2012. Epigenetic impact of dietary polyphenols in cancer chemoprevention: Lifelong remodeling of our epigenomes. *Pharmacologial Res*earch 65: 565-576.

Biedermann, K. A. and Landolph, J.R. 1990. Role of valence state and solubility of chromium compounds on induction of cytotoxicity, mutagenesis, and anchorage independence in diploid human fibroblasts. Cancer Research 50: 7835-7842

Bielicka, A., Bojanowska, I. and Wiśniewski. A. 2005. Two Faces of Chromium - Pollutant and Bioelement. *Polish Journal of Environmental Stud*ies 14(1): 5-10.

Blankenship, L. J., Carlisle, D. L., Wise, J. P., Orenstein, J. M., Dye, L. E., III, and Patierno, S. R. 1997. Induction of apoptotic cell death by particulate lead chromate: Differential effects of vitamins C and E on genotoxicity and survival. *Toxicology and Applied Pharmacology 146* (2): 270-280.

Bloching, M., Hofmann , A., Lautenschlager, C., Berghaus, A., Grummt, T. 2000. Exfoliative cytology of normal buccal mucosa to predict the relative risk of cancer in the upper aerodigestive tract using the MN assay. *Oral Oncol* 36: 550-555.

Blommaart, E.F., Krause, U., Schellens, J.P., VreelingSindelarova, H., Meijer, A.J. 1997. The phosphatidylinositol 3kinase inhibitors wortmannin and LY294002 inhibit autophagy in isolated rat hepatocytes. European Journal of Biochemistry 243: 240–6.

Bohula, E.A., Playford, M.P. and Macaulay, V.M. 2003. Targeting the type 1 insulin-like growth factor receptor as anticancer treatment. *Anticancer Drugs* 14: 669–682.

Bolognesi, C., Martini, F., Tognon, M. 2005.A molecular epidemiology case control study on pleural malignant mesothelioma. *Cancer Epidemiology, Biomarkers and Prevention* 14: 1741– 1746.

Bonassi, S., El-Zein, R., Bolognesi, C. and Fenech M. 2011. Micronuclei frequency in peripheral blood lymphocytes and cancer risk: evidence from human studies. *Mutagenesis* 26: 93–100.

Bonassi, S., Znaor, A., Ceppi, M. 2007. An increased micronucleus frequency in peripheral blood lymphocytes predicts the risk of cancer in humans. *Carcinogenesis* 28: 625–631.

Bonde, J.P and Ernst, E. 1992.Sex hormones and semen quality in relation to chromium exposure among welders. *Human Environmental Toxicology* 11, 259–263

Borges, K. M., Boswell, J. S., Liebross, R. H. and Wetterhahn, K. E. 1991. Activation of chromium (VI) by thiols results in chromium- (V) formation, chromium binding to DNA and altered DNA conformation. *Carcinogenesis* 12: 551–561.

Boya, P., Gonzalez-Polo, R.A., Casares, N., Perfettini, J.L., Dessen, P., Larochette, N., Metivier, D., Meley, D., Souquere, S., Yoshimori, T., Pierron, G., Codogno, P. and Kroemer G. 2005. Inhibition of macroautophagy triggers apoptosis. *Molecular and Cellular Biol*ogy 25:1025–1040.

Brito, D.A. and *Rieder* C.L. *2006*. Mitotic checkpoint slippage in humans occurs via cyclin B destruction in the presence of an active checkpoint. Current Biology 16(12):1194-200.

Burkill, H.M. 1994. Useful plants of West Tropical Africa. Vol. 2. Families E-I. Royal Botanical Gardens, Kew.

Bullok, K. E., Maxwell, D. and Kesarwala, A.H. 2007. Biochemical and in vivo characterization of a small, membrane-permeant, caspase-activatable far-red fluorescent peptide for imaging apoptosis, *Biochemistry* 46: 4055–4065.

Beutler, E., Duron, O. and Kelly, B.M. 1963. An improved method for the detection of blood glutathione. Journal Laboratory and Clinical Medicine 61: 882–888

Celik, A., Mazmanci, B., ¸Camlica,Y., Askin, A. and Comelekogglu, U. 2005. Induction of micronuclei by lambda-cyhalothrin in Wistar rat bone marrow and gut epithelial cells. *Mutagenesis* 20: 25–129.

Cadet, J., Berger, M., Douki, T. and Ravanat, J.L. 1997. Oxidative damage to DNA: formation, measurement, and biological significance. *Review of Physiology, Biochemistry, Pharmacol*ogy131: 1–87.

Chan, K.F., Siegel, M.R., Lenardo, J.M. 2000. Signaling by the TNF receptor superfamily and T cell homeostasis. *Immunity* 13:419–422.

Chen, N. and Vassiliki, K. 2009. Role and regulation of autophagy in cancer. *Biochimical and Biophysical Acta.* 1793: 1516–1523.

Cheng, L., Sonntag, D. M., de Boer, J. and Dixon, K. 2000. Chromium (VI)-induced mutagenesis in the lungs of big blue transgenic mice. *Journal of Environmental Pathology Toxicology and Oncology* 19: 239–249.

Chen, X. , Yu, L., Qiushi, L., Yan, W., Hong S., Jian W., Guoquan, C., Li, C. and Xiaoqun, D. 2014. Tea polyphenols induced apoptosis of breastcancer cells by suppressing the expression of Survivin. *Scientific Reports* 4: 4416 DOI: 10.1038/srep 044163.

Cheng, H., Tan, Z., Qian, L., Lu, L. and Chunye, L. 2014. Anthropogenic chromium emissions in China from 1990 to 2009. *PLoS ONE* 9 (2): e87753.doi:10.1371/ journal.pone.0087753.

Cheng, J., Zhou, T., Liu, C., Shapiro, J.P., Brauer, M.J., Kiefer, M.C., Barr, P.J. and Mountz, J.D. 1994. Protection from Fas-mediated apoptosis by a soluble form of the Fas molecule. *Science* 263:1759–62.

Cheeseman, K.H. and Slater T.F. 1993. An introduction to free radicals chemistry. *British Medical Bull*etin 49: 481–93.

Chelikani, P., Fita, I. and Loewen, P.C. 2004. Diversity of structures and properties among catalases. *Cellular and Molecular Life Sci*ence 61: 192- 208.

Chiarelli, R. and Maria, C. R. 2012. Heavy metals and metalloids as autophagy-inducing agents: focus on cadmium and arsenic. *Cells* 1: 597-616.

Chipuk, L. and Bouchier-Hayes, D.R. 2004. Mitochondrial outer membrane permeabilization during apoptosis: the innocent bystander scenario. *Cell Death and Differentiation* 13:1396–1402.

Chunlan, Y. , Joon, S. O, Seung, H. Y., Jee, S.L., Young, G.Y., Yoo, J. O., Min, S. J., Sang, Y. L., Jun, Y., Sang, H., Hye, Y.K. and Young, H. Y. (2013): The targeted inhibition of mitochondrial Hsp90 overcomes the apoptosis resistance conferred by Bcl-2 in Hep3B cells via necroptosis. *Toxicology and Applied Pharmacology* 266: 9–18.

Ciapetti, G., Granchi, D. Savarino L. 2002. *In vitro* testing of the potential for orthopedic bone cements to cause apoptosis of osteoblast-like cells. *Biomaterials* 23(2): 617– 627.

Cliby, W.A., Roberts, C.J., Cimprich, K.A., Stringer, C.M., Lamb, J.R., Schreiber, S.L. and Friend, S.H. 1998. Overexpression of a kinase-inactive ATR protein causes sensitivity to DNA-damaging agents and defects in cell cycle checkpoints. *European Molecular Biology Organisation Journal* 17:159–169.

,Clifford, D. and Chau, D. M. 1988. The fate of chromium (III) in chlorinated water. EPA document 600/S2-87/100.

Conceição S. and Eleazar R. 2012. *Review on Some Emerging Endpoints of Chromium (VI) and Lead Phytotoxicity.* Mworia J. (Ed.), ISBN: 978-953- 51-0355-4, Retrived June 15, 2014 from http://www.intechopen.com/books/botany/review- on-emerging-endpoints-of-chromium-vi-and-leadphytotoxicityMarch, 2012.

Cong, Z, Kang, S., Zhang, Y. and Li, X. 2010. Atmospheric wet deposition of trace elements to central Tibetan Plateau. *Applied Geochemistry* 25: 1415–1421.

Costa, M.1997. Toxicity and carcinogenicity of Cr(VI) in animal models and humans. *Critical Review of Toxicology* 27:431–442.

Costa, M. and Klein, C.B. 2008. Toxicity and carcinogenicity of chromium compounds in humans. *Critical Review of Toxicology* 36(2):155 – 163.

Cotran RS, Kumar V and Collins T 1999. Cellular pathology I: cell injury and cell death. *Robbins Pathologic Basis of Disease*. R.S. Cortan, V. Kumar and T.Collins, Eds. Saunders Co; Philadelphia. 1–29.

Cretu, A., Xiaojin, S., Tront, J., Hoffman, B. and Liebermann Dan. 2009. Stress sensor Gadd45 genes as therapeutic targets in cancer. *Cancer Therpeutical*: 7: 268–276

Cuervo, A.M. 2004. Autophagy: many paths to the same end. *Molecular and Cellular Biochem*.263: 55-72.

D'Agnostini, F., Alberto, I., Carlo, B., Anna, C., Elena, T. and De Flora S. 2002. Induction of apotosis in the lung but in the liver of rats receiving receiving intra-tracheal instillations of chromium(VI) *Carcinogenesis* 23(4): 587-593.

Dalager, N.A., Mason, T.J., Fraumeni, J.F., Jr., Hoover, R., and Payne, W.W. 1980. Cancer mortality among workers exposed to zinc chromate paints. *Journal of Occupational Medicine* 22: 25-29.

Dai, R., Yu, C., Liu, J., Lan, Y. and Deng, B. 2003.Photooxidation of Cr (III)-citrate complexes forms harmful Cr (VI). *Environmental Science Technol*ogy 44: 6959–6964.

Darzynkiewicz, Z., Juan, G., Xun, L., Wojciech, G., Tomoyuki, M., and Frank T. 1997. Cytometry in cell necrobiology: analysis of apoptosis and accidental cell death (necrosis). *Cytometry* 27:1–20.

Darzynkiewicz, Z., Juan, G., Li, X., Gorczyca,W., Tomoyuki M., and Das, A.P. and Mishra S. 2008. Hexavalent Chromium (VI): Environment Pollutant and Health Hazard. *Journal of Environmental Research and Develop*ment 2(3): 386-392.

Debunne, M., Christophe, P., Bruno, D., Ebba, B., Francoise, L., Jean-Paul,H., Heidi, L., Pauline, N., Marc, M., Anthony, R., Pierre-Yves, R., Christian, T., and Vincent, R. 2011. *In vitro and ex vivo* evaluation of Smart Infra-Red Fluorescent Caspase-3 probes for molecular imaging of cardiovascular apoptosis. *International Journal of Molecular Imaging* 2011, Article ID 413290, doi:10.1155/2011/413290.

De Flora, S. 2000.Threshold mechanisms and site specificity in chromium (VI) carcinogenesis. *Carcinogenesis* 21: 533–541.

Degterev, A., Huang, Z., Boyce, M., Li, Y., Jagtap, P., Mizushima, N., Cuny, G.D., Mitchison, T.J., Moskowitz, M.A. and Yuan, J. 2005. Chemical inhibitor of nonapoptotic cell death with therapeutic potential for ischemic brain injury. *Nature Chemical Biology* 1: 112–119.

.Degenhardt, K., Mathew, R., Beaudoin, B., Bray, K., Anderson, D., Chen, G. 2006. Autophagy promotes tumor cell survival and restricts necrosis, inflammation, and tumorigenesis. *Cancer Cell* 10:51–64.

Dennis, P. B. 2001. Mammalian TOR: a homeostatic ATP sensor. *Science* 294: 1102 –1105.

Deter, R.L and De Duve C. 1967. Influence of glucagon, an inducer of cellular autophagy, on some physical properties of rat liver lysosomes. *Journal of Cellular Biol*ogy 33: 437–449.

Dice, J.F. 2000. Lysosomal Pathways of Protein Degradation. *LandesBioscience, Austin*, Texas

Dunai, Z., Bauer, P.I. and Mihalik, R.2011. Necroptosis: biochemical, physiological and pathological aspects. *Pathology Oncology Res*earch 17:791–800.

Dunn, S.E., Hardman, R.A., Kari, F.W. and Barrett, J.C. 1997. Insulinlike growth factor 1 (IGF-1) alters drug sensitivity of HBL100 human breast cancer cells by inhibition of apoptosis induced by diverse anticancer drugs. *Cancer Research* 57 2687–2693.

Edel, J. and Sabbioni, E. 1985. Pathways of Cr (lII) and Cr (VI) in the rat after intratracheal administration. *Human Toxicology* 4**:** 409–416.

Elias, Z., Poirot, O., Pezerat, H., Suquet, H., Schneider, O., Daniere, M. C., Terzetti, F.,

Baruthio, F., Fournier, M., and Cavelier, C. 1989. Cytotoxic and neoplastic transforming effects of industrial hexavalent chromium pigments in Syrian hamster embryo cells. *Carcinogenesis 10* (11): 2043-2052.

Elmore, S. 2007. Apoptosis: A Review of Programmed Cell Death.*Toxicology and Pathol*ogy 35(4): 495–516.

El-Zein, R. A., Schabath M. B., Etzel C. J., Lopez M. S., Franklin J. D. and Spitz M. R. 2006. Cytokinesis-blocked micronucleus assay as a novel biomarker for lung cancer risk. *Cancer Research*. 66: 6449–6456.

Endersen, P.C., Prytz, P.S., Aarbakke, J. 1995. A new flow cytometric method for discrimination of apoptotic cells and detection of their cell cycle specificity through staining of F-actin and DNA. *Cytometry* 20: 162– 171.

Environmental Protection Agency, USA 1984. *Health assessment document for chromium*. Final report No. EPA600/8-83-014F. Research Triangle Park, NC, United States

Eskelinen, E.L. 2008. Fine structure of the autophagosome. *Methods in Molecular Biology* 445:11–28

Esterbauer, H., Cheeseman K.H. 1990. Determination of aldehydic lipid peroxidation products: malonaldehyde and 4hydroxynonenal. *Methods in Enzymology* 186: 407-421.

Evan, G.I., Brown, L., Whyte, M., and Harrington E. 1995. Apoptosis and the cell cycle. *Current Biol*ogy 7:825-34.

Evan, G.I., Wyllie, A.H., Gilbert C.S., Littlewood, T.D., Land, H., Brooks, M., Waters, C.M, Penn, L.Z., and Hancock, D.C. 1992. Induction of apoptosis in fibroblasts by c-myc protien. *Cell* 69: 119-28.

Evenson, D.P, Jost L.K. and Baer R.K. 1993. Effects of methyl methanesulfonate on mouse sperm chromatin structure and testicular cell kinetics. *Environmental and Molecular Mutagenesis* 21:144–153.

Fandeur, D., Juillot, F., Morin, G., Olivi, L., Cognigni, A., Webb, S. M., Ambrosi, J. P., Fritsch, E., Guyot, F. and Brown, G. E. Jr. 2009. XANES evidence for oxidation of Cr(III) to Cr(VI) by Mn-oxides in a lateritic regolith developed on serpentinized ultramafic rocks of New Caledonia. *Environmental Science Technology*. 43:7384–7390.

Fadeel, B. and Orrenius, S. 2005. Apoptosis: a basic biological phenomenon with wide-ranging

implications in human disease. *Journal of Internal Medicine* 258 (6): 479–517.

Fan, T.J., Han, L.H., Cong, R.S. and Liang, J. 2005. Caspase family proteases and apoptosis. *Acta Biochemical and Biophysics Shanghai* 37: 719–727.

Fenech, M., Holland, N., and Zeiger, E. 2011. The HUMN and HUMNxL international collaboration projects on human micronucleus assays in lymphocytes and buccal cells–past, present and future. *Mutagenesis* 26: 239–245.

Fenech, M. 2002. Chromosomal biomarkers of genomic instability relevant to cancer. *Drug Discovery Today***7**: 1128–1137.

Ferlay, J., Shin, H.R., Bray, F., Forman, D., Mathers, C.D. and Parkin D. 2008. *GLOBOCAN 2008, Cancer Incidence and Mortality Worldwide*: IARC CancerBase No.10 [Internet]. Lyon, France: International Agency for Research on Cancer. 2010;Retrived September 10,2015 from: http://globocan.iarc.fr.

Fishbein, L .1981. Sources, transport and alterations of metal compounds: an overview. I. Arsenic, beryllium, cadmium, chromium, and nickel. *Environmental Health Perspectives* 40: 43.

Fornace, A.J Jr, Nebert, D.W., Hollander, M.C., Luethy, J.D., Papathanasiou, M., Fargnoli, J., Holbrook, N.J. 1991. Induction by ionizing radiation of the Gadd45 gene in cultured human cells: lack of mediation by protein kinase C. *Molecular Cell Biology* 11:1009–16.

Francoa Frank, T.1997. Cytometry in cell necrobiology: analysis of apoptosis and accidental cell death (necrosis). *Cytometry* 27:1–20.

Frisch, S. M., and Screaton, R. A. 2001. Anoikis mechanisms. *Current Opinion in Cell Biology* 13:555–562.

Fujita N. 2008. The Atg16L complex specifies the site of LC3 lipidation for membrane biogenesis in autophagy. *Molecular Biology of the Cell* 19: 2092–2100.

Ganem, N.J., Storchova Z. and Pellman, D.2007. Tetraploidy, aneuploidy and cancer. *Current Opinion in Genetics and Development* 217(2):157-62.

Geng, D.J. and Klionsky D.J. 2008.The Atg8 and Atg12 ubiquitin-like conjugation systems I macroautophagy. *European Molecular Biology Organisation Report* 9: 859–864.

Ghadially, F.N.1988. Ultrastructural pathology of the cell and matrix, 3rd ed. Guildford, UK: Butterworth.

Gibbs, H., Lees, P., Pinsky, P., Rooneym and Ling B. 2000. Cancer among workers in chromium chemical production. *American Journal of Industrial Medicine*.38**:** 115-126.

Glick, D., Barth, S. and Macleod, K.F. 2010. Autophagy: cellular and molecular mechanisms. *Journal of Pathology* DOI 10:1002/path.2697.

Gioacchino, M. D., Petrarca, C., Perrone, A., Martino S., Esposito, Diana L., Vittoria L. L. and Mariani-Costantini R. 2008. Autophagy in hematopoietic /progenitor cells exposed to heavy metals: biological implication and toxicological relevance. *Autophagy* 4: 537-539.

Grotto, D., Santa M., Boeira, L., Valentini,S., Charão, J. Moro, M., Nascimento, A., PPomblum, V. and Garcia, S .2007.Rapid quantification of malondialdehyde in plasma by high performance liquid chromatography-visible detection. *Journal Pharmaceutical and Biomedical Analysis 43*: 619–624.

Goldstein, J.C., Waterhouse, N.J., Juin, P., Evan, G.I., Green, D.R. 2000. The coordinate release of cytochrome *c* during apoptosis is rapid, complete and kinetically invariant. *Nature Cell Biol*ogy 2:156–62

Gouill, S.L., Klaus, P., Jean-Luc H. and Kenneth, C. A. 2004. Mcl-1 regulation and its role in multiple myeloma. *Cell Cycle* 3(10): e107-e110.

Grabarek, J., Amstad, P. and Darzynkiewicz, Z. 2002. Use of fluorescently labeled caspase inhibitors as affinity labels to detect activated caspases. *Human Cell* 15:1–12.

Gross, A., McDonnell, J.M. and Korsmeyer, S.J. 1999. BCL-2 family members and the mitochondria in apoptosis. *Genes and Development*13: 1899–1911.

Gu, J., Kawai, H., Wiederschain, D. and Yuan. Z.M. 2001. Mechanism of functional inactivation of a Li-Fraumeni syndrome p53 that has a mutation outside of the DNA-binding domain. *Cancer Research* 61:1741–6.

Guha M. D., Das G.J and Santra A. 1998. Chronic arsenic toxicity in West Benga:the worst calamity in the world. *Journal of Indian Medical Association* 96: 4-7.

Gunaratnam, M. and Grant, M.H. 2004. Damage to F-actin and cell death induced by chromium VI and nickel in primary monolayer cultures of rat hepatocytes. *Toxicology In Vitro* 18: 245–253.

Gurtu, V., Kain, S.R. and Zhang, G. 1997. Fluorometric and colorimetric detection of caspase activity associated with apoptosis. Annals of Biochemistry 251:98–102.

Gutteridge, J.M.C.1995. Lipid peroxidation and antioxidants as biomarkers of tissue damage. *Clinical Chemistry* 41:1819–1828

Guttmann, D., Poage, G., Johnston, T. and Zhitkovich, A. 2008. Reduction with glutathione is a weakly mutagenic pathway in chromium(VI) metabolism. *Chemical Research Toxicol*ogy 21: 2188–2194.

Habig, W.H, Pabast, M.J, Jakoby, W.B. 1974. Glutathione S- Transferase, the first enzymatic step in mercapturic acid formation. *Journal of Biologial Chemistry* 249: 7130- 7139.

Hale, A. J., Smith, C. A., Sutherland, L. C., Stoneman, V. E. A., Longthorne, V. L., Culhan, A.C. and Williams G.T. 1996. Apoptosis: molecular regulation of cell death. *European Journal Biological Chemistry 268* (*236*): 1226.

Halliwell, B. 1995. How to characterize an antioxidant- An update. *Biochemistry Society Symposium* 61:73–101.

Halliwell, B. and Gutteridge, J. 1999. Free Radicals in Biology and Medicine, New York: Oxford University Press. 105–245.

Hamatake, M., Kazuhiro, I., Kazuyuki, H. and Ryoji, I. 2000. Zinc induces mixed types of cell death, necrosis, and apoptosis in Molt-4 *cells. Journal Biochem*istry 128: 933-939.

Hanada T. N., Satomi, N.N., Ichimura, Y., Fujioka,Y., Takao,Y., Inagaki,T. F. and Ohsumi, Y. 2007. The Atg12-Atg5 conjugate has a novel E3-like activity for protein lipidation in autophagy. *Journal Biological Chemistry* 282: 37298– 37302.

Hanahan, D. and Weinberg, R. A..2011. Hallmarks of Cancer: The Next Generation. *Cell* 144: 646-74.

Hanahan, D. and Weinberg, R.A. 2000.The hallmarks of cancer. *Cell* 100: 57–70.

Harris M.H. and Thompson C.B. 2000. The role of the Bcl-2 family in the regulation of outer mitochondrial membrane permeability. *Cell Death and Differentiation* 7: 1182–1191.

Hayashi-Nishino, M., Fujita, N., Noda, T., Yamaguchi, A., Yoshimori, T. and Yamamoto, A. 2009. A sub-domain of the endoplasmic reticulum forms a cradle for autophagosome formation. *Nature Cell Biol*ogy 11: 1433– 1437.

Hayashi, Y. , Takashi, K. ,Qing-Li, Z. , Ryohei, O. , Zheng-Guo, C. , Loreto, B. F.Jr, Hidetoyo, T. and Minoru, K. 2004. Signal transduction of p53-independent apoptotic pathway

induced by hexavalent chromium in U937 cells. *Toxicology and Applied Pharmacology* 197(2): 96–106

He, W., Wang, Q Xu, J. Xu X. , Padilla, M. T. Ren, G., Gou, X. and Li Y. 2012. Attenuation of TNFSF10/TRAIL-induced apoptosis by an autophagic survival pathway involving TRAF2- and RIPK1/RIP1-mediated MAPK8/JNK activation. *Autophagy* 8(12): 1811–1821.

Hodges, N.J., Adam, B. Lee, A.J., Cross, H.J., Chipmann J.K. 2001. Induction of DNA strand breaks in human peripheral blood lymphocytes and A549 lung cells by sodium dichromate: association with 8-oxo-2-deoxyguanosine formation and inter –individual variability. Mutagenesis 16: 467-474.

Holcik, M., Gibson, H. and Korneluk, R.G. 2001. XIAP: apotosis brake and promising therapeutic target. *Apoptosis* 6: 253- 261.

Holy, J. M. 2002. Curcumin disrupts mitotic spindle structure and induces micronucleation in MCF-7 breast cancer cells. *Mutation Research* 518: 71–84.

Hua, C., Shuan, F.L., Jie L., Bhalchandra A.D., Barrett, J.C., and Waalkes, M.P. 2004. Chronic inorganic arsenic exposure induces hepatic global and individual gene hypomethylation: implications for arsenic hepatocarcinogenesis. *Carcinogen*esis 25 (9): 1779-1786.

Huang, C., Ke, Q., Costa, M. and Shi, X. 2004. Molecular mechanisms of arsenic carcinogenesis. *Molecular Cell Biochemistry* 255:57–66.

Huang, J., Plass, C. and Gerhauser, C. 2011. Cancer chemoprevention by targeting the epigenome. *Current Drug Targets* 12:1925–56.

Hueper, W.C. and Payne, W.W. 1959. Experimental cancers in rats produced by chromium compounds and their significance to industry and public health. *America Industrial Hygiene .Association.Journal*. 1959; 20:274–280

Hellawell, G.O., Turner, G.D., Davies, D.R., Poulsom R., Brewster S.F. and Macaulay, V.M. 2002. Expression of the type 1 insulin-like growth factor receptor is up-regulated in primary prostate cancer and commonly persists in metastatic disease. *Cancer Research* 62: 2942–2950.

Holmes, A. L. ,Sandra, S. W., Stephen C. P., Abou, E. A., Wilma, L.,Jeffery S. ,Jamie G. and Wise J Pi., Sr. 2010. Chronic exposure to zinc chromate induces centrosome amplification and spindle assembly checkpoint bypass in human lung fibroblasts. *Chemical Research Toxicol*ogy 23(2): 386.

Holmes, A.L., Wise, S.S. and. Wise, J.P Sr. 2008. Carcinogenicity of hexavalent chromium. *Indian Journal of Medical Research* 128: 353-372.

Iarmarcovai, G., Ceppi, M., Botta, A., Orsière, T. and Bonassi, S. 2008. Micronuclei frequency in peripheral blood lymphocytes of cancer patients: a meta-analysis. *Mutation Res*earch 659: 274–283.

Igney, F.H. and Krammer, P.H. 2002. Death and anti-death: tumour resistance to apoptosis. *Nature Review Cancer* 2: 277–88.

Ishikawa,Y.,Nakagawa,K.,Satoh,Y.,Kitagawa,T.,Sugano,H.,Hirano,T.,Tsuchiya, E. 1994a Characteristics of chromate workers' cancers, chromium lung deposition and precancerous bronchial lesions: an autopsy study. *British Journal of .Cancer* 70:160–166.

Ishikawa, Y., Nakagawa, K., Satoh, Y., Kitagawa, T., Sugano, H., Hirano, T., Tsuchiya, E. 1994b. "Hot spots" of chromium accumulation at bifurcations of chromate workers ' bronchi. *Cancer Res*earch 54: 2342–2346.

Iwu, M.M. and Court W.E. 1982. Stem bark alkaloids of Rauwolfia vomitoria. *Oxford Textbook of Clinical Nephrology*. *Planta Med*icine 45(6): 105111.

Jiang, S., Li,D., Li,Y., Zhu,Y, Luo,R., Wu, X., Zhang, M., Tang,J., Qin, W., Li, Z., Wang, X., Feng, G., Jia, W., Deng,R. and Zhu, X. 2011. Intensive expression of UNC-51-like kinase 1 is a novel biomarker of poor prognosis in patients with esophageal squamous cell carcinoma. *Cancer Science* 102: 1568–1575

Johansen, M., Overgaard, E. and Toft, A. 1994. Severe chronic inflammation of the mucous membranes in the eyes and upper respiratory tract due to work-related exposure to hexavalent chromium. *Journal of Laryngology and Otology* 108(7):591–592.

Jomovaa K,and Valko M. 2011. Advances in metal-induced oxidative stress and human disease. *Toxicology* 283: 65–87

Joseph, P., He, Q. and Umbright, C. 2008. Heme-oxygenase 1 gene expression is a marker for

hexavalent chromium-induced stress and toxicity in human dermal fibroblasts. *Toxicological Science* 103:325–334.

Kadiiska, M.B., Xiang, Q.H. and Mason, R.P. 1994. *In vivo* free radical generation by chromium(VI): An electron spin resonance spin-trapping investigation. *Chemical Research Toxicology* 7:800–805

Kadowaki, M. and Karim, M.R. 2009. Cytosolic LC3 ratio as a quantitative index of macroautophagy. *Methods in Enzymology* 452: 199–213.

Kakunaga, T. H. and Kamasaki, H. 1985. *Transformation assay of established cell lines: mechanisms and application*. IARC Scientific Publications No 67. 225.

Karaczyn, A., Ivanov, S., Reynolds, M., Zhitkovich, A., Kasprzak, K. S. and Salnikow K. 2006. Ascorbate depletion mediates upregulation of hypoxia-associated proteins by cell density and nickel. *Journal of Cell Biochemistry* 97: 1025–1035.

Kamat, C.D. , Green D.E., Curilla S., Warnke L., Hamilton J.W., Sturup S., Clark C. and Ihnat M.A. 2005. Role of HIF signaling on tumorigenesis in response to chronic low-dose arsenic administration. *Toxicological Sci*ence 86 248–257.

Karantza-Wadsworth, V., Patel, S., Kravchuk, O., Chen, G., Mathew, R., Jin, S., and White, E. 2007. Autophagy mitigates metabolic stress and genome damage in mammary tumorigenesis. *Genes and* Development. 21: 1621–1635.

Kerr, J.F., Winterford, C.M. and Harmon, B.V. 1994. Apoptosis. Its significance in cancer and cancer therapy. *Cancer* 73:2013–26.

Kerr, J.F., Wyllie, A.H. and Currie, A.R. 1972. Apoptosis: a basic biological phenomenon with wide-ranging implications in tissue kinetics. *British Journal of Cancer* 26: 239-257.

Kimura, S., Noda, T. and Yoshimori, T. 2007. Dissection of the autophagosome maturation process by a novel reporter protein, tandem fluorescent-tagged LC3. *Autophagy* 3: 452–460.

Klaunig, J.E. and Kamendulis, L.M. 2004. The role of oxidative stress in carcinogenesis. *Annual Review of Pharmacology and Toxicology* 44: 239–267

Klehues, P. and Stewart, B.W. 2003. *World cancer report*. International Agency for Research on Cancer Lyon, France

Klionsky, D.J and Emr, S.D. 2000. Autophagy as a regulated pathway of cellular degradation. *Science*: 290:1717–21.

Klionsky, D.J., Agostinis, P., Agrawal, D.K, Bamber, B.A, Bassham, D.C, Bergamini, E. 2008. Guidelines for monitoring autophagy in higher eukaryotes. *Autophagy* 4:151–175.

.Koukourakis, M.I., Giatromanolaki, A., Sivridis, E., Pitiakoudis, M., Gatter, K.C. and Harris, A.L. 2010. Beclin 1 over- and underexpression in colorectal cancer: distinct patterns relate to prognosis and tumour hypoxia. *British Journal of Cancer*. 103:1209–14.

Korichneva, I. and Hammerling, U. 1999. F-actin as a functional target for retro-retinoids: a potential role in anhydroretinol-triggered cell death. *Journal of Cell Science* 112:2521–2528.

Korsmeyer, S.J**.** 1999. BCl-2 gene family and the regulation of programmed cell death. *Cancer Research* 59: 1693-1700.

Kroemer, G. and Levine, B. 2008. Autophagic cell death: the story of a misnomer. Nat. Rev. *Molecular Cell Biol*ogy 9: 1004–1010.

Krinsky, N.I. 1992. Mechanism of action of biological antioxidants. *Proceedings of the Society for Experimental Biology and Medicine* 200(2):248-54.

Kuma, A., Hatano, M., Matsui, M., Yamamoto, A., Nakaya, H., Yoshimori, T., Ohsumi, Y., Tokuhisa, T. and Mizushima, N. 2004. The role of autophagy during the early neonatal starvation period. *Nature* 432: 1032–1036.

Kuo, C.Y., Wong, R.H., Lin, J.Y., Lai, J.C. and Lee, H. 2006. Accumulation of chromium and nickel metals in lung tumors from lung cancer patients in Taiwan. *Journal of Toxicology and Environmental Health, Part A* 69: 1337–1344.

Kwak, M.K. and Kensler, W.K. 2010: Targeting NRF2 signaling for cancer chemoprevention. *Toxicology and Applied Pharmacol*ogy 244:66-76.

Lash, L.H., Putt, D.A., Hueni, S.E. and Horwitz, B.P. 2005. Molecular markers of trichloroethylene-induced toxicity in human kidney cells. Toxicology and Applied Pharmacology 206:157–68.

Lay, P. S., and Levina, A. 1998.Activation of molecular oxygen during the reactions of chromium (VI/V/IV) with biological reductants: implications for chromium-induced

genotoxicities. *Journal of American Chemistry Society* 120: 6704–6714.

Lebovitz, C.B., Svetlana B. B. and Sharon, M. G. 2012. Here, there bedragons: charting autophagy-related alterations in human tumours. *Clinical Cancer Research* 18:1214-1226.

Levina, A., Harris, H. H. and Lay, P. A. 2007. X-ray absorption and EPR spectroscopic studies of the biotransformations of chromium- (VI) in mammalian cells. Is chromodulin an artifact of isolation methods? *Journal of American Chemistry Society* 129: 1065–1075.

Levine, B., and Yuan, J. 2005. Autophagy in cell death: an innocent convict. *Journal of Clinical Investigation* 115: 2679–2688.

Levy, L.S. and Venitt, S. 1986. Carcinogenicity and mutagenicity of chromium compounds: the association between bronchial metaplasia and neoplasia. *Carcinogenesis*7: 831–835

Lewis D.R., Southwick J.W., Ouellet-hellstrom R., Rench J., and Calderon, R.L. 1999. Drinking water arsenic in Utah: a cohort mortality study. *Environmental Health Perspect*ive107: 359-365.

Li, W., Zhao, Y. and Chou, I.N. 1992. Cytoskeletal injury induced by hexavalent chromate. *Toxicology In Vitro* 6: 433–444.

Limon-Pacheco, J. and Gonsebatt, M. E. 2009. The role of antioxidants and antioxidant-related enzymes in protectiveresponses to environmentally induced oxidative stress. *Mutation Res*earch 674: 137–147

Lin, C.C., Wu, M.L., Yang, C.C., Ger, J., Tsai, W.J., Deng, J.F. 2009. Acute severe chromium poisoning after dermal exposure to hexavalent chromium. *Journal of Chinese Medical Association* 72 (4): 219–221.

Liu, W., Zhang X., and Liu M. 2001.Chromium Pollution and Control in the Leathermaking Industry. *Leather Science and Engineering:* 11: 1–6.

Listenberger, L.L., Han, X., Lewin, S.E., Cases,S., Farese, R.V., Ory, D.S. and Schaffer, J.E. 2003.Triglyceride accumulation protects against fatty acid-induced lipotoxicity. *Proceedings of the National Academy of Science USA* 100: 3077–3082.

Liu, Z.G. 2005. Molecular mechanism of TNF signaling and beyond. *Cell Research*15:24–27.

Lobo, V. , Patil, A., Phatak, A., and Chandra, N. 2010. Free radicals, antioxidants and functional

foods: Impact on human health. *Pharmacognosy Rev*iew 4(8): 118–126.

Locksley, R.M., Killeen, N. and Lenardo, M.J. 2001. The TNF and TNF receptor superfamilies: integrating mammalianbiology. *Cell* 104:487–501.

Loubieres, Y., de Lassence, A., Bernier, M., Vieillard-Baron, A., Schmitt, J.M., Page, B. and Jardin, F. 1999. Acute, fatal, oral chromic acid poisoning.*Journal of Toxicology Clinical Toxicology* 37, 333–336

Love, S., Barber, R . and Wilcock, G.K. 1999. Increased poly(ADP- ribosyl)ation of nuclear proteins in Alzheimer's disease. *Brain*: 122: 247–53.

Luca, M. R., Raluca, C., Cristiana, I. C., Valentina, M., Anisoara, C, and Dana, I. 2007. Response of antioxidant defence system to chromium VI induced oxidative stress in embryonary fibroblasts. *Romania Journal of Biophysics.* 17 (1): 9-20.

Lum, J.J., Bauer, D.E., Kong, M., Harris, M.H., Li, C., Lindsten, T., and Thompson, C.B. 2005. Growth factor regulation of autophagy and cell survival in the absence of apoptosis. *Cell* 120: 237–248.

Macfie, A., Hagan, E. and Zhitkovich, A. 2010. Mechanism of DNA-protein cross-linking by chromium. *Chemical Research Toxicol*ogy 23: 341–347.

Maduabuchi J-M. U, Adigba,, E. O., Nzegwu, C. N., Oragwu, C. I., Okonkwo, I. P. and Orisakwe, O. E. 2007. Arsenic and Chromium in Canned and Non-Canned Beverages in Nigeria: A Potential Public Health Concern. *International Journal of Environmental Research and Public Health 4(1)*: 28-33.

Maffe, I .F., Juan, M., Zolezzi, M., Sabrina, A., Corrado, Z., Muriel, M., Davide, F., Cantelli-Forti, G, and Patrizia, H. 2014. Micronucleus frequency in human peripheral blood lymphocytes as a biomarker for the early detection of colorectal cancer risk. *Mutagenesis* 29 (3): 221–225.

Majno, G and Joris, I. 1995. Apoptosis, oncosis, and necrosis. An overview of cell death. *American Journal Pathology* 146:3–15.

Masella, R., Di Benedetto, R., Vari, R., Filesi, C., Giovannini, C. 2005. Novel mechanisms of natural antioxidant compounds in biological systems: involvement of glutathione and glutathione related enzymes. *Journal of Nutrition Biochem*istry 16: 577-586.

Mathew, R., Kongara, S., Beaudoin, B., Karp, C.M., Bray, K., Degenhardt, K., Chen, G., Jin, S., and White, E. 2007. Autophagy suppresses tumor progression by limiting chromosomal

instability. *Genes* and *Development* 21**:** 1367–1381.

Mathew, R., Karp C.M., Beaudoin, B., Vuong, N., Chen, G., and Chen H.Y. 2009. Autophagy suppresses tumorigenesis through elimination of p62. *Cell* 137:1062–75.

Martin, B., Schoenhard, J., Hwang, J., Sugden, K. 2006.Ascorbate is a pro-oxidant in chromium-treated human lung cells. *Mutation Research*. 610: 74-84.

Mates, J.M., Perez-Gomez, C. and De Castro, I.N. 1999. Antioxidant enzymes and human diseases, *Clinical Biochem*emistry 32 595–603.

Matsui, Y., Takagi, H., Qu, X., Adbellatif, M., Sakoda,H. and Asano, T. (2007): Distinct roles of autophagy in the heart during ischemia and reperfusion: roles of AMP-activated protein kinase and Beclin 1 in mediating autophagy. *Circulation Res*earch 100: 914–922.

Maxwell, D., Chang,Q., Zhang,X.U., . Barnett, E.M. and Piwnica-Worms, D. 2009. An Improvedcell-penetrating, caspaseactivatable, near-infrared fluorescent peptide for apoptosis imaging. *Bioconjugate Chemistry* 20 (4): 702–709.

Mavournin, K.H., Blakey, D.H., Cimino, M.C., Salamone, M.F. and Heddle, J.A. 1990. The *in- vivo* micronucleus assay in mammalian bone marrow and peripheral blood. A report of the U.S. Environmental Protection Agency Gene-Tox Program. *Mutation Res*earch 239: 29–80.

McCarthy, T. C., Pollak, P. T., Hanniman, E. A., and Sinal, C. J. 2004. Disruption of hepatic lipid homeostasis in mice after amiodarone treatment is associated with peroxisome proliferator-activated receptor-alpha target gene activation. *Journal of Pharmacology and Experimental Ther*apeutics 311: 864–873.

McConkey, D.J, Nicotera, P., Hartzell, P., Bellomo, G., Wyllie, A.H, and Orrenius, S. 1989. Glucocorticoids acticvate a suicide process in thymocytes through an elevation of cytosolic Ca^{2+} concentration. *Archives of Biochemistry Biophysics* 269:365–370.

Mecha, I., Adegbola, T.A. and le Houerou, H.N. 1980. Chemical composition of some southern Nigeria forage eaten by goats. *Browse in Africa*., International Livestock Centre for Africa, Addis Ababa, Ethiopia 303-306

Medan, D., Luanpitpong, S. , Azad, N. Wang, L. Jiang, B. Davis, M. E. Barnett, J.B.' Guo, L. and Rojanasakul Y. 2012. Multifunctional role of Bcl-2 in malignant transformation and tumorigenesis of Cr(VI)-transformed lung cells.

Melendez, A., Talloczy, Z., Seaman, M., Eskelinen, E.L., Hall, D.H., Levine, B. 2003 Autophagy genes are essential for dauer development and life-span extension in *C. elegans*. *Science* 301: 1387–1391.

Melino, G., Bernassola, F., Ranalli, M., Yee, K., Zong, W.X., Corazzari, M., Knight, R.A., Green, D.R., Thompson, C. and Vousden, K.H. 2004. p73 Induces apoptosis via PUMA transactivation and Bax mitochondrial translocation. *Journal of Biological Chem*istry 279: 8076–8083.

Mesri, M., Wall, N.R., Li, J., Kim, R.W. and Altieri, D.C. 2001. Cancer gene therapy using a survivin mutant adenovirus. Journal Clinical Investigation 108: 981-990

Messer, J., Reynolds, M., Stoddard, L. and Zhitkovich, A. 2006. Causes of DNA single-strand breaks during reduction of chromate by glutathione in vitro and in cells. *Free Radical Biology and Med*icine 40: 1981–1992.

Messinaand, M. and Hilakivi-Clarke, L. 2009. Early intake appears to be the key to the proposed protective effects of soy intake against breast cancer. *Nutrition and Cancer* 61:792–8.

Michel R, Nolte M, Reich M, Löer F.1991. Systemic effects of implanted prostheses made of cobalt-chromium alloys. *Archives of Orthopedics Trauma and Surgery*. 110 (2): 61-74.

Mills, J. C., Stone N. L. and Pittman, R. N. 1999. Extranuclear apoptosis: the role of the cytoplasm in the execution phase. *Journal of Cell Biology* 146:703–707.

Mitelman, F. Catalog of Chromosome Aberrations in Cancer. 5th edn. New York: Wiley-Liss.

Miura, T., Patierno, S. R., Sakuramoto, T., and Landolph, J. R. l989. Morphological and Neoplastic Transformation of C3H/10T1/2 Cl 8 Mouse Embryo Cells by Insoluble Carcinogenic Nickel Compounds. *Environmetnal and Molecular Mutagenesis* 14: 65-78.

Mohan, S., Bustamam, A., Ibrahim, S., Al-Zubairi, A., Aspollah, M., Abdullah, R. and El-Hassan M. 2011. *In Vitro* Ultramorphological Assessment of Apoptosis on CEMss Induced by Linoleic Acid-RichFraction from Typhonium flagelliforme Tuber. *EvidenceBased Complementary and Alternative Medicine* 2011: 421894 – 21785623.

Molecular Probes 2010. Premo autophagy sensors (LC3B-FP) BacMam 2.0 manual. U.S. Patent No. 5,348,886.

Moreau, K., Luo, S. and Rubinsztein, D.C. 2010. Cytoprotective roles for autophagy. *Current Opinion in Cell Biol*ogy 22: 206–211.

Morita, T., Asano, N., Awogi,T. 1997. Evaluation of the rodent micronucleus assay in the screening of IARC carcinogens Group 1, 2A and 2B. The summary report of the 6th collaborative study by CSGMT/JEMS MMS. *Mutation Res*earch 389: 3–122.

Mouallem, M., Antipov, N., Mayan, H., Sela, B. A. and Farfel, Z. 2007. Hyperglobulinemia in amiodarone-induced pneumonitis. *Cardiovascular Drugs and Therapy*. 21: 63–67.

Muñoz A.and Costa M. 2012. Elucidating the mechanisms of nickel compound uptake: A review of particulate and nano-nickel endocytosis and toxicity. *Toxicology and Applied Pharmacol*ogy 260(1): 1–16.

Munshi, A., Hobbs, M., and Meyn, R.E. 2005. Clonogenic Cell Survival Assay. *In vitro Assay Chemosensitivity* Vol. 1, Bluementhal, R.D. (Ed.)

Murray, K. J. and Tebo, B. M2007. Cr (III) is indirectly oxidized by the Mn(II)-oxidizing bacterium Bacillus sp. strain SG-1. *Environmental Science Technol*ogy 41: 528–533.

Mustafa, T.A, Kadriye, O., Saygi, A., Isa, K.B, and Mustafa, S. 2010. Selective speciation and determination of inorganic arsenic in water, food and biological samples. *Food and Chemical Toxicol*ogy 48: 41–46.

National Research Council 1999. Arsenic in Drinking Water. National Academy Press, Washington, DC.

National Toxicology Program 2005. 11th Report on Carcinogens. *Reproductive Carcinogen*. 11: 1-A32.

National Toxicology Program 2008. Toxicology and Carcinogenesis Studies of Sodium Dichromate Dihydrate (CAS No. 7789–12–0) in F344/N Rats and B6C3F1 Mice (Drinking Water Studies*). National Toxicology Program Technical Report and Services* 546:1–192.

Nechushtan, A., Smith, C.L., Lamensdorf, I., Yoon, S.H. and Youle, R.J. 2001. Bax and Bak coalesce into novel mitochondria-associated clusters during apoptosis. *Journal of Cell Biology* 153: 1265–1276.

Nesnow, S., Garland, H. and Curtis, G 1980.Improved transformation of C3H/10T1/2 cells by direct and indirect acting carcinogens. *Carcinogenesis* 3:397-380.

Nickens K. P., Patierno S. R. and Ceryak S. 2010 Chromium genotoxicity: a double-edged sword. *Chemico-Biology Interact*ion 188(2): 276–288.

Noda T., Fujita N. and Yoshimori T. 2009. The late stages of autophagy: how does the end begin? *Cell Death and Differentiation* 16: 984–990.

Nonoyama, T., and Fukuda, R. 2008. Drug-induced phospholipidosispathological aspects and its prediction. *Journal of Toxicology and Pathology* 21: 9–24.

Obembe, E., Sokomba S., Olorunfemi O. and Alemika T. 1994. Antipsychotic effects and tolerance of crude *Rauvolfia vomitoria* in Nigerian psychiatric in-patients. *Phytotherapy. Research* 8(4): 218- 223.

Oberhammer, F., Wilson, J. W., Dive, C., Morris, I. D., Hickman, J. A., Wakeling, A. E., Walker, P. R. and Sikorska M. 1993. Apoptotic death in epithelial cells: cleavage of DNA to 300 and/or 50 kb fragments prior to or in the absence of internucleosomal fragmentation. *Europen Molecular Biology Organisation Journal 12*: 3679-3684.

Oberst, A., Pop, C., Tremblay, A.G., Blais, V., Denault, J.B., Salvesen, G.S. and Green, D.R. 2010. Inducible dimerization and inducible cleavage reveal a requirement for both processes in caspase-8 activation. *Journal of Biological Chem*istry 285: 16632–16642.

O'Brien, T.J, Ceryak, S. and Patierno, S.R. 2003. Complexities of chromium carcinogenesis: role of cellular response, repair and recovery mechanisms. *Mutation Research*. 533: 3–36.

O'Brien,T., Mandel,H.G., Pritchard, D.E. and Patierno,S.R. 2002. Critical role of chromium (Cr)–DNA interactions in the formation of Cr-induced polymerase arresting lesions. *Biochemistry* 41: 12529–12537.

O'Brien, T. J., Brooks, B. R., and Patierno, S. R. 2005. Nucleotide excision repair functions in the removal of chromium induced DNA damage in mammalian cells. *Molecular and Cellular Biochem*istry 279: 85–95.

Ochi, T. 2002. Methylmercury, but not inorganic mercury, causes abnormality of centrosome integrity (multiple foci of γ-tubulin), multipolar spindles and multinucleated cells without microtubule disruption in cultured Chinese hamster V79 cells. *Toxicology* 175:111–21.

Occupational and Health Safety Administration 2006. *Health Effects of Hexavalent Chromium* . U.S. Department of Labor.

Odunola, O.A., Uka, E. , Akinwumi , K.A. Gbadegesin, M. A. and Osifeso,O.O. 2008. Exposure of laboratory mice to domestic cooking gas: risk implication for toxicity. *International Journal of Environmental Research and Public Health* 5 (3):170-175.

Odunola, O.A., Akinwumi, K.A., Ogunbiyi, B. and Tugbobo O. 2007. Interaction and enhancement of the toxic effects of sodium arsenite and lead acetate in wistar rats. *African Journal of Biomedical Research* 10: 59 – 65.

Ojo, O., Soretiwa,O., Ajayi S., and Owolabi, L.O. 2012. Phytochemical screening, anti-nutrient composition, proximate analyses and the antimicrobial activities of the aqueous and organic extracts of bark of *Rauvolfia vomitoria* and leaves of *Peperomia pellucid. International Research Journal of Biochemistry and Bioinformatics*. 2(6): 127-134.

O'Hara, K.A., Nemec, A.A., Alam, J., Klei, L.R., Mossman, B.T., Barchowsky, A.2006. Chromium (VI) inhibits heme oxygenase-1 expression in vivo and in arsenic-exposed human airway epithelial cells. *Journal of Cell Physiology*: 113-21.

Ortega, R., Fayard, B., Salome, M., Deves, G. and Susini, J. 2005.Chromium oxidation state imaging in mammalian cells exposed in vitro to soluble or particulate chromate compounds. *Chemical Research Toxicol*ogy 18: 1512–1519.

OSHA 2006. *Occupational exposure to hexavalent chromium*. Final rule Federal Registry. 71, 10099-10385

Otsuki, Y., Li, Z., Shibata, M.A. 2003. Apoptotic detection methods–from morphology to gene. *Progress in Histochemistry and Cytochem*istry 38:275–339.

Oze, C., Bird, D. K. and Fendorf, S. 2007. Genesis of hexavalent chromium from natural sources in soil and groundwater. *Proceedings of the National Academy of Science*104: 6544–6549

Patel, T., Gores, G.J. and Kaufmann,S.H.1996. The role of proteases during apoptosis. *Federation of American Societies for Experimental Biology Journal* 10: 587–597.

Papathanasiou, M.A., Kerr, N.C., Robbins J.H., McBride, O.W., Alamo I. Jr, Barrett S.F, Hickson I.D, Fornace A.J. Jr. 1989. Mammalian genes coordinately regulated by growth arrest signals and DNA-damaging agents. *Molecular Cell Biology* 10: 4196–203.

Parys, S., Kehraus, S., Krick, A., Glombitza, K.W., Carmeli, S. and Klimo, K. 2010. In vitro chemopreventive potential of fucophlorethols from the brown alga *Fucus*

vesiculosus L. by anti-oxidant activity and inhibition of selected Cytochrome P450 enzymes. *Phytochemistry* 71: 221-229.

Patierno, S., Banh, D. and Landolph J. 1988. Transformation of C3H/10T1/2 mouse embryo cells to focus formation and achorage independence by insoluble lead chromate but not soluble calcium chromate: relationship to mutagenesis and internalization of lead chromate particles. *Cancer Research* 48: 5280-5288.

Patlolla, A.K., Barnes C., Hackett, D. and Tchounwou P.B. 2009. Potassium dichromate induced cytotoxicity, genotoxicity and oxidative stress in human liver carcinoma (HepG2) cells. .*International Journal of Environmental Research and Public Health*. 6: 643–653.

Pelicano, H., Carney, D. and Huang, P. 2004. ROS stress in cancer cells and therapeutic implications. *Drug Resistance Update* 7: 97–110.

Pellerin, C. and Booker, S. M. 2000. Reflections on hexavalent chromium: health hazards of an industrial heavyweight. *Environmental Health Perspect*ive 108: A402–407.

Perez, A., Ramirez-Ramos, M., Calleja,C., Martin,D., Namorado,M., Sierra,G.,Ramirez –Ramos, M.E., Paniagua, R., Sanchez,Y., Arreola,L. and Reyes, J.L. 2004. Beneficial effect of retinoic acid on the outcome of experimental acute renal failure, *Nephrology Dialysis and Transplantation* 19:2464-2471.

Pettit, D.K., Hoffman, A.S. and Horbett T.A. 1994. Correlation between corneal epithelial cell outgrowth and monoclonal antibody binding to the cell binding domain of absorbed fibronectin. *Journal of Biomedical Material Research* 28 (6): 685-91.

Piacentini, M., Fesus, I., Farrace, M.G., Ghibelli, L., Piredda, L., and Meline, G. 1995. The expression of ‘‘tissue’’ transglutaminase in two human cancer cell lines is related to with programmed cell death (apoptosis*). European Journal of Cell Biol*ogy 54:246–254.

Pillay, K., von Blottnitz, H. and Petersen, J. 2003. Ageing of chromium (III)-bearing slag and its relation to the atmospheric oxidation of solid chromium (III)-oxide in the presence of calcium oxide. *Chemosphere* 52: 1771–1779.

Poljsak, B., Gazdag, Z., Jenko-Brinovec, S., Fujs, S., Pesti, M., Belagyi, J., Plesnicar, S., Raspor, P. 2005. Pro-oxidative vs antioxidative properties of ascorbic acid in chromium (VI) induced damage: an in vivo and in vitro approach. *Journal of Applied Toxicol*ogy 25: 535-548.

Pop, C. and Salvesen, G.S. 2009. Human caspases: activation, specificity, and regulation. *Journal of Biological Chem*istry 284: 21777–21781.

Promega 2012. Technical bulletin for caspase-glo3/7 assay instructions for use of products G8090, G8091, G8092 AND G8093. U.S. Pat. No. 6,602,677 and 7, 241,584.

Pousset,,J.L., Poisson, J. 1965. Rauwolfia alkaloids: New alkaloids from the leaves of *Rauwolfia vomitoria Afz***.** *Annals of Pharmarcy Fr*. 23(12): 733-38.

Principe, P. 1989. *Economic and Medicinal Research*. Wagner H., Hikino H., Farnsworth, N.R. eds. Vol. 3 London: Academic Press. pp 1-17.

Qiagen 2012. RT^{2}Profiler PCR Array Handbook .U.S. Pat. No.5,994,056 and 6,171,785.

Quievryn, G., Messer, J. and Zhitkovich, A. 2002. Carcinogenic chromium (VI) induces cross-linking of vitamin C to DNA in vitro and in human lung A549 cells. *Biochemistry* 41: 3156–3167.

Quievryn, G., Peterson, E., Messer, J. and Zhitkovich A. 2003. Genotoxicity and mutagenicity of chromium (VI) / ascorbate generated DNA adducts in human and bacterial cells. *Biochemistry* 42: 1062–1070.

Quinteros, F. A., Leticia, I. M., Miler, E. A. , Jimena, P. C. and Beatriz, H. D. 2008. Mechanisms of chromium (VI)-induced apoptosis in anterior pituitary cells. *Toxicology* 249: 109–115.

Qu X. and Qing L. 2004. Abrin induces HeLa cell apoptosis by cytochrome c release and caspase activation. *Journal of Biochemistry and Molecular Biol*ogy 37: 445–453.

Raman N. and Atkinson S.J. 1999. Rho controls actin cytoskeletal assembly in renal epithelial cells during ATP depletion and recovery. *American Journal of Physiology*: 276: C1312-24.

Ramadan S., Terrinoni A., Catani M.V., Sayan A.E., Knight R.A., Mueller M., Krammer P.H., Melino G. and Candi E. 2005. p73 induces apoptosis by different mechanisms. *Biochemical and Biophysics Research Commun*ication 331: 713–717.

Rao, J. Y., Y. S. Jin, Q. Zheng, J. Cheng, J. Tai, and Hemstreet, G. P. 1999. Alterations of the actin polymerization status as an apoptotic morphological effector in HL-60 cells. *Journal Cell Biochemistry* 75:686–697.

Reed, J.C. 1999. Mechanisms of apoptosis avoidance in cancer. *Current Opinion in Oncology* 11*:* 68-75.

Reynolds, M., and Zhitkovich, A. 2007. Cellular vitamin C increases chromate toxicity via a death program requiring mismatch repair but not p53. *Carcinogenesis* 28: 1613–1620.

Reynolds, M., Peterson, E., Quievryn, G. and Zhitkovich, A. 2004. Human nucleotide excision repair efficiently removes chromium- DNA phosphate adducts and protects cells against chromate toxicity. *Journal of Biological Chem*istry 279: 30419–30424.

Reynolds, M., Stoddard, L., Bespalov, I. and Zhitkovich, A. 2007. Ascorbate acts as a highly potent inducer of chromate mutagenesis and clastogenesis: linkage to DNA breaks in G2 phase by mismatch repair. *Nucleic Acids Res*earch 35: 465–476.

Reznikoff, C.A., Brankow, D.W. and Heidelberger, C. l973a. Establishment and characterization of a cloned line of C3H Mouse embryo cells sensitive to post confluence Inhibition of division. *Cancer Research* 33: 3231-3238.

Reznikoff, C., Bertram, J., Brankow, D., and Heidelberger, C 1973b. Quantitative and qualitative studies of chemical transformation of cloned C3H mouse embryo cells sensitive to postconfluence inhibition of cell division. *Cancer Research* 33**:** 3239-3249.

Reitman S. and Frankel S. 1957. A colorimetric method for the determination of serum glutamate oxaloacetic and glutamate pyruvic transaminases. *American Journal of Clinical Pathology* 28(1): 56-63.

Ríos-Arrabal, S, Artacho-Cordón, Francisco, León, Josefa, Román-Marinetto, E., Salinas-Asensio M., Calvente, I. and Núñez, M. I. 2013. Involvement of free radicals in breast cancer. *SpringerPlus* 2: 404.

Rudolf, E. and Červinka, M. 2006. The role of intracellular zinc in chromium (VI)-induced oxidative stress, DNA damage and apoptosis. *Chemico-Biological Interactions* 162: 212–227.

Rose, R.C. 1988. Transport of ascorbic acid and other water-soluble vitamins. *Biochimica Biophysica Acta.*947, 335–366

Saygi, *K.O.,* Tuzen, *M.* , Soylak, *M.* and Elci, L. 2008. Chromium speciation by solid phase extraction on Dowex M 4195 chelating resin and determination by atomic absorption spectrometry. *Journal of Hazardous Materials* 153: 1009–1014.

Saha, K.C. 1995. Chronic arsenical dermatosis from tube-well water in West Bengal during 1983–87. *Indian Journal of Dermatology* 40**:** 1–12.

Salnikow, K., Donald, S. P., Bruick, R. K., Zhitkovich, A., Phang, J. M. and Kasprzak, K. S. 2004. Depletion of intracellular ascorbate by the carcinogenic metals nickel and cobalt results in the induction of hypoxic stress. *Journal of Biological Chemistry* 279: 40337–40344.

Salnikow, K. and Zhitkovich, A. 2008. Genetic and epigenetic mechanisms in metal carcinogenesis and cocarcinogenesis: nickel, arsenic and chromium. *Chemical Research Toxicology* 21: 28–44.

Savill, J. and Fadok, V. 2000. Corpse clearance defines the meaning of cell death. *Nature* 407 : 784–788.

Scherz-Shouval, R, Shvets, E, Fass, E, Shorer, H, Gil, L. and El Azar, Z. 2007: Reactive oxygen species are essential for autophagy and specifically regulate the activity of Atg4. *European Molecular Biology Association* Journal 26: 1749–1760.

Schnekenburger, M., Talaska, G. and Puga, A. 2007. Chromium cross-links histone deacetylase 1-DNA methyltransferase 1 complexes to chromatin, inhibiting histone-remodeling marks critical for transcriptional activation. *Molecular Cell Biol*ogy 27: 7089–7101.

Schmid, W. 1975. Chemical mutagen testing on *in-vivo* somatic mammalian cells. Agents and Action 3: 77-85

Schmid, W. 1973. The micronucleus test. *Mutation Research* 31:9- 15

Schnekenburger, M., Talaska, G. and Puga, A. 2007. Chromium cross-links histone deacetylase 1-DNA methyltransferase 1 complexes to chromatin, inhibiting histone-remodeling marks critical for transcriptional activation. *Molecular and Cellular Biol*ogy 27: 7089–7101.

Scorrano, L., Ashiya M., Buttle, K, Weiler, S., Oakes, S.A. , Mannella, C.A,. Korsmeyer SJ 2002. A distinct pathway remodels mitochondrial cristae and mobilizes cytochrome c during apoptosis. *Developmental Cell.* 2: 55–67.

Seager, A. L., Ume-Kulsoom, S., Katja, Brüsehafer, J. Wills, B., Manshian, K. E. , Chapman, A. , Thomas D., , Andrew, D. S., Ann, T. D., Shareen, H. D., George, E. J. and Gareth,

J., Jenkins S. 2014. Recommendations, evaluation and validation of a semi-automated, fluorescent-based scoring protocol for micronucleus testing in human cells. *Mutagenesis* 29:155–164.

Sedman, R.M., Beaumont, J. McDonald, T.A., Reynolds, S., Krowech G. and Howd R. 2006. Review of the evidence regarding the carcinogenicity of hexavalent chromium in drinking water. *Journal of Environmental Science Health, Environmental Carcinogenesis and Ecotoxicology Review* 24: 155–182.

Shadreck, M. and Mugadza, T. 2013. Chromium, an essential nutrient and pollutant: A review. *African. Journal of Pure and Applied Chemistry* 7: 310-17.

Sheehan D., Meade, G., Foley V. M. and Dowd C. A. 2001. Structure, function and evolution of glutathione transferases: implications for classification of non-mammalian members of an ancient enzyme superfamily. *Biochemistry Journal 360*: 1-16.

Shen, K., Ji, L., Chen, Y., Yu, Q. and Wang, Z. 2011. Influence of glutathione levels and activity of glutathione-related enzymes in the brains of tumor-bearing mice. *Bioscience trends* 5(1): 30–37.

Shi, H., Shi, X., Liu, K.J. 2004. Oxidative mechanisms of arsenic toxicity and carcinogenesis. *Molecular Cell Biochemistry* 255: 67–78.

Shi, X. 1999. Reduction of Chromium (VI) and Its Relationship to Carcinogenesis. *Journal of Toxicology and Environmental Health* 2: 87-104.

Shimizu, S., Kanaseki, T., Mizushima N., Mizuta T., Arakawa-Kobayashi S., Thompson C.B., Tsujimoto Y. 2004. Role of Bcl-2 family proteins in a non-apoptotic programmed cell death dependent on autophagy genes. *Nature Cell Biology* 6: 1221–1228.

Shindo, Y., Toyoda, Y. and Kawamura, K. 1989: Micronucleus test with potassium chromate (VI administered intraperitoneally and orally to mice. *Mutation Research 223*: 403–6.

Shu, X.O., Zheng Y., Cai, H., Gu. K, Chen, Z., Zheng, W. 2009. Soy food intake and breast cancer survival. *Journal of American Medical Association* 302: 2437–43.

Siegel, R. M. 2006. Caspases at the crossroads of immune-cell life and death. *Nature Reviews Immunology* 6 (4): 308–317.

Singh, R.P., Banerjee, S., Kumar, P.V.S., Raveesha, K.A., and Rao, A.R. 2006. Tinospora cordifolia induces enzymes of carcinogen/drug metabolism and antioxidant system and inhibits lipid peroxidation in mice. *Phytomedicine*13: 74-84.

Singh, J., Carlisle, D.L., Pritchard, D.E. and Patierno, S.R. 1999.Chromium-induced genotoxicity and apoptosis: relationship to chromium carcinogenesis (review*). Oncology Rep*ort 5: 1307–1318.

Skovbjerg, L.L., Stipp, S.L.S., Utsunomiya, S., and Ewing, R.C. 2006. The mechanisms of reduction of hexavalent chromium by green rust sodium sulfate: Formation of Cr-goethite. *Geochimica et Cosmochimica Acta*. 70: 3582-3592.

Slade, P. G., Priestley, N. D., and Sugden, K. D. 2007. Spiroiminodihydantoin as an oxo-atom transfer product of 8-oxo-20- deoxyguanosine oxidation by chromium(V). *Organic Lett*ers 9: 4411–4414.

Smyth, M.J., Godfrey, D.I. and Trapani, J.A. 2001. A fresh look at tumor immunosurveillance and immunotherapy. *Nature Immunology* 2: 293–9.

Sofowora, A.E. 1993. Medicinal plants and traditional medicine in Africa. 2nd Ed. Ibadan: Spectrum Book Ltd.

Son, Y.O., Hitron, J.A., Wang, X., Chang, Q., Pan, J., Zhang, Z., Liu, J., Wang, S., Lee, J.C. and Shi, X. 2010. Cr(VI) induces mitochondrial-mediated and caspase-dependent apoptosis through reactive oxygen species-mediated p53 activation in JB6 Cl41 cells. *Toxicology and Applied pharmacology* 245(2): 226-35.

Song, M., Youn-Jung, K., and Jae-Chun, R. 2011. Phospholipidosis induced by PPARc signaling in Human Bronchial Epithelial (BEAS-2B) cells exposed to Amiodarone. *Toxicological Science* 120(1): 98–108.

Steffee, C.H. and Baettjer A.M. 1965. Histopathologic effects of chromate chemicals. Archive Environment Health 11: 66–75.

Sugden, K. D., Campo, C. K. and Martin, B. D. 2001 Direct oxidation of guanine and 7,8-dihydro-8 oxoguanine in DNA by a highvalent chromium complex: a possible mechanism for chromate genotoxicity. *Chemical Research Toxicology* 14: 1315–1322.

Sugiyama, M., Tsuzuki, K., and Ogura, R. 1991.Effect of ascorbic acid on DNA damage, cytotoxicity, glutathione reductase, and formation of paramagnetic chromium in Chinese hamster V-79 cells treated with sodium chromate(VI). *Journal Biological Chemical 266* (6): 3383- 3386.

Standeven, A. M. and Wetterhahn, K. E. 1992. Ascorbate is the principal reductant of chromium (VI) in rat lung ultrafiltrates and cytosols, and mediates chromium-DNA binding in vitro. *Carcinogenesis* 13:1319–1324.

Standeven, A. M. and Wetterhahn, K.E. 1989. Chromium(VI) Toxicity: Uptake, Reduction, and DNA Damage. *International Journal of Toxicology* 8 (7): 1275-1283

Stern, A. H., Fagliano, J. A., Savrin, J. E., Freeman, N. C., and Lioy, P. J. 1998. The association of chromium in household dust with urinary chromium in residences adjacent to chromate production waste sites. *Environental Health Perspective* 106: 833–839.

Suzuki, Y. and Fukuda, K. 1990. Reduction of hexavalent chromium by ascorbic acid and glutathione with special reference to the rat lung. *Archives of Toxicol*ogy 64: 169–176.

Surh, Y.J. 2003. Cancer chemoprevention with dietary phytochemicals. *Nature Review Cancer* 3: 768-780.

Taylor, B.F, McNeely, S.C., Miller, H.L., States, J.C. 2008. Arsenite-induced mitotic death involves stress response and is independent of tubulin polymerization. *Toxicology and Applied Pharmacol*ogy 230:235–46.

Talasz, H., Helliger, W., Sarg, B., Debbage, P.L., Puschendorf, B. and Lindner, H. 2002. Hyperphosphorylation of histone H2A.X and dephosphorylation of histone H1 subtypes in the course of apoptosis. *Cell Death and Differentiation*. 9: 27–39.

.Tennant, D.A., Duran, R.V. and Gottlieb, E. 2010. Targeting metabolic transformation for cancer therapy. *Nature Review Cancer* 10: 267–77.

Tian, H., Cheng, K., Wang, Y., Zhao, D., Lu, L., 2012. Temporal and spatial variation characteristics of atmospheric emissions of Cd, Cr, and Pb from coal in China. *Atmospheric Environment* 50: 157–163.

Tseng, C.H., Tseng, C.P., Chiou, H.Y., Hsueh, Y.M., Chong, C.K., and Chen C.J. 2002. Epidemiologic evidence of diabetogenic effect of arsenic. *Toxicological Letters* 133: 69–76.

Tziritis, E., Kelepertzis, E., Korres, G., Perivolaris, D and Repani, S. 2012. Hexavalent chromium contamination in groundwaters of Thiva Basin, Central Greece. *Bulletin of Environmental Contamination and Toxicology* 89: 1073.

Ujihara, Y., Miyazak, H. and Wada, S. 2008. Morphological study of fibroblasts treated with cytochalasin D and colchicine using a Confocal Laser Scanning Microscopy. *Journal Physiological Science* 58 (7): 499–506.

Urbano, A., Carlos M., Rodrigues, F.D. and Maria, C. A. 2008. Hexavalent chromium exposure, genomic instability and lung cancer. *Gene Therapy and Molecular Biol*ogy 12: 219-238.

U.S. EPA 1999. Integrated Risk Information System on Chromium. Washington D.C.: U.S

Vakkila J. and Lotze, M.T. 2004. Inflammation and necrosis promote tumour growth. *Nature Reviews Immunology* .4: 641-648.

Valko, M., Rhodes,C.J., Moncol, J., Izakovic,M., and Mazur M. 2006. Free radicals, metals and antioxidants in oxidative stress-induced cancer. *Chemico-Biological Interactions* 160: 1–40.

Vallat, L., Magdelenat, H., Merle-Beral, H., Masdehors, P. , de Montalk, G., Davi, F., Kruhoffer, M., Sabatier, L., Orntoft, T.F., Delic, J. 2003. The resistance of B-CLL cells to DNA damage-induced apoptosis defined by DNA microarrays. *Blood* 101: 4598–606.

Vega, L., Gosebett, M.E. and Ostroky, W.P. 1995. Aneugenic effects of sodium arsenite on human lymphocytes in vitro: an individual susceptibility effects and defects. *Mutation Res*earch 334 (3): 356- 378.

Vel Szic, K.S., Ndlovu, M.N., Haegeman, G., Vanden Berghe W. 2010. Nature or nurture: let food be your epigenetic medicine in chronic inflammatory disorders. *Biochemical Pharmacology* 80:1816–32.

Vincent, J.C., Robert, A.B., Kurt, S., Yann, G., Marie, B.S., Fathia, EG and Kleihues, P. 2004. The science of practice of carcinogen identification and evaluation. *Evironmental Health Persp*ective 112 (13): 1269-1274.

Vogelstein, B. and Kinzler, K.W. 2004. Cancer genes and the pathways they control. *Nature Medicine.*10:789-799.

Voitkun, V., Zhitkovich, A. and Costa, M. 1998. Cr (III)- mediated crosslinks of glutathione or amino acids to the DNA phosphate backbone are mutagenic in human cells. *Nucleic Acids Research* 26: 2024–2030.

Wang, X.W. and Harris C.C. 1997. *p53* tumor-suppressor gene: clues to molecular carcinogenesis. *Journal Cell Physiol*ogy: 173:247–55.

Watanabe, K., Sakamoto, K. and Sasaki, T. 1998. Comparisons on chemically-induced mutation among four bacterial strains, Salmonella typhimurium TA102 and TA2638, and *Escherichia coli* WP2/ pKM101 and WP2 uvrA/pKM101: collaborative study II. *Mutation Res*earch 412: 17–31.

Wattenberg L. W. 1997. An overview of chemoprevention: current status and future prospect. *Proceedings of the Society for Experimental Biology and Med*icine 216**:**133-144.

Weber, H. 1983. Long-term study of the distribution of soluble chromate-51 in the rat after a single intratracheal administration. *Journal of Toxicology and Environmental Health* 11**:** 749–764.

Weichselbaum, T.E. 1946. An accurate and rapid method for the determination of proteins in small amounts of blood serum and plasma. *American Journal of Clinical Pathology* 10:40-9

Wiegand, H.J. 1984. Disposition of intratracheally administered chromium (III) and chromium (VI) in rabbits. *Toxicology Letters* 22**:** 273–276

Wise, S.S., Holmes, A.L., Qin, Q., Xie, H., Katsifis. S.P., Thompson, W.D., Wise, J.P. 2009. Comparative genotoxicity and cytotoxicity of four hexavalent chromium compounds in human bronchial cells. *Chemical Research Toxicol*ogy 23: 365–372.

Wise, S.S., Holmes, A.L., Xie, H., Thompson, W.D. and Wise, Sr, J.P. 2006. Chronic exposure to particulate chromate induces spindle assembly checkpoint bypass in human lung cells. *Chemical Research Toxicology* 19: 1492–1498

Wise, J. P., Sr., Orenstein, J. M., and Patierno, S. R. 1993. Inhibition of lead chromate clastogenesis by ascorbate: Relationship to particle dissolution and uptake. *Carcinogenesis 14* (3): 429-434.

White, M.K. and Cinti, C. 2004. A morphologic approach to detect apoptosis based on electron microscopy. *Methods in Molecular Biol*ogy 285: 105–11.

White, S. R., Williams, P., Wojcik, K. R., Sun, S., Hiemstra, P. S., Rabe, K. F. and Dorscheid, D. R. 2001. Initiation of apoptosis by actin cytoskeletal derangement with cytochalasin D and jasplakinolide in human airway epithelial cells. *American Journal of Respiratory and Cell Molecular Biologgy* 24:282–294.

White, E. and DiPaola, R.S. 2009.The double-edged sword of autophagy modulation in cancer. *Clinical Cancer Res*earch 15:5308–16.

Wojtczak, L. and Schonfeld, P. 1993. Effect of fatty acids on energy coupling processes in mitochondria. *Biochimical Biophys*ics *Acta* 1183: 41–57.

World Health Organisation 2000. Chromium. World Health Organisation Regional Office for Europe, Copenhagen, Denmark.

Wu, N., Zu, Y., Fu, Y., Kong, Y., Zhao, J., Li, X., Li, J., Wink, .M., and Efferth T. 2010. Antioxidant activities and xanthine oxidase inhibitory effects of extracts and main polyphenolic compounds obtained from Geranium sibiricum L. *Journal of Agricultural Food Chemistry* 58(8):4737-43.

Wyllie, A. H. 1980. Glucocorticoid-induced thymocyte apoptosis is associated with endogenous endonuclease activation. *Nature* 284: 555–6.

Xiao, F., Feng, X., Zeng, M., Guan, L., Hu, Q., and Zhong, C. 2012. Hexavalent chromium induces energy metabolism disturbance and p53-dependent cell cycle arrest via reactive oxygen species in L-02 hepatocytes. *Molecular and Cellular Biochemistry* 371 (1-2): 65-76.

Xie, H., Wise,S.S., Holmes,A.L., Xu,B., Wakeman,T.P., Pelsue,S.C., Singh,N.P. and Wise,J.P., Sr. 2005. Carcinogenic lead chromate induces DNA double-strand breaks in human lung cells. *Mutation Research* 586: 160-172.

Xie, H., Holmes, A.L., Wise, S.S., Gordon, N., and Wise, J.P., Sr. 2004. Lead chromate-induced chromosome damage requires extracellular dissolution to liberate chromium ions but does not require particle internalization or intracellular dissolution. *Chemical Research Toxicology* 17, 1362-1367.

Xu, Y., Kim, S.O., Li, Y. and Han, J. 2006. Autophagy contributes to caspase-independent

macrophage cell death. *Journal of Biological Chemistry* 281: 19179–19187.

Yamanaka, F. , Takabayashi, K., Mizoi, M., An, Y., Hasegawa, A., and Okada S. 2007. Oral exposure of dimethylarsinic acid, a main metabolite of inorganic arsenics, in mice leads to an increase in 8-oxo- 2'-deoxyguanosine level, specifically in the target organs for arsenic carcinogenesis. *Biochemical Biophysics Research Comm*unication 287: 66–70.

Yang, C.Y., Chang, C.C., Tsai, S.S., Chuang, H.Y., Ho, C.K and Wu, T.N. 2003. Arsenic in drinking water and adverse pregnancy outcome in an arsenic-endemic area in northeastern Taiwan. *Environmental Research. 91***:** 29–34.

Yi, H., Wua, L., and Jianga L. 2007. Genotoxicity of arsenic evaluated by Allium-root micronucleus assay. *Science of the Total Environ*ment 383:232–236.

Yla-Anttila P., Vihinen H., Jokitalo, E. and Eskelinen, E.S.2009. 3D tomography reveals connections between the phagophore and endoplasmic reticulum. *Autophagy* 5: 1180–1185.

Yokota, S. 1993. Formation of autophagosomes during degradation of excess peroxisomes induced by administration of dioctyl phthalate. European Journal Cell Biology 61:67–80.

Yoshimori, T. 2004. Autophagy: a regulated bulk degradation process inside cells. *Biochemical Biophysics Research Communication* 313 (2): 453–458.

Young, I.S. and Woodside, J.V. 2001. Antioxidants in health and disease. *Journal of Clinical Pathol*ogy 54:176–86.

Youle, R.J. and Strasser, A. 2008. The BCL-2 protein family: opposing activities that mediate cell death. *Nature Review Molecular and Cell Biology* 9: 47–59.

Yu, J., Yan, M., Jeanne, D., Chen, Q. 2013. Antitumor activities of *rauwolfia vomitoria* Extract and potentiation of carboplatin effects against ovarian cancer. *Current Therapeutic Research* 75: 8-14.

Yu, L., Alva,A., . Su, H, Dutt,P., Freundt, E., Welsh,S., Baehrecke, E.H. and Lenardo, M.J. 2004. Regulation of an ATG7-beclin 1 program of autophagic cell death by caspase-8. *Science:* 1500–1502.

Zayed, A .M. and Terry. N. 2003. Chromium in the environment: factors affecting biological remediation. *Plant Soil* 249: 139-156.

Zecevic, A., Hagan, E., Reynolds, M., Poage, G., Johnston, T. and Zhitkovich, A. 2010. XPA impacts formation but not proteasome sensitive repair of DNA-protein crosslinks induced by chromate. *Mutagenesis* 25:381–388.

Zhang, N., Chen, Y., Jiang, R., Li, E., Chen, X., Xi, Z., Guo, Y., Liu, X., Zhou, Y., Che, Y.and Jiang, X. 2011. PARP and RIP 1 are required for autophagy induced by 11'-deoxyverticillin A, which precedes caspase-dependent apoptosis. *Autophagy* 7:598–612.

Zhang, Z., Fan,J. , and Cheney, P. P. 2009. Activatable molecular systems using homologous near- infrared fluorescent Probes for monitoring enzyme activities in vitro, in pCellulo, and *in vivo, Molecular Pharmaceutics* 6 (2) : 416–427.

Zhang, J., Campbell, R.E., Ting, A.Y. and Tsien, R.Y. 2002. Creating new fluorescent probes for cell biology. *Nature Review Molecular and Cell Biology* .3: 906–18.

Zhang, Z., Leonard, S.S., Wang, S., Vallyathan, V., Castrano,V., and Shi, X. 2001. Cr (VI) induces cell growth arrest through hydrogen peroxide-mediate reactions. *Molecular Cell Biochemistry 222* (1–2):77–83.

Zhitkovich, A. 2005. Importance of chromium-DNA adducts in mutagenicity and toxicity of chromium (VI). *Chemical Research Toxicol*ogy 18: 3–11.

Zhitkovich, A., Song, Y., Quievryn, G.. and Voitkun, V. 2001. Nonoxidative mechanisms are responsible for the induction of mutagenesis by reduction of Cr(VI) with cysteine: role of ternary DNA adducts in Cr(III)-dependent mutagenesis. *Biochemistry* 40: 549–560.

Zhitkovich, A., Voitkun, V. and Costa, M. 1995. Glutathione and free amino acids form stable adducts with DNA following exposure of intact mammalian cells to chromate. *Carcinogenesis* 16: 907–913.

Zucker, R.M., Hunter, E.S. and Rogers, J.M. 2000. Confocal laser scanning microscopy of morphology and apoptosis in organogenesis-stage mouse embryos. *Methods in Molecular Biol*ogy 135:191–202.

APPENDIX 1

Table A1: Plating Efficiency (PE) of 10T½ cells treated with $PbCrO_4$ and Lower Concentrations of Ascorbate (Asc).

Treatment	PE 1± SD (%)	PE 2± SD (%)	Avg PE± SD (%)
No Addition	33.1 ± 2.5	36.5 ± 2.4	34.8 ± 2.4
Acetone	28.5 ± 5.3	34.9 ± 1.5	31.7 ± 4.5
PbS	30.3 ± 2	34.3 ± 2.1	32.3 ± 2.8
Ac+PbS	33.2 ± 3.5	36.1 ± 16.2	34.7 ± 5.0
PbCrO4	19.1 ± 2.5	31.7 ± 3.1	25.4 ± 8.9
0.0025 Asc	31.7 ± 1.8	32.5 ± 1.4	32.1 ± 0.6
0.005 Asc	23.1 ± 4.5	34 ± 1.6	28.6 ± 7.7
0.00625 Asc	28.5 ± 1.1	33.7 ± 0.8	31.1 ± 3.7
0.01 Asc	22.6 ± 5.9	35.4 ± 3	29.0 ± 9.1
0.0125 Asc	22.5 ± 2.9	34.6 ± 3.3	28.6 ± 8.6
0.015 Asc	21.8 ± 2.7	35.4 ± 3.5	28.6 ± 9.6
0.02 Asc	28.1 ± 0.9	33.8 ± 3.7	31.0 ± 4.0
0.025 Asc	29.9 ± 0.8	35 ± 1	32.5 ± 3.6
0.0025 Asc +PbCrO4	17 ± 11.3	26.7 ± 1.3	21.9 ± 6.9
0.005 Asc +PbCrO4	8.3 ± 4.7	29.1 ± 2.7	18.7 ± 14.7
0.00625 Asc +PbCrO4	10.9 ± 6.4	24.4 ± 11.4	17.7 ± 9.5
0.01 Asc +PbCrO4	8.9 ± 7.1	26.2 ± 14.8	17.6 ± 12.2
0.0125 Asc +PbCrO4	11.9 ± 3.8	20.9 ± 12.1	16.4 ± 6.4
0.015 Asc +PbCrO4	15.5 ± 8.3	21.8 ± 12.4	18.7 ± 4.4
0.02 Asc +PbCrO4	21.9 ± 4.2	29.1 ± 2.4	25.5 ± 5.1
0.025 Asc +PbCrO4	9.9 ± 3.3	25.7 ± 3.1	17.8 ± 11.2

Table A2: Plating Efficiency (PE) of 10T½ cells treated with $PbCrO_4$ and Lower Concentrations of Dehydroascorbate (DeAsc).

Treatment	PE 1 ± SD (%)	PE 2 ± SD (%)	Avg PE ± SD (%)
No Addition	33.1 ± 2.5	36.5 ± 2.4	34.8 ± 2.4
Acetone	28.5 ± 5.3	34.9 ± 1.5	31.7 ± 4.5
PbS	30.3 ± 2	34.3 ± 2.1	32.3 ± 2.8
Ac+PbS	33.2 ± 3.5	36.1 ± 16.2	34.7 ± 2.1
PbCrO4	19.1 ± 2.5	32.6 ± 3.3	25.9 ± 9.5
0.00025 De Asc	29.6 ± 13.5	37.9 ± 2.9	33.8 ± 5.9
0.0005 DeAsc	27.7 ± 2.7	30.8 ± 2.4	29.3 ± 2.2
0.001 De Asc	30.6 ± 2	34.4 ± 2.2	32.5 ± 2.7
0.002 De Asc	31.4 ± 4.3	36.9 ± 2.5	34.1 ± 3.9
0.0003 De Asc	27.8 ± 2.7	37 ± 3.2	32.4 ± 6.5
0.004 De Asc	30.9 ± 1.8	33.4 ± 3.8	32.2 ± 1.8
.005 De Asc	26 ± 1.4	34 ± 3	30.0 ± 5.7
.00025 DeAsc +PbCrO4	20.2 ± 10.7	25.3 ± 14.6	22.8 ± 3.6
0.0005 DeAsc+PbCrO4	16.6 ± 15.3	26.4 ± 5.4	21.5 ± 6.9
0.001 DeAsc+PBCrO4	18.8 ± 7.5	21.4 ± 10.5	20.1 ± 1.8
0.002 DeAsc+PBCrO4	17.4 ± 6.3	15.6 ± 14.5	16.5 ± 1.3
0.003 DeAsc +PBCrO4	13.6 ± 6.7	22.5 ± 12.9	18.1 ± 6.3
0.004 DeAsc+PBCrO4	23.1 ± 1.8	24.7 ± 14.2	23.9 ± 1.1
0.005 DeAsc+PbCrO4	20.2 ± 10.9	16.8 ± 14.7	18.5 ± 2.4

Table A3: Percentage plating efficiency of 10T½ cells treated with unsonicated lead chromate

Treatment	PE 1 ± SD (%)	PE 2 ± SD (%)	PE 3 ± SD (%)	Avg PE ± SD (%)
No Addition	49.1 ± 1.4	46.3 ± 1.7	46.6 ± 4.3	47.3 ± 1.5
Acetone	45.5 ± 7.2	46.5 ± 3.6	47.5 ± 3	46.5 ± 1.0
0.5 µg/mL	43.3 ± 3	41.9 ± 3.1	38.9 ± 3.6	41.4 ± 2.2
1 µg/mL	39.1 ± 4.7	40.9 ± 5.6	36.7 ± 5.8	38.9 ± 2.1
1.62 µg/mL	35.4 ± 2.5	30.9 ± 2.9	34.1 ± 9.1	33.5 ± 2.3
2.5 µg/mL	31.6 ± 3.7	28.9 ± 7.2	32.6 ± 7.9	31 ± 1.9
5.0 µg/mL	5.8 ± 4.7	4.5 ± 4.2	1.5 ± 0.4	3.9 ± 2.2
7.5 µg/mL	5.8 ± 11.5	0.3 ± 0.5	0.3 ± 0.4	2.1± 3.2
10 µg/mL	0 ± 0	0 ± 0	0 ± 0	0 ± 0

Table A4: Plating efficiency of 10T½ cells treated with sonicated lead chromate

Treatment	PE1± SD (%)	PE2± SD (%)	Average PE± SD (%)
No Addition	18.6 ± 1.9	16.8 ± 3.4	17.7 ± 1.3
Acetone	17 ± 6.2	14.3 ± 4.3	15.65 ± 1.9
0.5 µg/mL	8.25 ± 1.3	8.375 ± 4.2	8.3125 ± 0.1
1 µg/mL	6.3 ± 1.3	7.7 ± 1.7	7 ± 1.0
1.62 µg/mL	6.6 ± 0.7	6.9 ± 1.4	6.75 ± 0.2
2.5 µg/mL	0 ± 0	0.4 ± 0.4	0.2 ± 0.3
5.0 µg/mL	0 ± 0	0 ± 0	0 ± 0
7.5 µg/mL	0 ± 0	0 ± 0	0 ± 0
10 µg/mL	0 ± 0	0 ± 0	0 ± 0

Table A5: Plating efficiency of 10T½ cells treated with Unsonicated $BaCrO_4$.

Treatment	PE 1 ± SD (%)	PE 2 ± SD (%)	PE 3 ± SD (%)	Avg PE± SD (%)
No Addition	43.7 ± 3.3	43.8 ± 4.2	44.5 ± 2.6	44 ± 0.4
Acetone	40.7 ± 4.2	41.6 ± 3	41.5 ± 3.7	41.3 ± 0.5
0.5 µg/mL	34.2 ± 2.1	35.6 ± 4	33.4 ± 5.9	34.4 ± 1.1
1.0 µg/mL	19.8 ± 9	18.5 ± 2.9	21.8 ± 7.8	20 ± 1.6
2.5 µg/mL	9.9 ± 5.9	10 ± 0.6	10.1 ± 3.5	10 ± 0.1
5 µg/mL	7.5 ± 2.7	5.4 ± 2.1	5.8 ± 3.7	6.2 ± 1.1
7.5 µg/mL	2.9 ± 1.6	3.7 ± 2.6	1.8 ± 0.9	2.8 ± 1.0
10 µg/mL	1.2 ± 1.4	2.2 ± 1.3	2.8 ± 0.9	2.1 ± 0.8

Table A6: **Plating efficiency of 10T½ cells treated with sonicated $BaCrO_4$ chromate.**

Treatment	PE 1 ± SD (%)	PE 2± SD (%)	Avg PE± SD (%)
No Addition	27.3 ± 3.5	22.7 ± 2	25 ± 3.2
Acetone	22.4 ± 3.3	22.4 ± 3	22.4 ± 0
0.5 µg/mL	11.8 ± 0.8	9.9 ± 2.2	10.85 ± 1.3
1.0 µg/mL	5.8 ± 1.1	7.1 ± 2.3	6.45 ± 0.9
2.5 µg/mL	5.5 ± 1.3	5.8 ± 1.3	5.65 ± 0.2
5 µg/mL	3 ± 1.4	3.7 ± 1.2	3.35 ± 0.5
7.5 µg/mL	1.3 ± 0.9	2.6 ± 0.7	1.95 ± 0.9
10 µg/mL	0.9 ± 0.7	1.1 ± 1.1	1 ± 0.1

Table A7: Percentage Plating Efficiency of 10T½ cells treated with lower concentrations of unsonicated $SrCrO_4$.

Treatment	PE 1 ± SD (%)	PE 2 ± SD (%)	PE 3 ± SD (%)	Avg PE± SD (%)
No Addition	30 ± 2.0	28.9 ± 3.5	30 ± 2.0	29.6 ± 0.6
Acetone	29.1 ± 2.4	27.6 ± 12.4	29.4 ± 1.8	28.7 ± 1.0
0.125 ug/mL	23.7 ± 2.8	23.6 ± 11.5	18.8 ± 1.5	22 ± 2.8
0.25 ug/mL	21.875 ± 10.1	18.1 ± 8.4	15.9 ± 3.4	18.6 ± 3.0
0.5 ug/mL	11.2 ± 2	11.9 ± 6.5	10 ± 6.2	11 ± 1.0
1.0 ug/mL	9.5 ± 4.4	2.4 ± 2.7	6.8 ± 5.4	6.2 ± 3.6
2.5ug/mL	0.2 ± 0.3	0 ± 0	2.7 ± 2.3	1 ± 1.5
5 ug/mL	0 ± 0	0 ± 0	0 ± 0	0 ± 0

TableA8: Percentage Plating Efficiency 10T½ cells treated with lower concentrations of sonicated $SrCrO_4$.

Treatment	**PE1 ± SD (%)**	**PE2 ± SD (%)**	**PE 3 ± SD (%)**	**Avg PE ± SD (%)**
No Addition	28.9 ± 3.5	30 ± 2.0	29.8 ± 2.9	29.6 ± 0.6
Acetone	28.4 ± 2.2	29.1 ± 2.4	29.4 ± 1.8	29.0 ± 0.5
0.125 ug/mL	24.875 ± 11.8	16.6 ± 3	20.125 ± 9.1	20.5 ± 4.2
0.25 ug/mL	22.1 ± 1.9	14.9 ± 2.9	12.375 ± 6.1	16.5 ± 5.0
0.5 ug/mL	13.5 ± 6.5	11.5 ± 5.8	11.875 ± 5.6	12.3 ± 1.1
1.0 ug/mL	6.5 ± 4.5	3.8 ± 1.6	1.6 ± 1.3	4.0 ± 2.5
2.5 ug/mL	0 ± 0	0.4 ± 0.5	0.2 ± 0.4	0.2 ± 0.2
5.0 ug/mL	0 ± 0	0 ± 0	0 ± 0	0 ± 0

APPENDIX 2

Table A9: Pro-apoptosis genes in RT^2 profiler array

Symbol	Description
Abl1	C-abl oncogene 1, non-receptor tyrosine kinase
Apaf1	Apoptotic peptidase activating factor 1
Atp6v1g2	ATPase, H+ transporting, lysosomal V1 subunit G2
Bax	CD40 ligand
Bcl2l11	CD40 ligand
Birc2	CD40 ligand
Casp1	CD40 ligand
Casp3	Caspase 3
Casp6	CD40 ligand
Casp7	CD40 ligand
Casp9	CD40 ligand
Cd40	CD40 ligand
Cflar	CASP8 and FADD-like apoptosis regulator
Cyld	Cylindromatosis (turban tumor syndrome)
Dffa	DNA fragmentation factor, alpha subunit
Fas	Fas (TNF receptor superfamily member 6)
Fasl	Fas ligand (TNF superfamily, member 6)
Gadd45a	Growth arrest and DNA-damage-inducible 45 alpha
Nol3	Nucleolar protein 3 (apoptosis repressor with CARD domain)
Spata2	Spermatogenesis associated 2
Sycp2	Synaptonemal complex protein 2
Tnf	Tumor necrosis factor
Tnfrsf10b	Tumor necrosis factor receptor superfamily, member 10b
Trp53	Transformation related protein 53

Table A10: Anti apoptosis genes in RT^2 profiler array

Symbol	Description
Akt1	Thymoma viral proto-oncogene 1
Bcl2	B-cell leukemia/lymphoma 2
Bcl2a1a	B-cell leukemia/lymphoma 2 related protein A1a
Bcl2l1	Bcl2-like 1
Birc3	Baculoviral IAP repeat-containing 3
Casp2	Caspase 2
Igf1r	Insulin-like growth factor I receptor
Mcl1	Myeloid cell leukemia sequence 1
Tnfrsf11b	Tumor necrosis factor receptor superfamily, member 11b (osteoprotegerin)
Traf2	Tnf receptor-associated factor 2
Xiap	X-linked inhibitor of apoptosis

Table 11: Autophagy related genes in RT^2 profiler array

Symbol	Description
Akt1	Thymoma viral proto-oncogene 1
App	Amyloid beta (A4) precursor protein
Atg12	Autophagy-related 12 (yeast)
Atg16l1	Autophagy-related 16-like 1 (yeast)
Atg3	Autophagy-related 3 (yeast)
Atg5	Autophagy-related 5 (yeast)
Atg7	Autophagy-related 7 (yeast)
Bax	Bcl2-associated X protein
Bcl2	B-cell leukemia/lymphoma 2
Bcl2l1	Bcl2-like 1
Becn1	Beclin 1, autophagy related
Casp3	Caspase 3
Ctsb	Cathepsin B
Ctss	Cathepsin S
Eif5b	Eukaryotic translation initiation factor 5B
Esr1	Estrogen receptor 1 (alpha)
Fas	Fas (TNF receptor superfamily member 6)
Gaa	Glucosidase, alpha, acid
Htt	Huntingtin
Ifng	Interferon gamma
Igf1	Insulin-like growth factor 1
Igf1r	Insulin-like growth factor I receptor
Ins2	Insulin II
Irgm1	Immunity-related GTPase family M member 1
Map1lc3a	Microtubule-associated protein 1 light chain 3 alpha
Mapk8	Mitogen-activated protein kinase 8
Nfkb1	Nuclear factor of kappa light polypeptide gene enhancer in B-cells 1, p105
Pik3c3	Phosphoinositide-3-kinase, class 3
Rps6kb1	Ribosomal protein S6 kinase, polypeptide 1
Snca	Synuclein, alpha
Sqstm1	Sequestosome 1
Tnf	Tumor necrosis factor
Trp53	Transformation related protein 53
Ulk1	Unc-51 like kinase 1 (C. elegans)

Table 12: Necrosis genes in RT^2 profiler array

Symbol	Description
Atp6v1g2	ATPase, H+ transporting, lysosomal V1 subunit G2
Ccdc103	Coiled-coil domain containing 103
Bmf	Bcl2 modifying factor
Commd4	COMM domain containing 4
Cyld	Cylindromatosis (turban tumor syndrome)
Defb1	Defensin beta 1
Dpysl4	Dihydropyrimidinase-like 4
Foxi1	Forkhead box I1
Galnt5	UDP-N-acetyl-alpha-D-galactosamine:polypeptide N-acetylgalactosaminyltransferase 5
Grb2	Growth factor receptor bound protein 2
Hspbap1	Hspb associated protein 1
Kcnip1	Kv channel-interacting protein 1
Mag	Myelin-associated glycoprotein
Parp1	Poly (ADP-ribose) polymerase family, member 1
Parp2	Poly (ADP-ribose) polymerase family, member 2
Pvr	Poliovirus receptor
Rab25	RAB25, member RAS oncogene family
Spata2	Spermatogenesis associated 2
Sycp2	Synaptonemal complex protein 2
Tmem57	Transmembrane protein 57
Tnfrsf1a	Tumor necrosis factor receptor superfamily, member 1a
Olfr1404	Olfactory receptor 1404
S100a7a	S100 calcium binding protein A7A
Jph3	Junctophilin 3
9430015G10Rik	RIKEN cDNA 9430015G10 gene